The Importance of the Antiperiplanar Effect in the Nucleophilic Addition of Hydride to a Carbonyl Group

by

Neil Charles Faibish
B. Sc. (Honours), York University, 1990

A Thesis Submitted to the School of Graduate Studies and Research In Partial Fulfillment of the Requirements for the Degree of
Doctor of Philosophy

Ottawa-Carleton Chemistry Institute
Department of Chemistry
University of Ottawa
Ottawa, Ontario
Canada

Candidate

Neil C. Faibish

Supervisor

Professor R.R. Fraser

National Library
of Canada

Acquisitions and
Bibliographic Services Branch

395 Wellington Street
Ottawa, Ontario
K1A 0N4

Bibliotheque nationale
du Canada

Direction des acquisitions et
des services bibliographiques

395, rue Wellington
Ottawa (Ontario)
K1A 0N4

Your file Votre référence

Our file Notre référence

ISBN 0-612-19955-X

Canada

UNIVERSITÉ D'OTTAWA
UNIVERSITY OF OTTAWA

To my mother and father.

Abstract

The factors responsible for π-facial selectivity in the nucleophilic addition to ketones have been at the focus of attention for the last forty years. Currently, two main explanations have been cited, that of Cieplak involving non-classical orbital-orbital interactions and that of Felkin-Houk involving torsional and electrostatic effects. However, in contrast to previous studies which have measured π-facial selectivity (i.e. diastereoselectivity), we have chosen to determine π-facial reactivity. More specifically, we have measured the relative rates for addition of lithium aluminum hydride, sodium borohydride and triethylsilane to the conformationally fixed ketone **44** and its α-methyl, -methylthio, -methoxy, -chloro and -fluoro quasi-axial and quasi-equatorial derivatives **45-53**.

On the basis of a molecular mechanics study of the α-chloro derivatives of **44**, we have demonstrated that our bridge biaryl ketone is a suitable model to test the importance of the antiperiplanar effect as proposed by Cieplak or Anh. In addition to providing greater inflexibility over the normally employed cyclohexanone model, the calculations revealed, unlike 2-substituted cyclohexanones, only one energy minimum.

The α-fluoro derivative of our bridge biaryl ketone exhibits an extremely large preference for the equatorial conformation. However, for the α-methylthio derivative of **44**, the axial diastereomer is favoured, even in the highly polar solvent acetonitrile. In order to aid our understanding of this variability and to clarify the data in the literature, we conducted a conformational analysis of 2-methoxy- and 2-methylthiocyclohexanone in five solvents using 500 MHz ^{1}H NMR spectroscopy. Both compounds show a strong solvent dependence with the α-methylthio group existing mainly in its axial conformer (n_a = 0.94) while the α-methoxy group shows only a marginal preference in the same solvent (n_a = 0.56). Employing these results and those known for the α-halo cyclohexanones provides the following order of increasing axial preference: fluoro<methoxy<chloro

<bromo<methylthio. On the basis of molecular mechanics calculations, it is concluded that this order may simply reflect the varying strength in the van der Waals interaction between the carbonyl group and the 2-equatorial substituent.

Our competitive reduction rate study has demonstrated with the aid of log (k_R^{app}/k_H) and (k_R^{ac}/k_H) versus σ_I plots that the π-facial reactivity is mainly governed by sigma-inductive effects and not app orbital-orbital interactions as put forward by Cieplak or Anh. The results indicate an early transition state for reduction by LAH, while reduction by SBH exhibits a much later transition state. In both instances, the reactivity increased as the electron withdrawing ability of the α-substituent increased. In the reduction using triethylsilane, the opposite trend was found. As the electron withdrawing ability of the α-substituent increased, the reactivity decreased.

Since the π-facial reactivity for reduction with LAH shows the least influence from inductive effects, it should be the most likely to reveal an app effect. However, both the Cieplak and Anh theories do not predict the observed results. In addition, assuming that the face reactivity for the axial substituents represents a combination of inductive and app effects (Cieplak or Anh) and for the equatorial substituents represents only inductive effects, the study indicates, for all three reducing agents, a series of inconsistent results.

The plots of log (k_R^{app}/k_H) and (k_R^{ac}/k_H) versus σ_I do not exhibit a strong correlation. For all three reducing agents, the data for the methoxy substituents show the largest deviation. In addition to steric and torsional strain, we have reasoned this lack of linearity arises from a variable dipole-dipole interaction. It is concluded that this field effect is responsible for deviation in the methoxy data and the differences in susceptibility constants for the axial and equatorial substituents.

Acknowledgments

I wish to express my sincerest gratitude to my supervisor Professor R.R. Fraser for all his guidance and support. Professor Fraser has been extremely generous with his time. I appreciate that I was able to approach him to discuss any problems or answer any questions that I may have had.

I would like to thank Professor R. Roy and the members of his group for making my stay in Ottawa a pleasurable experience. Thanks especially to Serge Meunier, Denis Carriere, Bernd Kratzer and U.K. Saha for their friendship and for making our time together sharing laboratory space so enjoyable.

I would also like to extend my thanks to Mr. Q.Q. Wu for his friendship and for his contribution to the syntheses of several of the compounds under study. I would next like to thank Dr. Fanzuo Kong and Krzysztof Bednarski for their contribution to this project.

In addition, I would like to thank the Chemistry Department staff, graduate students and postdoctoral fellows, especially to Dr. G. Facey and Mr. Raj Capoor for their invaluable assistance with many NMR experiments.

Finally, I would like to extend my deepest gratitude to my parents, Bernard and Eleanor Faibish, and my brother Paul for their encouragement and support.

Table of Contents

Dedication		i
Abstract		ii
Acknowledgments		iv
Table of Contents		v
List of Tables		ix
List of Figures		xii
List of Abbreviations		xvii
Chapter 1	**General Introduction**	1
1.1	π-Facial Selectivity in Acyclic Systems	1
1.2	Additional Theoretical Support of the Felkin Model	9
1.3	π-Facial Selectivity in Cyclohexanone Based Substrates	11
1.3.1	Product Development and Steric Approach Control	13
1.3.2	Torsional Strain	14
1.3.3	Cieplak's Model	16
1.4	Recent Theoretical Calculations	18
1.5	Recent Experimental Investigations	19
1.5.1	π-Facial Selectivity Study of le Noble	20
1.5.2	Cieplak and Johnson's Investigation of π-Facial Selectivity	22
1.5.3	Halterman's Examination of π-Facial Selectivity	24
1.5.4	π-Facial Selectivity Study of Mehta	26
1.5.5	Okada's Examination of π-Facial Selectivity	27
1.5.6	Wipf's Study of π-Facial Selectivity	27
1.5.7	Houk's Study of π-Facial Selectivity	29

Chapter 2 **Syntheses of 5,7-dihydro-1,11-dimethyl-6*H*-dibenzo[a,c]cyclohepten- 6-one and its α-methyl, -methylthio , -methoxy, -chloro and -fluoro Derivatives** 34

2.1 Introduction 34

2.2 Syntheses of the α-methyl, -methoxy and -chloro derivatives of 5,7-dihydro-1,11-dimethyl-6*H*-dibenzo[a,c]cyclohepten-6-one 38

2.3 Syntheses of the α-methylthio derivatives of 5,7-dihydro-1,11-dimethyl-6*H*-dibenzo[a,c]cyclohepten-6-one 38

2.4 Synthesis of the Equatorial α-fluoro Derivative of 5,7-dihydro-1,11-dimethyl-6*H*-dibenzo[a,c]cyclohepten-6-one 40

2.5 Characterization of 5,7-dihydro-1,11-dimethyl-6*H*-dibenzo[a,c] cyclohepten-6-one and its α-Substituted Reduction Products 46

Chapter 3 **Conformational Study of the α-Derivatives of 5,7-dihydro-1,11-dimethyl-6*H*-dibenzo[a,c]cyclohepten-6-one and their Cyclohexanone Analogues** 51

Part A α-Derivatives of 5,7-dihydro-1,11-dimethyl-6*H*-dibenzo[a,c]cyclohepten-6-one 51

3.1 Introduction 51

3.2 Results and Discussion 52

3.2.1 Determination of the Viability of the α-chloro Derivatives of **44** as a Stereochemical Model 52

3.3 Conclusions 56

Part B Conformational Analysis of 2-Substituted Cyclohexanones 56

3.4 Introduction 56

3.5 Results and Discussion 60

3.5.1 Factors Influencing the Conformational Equilibrium 66

3.5.2 Molecular Mechanics Calculations 69

3.6 Conclusions 71

Chapter 4 Competitive Reduction Rates of 5,7-dihydro-1,11-dimethyl-6*H*-dibenzo[a,c]cyclohepten-6-one and its α-methyl, -methylthio, -methoxy, -chloro and -fluoro derivatives 72

4.1 Introduction 72

4.1.1 Reductions using Lithium Aluminum Hydride in Tetrahydrofuran 77

4.1.2 Reductions using Sodium Borohydride in Isopropanol 80

4.1.3 Boron Trifluoride Etherate Catalyzed Reductions using Triethylsilane 83

4.2 Results 85

4.2.1 Competitive Rates using Lithium Aluminum Hydride 85

4.2.2 Competitive Rates using Sodium Borohydride 98

4.2.3 Competitive Rates using Triethylsilane/Boron Trifluoride Etherate 103

4.3 Discussion 108

4.3.1 Axial versus Equatorial Substituents 117

4.3.2 A Closer Look at the Axial and Equatorial Plots 119

4.4 Conclusions 128

Chapter 5	**Experimental**		130
	5.1	General Experimental	130
	5.2	Experimental for Chapter 2	131
	5.3	Experimental for Chapter 3 Part B	140
	5.4	Experimental for Chapter 4	140

References 144

Claims to Original Research 156

Appendix 1: X-ray Data for Ketones **46** and **53** 158

Appendix 2: Competitive Reduction of Ketones **44-53** using LAH, SBH and Triethylsilane 186

Appendix 3: Supplementary ^{1}H NMR Spectra 192

List of Tables

Table 1.1	Selected examples of 1,2-asymmetric induction for racemic acyclic ketones/aldehydes.	2
Table 1.2	Selected examples of stereoselectivity for the reduction of cyclohexanone derivatives.	12
Table 1.3	Attack ratios of *syn*:*anti* approach for the reduction of **16-18** by $NaBH_4$.	21
Table 1.4	Percent axial (*syn*) attack in the nucleophilic addition to 3-substituted cyclohexanones.	23
Table 1.5	Diastereoselectivity for the reduction of cyclopentanones **19a-f**.	24
Table 1.6	Experimental attack ratios for the nucleophilic addition to 7-norbornanones **22a-e**.	25
Table 1.7	Experimental attack ratios (*syn*:*anti*, **27**:**28**) for the reduction of ketones **26a-f**.	26
Table 1.8	Summary of Wipf's results on the nucleophilic addition to dienones **29-37**.	29
Table 1.9	Diastereoselectivities for the reduction of *trans*-decalones **46a-i**.	30
Table 2.1	Attempted epimerization of ketone **53**.	43
Table 2.2	Spin simulation spectral parameters.	44
Table 2.3	Vicinal coupling constants (Hz) for **65** and its α-substituted derivatives.	50
Table 2.4	π-Facial selectivity for the nucleophilic addition of $LiAlH_4$ to ketones **45-53**.	50
Table 3.1	Spectral parameters for the simulation of (a) 4-*t*-butylcyclohexanone (**6**, in acetone-d_6) and (b) 2-methylthiocyclohexanone (**73**, in $CDCl_3$).	62
Table 3.2	Conformational equilibrium data for 2-methylthiocyclohexanone (**73**).	64
Table 3.3	Conformational equilibrium data for 2-methoxycyclohexanone.	66
Table 3.4	Solvent effects on 2-substituted cyclohexanones.	68

Table 3.5	Molecular mechanics calculations of steric energies of 2-substituted cyclohexanones.	70
Table 4.1	Face reactivity for the electrophilic addition of *p*-nitroperbenzoic acid in dichloromethane at 0°C.	74
Table 4.2	Competitive reduction of ketones **44** versus **45** with LAH in 4 mL THF at 0°C (20 sec quench, 0.05 mmol of total ketones).	94
Table 4.3	Competitive reduction of ketones **50** versus **46** with LAH in 4 mL THF at 0°C (20 sec quench, 0.05 mmol of total ketones).	96
Table 4.4	π-Facial reactivity of the α-derivatives of **44** for reduction by LAH.	98
Table 4.5	Ketone reduction by SBH in isopropanol at rt.	100
Table 4.6	Competitive reduction of ketones **45** versus **44** for SBH in *i*-PrOH at rt.	101
Table 4.7	π-Facial reactivity of the α-derivatives of **44** for reduction by SBH.	103
Table 4.8	Competitive reduction of ketones **45** versus **44** with $Et_3SiH/BF_3{\cdot}Et_2O$ in CH_3CN at 0°C.	105
Table 4.9	π-Facial reactivity of the α-derivatives of **44** for reduction by $Et_3SiH/BF_3{\cdot}Et_2O$.	107
Table 4.10	Facial reactivity of the α-derivatives of **44**.	109
Table 4.11	Correlation coefficients and susceptibility constants of the Taft plots.	112
Table A2.1a	Competitive reduction of ketones A (unsubstituted) versus B (axial α-substituted) for $LiAlH_4$ in 4 mL THF at 0°C (20 sec quench).	187
Table A2.1b	Competitive reduction of ketones A (unsubstituted) versus B (equatorial α-substituted) for $LiAlH_4$ in 4 mL THF at 0°C (20 sec quench).	188
Table A2.2a	Competitive reduction of ketones A (unsubstituted) versus B (axial α-substituted) for $NaBH_4$ (1 equiv) in 20 mL *i*-PrOH at 23°C (45 sec quench).	189
Table A2.2b	Competitive reduction of ketones A (unsubstituted) versus B (equatorial α-substituted) for $NaBH_4$ (1 equiv) in 20 mL *i*-PrOH at 23°C (45 sec quench).	190

Table A2.3 Competitive reduction of ketones A (unsubstituted) versus B (α-substituted) for Et_3SiH (1 equiv)/BF_3-Et_2O (3 equiv) in 5 mL CH_3CN at 0°C (2 min quench). 191

List of Figures

Figure 1.1	Cram's (a) original, (b) modified and (c) chelation controlled models for 1,2-asymmetric induction (S = small sized group, M = medium sized group and L = large sized group).	4
Figure 1.2	The (a) Cornforth, (b) Karabatsos and (c) Felkin models for 1,2-asymmetric induction.	5
Figure 1.3	The Felkin model for 1,2-asymmetric induction.	7
Figure 1.4	Liotta's frontier molecular orbital model for the Bürgi-Dunitz angle.	8
Figure 1.5	The Anh molecular orbital interpretation of Felkin's model.	9
Figure 1.6	Definition of inside, outside and anti positions.	10
Figure 1.7	Stereochemistry for the reduction of 4-*t*-butylcyclohexanone and 3,3,5-trimethylcyclohexanone.	13
Figure 1.8	The Felkin model for 4-*t*-butylcyclohexanone.	15
Figure 1.9	Anh's flattening rule.	16
Figure 1.10	The Cieplak model for the nucleophilic addition to cyclohexanone.	17
Figure 1.11	Representation of Wipf's proposed "vinylogous Cieplak effect".	28
Figure 2.1	Structural and three-dimensional representation of **44-53**.	35
Figure 2.2	Structural representation of the chair, C_s boat, C_1 boat and twist boat conformers of cyclohexanone.	36
Figure 2.3	Molecular mechanics calculations of the three rotamers about the S-C2 bond for ketone **46** and their respective steric energies (E) in kcal/mol.	40
Figure 2.4	The 500 MHz ^{1}H NMR spectrum of **53** in $CDCl_3$. The inset shows an expansion of the methylene protons on C15 (δ 3.44-3.53).	42
Figure 2.5	The 500 MHz ^{1}H NMR spectrum of the mother liquor from the crystallization of **53** in $CDCl_3$: (a) spectrum (δ 0-10); (b) expansion of (a) (δ 5.64-5.79); (c) spectrum calculated by PCPMR employing the parameters given in Table 2.2.	45

Figure 2.6 The 300 MHz ^{1}H NMR spectrum of **65** in benzene-d_6. The inset shows an expansion of the four benzylic protons on C2 and C15 (δ 1.95-2.95). 48

Figure 2.7 Syntheses and three-dimensional representation of alcohols **65-69**. 49

Figure 3.1 A plot of steric energy (kcal/mol) versus the torsional angle (deg) about C1-C2 for (a) **44**, (b) **48** and (c) **52**. 53

Figure 3.2 A plot of steric energy (kcal/mol) versus the torsional angle (deg) about C1-C2 for (a) **44**, (b) cyclohexanone, (c) axial 2-chlorocyclohexanone (**70**), dielectric constant = 1.5 and (d) axial 2-chlorocyclohexanone (**70**), dielectric constant = 6.0. 55

Figure 3.3 A portion of the 500 MHz ^{1}H NMR spectrum for 4-*t*-butylcyclohexanone in acetone-d_6: (a) the absorption for the axial (δ 2.31-2.39) and the equatorial (δ 2.21-2.26) protons at C2 and C6; (b) the spectrum calculated by PCPMR employing the parameters given in Table 3.1. 61

Figure 3.4 The 500 MHz ^{1}H NMR spectrum of 2-methylthiocyclohexanone (**73**) in $CDCl_3$. The inset shows the expansion of the octet for H6 at δ 2.94. 63

Figure 3.5 Estimation of J_{aa} and J_{ee} for 2-methoxycyclohexanone. 65

Figure 3.6 The (a) steric, (b) dipole-dipole repulsive interaction and (c) orbital-orbital interaction used to rationalize the conformational equilibrium in 2-substituted cyclohexanones. 67

Figure 4.1 Relative rates of addition for axial (ax) and equatorial attack. 76

Figure 4.2 Proposed mechanism for the reduction of ketones with LAH in THF. 80

Figure 4.3 Proposed transition state for sodium borohydride reduction in isopropanol. 83

Figure 4.4 Proposed mechanisms for the reduction of ketones using $Et_3SiH/BF_3{\cdot}Et_2O$. 84

Figure 4.5 The 500 MHz ^{1}H NMR spectrum in $CDCl_3$ for the competitive reduction of entry 7 in Table 4.2. 88

Figure 4.6 The 500 MHz ^{1}H NMR spectrum of the unsubstituted ketone **44** in $CDCl_3$. 89

Figure 4.7	The 500 MHz ^{1}H NMR spectrum of the axial α-methyl ketone **45** in $CDCl_3$.	90
Figure 4.8	The 300 MHz ^{1}H NMR spectrum of the unsubstituted alcohol **65** in $CDCl_3$.	91
Figure 4.9	The 300 MHz ^{1}H NMR spectrum of the axial α-methyl major alcohol **66a** in $CDCl_3$.	92
Figure 4.10	The 300 MHz ^{1}H NMR spectrum of the axial α-methyl minor alcohol **67a** in $CDCl_3$.	93
Figure 4.11	Kinetic plots for the reduction of (a) 1,3-diphenylacetone and (b) unsubstituted bridge biaryl ketone **44** by sodium borohydride (a = initial ketone concentration, b = initial borohydride concentration and x = concentration of ketone remaining at time *t*.	99
Figure 4.12	The 500 MHz ^{1}H and ^{1}H-^{1}H COSY NMR spectra of **84** in $CDCl_3$.	106
Figure 4.13	Plots of (a) log k_R^{app}/k_H and (b) log k_R^{ac}/k_H versus σ_I for LAH reduction of (a) **44-48** and (b) **44** and **49-53**.	110
Figure 4.14	Plots of (a) log k_R^{app}/k_H and (b) log k_R^{ac}/k_H versus σ_I for SBH reduction of (a) **44-48** and (b) **44** and **49-53**.	110
Figure 4.15	Plots of (a) log k_R^{app}/k_H and (b) log k_R^{ac}/k_H versus σ_I for triethylsilane reduction of (a) **44-48** and (b) **44** and **49-53**.	111
Figure 4.16	Free energy-reaction coordinate diagram representing reduction by lithium aluminum hydride.	113
Figure 4.17	Free energy-reaction coordinate diagram representing reduction by sodium borohydride.	114
Figure 4.18	Free energy-reaction coordinate diagram representing reduction by triethylsilane.	115
Figure 4.19	Plots of log k_R^{app}/k_H (■) and log k_R^{ac}/k_H (▲) versus σ_I for reduction by (a) LAH, (b) SBH and (c) triethylsilane.	118
Figure 4.20	Three-dimensional representations of the transition states for (a) the Taft hydrolysis of aliphatic esters and (b) the reduction of our α-X substituted bridged biaryl ketones.	122
Figure 4.21	Molecular mechanics calculations of the three rotamers about the O-C2 bond for the (a) axial α-methoxy ketone **47** and (b) equatorial α-methoxy ketone **51** and their respective steric energies (E) in kcal/mol.	124

Figure 4.22 Proposed electrostatic interaction for the reduction of the axial and equatorial chloro derivatives (a) and methoxy derivatives (b) by triethylsilane. 125

Figure 4.23 Proposed electrostatic interaction for the reduction of the axial and equatorial chloro derivatives (a) and methoxy derivatives (b) by sodium borohydride. 126

Figure 4.24 Proposed electrostatic interaction for the reduction of the axial and equatorial chloro derivatives (a) and methoxy derivatives (b) by lithium aluminum hydride. 127

Figure A3.1 The 500 MHz ^{1}H NMR spectrum of the axial α-methylthio ketone **46** in $CDCl_3$. 193

Figure A3.2 The 500 MHz ^{1}H NMR spectrum of a mixture of the axial and equatorial α-methylthio ketones **46** and **50** in $CDCl_3$ (**50**:**46**, 1.22:1; sample contained 5.6% of the unsubstituted ketone **44**). 194

Figure A3.3 The 300 MHz ^{1}H NMR spectrum of the equatorial α-methyl major alcohol **68a** in $CDCl_3$. 195

Figure A3.4 The 500 MHz ^{1}H NMR spectrum of the axial α-methylthio major alcohol **66b** in $CDCl_3$. 196

Figure A3.5 The 500 MHz ^{1}H NMR spectrum of the equatorial α-methylthio major alcohol **68b** in $CDCl_3$. 197

Figure A3.6 The 500 MHz ^{1}H NMR spectrum of the axial α-methoxy major alcohol **66c** in $CDCl_3$. 198

Figure A3.7 The 500 MHz ^{1}H NMR spectrum of the equatorial α-methoxy major alcohol **68c** in $CDCl_3$. 199

Figure A3.8 The 500 MHz ^{1}H NMR spectrum of the axial α-chloro major alcohol **66d** in $CDCl_3$. 200

Figure A3.9 The 500 MHz ^{1}H NMR spectrum of the equatorial α-chloro major alcohol **68d** in $CDCl_3$. 201

Figure A3.10 The 500 MHz ^{1}H NMR spectrum of the equatorial α-fluoro major alcohol **68e** in $CDCl_3$. 202

List of Abbreviations

a or ax	axial
Ac	acetyl
ac	anticlinal
app	antiperiplanar
n-Bu	*n*-butyl
t-Bu	*tert*-butyl
calcd	calculated
COSY	correlation spectroscopy
d	doublet
dd	doublet of doublets
ddd	doublet of doublet of doublets
dq	doublet of quartets
deg	degrees
DME	dimethoxyethane
e or eq	equatorial
EI	electron ionization
Et	ethyl
equiv	equivalent
exptl	experimental
h	hours
HMQC	heteronuclear multiple quantum coherence
HRMS	high resolution mass spectrometry
Hz	hertz
i-Pr	isopropyl
kcal	kilocalories

L	litre
LAH	lithium aluminum hydride
LDA	lithium diisopropylamide
LHMDS	lithium 1,1,1,3,3,3-hexamethyldisilazide
m	multiplet
M	molar or metal
M^+	parent molecular ion
Me	methyl
MHz	megahertz
min	minutes
mg	milligrams
µL	microlitres
mL	millilitres
mm	millimetres
mmol	millimoles
mol	moles
mp	melting point
mT	milliTorr
m/z	mass to charge ratio
NMR	nuclear magnetic resonance
NOE	nuclear Overhauser enhancement
Nu	nucleophile
Ph	phenyl
ppm	parts per million
q	quartet
ref	reference(s)
rt	room temperature

s	singlet
SBH	sodium borohydride
sc	synclinal
sec	seconds
sp	synperiplanar
TFA	trifluoroacetic acid
THF	tetrahydrofuran
TLC	thin layer chromatography
TMS	tetramethylsilane
unsub	unsubstituted
vs	versus
v/v	volume to volume ratio

Chapter 1 General Introduction

1.1 π- Facial Selectivity in Acyclic Systems

The addition of nucleophiles to a carbonyl group (C=O) possessing two distinct faces may yield two diastereomeric products in unequal proportions. More precisely, the addition may occur with some diastereoselectivity. Acyclic ketones or aldehydes possessing one or more asymmetric carbon atoms meet the above criterion and thus may provide a valuable method for asymmetric synthesis. McKenzie and other researchers have recognized this fact and have exploited it with some success since the beginning of this century.[1]

In order to provide the maximum influence on the diastereoselectivity for the addition of nucleophiles to an open chain aldehyde/ketone having one asymmetric carbon atom, the asymmetric environment of the chiral centre should be adjacent to the carbonyl group. This type of asymmetric synthesis was later termed 1,2-asymmetric induction and has been employed by a large number of research groups with some representative examples listed in Table 1.1.[2]

Several models have been proposed to explain and, it is hoped, predict the observed stereochemical course of these reactions.[7] The models have focused primarily on the nucleophilic addition of organometallic and complex metal hydride reagents to chiral ketones and aldehydes. Each model makes assumptions about the exact conformation of the transition state and the relative importance of various factors such as steric strain, torsional strain, dipolar effects, hyperconjugative orbital-orbital interactions and chelation effects. The terms steric and torsional strain warrant further comment at this point. Torsional strain is defined as the excess strain present in a molecule caused by the torsional angles deviating from their ideal values (usually 60° in saturated molecules, i.e. gauche interactions). Steric strain is defined as the nonpolar nonbonded or van der Waals

interactions between two atoms. This interaction is attractive at larger distances and repulsive as the interatomic distance decreases.

Table 1.1 Selected examples of 1,2-asymmetric induction for racemic acyclic ketones/aldehydes.

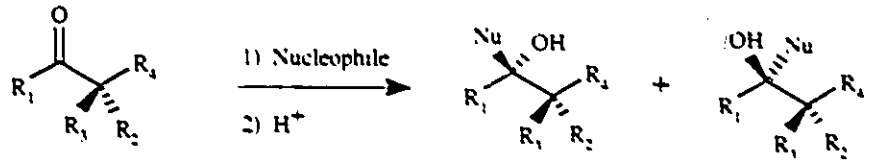

1a-h **2a-h** **3a-h**

	Compound	Nucleophile	Stereochemical Ratio of Products (2:3)	Ref.
1a	R_1 = Me, R_2 = C_6H_{11}[a], R_3 = H, R_4 = Me	$LiAlH_4$[b]	62:38	3a
b	R_1 = *i*-Pr, R_2 = C_6H_{11}, R_3 = H, R_4 = Me	$LiAlH_4$[b]	80:20	3a
c	R_1 = Me, R_2 = Ph, R_3 = H, R_4 = Me	$LiAlH_4$[b]	74:26	3a
d	R_1 = *i*-Pr, R_2 = Ph, R_3 = H, R_4 = Me	$LiAlH_4$[b]	83:17	3a
e	R_1 = Ph, R_2 = Me, R_3 = Ph, R_4 = OH	MeLi[c]	8:92	5
f	R_1 = Me, R_2 = Me, R_3 = Ph, R_4 = OMe	PhLi[c]	10:90	5
g[f]	R_1 = H, R_2 = H, R_3 = *n*-Bu, R_4 = Cl	EtMgBr[d]	70:30	6
h[f]	R_1 = *n*-Bu, R_2 = H, R_3 = Et, R_4 = Cl	$NaBH_4$[e]	80-85:15-20	6

[a] C_6H_{11} represents a cyclohexyl group. [b] In Et_2O at 35°C. [c] In Et_2O at 0°C. [d] In Et_2O at -70°C. [e] In aqueous EtOH at rt. [f] Optically pure ketones were employed.

In 1952, Cram was the first to propose a rule which proved to be very effective for correlating and predicting the stereochemical direction of approach of nucleophiles in 1,2-asymmetric induction reactions.[4] Cram termed his explanation as the "open-chain model". The model predicts that "in noncatalytic (kinetically controlled) reactions of the type shown (**1a-b** $\rightarrow$ **2a-b + 3a-b**) that diastereomer will predominate which would be formed by the approach of the entering group (nucleophile) from the less hindered side of the double bond when the rotational conformation of the C-C bond is such that the double bond is flanked by the two least hindered bulky groups (M and S) attached to the asymmetric centre".[4] Therefore Cram's model assumes that the reaction occurs via a reactant-like transition state in which the conformation of the transition state closely represents the conformation of starting ketone/aldehyde. Cram concluded that based solely on steric reasons the conformation shown in Figure 1.1(a) is adopted in which the R_1 group eclipses L (i.e. the R_1-C-C-L dihedral angle $\theta \sim 0^\circ$) and thus causes the bulky oxygen to be placed between the two least bulky groups, M and S, on the adjacent asymmetric carbon atom. Cram offered the explanation that during the course of the reaction the metal cation of the nucleophile (e.g. Li^+ of $LiAlH_4$ of Mg^{2+} of RMgX) becomes coordinated to the carbonyl group and thus renders the oxygen as the bulkiest group. In addition, it is assumed that the nucleophile attacks perpendicular to the carbonyl plane since this allows for the maximum π orbital overlap.

In a subsequent paper on the same subject Cram and Kopecky modified their original conformation to a R_1-C-C-L dihedral angle of approximately 30° as shown in Figure 1.1(b).[5] In this model no specifics were given about the precise mechanism for nucleophilic addition.

In systems in which the adjacent asymmetric centre possesses a substituent such as OR or NR_2 capable of complexing to the organometallic reagent (e.g. **1e** or **1f** in Table 1.1), Cram advanced a third model termed the chelation controlled, cyclic or rigid model to explain the observed stereochemical result in this rather unique situation.[4,5,8] In the

cyclic model the carbonyl oxygen atom and the α-heteroatom (R_4 in Table 1.1) are held in an approximately coplanar arrangement by chelation to the metal (Z). The nucleophile then attacks perpendicular to the carbonyl plane from the face bearing the smaller of the two remaining groups on the α-asymmetric carbon atom. As in the previous model, Cram provided no specifics regarding the mechanism of the reaction. The open chain model and the cyclic model predict the same result when the α-heteroatom is the medium group (M), but the models predict the opposite result when the α-heteroatom is the large (L) or the small substituent (S) (see Figure 1.1(c)).

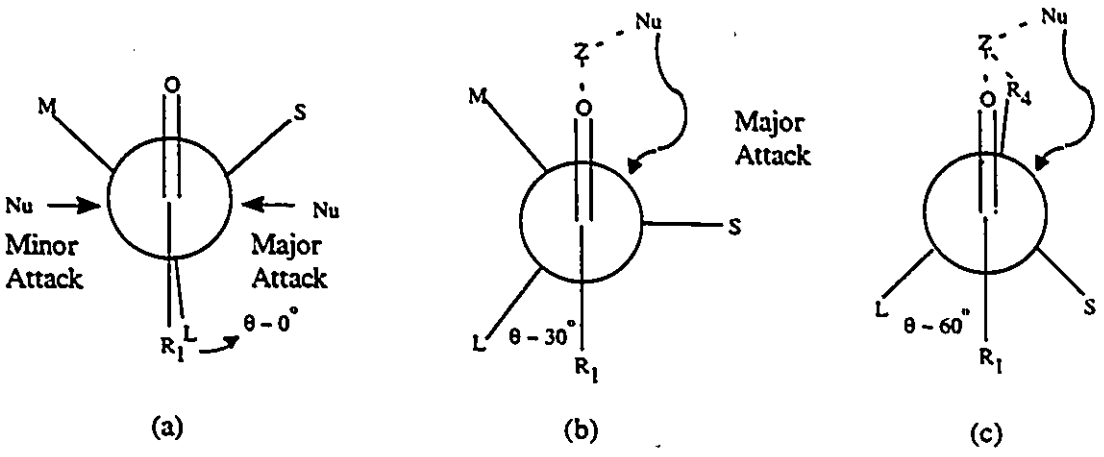

Figure 1.1 Cram's (a) original, (b) modified and (c) chelation controlled models for 1,2-asymmetric induction (S = small sized group, M = medium sized group and L = large sized group).

The open-chain model usually exhibits significantly less stereoselectivity than the cyclic model. Presumably, the rigid conformation involved in the cyclic model allows for greater discrimination between the two faces of the carbonyl group.*

A few years after the appearance of Cram's open-chain and cyclic models, Cornforth recognized that if one of the substituents on the asymmetric carbon is a highly

* The chelation controlled model has been included for the sake of completeness, but will not be further discussed in this thesis. All subsequent discussions of Cram's model will refer to Cram's open-chain model.

polar group (e.g. halogen, R_4 in Table 1.1) neither the cyclic nor the open-chain model no longer predicts the observed stereochemical outcome (see **1g** and **1h** in Table 1.1).[6] Cornforth pointed out that the $^{\delta+}C{=}O^{\delta-}$ and the $^{\delta+}C\text{-}R_4{}^{\delta-}$ bonds are likely to orient themselves in an antiperiplanar (app) relationship since this minimizes the electrostatic repulsive interaction between these two dipoles (see Figure 1.2(a)). In Cornforth's model, the electronegative substituent R_4 plays the role of the large (L) substituent in Cram's model, even though it may not be so on purely steric grounds. Therefore dipolar interactions outweigh the influence of steric factors. Sauleau discussed the Cornforth model and concluded that it is applicable when R_4 = C:, but only in some instances when R_4 = OH.[9]

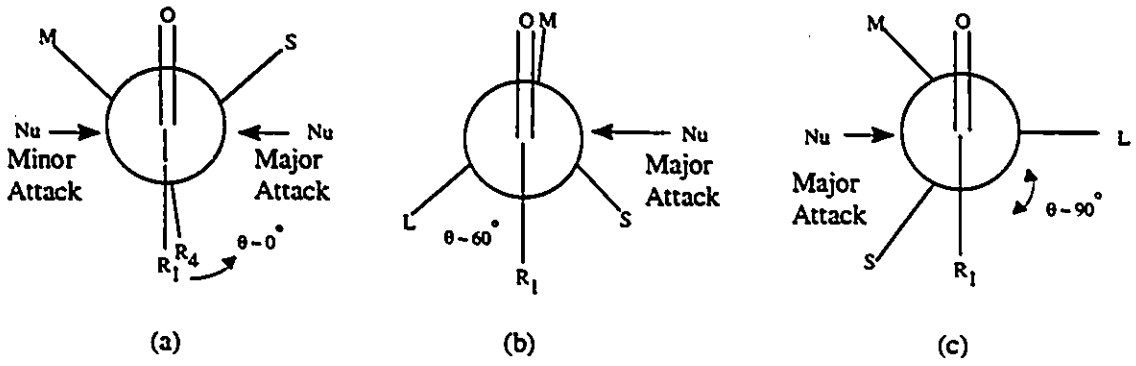

Figure 1.2 The (a) Cornforth, (b) Karabatsos and (c) Felkin models for 1,2-asymmetric induction.

Since being proposed by Cram[4] in 1952, the open-chain model has failed to rationalize several experimental results. In addition, spectroscopic studies by Karabatsos indicated that the preferred conformation of aldehydes and ketones possess a substituent on the adjacent carbon eclipsed with the C=O group.[10] These facts led Karabatsos in 1967 to propose a new model for predicting the stereochemical outcome of 1,2-asymmetric induction.[11] In his model, as in the previous models, it is assumed that the nucleophilic addition to the carbonyl occurs via a reactant-like transition state and thus the eclipsed

ground state conformation of the substrate aldehyde/ketone provides a good representation of the conformation in the transition state. Karabatsos assumed that the substrate adopts the conformation with the medium sized group (M) eclipsed with the carbonyl group; nucleophilic attack then occurs from the less hindered face as shown in Figure 1.2(b).

In 1968 Felkin noted two serious deficiencies in both the Cram and Karabatsos models. More specifically, neither the Cram nor the Karabatsos model could account for the effect of varying the size of the carbonyl R_1 group (see **1c-d** in Table 1.1) and the stereoselectivity observed in the reduction of cyclohexanone based systems (see Table 1.2 and Section 1.3.2). These facts led Felkin to put forward a new model (see Figure 1.2(c)) for 1,2-asymmetric induction which was premised on the following assumptions:[3] (1) the reaction occurs via a reactant-like transition state; (2) as pointed out by Schleyer[12a,b] for *endo* versus *exo* deprotonation of norbornanone and Garbisch for diimide reduction[12c], torsional strain involving partially formed bonds in the transition state represents a significant fraction of the strain present in fully formed bonds, even in the case when the degree of bonding is quite small; thus, in order to minimize torsional strain, a staggered conformation is preferred; (3) the dominant steric interaction is between the incoming nucleophile and the large (L) group and hence nucleophiles approach the substrate antiperiplanar (app) to L; (4) steric interactions between R and M/S are more important than those between the carbonyl's oxygen atom and M/S; this assumption represents an obvious weakness in Felkin's model, especially in the case of aldehydes (R_1 = H); (5) if one of the three substituents of the α-asymmetric carbon is a polar group, it takes the role of the large substituent L; as in the Cornforth model, dipolar effects take precedence over steric effects.

Therefore the degree of diastereoselectivity depends of the relative population of the major conformer **4** and the minor conformer **5** which, in turn, is dependent on the

difference in the gauche interactions between the R_l and S groups and the R_l and M groups (see Figure 1.3).

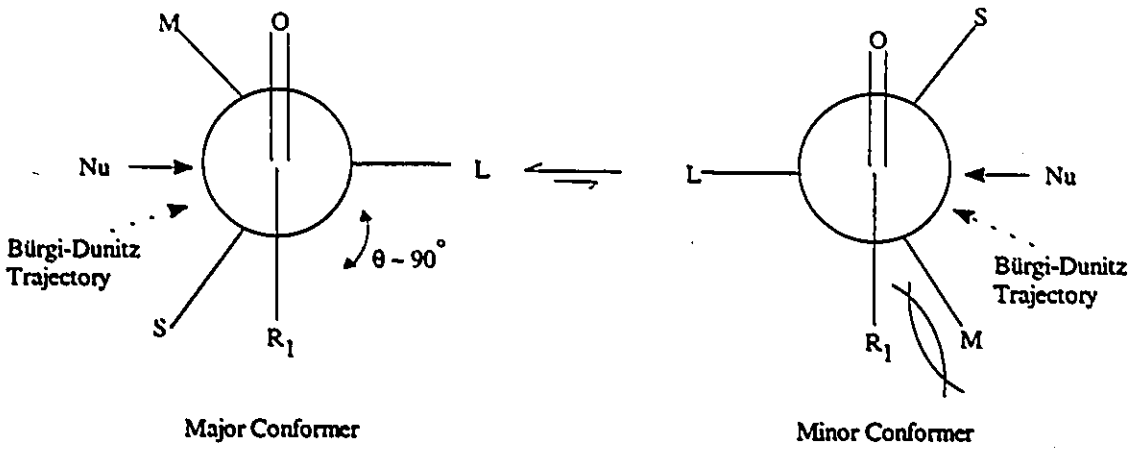

Figure 1.3 The Felkin model for 1,2-asymmetric induction.

Anh conducted an *ab initio* study of 1,2-asymmetric induction (at the STO-3G level) for the nucleophilic attack of hydride (H^-) to 2-chloropropanal and 2-methylbutanal.[13] In both cases, Anh found that the lowest energy conformation of the transition states corresponded closely to the conformation predicted by Felkin. For 2-chloropropanal, the Felkin transition state conformer was ≥4 kcal/mol more stable than the conformers predicted by Cram, Cornforth or Karabatsos. For the second substrate, 2-methylbutanal, the Felkin transition state conformer was determined to be at least 2.7 kcal/mol more stable than either the Cram or Karabatsos models. When Anh took into account carbonyl complexation (with Li^+) and the Bürgi-Dunitz angle[14] for hydride attack, both of which are now widely accepted, his calculations revealed an even greater preference for the Felkin transition states.

In combination with the Bürgi-Dunitz trajectory, the Felkin model no longer requires the assumption, for even aldehydes, that the steric interactions between R_l and

M/S are more important than those between O and M/S. Therefore, the nucleophile attacks preferentially past the least sterically encumbered S substituent in **4**.

Bürgi and Dunitz reported on the basis of crystallographic and theoretical evidence that the optimal angle of attack of hydride to a carbonyl group is 105±5°.[14] Liotta later proposed a model which qualitatively agrees with the work of Bürgi and Dunitz by considering the stabilizing interactions of the nucleophile's HOMO with the π^* molecular orbital of the carbonyl group (see Figure 1.4).[15]

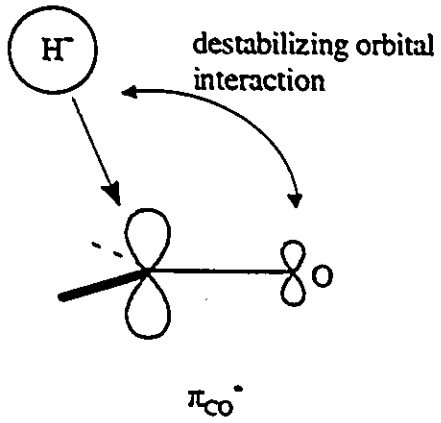

Figure 1.4 Liotta's frontier molecular orbital model for the Bürgi-Dunitz angle.

Anh concluded on the basis of frontier molecular orbital arguments that the substituent on the α-asymmetric carbon atom with the lowest lying σ^* orbital rather than the sterically bulkiest substituent occupies the app L position in Felkin's model. The app antibonding $\sigma_{C\text{-}L}^*$ orbital can mix with carbonyl's π_{CO}^* orbital which according to molecular orbital theory lowers the energy ($\Delta E'$ in Figure 1.5) of the π^* orbital. This stabilization of the π_{CO}^* molecular orbital reduces the separation (ΔE in Figure 1.5) between the nucleophile's HOMO and the carbonyl's LUMO and thus facilitates nucleophilic attack.[16] Therefore since polar and large substituents stabilize the σ^* orbital, these groups take the role of L in the Felkin model. Anh's calculations on ethanal, propanal and chloroethanal indicated the stabilization energies to be 35.5, 37.4 and 59.0

kcal/mol, respectively. Anh called this transition state stabilization the antiperiplanar (app) effect. The combination of these two mutually reinforcing theories has been termed the Felkin-Anh model.

In contrast to Anh's conclusions, Heathcock reported from a study of the reaction of a series of acyclic aldehydes with lithium enolates that the preference for substituents to be app to the incoming nucleophile is based not only on σ* orbital energies, but also on steric effects with the order being the following: MeO>*t*-Bu>Ph>*i*-Pr>Et>Me>H.[17]

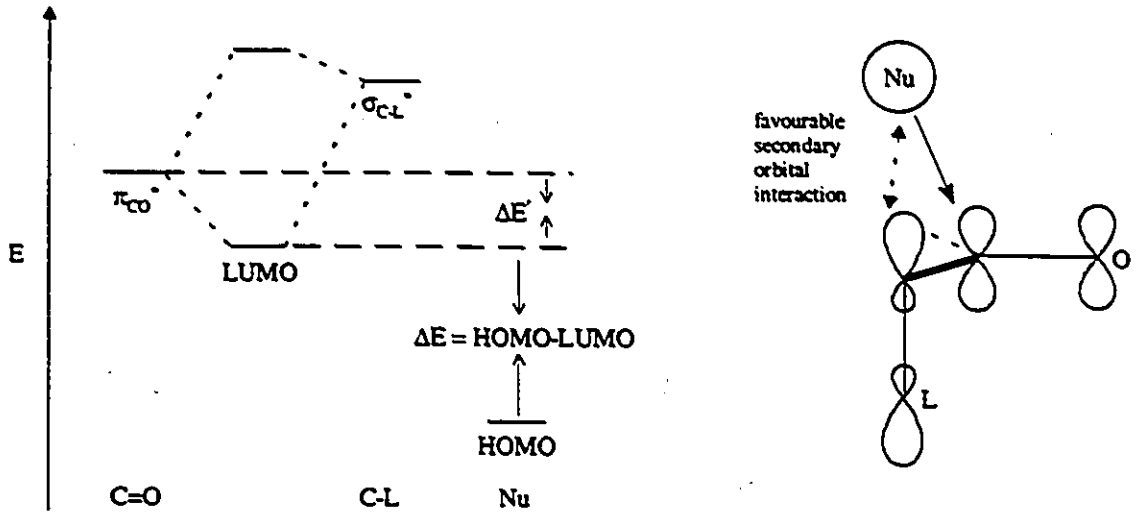

Figure 1.5 The Anh molecular orbital interpretation of Felkin's model.

1.2 Additional Theoretical Support of the Felkin Model

Force field models put forward by Houk[18], Wipke[19] and Müller[20] support Felkin's hypothesis that the stereoselectivity for the nucleophilic addition to acyclic aldehydes/ketones arises from a combination of torsional and steric effects. These models have also been used to support Felkin's model for the nucleophilic addition to cyclohexanone and other cyclic ketones (see Section 1.3.2).

Houk has shown that for the nucleophilic addition of hydride to propene and the addition of water to ethanal, the calculated rotational barriers involving torsional

interactions with the partially formed bonds suggest that they are as large (~3 kcal/mol) as fully formed bonds and thus supports Felkin's original assumption.[21]

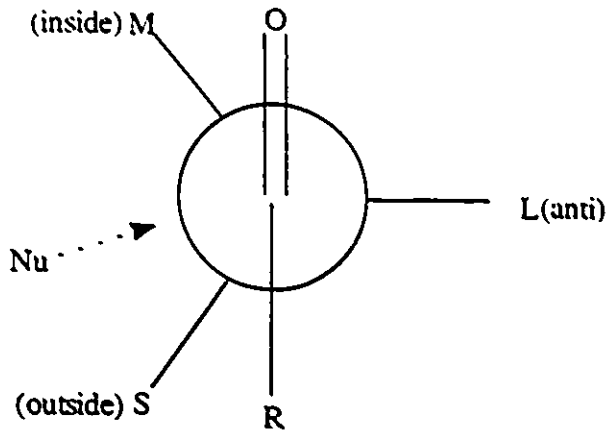

Figure 1.6 Definition of inside, outside and anti positions.

Ab initio calculations by Houk[18], Paddon-Row[22] and Frenking[23] on the transition state for NaH, LiH and CN^- addition to propanal indicate that, contrary to Anh's results, the lowest energy transition state occurs when the methyl group occupies the inside position rather than the anti position (see Figure 1.6 where R = H, S = H, M = Me and L = H). However, when the α-carbon is secondary (i.e. asymmetric), the Felkin-Anh geometry is adopted since an anti H results in unfavourable steric interactions for both the inside and outside alkyl groups (e.g. Figure 1.6 where R = H, S = H, M = Me and L = *t*-Bu).

In agreement with Anh's proposal, *ab initio* calculations by Paddon-Row[22a] and Frenking[23] on the addition of cyanide (CN^-) to fluoroethanal, 2-fluoropropanal and 2-chloropropanal places the substituent with the lowest lying σ^* orbital (i.e. F in fluoroethanal & 2-fluoropropanal and Cl in 2-chloropropanal) anti to the incoming cyanide ion. In addition, Frenking[23] has performed calculations on the addition of LiH to chloroethanal and 2-chloropropanal. For chloroethanal, Frenking found two favourable

transition sate conformations with the inside chloro conformer being slightly more stable than the anti chloro conformer. The result for 2-chloropropanal showed only one stable conformation with, as predicted by Anh, the chloro substituent occupying the anti position and the methyl occupying the inside position (i.e. R = H, S = H, M = Me and L = Cl in Figure 1.6).

However, subsequent ab initio studies by Paddon-Row[22b] at the 6-31G level have shown that for the attack of LiH to fluoroethanal and 2-fluoropropanal, the fluoro substituent preferably occupies the inside position. Paddon-Row concluded that the relative energies of the transition states is dependent on both Anh electronic effects and electrostatic factors.

In summary, all theoretical studies of 1,2-asymmetric induction support Felkin's staggered transition state, however by their very nature remain qualitative.

1.3 π-Facial Selectivity in Cyclohexanone Based Substrates

The nucleophilic addition of hydride to cyclic ketones such as conformationally rigid substituted cyclohexanones can yield two diastereomeric alcohol products. The free energy of activation ($\Delta G^{\ddagger}$) for attack at each face will be different and as this difference increases, the diastereoselectivity will increase.

The stereoselectivity of such substituted cyclohexanone systems has been extensively investigated and some representative examples are given in Table 1.2.[24] The data in Table 1.2 show that the addition occurs predominantly from the axial face of the carbonyl group and this preference diminishes as the steric bulk of the reducing agent increases.

Over the course of the last forty years, numerous models have been proposed to explain and predict this diastereoselectivity.[33] The impetus for the search into a general model was based on the unexpected high preference for nucleophiles to attack sterically unhindered cyclohexanones from the apparently more sterically encumbered axial face (see

Table 1.2). These models have subsequently been employed, where applicable, to explain the diastereoselectivities observed for other acyclic and cyclic ketones. However, only a few of the models have survived detailed investigation.

Table 1.2 Selected examples of stereoselectivity for the reduction of cyclohexanone derivatives.

Compound	Nucleophile (experimental conditions)[a]	% Axial Attack	Ref.
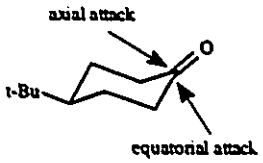 **6a-d**	**a** $NaBH_4$ (in *i*-PrOH)	85-87	25, 26, 27
	b $LiAlH_4$ (in THF)	88-93	25, 27
	c $LiAlH_4$ (in Et_2O)	91-93	25, 27, 28
	d $LiAl(OMe)_3H$ (in THF)	61	25
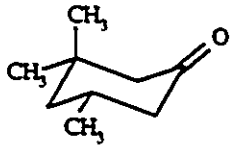 **7a-d**	**a** $NaBH_4$ (in *i*-PrOH)	38-43	26, 27, 29
	b $LiAlH_4$ (in THF)	18-20	27, 30
	c $LiAlH_4$ (in Et_2O)	42	27
	d $LiAl(OMe)_3H$ (in THF)	2-8	25, 31
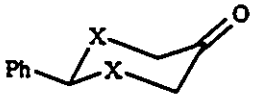 **8a-c**	$LiAlH_4$ (in Et_2O)		
	a X = CH_2	96	32
	b X = O	94	32
	c X = S[b]	15	32

[a] All reductions were performed at O°C unless otherwise specified. [b] At rt.

1.3.1 Product Development and Steric Approach Control

In 1953, Barton recognized that for cyclohexanone derivatives the "reduction with sodium borohydride and lithium aluminum hydride in general affords the equatorial epimer (e.g. **9** in Table 1.2) if the ketone group is not hindered, the axial epimer (e.g. **12** in Table 1.2) if it is hindered or very hindered" (see Figure 1.7).[34] This rule of thumb is generally valid, however it relies on the rather vague and subjective "hindered" and "not hindered" terms.

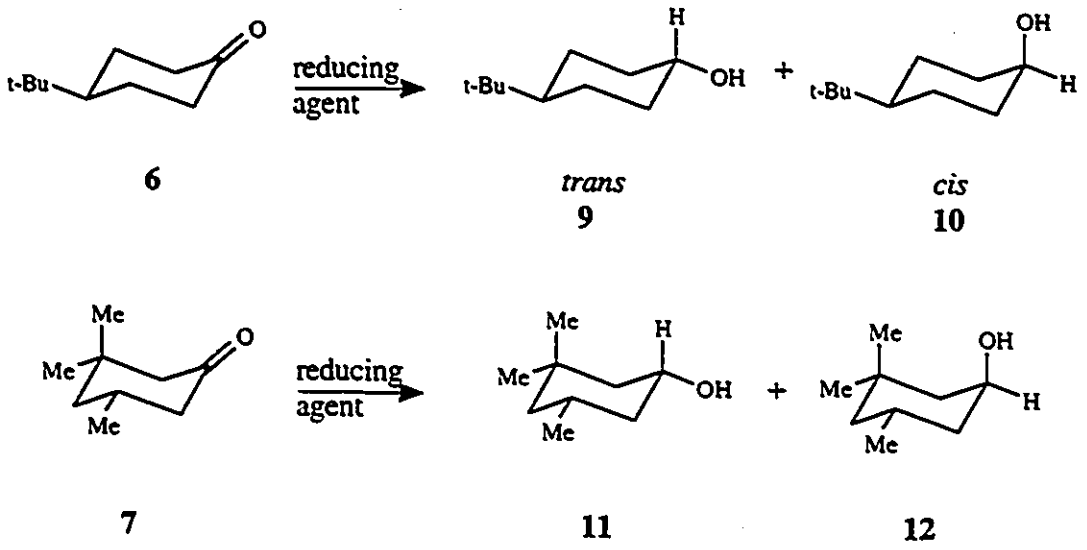

Figure 1.7 Stereochemistry for the reduction of 4-*t*-butylcyclohexanone and 3,3,5-trimethylcyclohexanone.

In order to explain the success of this rule and hence the results shown in Table 1.2, Dauben *et al.* introduced in 1956 the concepts of product development and steric approach control.[35] These concepts were subsequently supported by Brown after the investigation of several cyclic and bicyclic ketones.[36] Steric approach control is operative when the reduction of cyclohexanone derivatives occurs with a bulky reducing agent. Under these circumstances, the product ratio (e.g. **9**:**10** in Figure 1.7) is determined by the ease of approach of the nucleophile; thus, equatorial attack will predominate to afford mainly the axial alcohol (e.g. **10** in Figure 1.7). However, product development control is

operative for reductions involving simple metal hydrides, where the predominant product is the more stable equatorial alcohol (e.g. **9** in Figure 1.7).

The concept of steric approach control has never been questioned, however, the concept of product development control has not survived detailed scrutiny. For example, lithium aluminum hydride reductions are known to be highly exothermic and therefore according to the Hammond postulate[37] the transition state should be reactant-like for *both* hindered and unhindered cyclohexanones. For the reduction of 4-*t*-butylcyclohexanone (see **6a-c** in Table 1.2), **9** is formed in greater proportion (**9**:**10** = 10:1) than is found at equilibrium in *i*-PrOH (4:1) and in the more THF/Et_2O like solvent DME (2.4:1).[38] Eliel initially suggested that the difference in the experimental and thermodynamic ratios might be due to the fact that the alcohols are formed as lithium or aluminum complexes and not free alcohols.[38a] However, Eliel later questioned this explanation since he later found that the ratio of aluminum alkoxide derivatives of 4-t-butylcyclohexanone in THF was still significantly less (4.6:1) than the experimental 10:1 selectivity.[38b] The equilibrium data are inconsistent with Dauben's product development control hypothesis since the maximum ratio predicted should not exceed the thermodynamic ratio.[39] Lastly, based on competitive reduction studies of 4-*t*-butylcyclohexanone (**6**) and 3,3,5-trimethylcyclohexanone (**7**) and equilibrium studies on these ketones and their corresponding reduction products, Eliel concluded that the relative rate of equatorial attack for **6** versus **7** should be approximately 15-100:1 (i.e. the axial alcohol product **10** is significantly more stable than **12**) if product development control is operative. However, the opposite reactivity was observed with **7** being favoured by 1.1-1.7:1.[25]

1.3.2 Torsional Strain

In addition to rationalizing the observed stereoselectivities in acyclic systems (see Section 1.1), Felkin employed the same torsional strain model to explain the stereochemical course for the nucleophilic addition to cyclohexanone based substrates.[3b]

As in the case of the acyclic model, Felkin noted a serious deficiency in the Dauben model. Namely, it appeared very unlikely that there should be any fundamental difference between the factors which are responsible for the nucleophilic addition to acyclic or cyclic ketones. This realization led Felkin to propose a model which was based on the same assumptions as the acyclic system. However, the latter three assumptions are no longer necessary for a conformationally fixed substrate (e.g. **6**).

Unlike open-chain ketones, for nucleophilic attack of cyclohexanone derivatives, steric and torsional strain cannot be simultaneously minimized and thus, assuming there are no overriding dipolar influences, the most energetically favourable balance will be

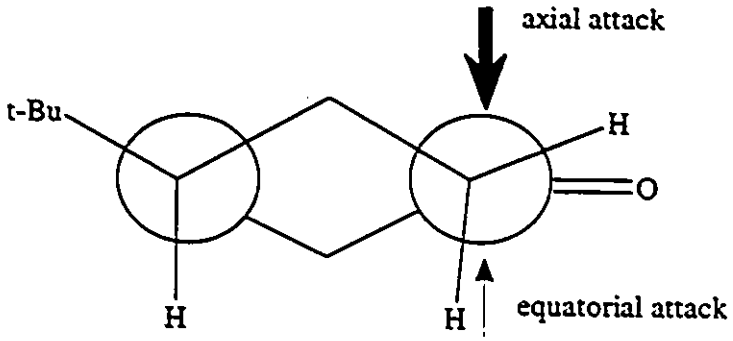

Figure 1.8 The Felkin model for 4-*t*-butylcyclohexanone.

followed. In the case of 4-*t*-butylcyclohexanone where the steric strain is relatively small (i.e. with axial protons substituted on C3 and C5), axial attack is favoured since it allows for the more staggered transition state as clearly shown in Figure 1.8. If the Bürgi-Dunitz trajectory is followed, both the steric strain in axial attack and the torsional strain in equatorial attack increases. Finally, in combination with Felkin's model and the app effect, Anh suggested that the more flattened the cyclohexanone ring, the more axial attack will occur.[13b] Since the antiperiplanarity between the incipient bond (C···Nu) and the adjacent sigma bond (C-H_{ax}) increases as the ring flattens, the greater will be the bias for axial attack (see Figure 1.9). If the ring puckers, this app stabilization is diminished and thus

more equatorial attack will occur. Anh assumed that the diminishment in axial attack is a result of a decrease in axial attack and not a result of an increase in equatorial attack. More precisely, because of poor orbital overlap the weak app interactions between the incipient bond, C···Nu, and the C2-C3/C5-C6 σ^* orbitals in equatorial attack are not considered.

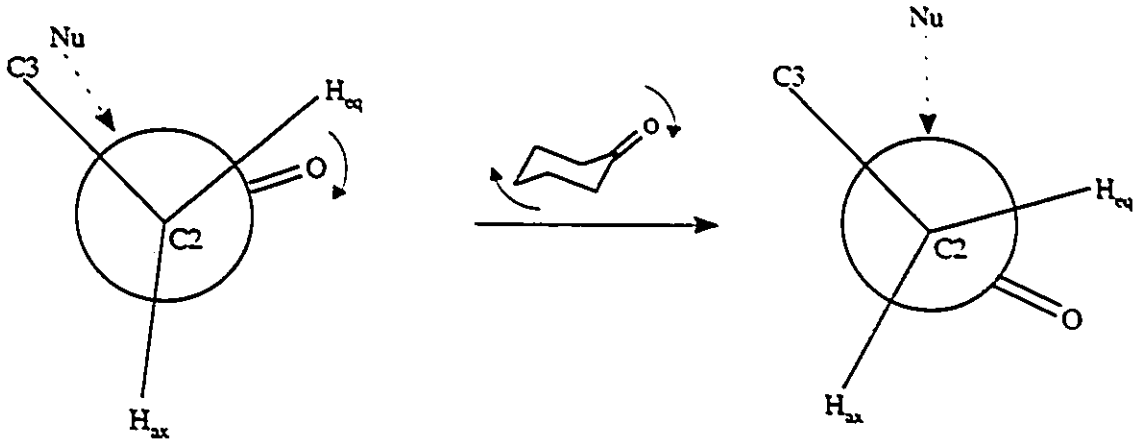

Figure 1.9 Anh's flattening rule.

1.3.3 Cieplak's Model

In order to explain the general phenomenon that nucleophiles attack mainly axially in unhindered cyclohexanone derivatives, Cieplak in 1981, like Anh, employed transition state hyperconjugation.[40] However, in Cieplak's model he assumes that the transition state of nucleophilic attack of cyclohexanones is stabilized by electron donation from the two types of app σ orbitals into the $\sigma^{*}_{C\cdots Nu}$ antibonding orbital, a low-lying vacant orbital of the forming bond. Therefore according to this model, nucleophilic attack should occur app to the best electron donating σ bond and the greater the difference in app electron donating ability, the greater the stereoselectivity should be. It should be stated, however, that the Cieplak proposal allows for only a qualitative estimation of the π-facial selectivity and the proposal considers only the two app interactions in axial and equatorial attack, but

ignores the two synclinal (sc) interactions with the C-H_{eq} bonds for axial and equatorial attack.

Cieplak objected to Anh's premise that the app orbital interaction with the C2-C3 and C5-C6 bonds for equatorial attack can be ignored since they only provide poor antiperiplanarity. Accordingly, in the transition state for axial addition, there are two app sigma bonds (C2-R_{ax} and C6-R_{ax}), while in the transition state for equatorial addition there are two app C-C bonds (i.e. C2-C3 and C5-C6). Cieplak assumes that the electron donating ability of some common σ bonds is C-S>C-H>C-C>C-N>C-O~C-Cl. Hence, for 4-*t*-butylcyclohexanone, Cieplak's theory predicts, as experimentally observed, that axial attack should be predominant since ΔE for axial attack is less than ΔE for equatorial attack (see Figure 1.10). It follows that as the electron donating ability of the C-R_{ax} increases or

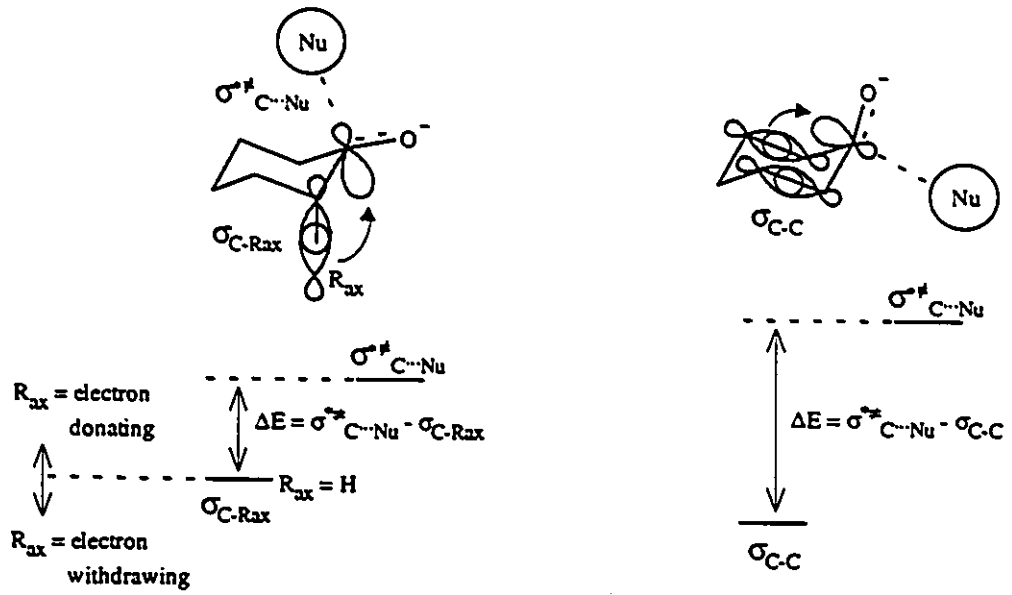

Figure 1.10 The Cieplak model for the nucleophilic addition to cyclohexanones.

the electron donating ability of the C2-C3 bond decreases, the proportion of axial attack will increase. In addition to the nucleophilic attack of cyclohexanones and other ketones, the Cieplak proposal has been used to rationalize the π-facial selectivity in many other

reactions including the electrophilic addition to exocyclic alkenes[40b,41], thermo- and photoaddition reactions[41a,42], the capture of radical intermediates[43], the nucleophilic capture of intermediate carbocations[44], sulphur oxidation[45], olefin-metal complexations[46] and sigmatropic rearrangements[41a,47].

Finally, as previously stated, in order for the Cieplak theory to be successful in rationalizing the unexpected large preference (10:1) for axial approach to unhindered cylohexanones[33], Cieplak assumes that a C-H sigma bond is a much better electron donor than a C-C sigma bond. However, there has been significant controversy as to the validity of this assumption with evidence favouring both C-C>C-H[48] and C-H>C-C[49].

1.4 Recent Theoretical Calculations

Ab initio calculations by Houk *et al.* on the reduction of cyclohexanone (**13**), 1,3-dithian-5-one (**14**) and 1,3-dioxan-5-one (**15**) with LiH indicated that torsional (see Section 1.3.2) and electrostatic factors (for cyclohexanones bearing polar substituents) and not orbital hyperconjugative interactions involving the C-C, C-H, C-O or C-S bonds as proposed by Anh[13] or Cieplak[40] were chiefly responsible for determining the preferred stereochemistry of attack.[48d,50] This conclusion was based on the fact that no significant bond length changes in **13**, **14** or **15** were found in the calculated axial and equatorial transition states.

13

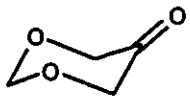

14

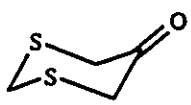

15

The calculations on the ground state conformation showed the ring to be flat for **14** and puckered for **15** relative to cyclohexanone. Subsequent transition state calculations revealed, as predicted by Anh[13b], the flatter the ring the greater the proportion

of axial attack occurred since it allowed for both the minimization of torsional and ring strain. For **15**, axial attack introduces severe ring strain and thus, again as predicted by Anh[13b], equatorial attack is dominant. For the cyclohexanone and LiH reaction, the calculations gave a near perfect staggered transition state for axial attack. However under equatorial attack, the transition state contains partial eclipsing between the nucleophile and the axial bond at C2, while simultaneously introducing some ring strain. Houk and coworkers concluded that if equatorial attack were to occur with an ideal staggered transition state, too much ring strain would be introduced and thus an energetic balance between these two types of strain is followed. *Ab initio* calculations by Coxon on the reduction of cyclohexanone with AlH_3 yielded similar results.[51]

In 1993, Boyd performed *ab initio* calculations on the transition state for the LiH reduction of cyclohexanone, 4-fluorocyclohexanone and 4-chlorocyclohexanone.[52] The results showed that the Cieplak theory failed on two fronts. Firstly, the electron density of the C2-H_{ax} bond in the 4-substituted compounds is greatest when the 4-substituent is axially oriented. Therefore the observed increase in axial attack for 4-axial substituents (see Section 1.5.7) should be a result of a stabilization of the axial transition state, but the calculations show the increase to be a result of an increase in the barrier for equatorial attack. Secondly, the electron density of the C2-C3 bonds in both 4-axial and 4-equatorial substituted cylohexanones are very similar and thus the barrier for equatorial attack should be similar; however, the calculations reveal a substantial difference.

1.5 Recent Experimental Investigations

In contrast to acyclic ketones, the conformation in the transition state can be relatively fixed in cyclic ketones, except perhaps for simple rings, and thus these substrates provide useful models for investigating the validity of the various aforementioned theories (see Section 1.3).[53] The vast majority of investigations have thus far been carried out by studying the π-facial selectivity of cyclic ketones bearing a range of substituents from

strongly electron donating to strongly electron withdrawing. As a result of the experimental results, a number of conclusions were drawn with some supporting the Cieplak explanation while others supported the torsional strain proposal of Felkin, dipolar effects or a balance thereof.

1.5.1 π-Facial Selectivity Study of le Noble

In 1986, le Noble first recognized that if one assumed that 5,7-disubstituted 2-adamantanones[§] **16a-m** are symmetric[#], a model ketone will be available to probe the factors responsible for π-facial selectivity.[44c] Under this symmetric assumption, steric effects can be omitted from the list of possible factors and thus an assessment of the remaining proposed factors (i.e. Cieplak, Anh or dipolar effects) by varying the electron donating and withdrawing ability of the four adjacent C-C bonds (i.e. C1-C8, C1-C9, C3-C4 and C3-C10) is possible.

In addition to the study on the $NaBH_4$ reduction of **16a-m**, le Noble investigated the π-facial selectivity of 5-azaadamantan-2-one-N-oxide (**17a**), 5,7-diazaadamantan-2-one-N-oxide (**17b**) and the perfluorinated derivatives **18a-b** (see Table 1.3). Again, compounds **17a-b** and **18a-b** were assumed to be free from distortion.[54] An additional advantage of these adamantanone derivatives is that they avoid the controversial problem of comparing C-H versus C-C sigma bond donating ability present in cyclohexanone based substrates.

le Noble interpreted the results for ketones **16** and **17** in terms of Cieplak's theory, which was later supported by a semiquantitative model by Mehta[56], since the attack of the complex metal hydride occurs preferentially *syn* to the C5 substituent in **16** and N5 in **17**

---

§ le Noble employed the adamantane skeleton for numbering atoms rather than using the system recommended by IUPAC.

Obviously, this assumption is not necessary for the symmetric 2-adamantanone **16g**.

Table 1.3 Attack ratios of *syn*:*anti* approach for the reduction of 16-18 by $NaBH_4$.

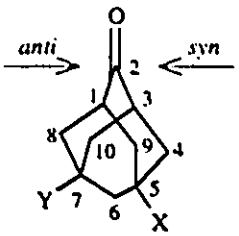

16

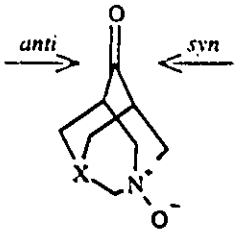

17

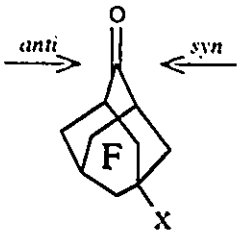

18

Compound	MeOH, 0°C	*i*-PrOH, 0°C	*i*-PrOH, rt	ref.
16a X = CF_3, Y = H		59 *syn*:41 *anti*		44c
b X = CO_2Me, Y = H	61 *syn*:39 *anti*			55a
c X = F, Y = H	59-62:38-41	58:42	62 *syn*:38 *anti*	44c, 55b
d X = Cl, Y = H	62-67:33-38	57:43	59:41	44c, 55b
e X = Br, Y = H	59:41			44c
f X = OH, Y = H	57:43			44c
g X = H, Y = H	50:50			44c
h X = *t*-Bu, Y = H	50:50[a]			44c
i X = $SiMe_3$, Y = H	49:51		45:55	55b,c
j X = $SnMe_3$, Y = H	47:53		43.5:56.5	55b,c
k X = *p*-$C_6H_4NO_2$, Y = C_6H_5			57:43	44a
l X = *p*- $C_6H_4NH_2$, Y = C_6H_5			44:56	44a
m X = *p*-$C_6H_4NO_2$, Y = *p*-$C_6H_4NH_2$			62:38	44a
17a X = CH		96:4[b]		55d
b X = N	88:12[c]			55e
18a X = H	58:42[d]			55f
b X = Cl	55:45[d]			55f

[a] $LiAlH_4$, rt. [b] Temperature not specified. [c] In D_2O at pH 13, rt. [d] $LiBH_4$ in Et_2O, 0°C.

with the greatest selectivity occurring for the strongest electron withdrawing N-oxide substituent in **17a**. In other words, as stated in Cieplak's model, the nucleophile attacks preferentially from the face app to the more electron rich C-C bond since this allows for the greater transition state stabilization (i.e. $\sigma_{C\text{-}C}$ electron donation into $\sigma^*_{C\text{-}Nu}$). le Noble rationalized the decrease in selectivity in **17b** as a result of partial transfer of the positive charge on the quaternary N5 to the neutral N7. Thus the difference in donating ability of the two pairs of carbon-carbon bonds is diminished which, in turn, reduces the stereoselectivity. For ketones **18a** and **18b**, the results in Table 1.3 reveal that, unlike **16** and **17**, the reduction with sodium borohydride exhibits a marginal selectivity with attack occurring app to the more electron deficient C-C sigma bond as predicted by Anh's transition state stabilization model. le Noble made the rather contradictory conclusion "that, under these unusual circumstances, the electron demand by the vicinal bonds is greater than that of the incipient and that Anh hyperconjugation accordingly becomes dominant".[55f]

Ab initio methods (3-21G* level) have provided evidence that the reduction of **16g** and **17a** with alane (AlH_3) show bond length changes in a four-centre transition state which are consistent with Anh's hyperconjugative stabilization.[57] However, these conclusions are based on <2% differences in bond lengths. Gung and Wolf have also performed *ab initio* calculations (6-31G* level) on **16g** and **17a** and showed that these ketones have distorted structures and thus refutes le Noble's symmetric claim.[58] However, again, the conclusions were based on <3.4° deviations in the torsional angles from that of adamantanone.

1.5.2 Cieplak and Johnson's Investigation of π-Facial Selectivity

Several years after the appearance of his initial model, Cieplak *et al.* in 1989 investigated the nucleophilic attack of 3-substituted cyclohexanones.[40b] Cieplak and Johnson assumed that under the conditions in which the experiments were performed (i.e.

at -78°C), the addition occurs through only the equatorial conformer. The goal of this study was to test and to determine the generality of the initial concepts developed in Cieplak's original paper. The results of their study are given in Table 1.4.

Cieplak and Johnson concluded that the data shown in Table 1.4 are consistent with the Cieplak hyperconjugative effect. More specifically, as the electron withdrawing ability of R increases, the electron donating ability of the C2-C3 bond decreases which enhances the difference between $\sigma_{C\text{-}C}$ and $\sigma^{*}_{C\text{-}Nu}$ and thus increases the activation energy for equatorial attack. The net result is an increase in axial attack.

Table 1.4 Percent axial (*syn*) attack in the nucleophilic addition to 3-substituted cyclohexanones.

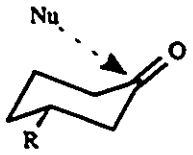	CH_3Li/Et_2O	$Li_2(CH_3)_3Cu/Et_2O$	CH_3Li/THF
R = TMS	15	2	22
R = *t*-Bu	19	3	27
R = H	21	6	
R = *p*-$OMeC_6H_4$	24	8	30
R = *p* - MeC_6H_4	23	8	30
R = C_6H_5	25	7	30
R = *p*-$CF_3C_6H_4$	28	10	36
R = C_6H_5	34	21	50
R = CF_3	50	42	58

1.5.3 Halterman's Examination of π-Facial Selectivity

In order to elucidate the factor or factors responsible for π-facial selectivity, Halterman and McEvoy in 1990 chose to study the sodium borohydride reduction of the 2,2-diphenylcyclopentanones **19a-e** (see Table 1.5).[59] The assumption, again, was made

Table 1.5 Diastereoselectivity for the reduction of cyclopentanones 19a-f.

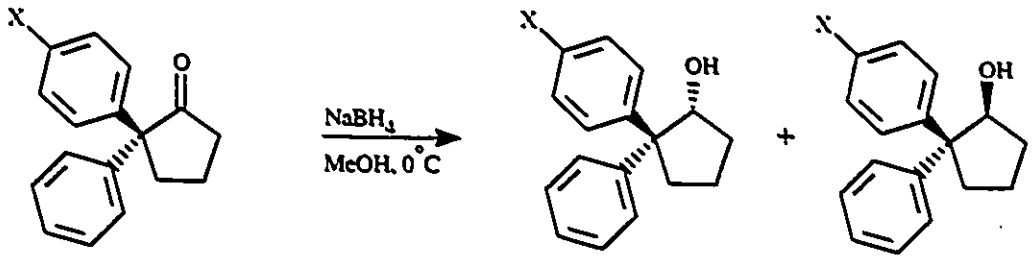

19	20 (*syn* attack)	21 (*anti* attack)
a X = NO_2	21	79
b X = Cl	37	63
c X = Br	37	63
d X = OCH_3	57	43
e X = OH	70	30
f X = NH_2	64	36

that the reduction occurs with a negligible amount of steric bias since the phenyl groups are approximately isosteric. In addition, Halterman thought it advantageous that the electronically tunable phenyl groups, which avoid the C-H versus C-C question, were located directly adjacent to the carbonyl group rather than several bonds removed.

The results in Table 1.5 prompted Halterman to infer that under his system the nucleophilic addition is governed by the Cieplak effect with attack occurring

predominantly app to the more electron rich p-XC_6H_4-C2 bond. The reductions were also carried out with $LiBH_4$ in THF and the same ratios of **20:21**, within 3%, were obtained. Although not explicitly stated in Halterman's paper, the lack of a solvent effect is presumably inconsistent with electrostatic control since reaction in the less polar THF solvent might enhance any dipolar effects.

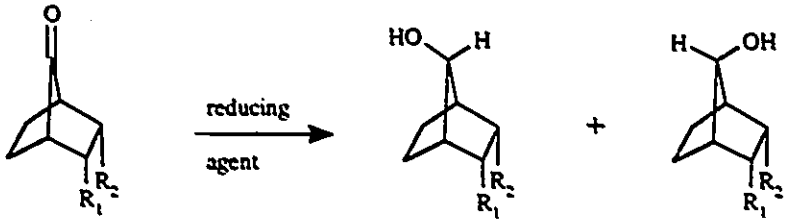

22a $R_1 = R_2 = CO_2CH_3$
22b $R_1 = R_2 = CH_2OCH_3$
22c $R_1 = R_2$ = vinyl
22d R_1 = vinyl, R_2 = ethyl
22e $R_1 = R_2$ = ethyl

23a-e (*syn* attack)

24a-e (*anti* attack)

Table 1.6 Experimental attack ratios for the nucleophilic addition to 7-norbornanones 22a-e.[a]

Compound	*syn*:*anti* (at ~0-10°C)		
	$NaBH_4$[b]	$LiAlH_4$[c]	$LiAl(O\text{-}t\text{-}Bu)_3H$[c]
22a	84:16	87:13	77:23
22b	40:60		
22c	36:64	35:65	34:66
22d	25:75		
22e	20:80	21:79	29:71

[a] Reference 59a. [b] In MeOH. [c] In Et_2O.

1.5.4 π-Facial Selectivity Study of Mehta

In Mehta's study into the origin of π-facial selectivity in the nucleophilic addition to the carbonyl group, he employed the bicyclic ketones 7-norbornanone (**22**) and 7-norbornenone (**25**).[60] As in the work of le Noble[44c,55] and Halterman[59], Mehta assumed that his model ketones were sterically unbiased and thus the reduction of **22** and **25** should be controlled by electronic effects. The results for the 7-norbornanone system are given in Table 1.6.

Initially the results for **22** were explained using Cieplak's model in which the nucleophile is biased towards attack app to the most electron donating C-C bond. However, subsequent calculations by Mehta[56] and Houk[61] revealed that the electrostatic effect is dominant (see Section 1.5.7).

Table 1.7 Experimental attack ratios (*syn*:*anti*, 27:28) for the reduction of ketones 26a-f.

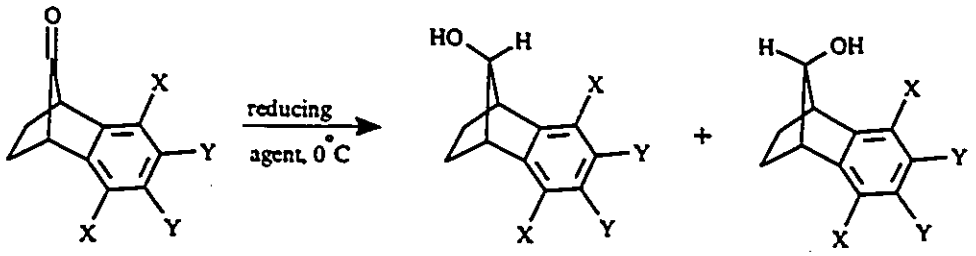

26a-f **27a-f** (*syn* attack) **28a-f** (*anti* attack)

	$LiAlH_4$ in THF	$LiAlH_4$ in Et_2O	$NaBH_4$ in EtOH
26a X = Y = F	100:0	100:0	100:0
b X = Y = Cl	92:8	95:5	95:5
c X = Y = H	62:38	81:19	81:19
d X = OMe, Y=H	45:55	79:21	79:21
e X = H, Y = OMe	51:49	64:36	81:19
f X = OMe, Y = OMe	59:41	78:22	89:11

1.5.5 Okada's Examination of π-Facial Selectivity

The stereochemistry in the metal hydride reduction of a number of substituted 1,2,3,4-tetrahydro-1,4-methanonaphthalen-9-ones (9-benzonorbornenones) was studied by Okada and coworkers.[62] The results of his investigation are shown in Table 1.7. Okada concluded that the data were in agreement with the Cieplak transition state stabilization model. This conclusion was later supported by Mehta's semiquantitative model[56] and based on the assumption that the observed changes in diastereoselectivity could not be a result of steric bias.

1.5.6 Wipf's Study of π-Facial Selectivity

During the course of their research on the total synthesis of the antitumor antibiotic aranorosin[63], Wipf and Kim observed an unexpectedly large diastereoselectivity in the 1,2-addition of the organometallic nucleophile $BnOCH_2Li$ to the 4,4-disubstituted dienone **31**. This observation prompted Wipf and Kim to conduct a thorough investigation of such a system with the hope of providing definitive experimental evidence as to factors responsible for the selectivity.[64] The results of Wipf's study are summarized in Table 1.8.

The data given in Table 1.8 show a large range in selectivity, despite seemingly modest structural changes, with the percentage of *syn* attack ranging from 3 to 50. In every case, except dienone **37**, the nucleophile attacked *anti* to the OR group preferentially. Wipf concluded that the results were in agreement with both Cieplak's and Anh's models since, in the case of Anh's model, the selectivity showed a general increase as the electron withdrawing ability increased (i.e. from 4-alkoxy to 4-acyloxy). In the case of Cieplak's model, Wipf considered as an alternative a "vinylogous Cieplak effect" in which "the stabilization of the transition state (occurs) by hyperconjugation of the newly formed σ^* bond by the σ-orbital of the 4-alkyl substituent via a σ-π^*-σ^* interaction"[64] (see

Figure 1.11). However, the Anh and Cieplak theories do not readily explain the large range in selectivity observed for, again, what appears to be subtle structural modifications.

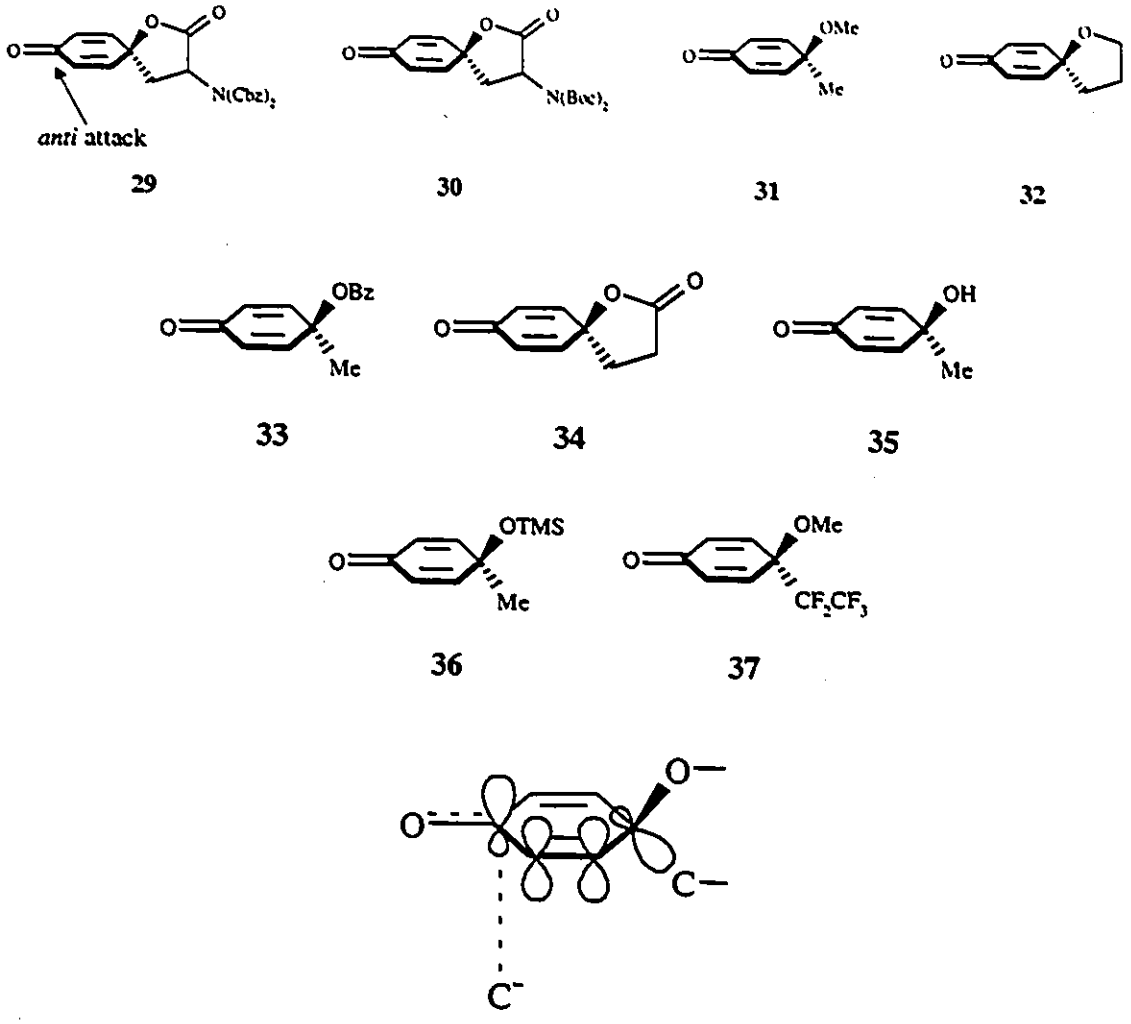

Figure 1.11 Representation of Wipf's proposed "vinylogous Cieplak effect".

These facts prompted Wipf and Kim to postulate that this dienone system is under electrostatic control since the calculated dipole moments showed a direct correlation with ln *anti/syn*. As a test of this theory, Wipf synthesized dienone **37** and reacted it with methyllithium. As predicted by the dipolar model and contrary to the Anh or Cieplak model, a 5:1 preference for *syn* attack was obtained.

Table 1.8 Summary of Wipf's results on the nucleophilic addition to dienones 29-37.

Compound	Nucleophile (exptl. conditions)	Selectivity *syn*:*anti* attack
29	$BnOCH_2Li$ (THF, -100°C)	17:83
30	MeMgBr (THF, -78°C)	14:86
31	MeMgBr (THF, -78°C)	17:83
31	$NaBH_4$ (MeOH, -35°C)	50:50
31	$LiAlH_4$ (Et_2O, -78°C)	50:50
31	HC≡CMgBr (THF, 0°C)	50:50
31	$H_9C_4C{\equiv}CLi$ (THF, 0°C)	48:52
31	PhMgBr (THF, -78°C)	22:78
31	MeLi (THF, -78°C)	32:68
31	MeLi (Et_2O, -78°C)	23:77
31	$BnOCH_2Li$ (THF, -78°C)	25:75
32	MeMgBr (THF, -78°C)	10:90
33	MeMgBr (THF, -78°C)	9:91
34	MeMgBr (THF, -78°C)	3:97
35	MeMgBr (THF, -78°C)	11:89
36	MeMgBr (THF, -78°C)	5:95
37	MeLi (THF, -78°C)	83:17

1.5.7 Houk's Study of π-Facial Selectivity

In order to allow for a critical assessment of the various theoretical explanations put forward to account for the bias towards axial attack in unhindered cyclohexanones, Houk conducted a study on the sodium borohydride reduction of a series of 4-substituted

trans-decalones.[48d] The resultant selectivities (see Table 1.9) were opposite to that predicted by Cieplak since if one assumes that electronegative equatorial substituents on C4 interact more strongly with the C2-C3 and C9-C10 bonds than do the axial substituents, then the electron donating ability of the C2-C3/C9-C10 bonds will be reduced. This decrease will, it turn, reduce the amount of equatorial attack. In other words, according to Cieplak and not supported by the data in Table 1.9, electron withdrawing equatorial substituents at C4 should increase the amount of axial attack and axial substituents should have a marginal influence on diastereoselectivity relative to the parent *trans*-decalone **38a**.

Houk reasoned that, in addition to torsional and steric effects, dipolar effects were deemed to play a critical role on the stereoselectivity. Therefore, as observed, electron

Table 1.9 Diastereoselectivities for the reduction of *trans*-decalones 46a-i.

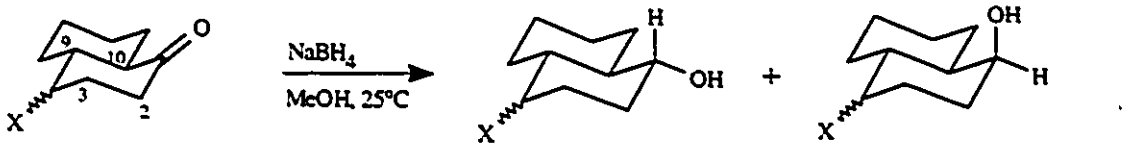

		axial addition	equatorial addition
38a	X = H	60	40
b	X = OH(eq)	61	39
c	X = OAc(eq)	71	29
d	X = Br(eq)	66	34
e	X = Cl(eq)	71	29
f	X = OH(ax)	85	15
g	X = OAc(ax)	83	17
h	X = Cl(ax)	88	12
i	X = F(ax)	87	13

withdrawing equatorial substituents should have a small influence on the diastereoselectivity, whereas axial substituents should have a significant influence. For 4-axial electron withdrawing substituents, equatorial attack is destabilized by an electrostatic repulsive interaction (**39**) whereas axial attack is favoured by the stabilizing antiparallel orientation of dipoles depicted in **40**. *Ab initio* methods in the same paper and a subsequent charge density study by Boyd[52] further supported the importance of the dipolar effect in the 4-substituted cyclohexanone system. Houk also used the dipolar model to provide an alternative rationalization for the results obtained by Cieplak[50b], Halterman[59],

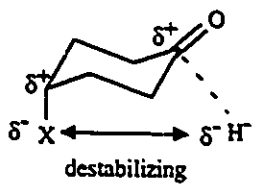

39

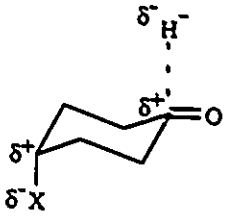

40

Mehta[60] and Okada[62]. For example, in Mehta's study of 2,3-endo,endo-disubstituted 7-norbornanones, it was found that as the electron withdrawing ability of the substituents in

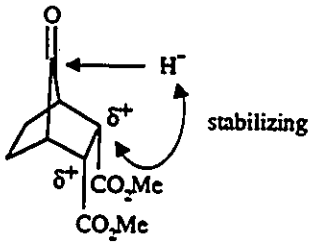

41

22 increased, the proportion of nucleophiles that attacked *syn* to these substituents to afford the **23** alcohols increased.[60] The electron withdrawing substituents induces a partial positive charge at C1 and C2, which as shown in **41** stabilizes nucleophilic addition *syn* to

these substituents. Although not stated in Houk's paper, this model can also be used to explain the results of le Noble's adamantanone study. Indeed, in 1994 Adcock *et al.* conducted a ^{13}C NMR study of various 5-substituted adamantanones and showed the substituent chemical shifts to be proportional to substituent field effects. As a result, Adcock and coworkers concluded that the nucleophilic addition to this system is governed mainly by electrostatic effects.[65]

In addition to the research of Houk[48d] and Wipf[64], earlier studies supported the importance of electrostatic effects. More specifically, Kwart found in 1962 that the ratios of reduction for various 4-substituted cyclohexanones with $NaBH_4$ in *i*-PrOH at O°C obeyed a linear free energy relationship (i.e. log k vs. σ_I) and thus indicated that the rates of reduction are governed by dipolar effects.[66] The fact that the amount of *cis* product produced increased as the electron withdrawing ability of the 4-substituent increased signified that this effect is predominantly occurring through the solvent medium (i.e. a field effect). In other words, although the number and type of bonds between the substituent X and the reaction centres are identical for the two transition states leading to the *cis* and *trans* alcohol products, the diastereoselectivity exhibits a stereochemical dependence and thus the dipolar effect is primarily a field effect as compared to a through bond effect. In Kwart's explanation he assumed that the reaction is occurring via a late transition state resembling the product. Under these circumstances, the transition state 42 leading to the

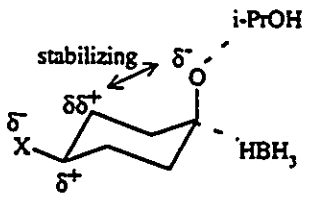

42

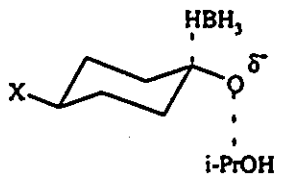

43

cis alcohol experiences an electrostatic stabilizing interaction whereas no such interaction exists in transition state **43**. Interestingly, these results are the opposite obtained by Houk and coworkers[48d] for their sodium borohydride reduction of the *trans*-decalones **38a-e**. Perhaps, the reduction in Kwart's mobile system is occurring through a twist boat conformation.

Chapter 2 Syntheses of 5,7-dihydro-1,11-dimethyl-6*H*-dibenzo[a,c]cyclohepten-6-one and its α-methyl, -methylthio, -methoxy, -chloro and -fluoro Derivatives

2.1 Introduction

The bridged biaryl ketone 5,7-dihydro-1,11-dimethyl-6*H*-dibenzo[a,c]cyclohepten-6-one, **44**, was originally synthesized by Mislow and coworkers in 1962.[67] Ketone **44** (R = H) is a chiral derivative of biphenyl which Mislow concluded on the basis of molecular models to possess a single "rigid" conformation with the two aromatic rings being approximately 60° to one another.[#] Mislow's observations were later supported by ^{1}H NMR which revealed two pairs of nonequivalent (i.e. diastereotopic) α protons. Further support of the resistance of the bridged biaryl ketone **44** to undergo conformational change was obtained in 1963 by Mislow who reported a 36 kcal/mol barrier to racemization (i.e. $\Delta G^{\ddagger}$).[68] The origin of this high energy barrier to inversion is mainly a result of the steric strain between the two *ortho* methyl groups at C7 and C10 present in the planar transition state. In the absence of these two *ortho* methyl groups (i.e. ketone **54**), the barrier to racemization decreases dramatically to approximately 14 kcal/mol.[69]

As a result of the C_2 axis which bisects the central seven-membered ring along the carbonyl double bond, two equivalent methylene groups exist α to the carbonyl group in **44**. Each hydrogen in the methylene group adopts two possible orientations which, due to the similarity to the α positions in cyclohexanone, are termed quasi-axial and quasi-equatorial (see Figure 2.1).[*]

[#] The conformational properties and the degree of rigidity present in ketone **44** and its α-subsituted derivatives will be the focus of discussion in Chapter 3 of this thesis.

[*] In order to avoid using subscripts in numbering the carbon atoms in compounds **44-53**, the IUPAC system has been altered to that shown on the left in Figure 2.1.

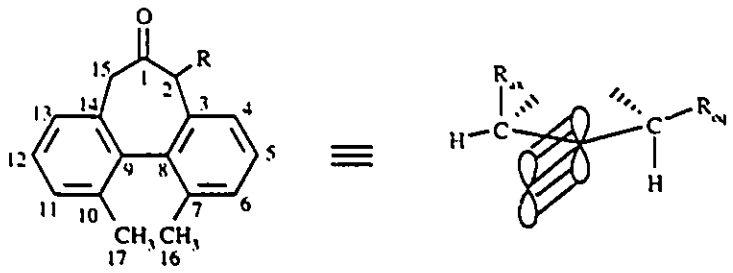

44	$R_{ax} = R_{eq} = H$	**49**	$R_{ax} = H, R_{eq} = CH_3$
45	$R_{ax} = CH_3, R_{eq} = H$	**50**	$R_{ax} = H, R_{eq} = SCH_3$
46	$R_{ax} = SCH_3, R_{eq} = H$	**51**	$R_{ax} = H, R_{eq} = OCH_3$
47	$R_{ax} = OCH_3, R_{eq} = H$	**52**	$R_{ax} = H, R_{eq} = Cl$
48	$R_{ax} = Cl, R_{eq} = H$	**53**	$R_{ax} = H, R_{eq} = F$

Figure 2.1 Structural and three-dimensional representation of 44 -53.

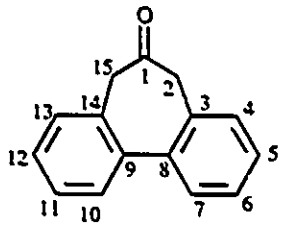

54

Cyclohexanone exhibits only a 4.0±0.1 kcal/mol free energy of activation ($\Delta G^{\ddagger}$) barrier to chair inversion (see equation [1], R = H).[70] Thus, in order to achieve a homogeneous conformational model, a 4-*t*-butyl substituent was normally employed,

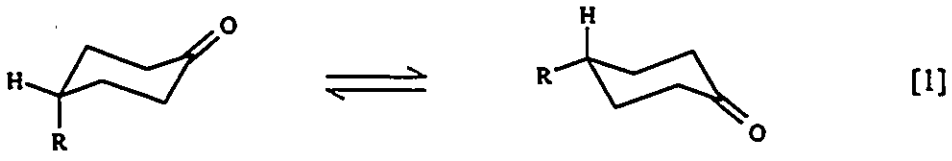

55 **56** [1]

whose energetic preference (i.e. A value) for the equatorial conformer **56** (R = *t*-butyl) is 4.9 kcal/mol.[71] However the conformational rigidity of the 4-*t*-butylcyclohexanone model

is suspect. The twist boat, C_1 and C_s boat conformations (see Figure 2.2) are only according to Allinger's MM3 calculations 3.09, 3.52 and 4.11 kcal/mol, respectively, less

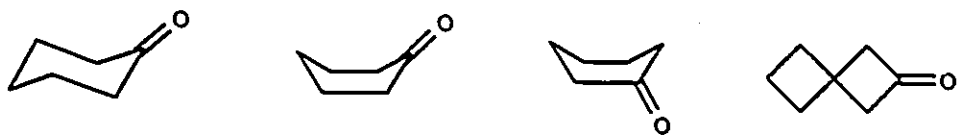

Chair C_s Boat C_1 Boat Twist Boat

Figure 2.2 Structural representation of the chair, C_s boat, C_1 boat and twist boat conformers of cyclohexanone.

stable than the chair conformation.[72] Therefore, the possibility exists that these less stable conformations may play a role in any stereochemical study employing cyclohexanones as model substrates.

The bridged biaryl ketones **44** and several of its α-substituted derivatives have been utilized in two stereochemical studies since it alleviated many of the above noted concerns present in the text-book model cyclohexanone. Firstly, ketone **44** has been used in a base catalyzed hydrogen-deuterium exchange reaction of the α quasi-axial and quasi-equatorial protons.[73] Fraser and Champagne reported an axial:equatorial rate ratio of 73:1. In contrast, 4-*t*-butylcyclohexanone showed a much lower 5:1 stereoselectivity[74] and thus reinforces Mislow's original conclusion. The preference for axial abstraction is thought to be a result of a stereoelectronic effect. That is, the C-H_{ax} sigma bond is better aligned with the carbonyl's π-system.[75] Overall, it would appear that our bridged biaryl ketone provides a model with both significantly greater inflexibility and no intermediate possible twist boat or boat conformations as present in cyclohexanone systems.

Secondly, Fraser measured the relative rates of acid catalyzed addition of $H_2{}^{18}O$ to the α-methyl, -methoxy and -chloro derivatives of **44** to investigate the app effect.[76] The study revealed a large rate retardation for antiperiplanar (app) attack to the axial methyl (Δ

$\Delta G^{\ddagger}$ = 2.3 kcal/mol) in ketone **45** and the axial chloro ($\Delta\Delta G^{\ddagger}$ = 2.8 kcal/mol) in ketone **48** relative to the unsubstituted ketone **44**. However, a negligibly small rate retardation was observed for attack app to an axial methoxy group ($\Delta\Delta G^{\ddagger}$ = 0.2 kcal/mol). Interestingly, the diaxial dimethyl derivative of **44** increased the change in the free energy of activation by only 0.4 kcal/mol (i.e. $\Delta\Delta G^{\ddagger}$ = 2.7 kcal/mol). If the assumption was made that steric effects were dominant, the data indicated that the value for the app effect (i.e. the Cieplak hyperconjugative effect) was only 0.4 and 0.7 kcal/mol for the axial methyl and chloro substituents, respectively, and a maximum of 0.2 kcal/mol for the axial methoxy substituent. Because of the assumptions associated with this conclusion and the viability of our bridged biaryl ketone as a stereochemical model, we were prompted to further probe both the mechanistic properties of reduction and the validity of the various proposed theoretical explanations (see Sections 1.1 and 1.3) that have gained widespread acceptance for predicting the preferred face of addition of nucleophiles to a carbonyl group. However, as in the ^{18}O isotopic exchange study and in contrast to most previous studies which have thus far investigated π-facial selectivity (see Section 1.5), we have chosen to measure the π-facial reactivity for the addition of lithium aluminum hydride, sodium borohydride and triethylsilane to our conformationally fixed model ketone **44** and its α-methyl, -methylthio, -methoxy, -chloro and -fluoro quasi-axial and quasi-equatorial derivatives **45-53**. Hydride was chosen as the nucleophile, since most, if not all, theories were based on the diastereoselectivity observed for this nucleophile. More specifically, we have chosen to measure the rate of addition of hydride to the two faces of the carbonyl group for our model ketone and its axial and equatorial α-substituted derivatives. The determination of π-facial reactivity provides a more definitive test of the aforementioned models than a study of π-facial selectivity, which only represents a ratio of the two diastereomeric products, since the reactivity is the actual cause of the observed diastereoselectivity. These substituents possess a wide range in induction and polarizability and hence would maximize the likelihood of observing either the Cieplak or

Anh effect. Finally, an additional advantage of our bridged biaryl ketone model is that there will be a minimal amount of direct steric interaction between the incoming hydride when approaching antiperiplanar (app) or anticlinal (ac) to the axial or equatorial α-substituents, respectively, and thus it is assumed that steric effects will not contribute to this π-facial reactivity.

2.2 Syntheses of the α-methyl, -methoxy and -chloro derivatives of 5,7-dihydro-1,11-dimethyl-6*H*-dibenzo[a,c]cyclohepten-6-one

The syntheses of ketones **45**, **47-49** and **51-52** (i.e. the axial and equatorial α-methyl, -methoxy and -chloro derivatives) were reported by Fraser and coworkers and were carried out accordingly.[76]

2.3 Syntheses of the α-methylthio derivatives of 5,7-dihydro-1,11-dimethyl-6*H*-dibenzo[a,c]cyclohepten-6-one

The axial compound **46** was prepared via reaction of the corresponding lithium enolate of **44** (generated with LHMDS) with the electrophile methyl methanethiolsulphonate ($CH_3SSO_2CH_3$)[77] to afford a 1.8:1 mixture of the axial:equatorial (i.e. **46:50**) ketones, unreacted starting ketone **44** and <10% of disubstituted SCH_3 products (see equation 2). Column chromatography afforded a mixture of the axial and the equatorial ketones which was induced to crystallize to yield pure **46** in 43% yield. Repeated attempts to isolate pure equatorial SCH_3 were unsuccessful; however, column

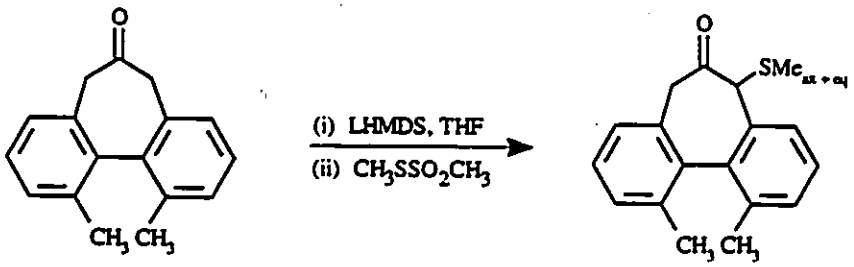

44 **46 + 50** (1.8:1) [2]

chromatography yielded enriched fractions that were subsequently used for our π-facial reactivity study (see Chapter 4). The purified equatorial SCH_3 samples were prepared by one of two methods. The first method involved the epimerization of **46** with sodium methoxide in acetonitrile to give a 2.4:1 (**46**:**50**) mixture. The second procedure involved collecting the mother liquor from the crystallization of **46** and subjecting it to further purification. In both instances the crude mixtures were purified by column chromatography to afford a **50**:**46** ratio of approximately 1:1 and 6:1, respectively. The resulting purified mixture of **46** and **50** was fully characterized by HRMS, ^1H and ^{13}C NMR spectroscopy and used for our π-facial reactivity study of **50** (see Chapter 4).

The configuration in ketone **46** was proven by X-ray analysis. The ORTEP plot for **46** and its corresponding X-ray data appear in Appendix 1 and clearly shows the axial methylthio geometry by the O1-C1-C2-S1 torsional angle of 93.2°. Consistent with the previously described α-methyl and -chloro derivatives of **44**[78,79], the torsional angle between the two aromatic rings is between 57.3 and 61.7°. Molecular mechanics calculations using the program PCMODEL[80] indicated that there exists three stable rotamers about the S-C2 bond as shown in Figure 2.3. The X-ray structure of **46** corresponds to structure **58** and thus the calculations are in acceptable agreement given the fact that they represent a system in the gas phase at a dielectric constant of 2.2. In addition to X-ray crystallography, the configuration of **46** was confirmed by NOE difference measurements. Irradiation of H2 (proton geminal to the SMe group) resulted in a 20% enhancement in the *ortho* proton H4 on the adjacent aromatic ring. The previous NOE results of Fraser *et al.*[76] indicated that only axially oriented α-substituted derivatives of **44** give an NOE and thus we concluded that the crystalline sample was indeed **46**.

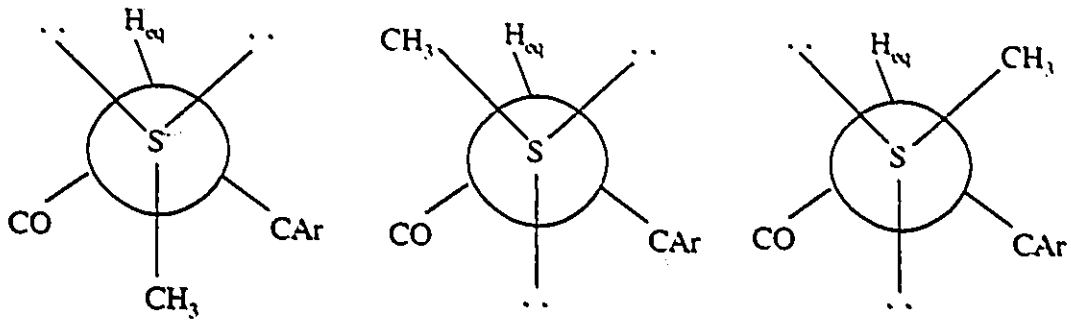

	57	58	59
E =	28.15	24.33	24.21

Figure 2.3 Molecular mechanics calculations of the three rotamers about the S-C2 bond for ketone 46 and their respective steric energies (E) in kcal/mol.

2.4 Synthesis of the Equatorial α-fluoro Derivative of 5,7-dihydro-1,11-dimethyl-6*H*-dibenzo[a,c]cyclohepten-6-one

The equatorial fluoro ketone **53** was prepared by treating the lithium enolate of **44** with N-fluorodibenzenesulphonamide.[81] The resulting crude reaction product showed, in addition to unreacted starting material and **53**, the presence of a minor (<5%) component (*vide infra*). Column chromatography afforded pure **53** in 46% yield (see equation 3).

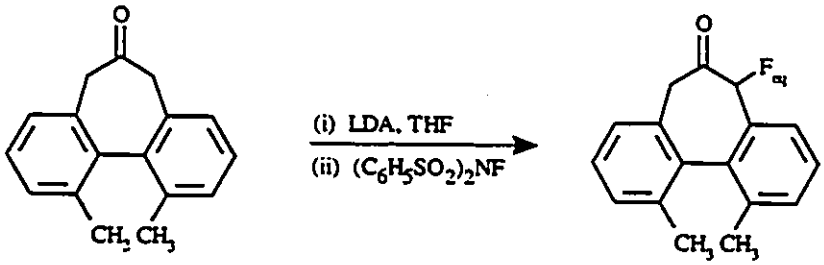

44 **53** [3]

The configuration of **53** was, again, confirmed by X-ray crystallography. Two crystallographically independent molecules **53a** and **53b** were found in the unit cell of **53**. The ORTEP plots and the X-ray data appear in Appendix 1. The torsional angles O1-C1-C2-F1 (-0.8°) and O2-C18-C19-F2 (0.9°) clearly show that the α-fluoro substituent

adopts an equatorial orientation. As in the crystal structure for **46**, the torsional angle about the benzene rings is 60±4°.

Finally, further evidence of the stereochemistry in our crystalline α-fluoro ketone **53** sample was provided by the 500 MHz ^{1}H NMR spectrum (see Figure 2.4). An expansion of the methylene protons on C15 is shown in the inset. In addition to the geminal coupling between these two protons ($^2J_{H15ax,H15eq}$ = 16.9 Hz), $H15_{eq}$ shows long range "W coupling" to the equatorial fluoro substituent ($^4J_{H15eq,Feq}$ = 3.3 Hz).[85] If the α-fluoro substituent adopted an axial geometry, the long range "W coupling" between $H15_{eq}$ and $H2_{eq}$ would not be observed as in the axial α-CH_3, -SCH_3, -OCH_3 or -Cl derivatives.

*Attempted Preparation of the Axial α-fluoro Derivative of **44***

It is well known that the conformational equilibrium of an α-halo substituted cyclohexanone is highly dependent on solvent (see equation 4).[82,83] For 2-fluorocyclohexanone in the nonpolar solvent cyclohexane, the equilibrium exhibits a slight preference for the equatorial conformer **61** with the equatorial:axial (X = F, **61**:**60**) ratio being 57:43. However, the equilibrium shown in equation 4 shifts to the right as the solvent polarity is increased. For example, in acetonitrile, the ratio increases to 87:13.[83,#] Thus, in order to maximize the proportion of the axial fluoro bridged biaryl

[4]

60 **61**

For a thorough discussion as to the cause of this shift in eq. 4 consult Chapter 3.

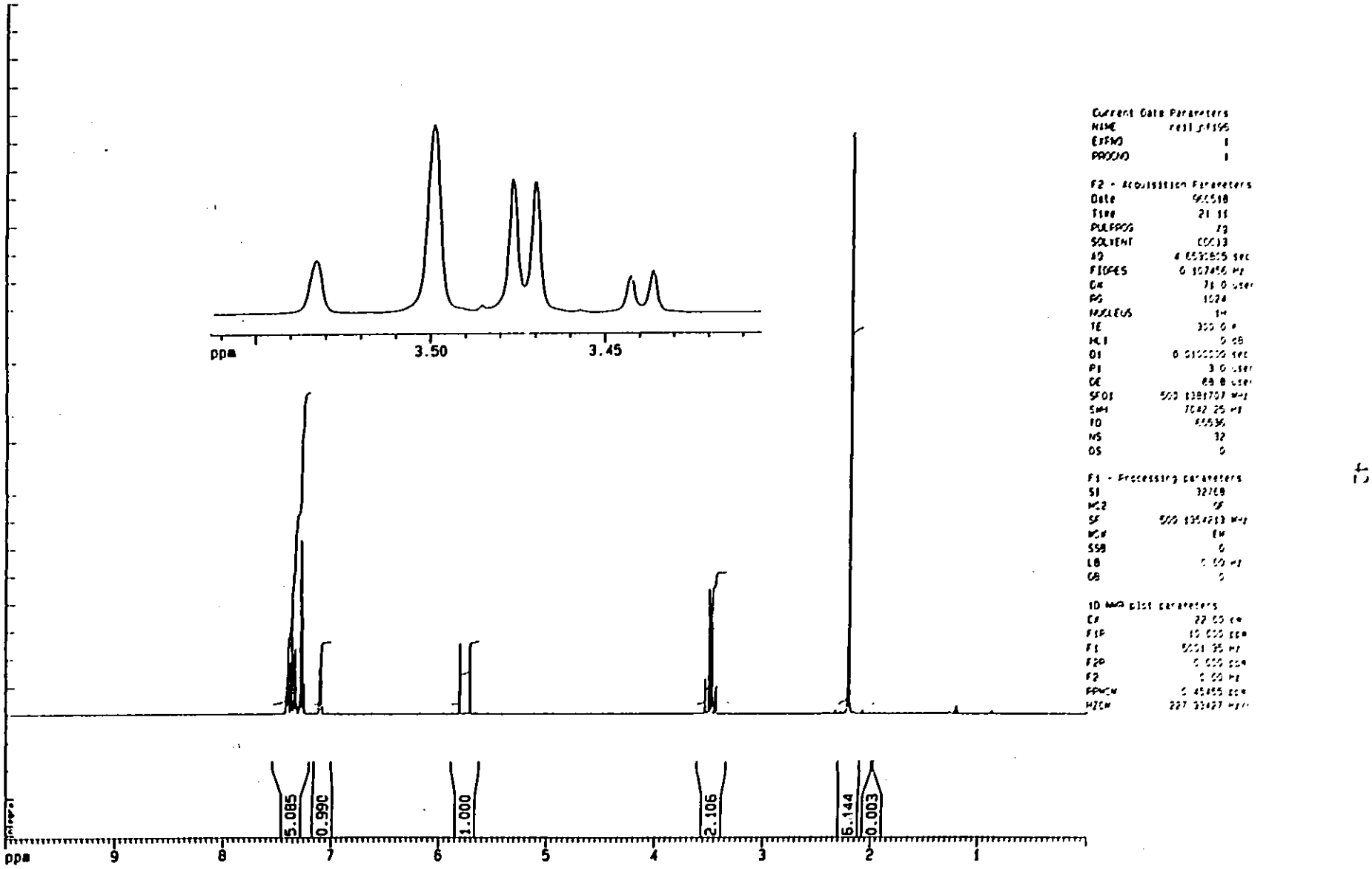

Figure 2.4 The 500 MHz ^{1}H NMR spectrum of 53 in $CDCl_3$. The inset shows an expansion of the methylene protons at C15 (δ 3.44-3.53).

ketone **62** at equilibrium, we undertook an epimerization study in nonpolar solvents. However, as shown in Table 2.1, a variety of both acid[84] and base catalyzed conditions afforded only unreacted **53** according to 200 MHz ^{1}H NMR.

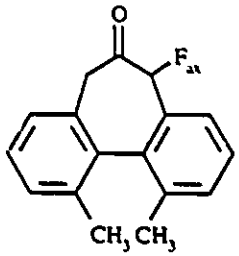

62

Table 2.1 Attempted epimerization of ketone 53.

Entry	Catalyst	Solvent	Time	Result[a]
1	HCl[b,c]	*p*-dioxane[c]	24 h	<5%
2	HCl[b,c]	benzene[c]	24 h	<5%
3	TFA	cyclohexane	16 h	<5%
4	LDA[d]	benzene[c]	24 h	<5%

[a] Percent epimerization. [b] Saturated HCl solution. [c] Anhydrous. [d] 0.1 equiv.

As previously mentioned, the reaction of N-fluorodibenzenesulphonamide with the lithium enolate of **44** produced, in addition to ketone **53**, an additional product in <5% yield. The 500 MHz ^{1}H NMR spectrum of the mother liquor after crystallization of **53** is shown in Figure 2.5. The expansion (Figure 2.5b) clearly shows the presence of an additional doublet of triplets centred at 5.72 ppm. In order to avoid the rather labour intensive process of isolating this minor component, tentative identification was carried out by simulating the ^{1}H NMR spectrum with the commercially available program PCPMR.[80] Because of the inherent preference for 2-fluorocyclohexanone to adopt the

equatorial conformation **61** (see Chapter 3) and the lack of any observable formation of **62** after epimerization of our bridged biaryl ketone **53**, we were led to believe that the minor component was the diequatorial difluoro ketone **63**. The initial parameters for this unusual A_2X_2 pattern were estimated from the literature and adjusted as necessary.[85] Employing the parameters gives in Table 2.2, we were able to reproduce the doublet of triplet pattern to within 0.1 Hz and thus the minor component appears to be **63** and not the required **62** (see Figure 2.5).

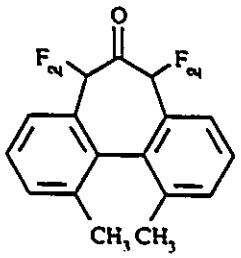

63

Lastly, as stated previously in the introduction (Section 2.1), the bridged biaryl ketone **44** possesses a high racemization barrier of 36 kcal/mol.[68] If, however, the *ortho* methyls are not present, the barrier drops to ~14 kcal/mol and thus an alternative route to epimerization is available via rotation about the C8-C9 bond. Accordingly, in order to

Table 2.2 Spin simulation spectral parameters.[a]

Chemical shifts (Hz from TMS): H1 9000, H15 9000, F1 -900, F15 -900
Coupling constants (Hz): $J_{H1F1} = 46.1$, $J_{H15F15} = 46.1$, $J_{F1F15} = 7.0$, $J_{H1F15} = -0.3$, $J_{H15F1} = -0.3$

[a] In order to maximize to chemical shift difference between H and F, the maximum dispersion allowed in PCPMR was used.

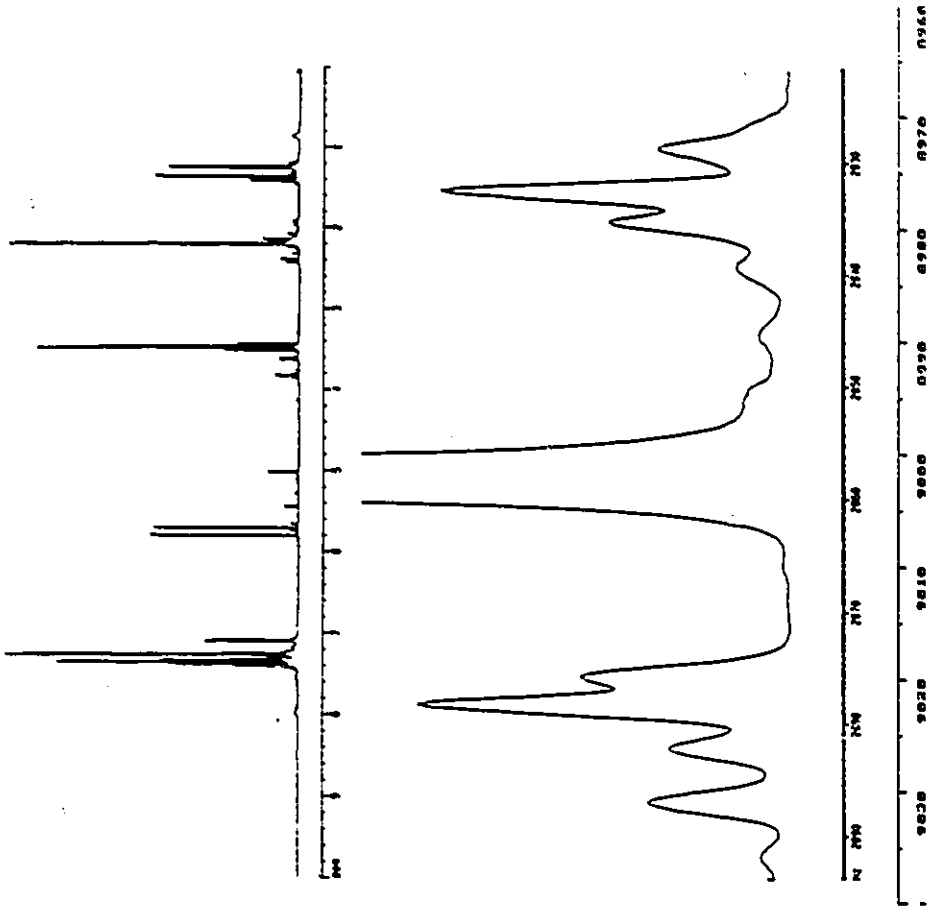

Figure 2.5 The 500 MHz ^{1}H NMR spectrum of the mother liquor from the crystallization of 53 in $CDCl_3$: (a) spectrum (δ 0-10); (b) expansion of (a) (δ 5.64-5.79); (c) spectrum calculated by PCMR employing the parameters given in Table 2.2.

determine the axial:equatorial ratio of our α-fluoro substituted bridged biaryl ketone at equilibrium, we synthesized compound **64** by similarly reacting the lithium enolate of **54** with N-fluorodibenzenesulphonamide. The 500 MHz ^{1}H NMR spectrum in CCl_4 revealed

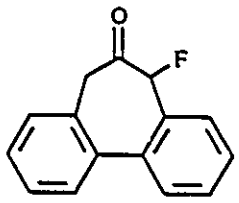

$$K = \frac{[\text{equatorial}]}{[\text{axial}]} \geq 200$$

64

only the presence of the equatorial conformer and confident that 500 MHz ^{1}H NMR would detect 0.5%, we assigned K a minimum value of 200 (i.e. ≤0.5% axial fluoro **64**). Therefore, our α-fluoro bridged biaryl ketone **53** exhibits an even greater bias than 2-fluorocyclohexanone towards the equatorial orientation.

2.5 Characterization of 5,7-dihydro-1,11-dimethyl-6*H*-dibenzo[a,c]cyclohepten-6-one and its α-Substituted Reduction Products

As mentioned previously in the introduction, the main focus of this thesis will be to conduct a π-facial reactivity study for the nucleophilic addition of hydride to our model bridged biaryl ketone and its α-substituted derivatives. Thus, it was necessary to prepare and fully characterize the various reduction products.[86] All alcohols were prepared by reducing the ketones **44-53** with a 25% excess of lithium aluminum hydride. Column or preparative thin layer chromatography afforded the pure alcohol products **65-69**. For unsubstituted ketone **44**, addition of hydride to the homotopic faces of the carbonyl yields a singie alcohol **65**. However, for the quasi-axial α-substituted derivatives of **44**, the addition of hydride may occur either antiperiplanar (app) to the substituent R_{ax} to afford the major alcohol **66** or synperiplanar (sp) to afford the minor alcohol **67**. For the quasi-

equatorial substituents, the addition of hydride may occur anticlinal (ac) to the substituent R_{eq} to give the major alcohol **68** or synclinal (sc) to give the minor alcohol **69** (see Scheme 2.3).

The 300 MHz ^{1}H NMR spectrum in benzene-d_6 of the unsubstituted alcohol **65** shows the presence of four magnetically nonequivalent benzylic protons (see Figure 2.6). Each benzylic proton is a doublet of doublets whose spacings represent a large geminal coupling and a smaller vicinal coupling (see inset). On the basis of molecular models, molecular mechanics calculations using the program PCMODEL[80] and the Karplus relationship[87], the four observed vicinal coupling constants of 10.1, 6.4, 4.8 and 1.8 Hz could be readily assigned. The dihedral angle about protons H_a and H_c is approximately 160° and thus $^3J_{a,c}$ was assigned to the large 10.1 Hz vicinal coupling. The dihedral angle between protons H_b and H_c is approximately 40° to which the 6.4 Hz coupling was assigned. Similarly, the dihedral angle about H_c and H_d is ~40° and $^3J_{c,d}$ was assigned to the 4.8 Hz coupling. Lastly, the torsional angle about H_c and H_e is around 80° and thus $^3J_{c,e}$ was ascribed to the smallest coupling of 1.8 Hz.

The stereochemistry of the axial and equatorial α-substituted reduction products **66-69** could be assigned by considering the vicinal proton-proton coupling constants in the three carbon bridge. More precisely, the presence or absence of the large (i.e. ~160° dihedral angle) or small (i.e. ~80° dihedral angle) coupling constants provided an unambiguous method for distinguishing between the major and minor alcohols **66** and **67** or **68** and **69**. For example, the minor axial methyl reduction product **67a** possessed a large 10.4 Hz vicinal coupling which was assigned to $J_{c,d}$ since the dihedral angle about H_c and H_d is approximately 160°. However, the major axial methyl alcohol **66a** exhibited vicinal coupling constants of no greater than 7.7 Hz and thus **66a** and **67a** could be readily distinguished. The minor equatorial methyl alcohol **69a** has a small ~2.7 Hz vicinal coupling due to the ~80° torsional angle about H_b and H_c, whereas no such small coupling

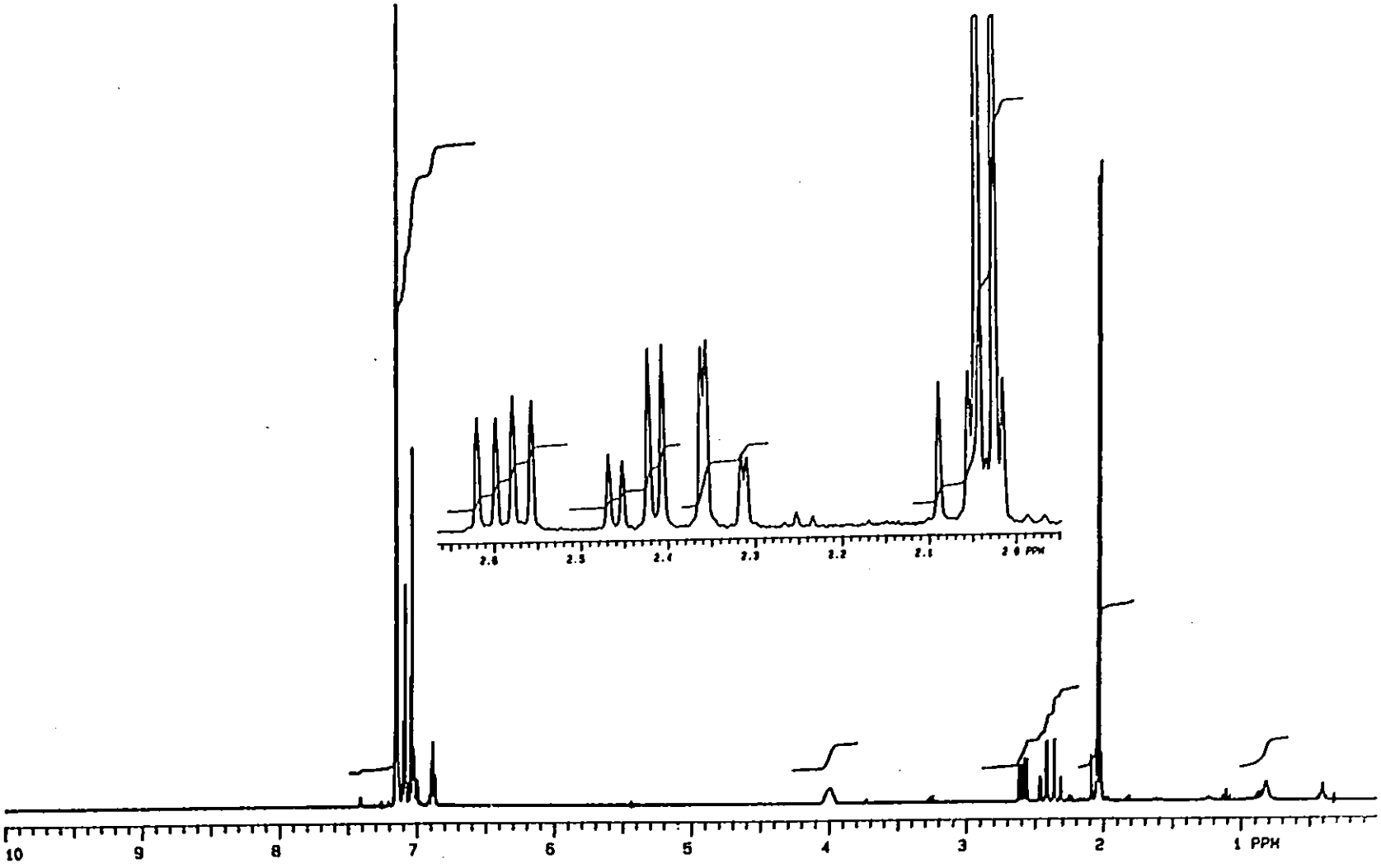

Figure 2.6 The 300 MHz ^{1}H NMR spectrum of 65 in benzene-d_6. The inset shows an expansion of the four benzylic protons on C2 and C15 (δ 1.95-2.95).

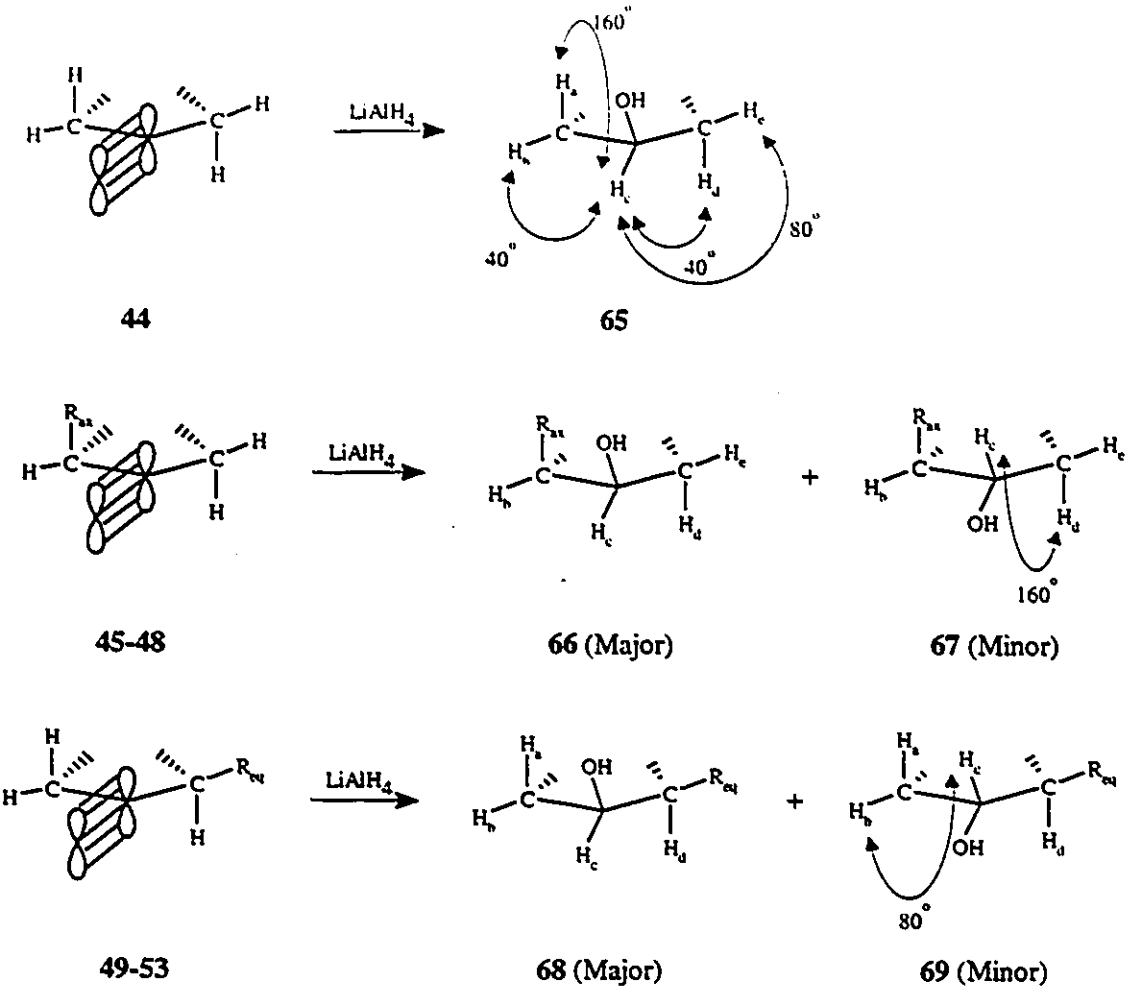

Figure 2.7 Syntheses and three-dimensional representation of alcohols 65-69.

was observed for the major equatorial methyl alcohol and thus, as before, the two alcohols **68a** and **69a** could be readily distinguished. In both the axial and equatorial methyl alcohol products the remaining coupling constants showed behavior consistent with that observed in **65** (see Table 2.3). In addition, the coupling constants of the remaining α-SCH_3, -OCH_3, -Cl and -F reduction products exhibited similar trends and hence, as before, the major and minor alcohols, where observed, could be unambiguously identified (see Table 2.3). Finally, the diastereoselectivities for LAH addition, from NMR integrals, are given in Table 2.4. All ketones exhibited high diastereoselectivity with the equatorial methyl derivative showing the minimum π-facial selectivity (i.e. ac:sc approach) of 5.7:1.

Table 2.3 Vicinal coupling constants (Hz) for 65 and its α-substituted derivatives.

Alcohol	$^3J_{a,e}$	$^3J_{b,e}$	$^3J_{c,d}$	$^3J_{c,e}$
65[a]	10.1	6.4	4.8	1.8
66a $R_{ax} = CH_3$		7.7	5.2	1.8
b $R_{ax} = SCH_3$		6.9	5.1	1.6
c $R_{ax} = OCH_3$		6.0	4.8	1.6
d $R_{ax} = Cl$		6.3	5.4	~0.0
67a $R_{ax} = CH_3$		~0.0	10.4	~5.9
68a $R_{eq} = CH_3$	9.8	6.7	4.0	
b $R_{eq} = SCH_3$	9.9	6.6	3.8	
c $R_{eq} = OCH_3$	10.0	6.8	4.5	
d $R_{eq} = Cl$	9.9	6.8	3.7	
e $R_{eq} = F$[b]		7.2	4.5	
69a $R_{eq} = CH_3$	~3.5	~2.7	9.2	
e $R_{eq} = F$[b]			7.5	

[a] Obtained from 300 MHz ^{1}H NMR spectrum in benzene-d_6. [b] Because of severe overlap, not all coupling constants could be determined.

Table 2.4 π-Facial selectivity for the nucleophilic addition of $LiAlH_4$ to ketones 45-53.

α-Substituent	app:sp	ac:sc
CH_3	9:1	6:1
SCH_3	≥19:1	≥19:1
OCH_3	≥19:1	≥19:1
Cl	≥19:1	8.2:1
F	-	7.6:1

Chapter 3 Conformational Study of the α-Derivatives of 5,7-dihydro-1,11-dimethyl-6*H*-dibenzo[a,c]cyclohepten-6-one and their Cyclohexanone Analogues

Part A α-Derivatives of 5,7-dihydro-1,11-dimethyl-6*H*-dibenzo[a,c]cyclohepten-6-one

3.1 Introduction

As previously mentioned in Section 2.1, the bridged biaryl ketone 5,7-dihydro-1,11-dimethyl-6*H*-dibenzo[a,c]cyclohepten-6-one, **44**, is a chiral derivative of biphenyl which Mislow concluded on the basis of molecular models to possess a single "rigid" conformation.[67] Mislow's observations were later supported by 1H NMR which revealed two pairs of nonequivalent α protons. An indication of this rigidity is the high 36 kcal/mol barrier to racemization ($\Delta G^{\ddagger}$).[68] However, in the absence of the two ortho methyl groups on C7 and C10 (i.e. ketone **54**), the barrier decreases significantly to approximately 14 kcal/mol and thus most of the rigidity present in **44** is lost.

In order to probe the degree of rigidity present in ketone **44** and its α-methyl derivatives (**45** and **49**) and to compare to their cyclohexanone analogues, Fraser and coworkers in 1993 conducted a qualitative conformational study using the molecular mechanics program PCMODEL.[80] The study revealed that **44** is significantly more rigid than cyclohexanone, however, **44** still possesses some flexibility. As validation of PCMODEL, Fraser and coworkers found that the X-ray crystal structure of **44** and its α-methyl derivatives could be satisfactorily reproduced.[78] As a continuation of this research, we have carried out a conformational study of the axial and equatorial α-chloro derivatives **48** and **52** in order to assess the degree of inflexibility present in these ketones relative to their cyclohexanone analogues.

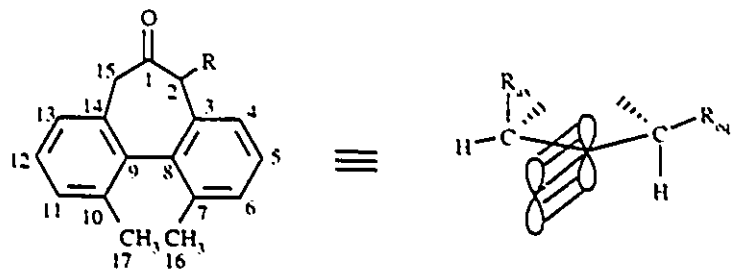

44	$R_{ax} = R_{eq} = H$	**49**	$R_{ax} = H, R_{eq} = CH_3$
45	$R_{ax} = CH_3, R_{eq} = H$	**50**	$R_{ax} = H, R_{eq} = SCH_3$
46	$R_{ax} = SCH_3, R_{eq} = H$	**51**	$R_{ax} = H, R_{eq} = OCH_3$
47	$R_{ax} = OCH_3, R_{eq} = H$	**52**	$R_{ax} = H, R_{eq} = Cl$
48	$R_{ax} = Cl, R_{eq} = H$	**53**	$R_{ax} = H, R_{eq} = F$

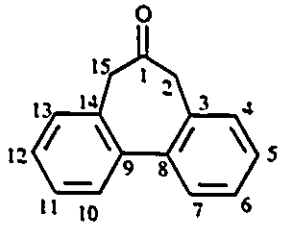

54

3.2 Results and Discussion

3.2.1 Determination of the Viability of the α-chloro Derivatives of 44 as a Stereochemical Model

In order to compare the conformational mobility of the chloroketones **48** and **52** with the bridged biaryl ketone **44**, we calculated their steric energies over a 40° increase and decrease in the torsional angle C15-C1-C2-C3 from their ground state conformations (see Figure 3.1). As observed for the unsubstituted bridged biaryl ketone and its α-methyl derivatives (i.e. **45** and **49**) and in contrast to 1,3-cycloheptadiene[92], only one minimum was found for **48** and **52**. The curve for the unsubstituted ketone **44** exhibits a steep energy well since a deviation of 15° in the torsional angle C15-C1-C2-C3 causes an approximate 1 kcal/mol increase in energy. However, the curves for the chloroketones **48** and **52** (see Figure 3.1a and b) show much broader plots and thus these substrates

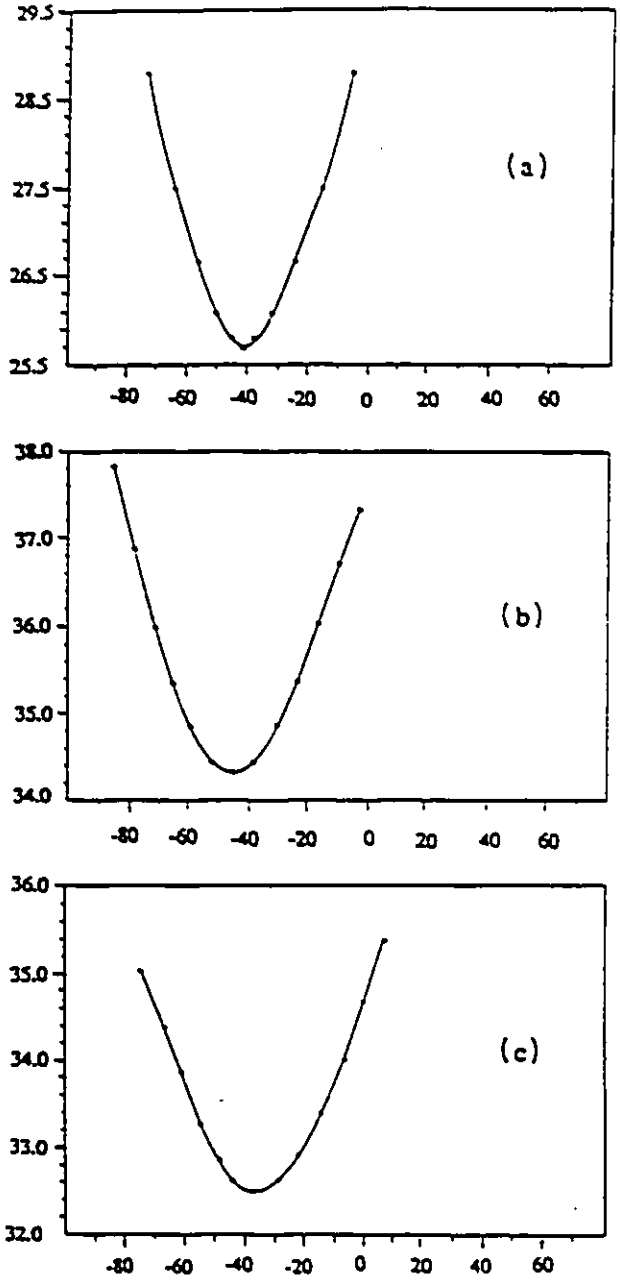

Figure 3.1 A plot of steric energy (kcal/mol) versus the torsional angle (deg) about C1-C2 for (a) 44, (b) 48 and (c) 52.

possess less rigidity than **44**. Fraser *et al.* observed a similar result for the α-methylketones **45** and **49**.[78]

The comparison of flexibility present in our model chloroketones **48** and **52** with their corresponding cyclohexanone analogues was carried out in a similar fashion. As before, we calculated a steric energy profile for cyclohexanone and axial 2-chlorocyclohexanone (**70**) over an 80° range in the internal torsional angle C6-C1-C2-C3

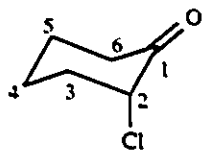

70

from their ground state conformations. The plots are presented in Figure 3.2. The curves for cyclohexanone and axial 2-chlorocyclohexanone (Figure 3.2a-b) exhibit similar energy profiles and hence are qualitatively equivalent in rigidity.

In molecular mechanics and other theoretical methods, the calculation of polar interactions (e.g. between the carbonyl group dipole and the C-Cl dipole in 2-chlorocyclohexanone) show a large dependence on the size of the dielectric constant for the surrounding medium. However, it is well recognized that the dielectric constant for the bulk medium does not normally represent the dielectric constant between the dipoles in question. Thus, in molecular mechanics calculations the effective dielectric constant should be employed. However, the proper value to use has been quite speculative. In most instances, a value between 2 and 5 has been employed.[93] Therefore, in order to determine the importance of the choice of dielectric constant, we recalculated the plot for **70** using a value of 6 for the dielectric constant. The plot shows no change in the magnitude of the torsional angle in the ground state conformation, but exhibits a slight increase in flexibility (see Figure 3.2c).

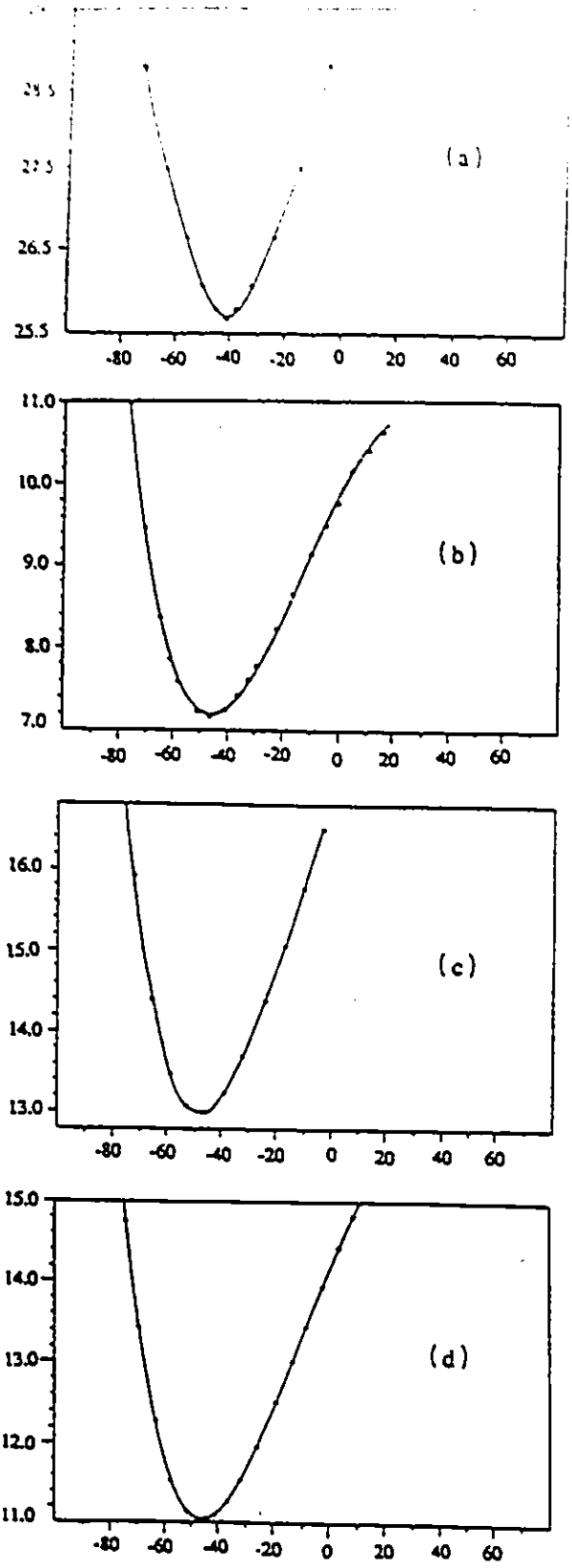

Figure 3.2 A plot of steric energy (kcal/mol) versus the torsional angle (deg) about C1-C2 for (a) 44, (b) cyclohexanone, (c) axial 2-chlorocyclohexanone (70), dielectric constant = 1.5 and (d) axial 2-chlorocyclohexanone (70), dielectric constant = 6.0.

3.3 Conclusions

If a compound is to be a suitable model for investigating stereoelectronic effects, its skeleton must be able to provide compounds of known stereochemistry. Accordingly, the greater the rigidity of the model, the more suitable it is for observing a stereoelectronic effect. Thus, from the previous results of Fraser[78] and the results shown in Figures 3.1 and 3.2, it appears that ketone **44** is a suitable model to test the importance of the antiperiplanar effect as proposed by Anh[13] or Cieplak[40]. In addition to providing greater rigidity over cyclohexanone, molecular mechanics calculations have shown that the unsubstituted bridged biaryl ketone and its α-methyl[78] and α-chloro derivatives have only one energy minimum, whereas cyclohexanone, 2-methylcyclohexanone[78] and 2-chlorocyclohexanone are in equilibrium with a twist boat conformation that is only 3-4 kcal/mol higher in energy. Thus, as previously stated, the possibility of the addition of hydride occurring through a twist boat conformation must be considered whenever cyclohexanones are to be employed as stereochemical models.

Part B Conformational Analysis of 2-Substituted Cyclohexanones

3.4 Introduction

As stated in Section 2.4.1, the α-fluoro derivative of our bridged biaryl ketone **44** exhibits an extremely strong preference for the equatorial conformation where the limit provided by **64** is ≤ 0.5% of the axial conformer (i.e. $\Delta G_{eq\text{-}ax} < -3.1$ kcal/mol). All attempts to epimerize the equatorial ketone **53** were unsuccessful. However, for the α-methylthio derivative of **44**, the axial diastereomer **46** was favoured, even in the highly polar solvent acetonitrile ($\Delta G_{eq\text{-}ax} = 0.72$ kcal/mol) which should presumably minimize the destabilizing dipolar interaction in the equatorial diastereomer **50**. In order to help understand this variability in conformational stability, we consulted the literature for the analogous 2-

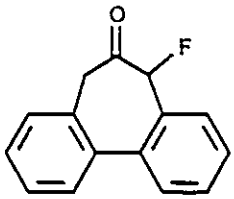

64

substituted cyclohexanones.[94] However, unlike our bridged biaryl ketone **44**, the axial and equatorial conformations of 2-substituted cyclohexanones rapidly equilibrate at room temperature (see equation 5). In equation 5, the protons are labeled to indicate either their cis (H) or trans (H′) stereochemical relationship with respect to the 2-substituent R.

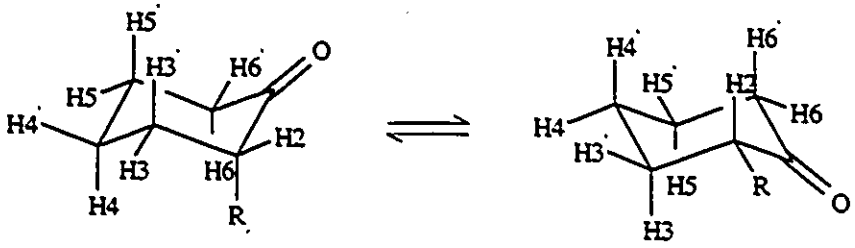

[5]

71 **72**

As previously stated in Section 2.4, the conformational properties of α-halo substituted cyclohexanones have been thoroughly investigated. Studies by Allinger and Stothers employing dipole moment measurements[95,96], infrared[95] and NMR spectroscopy[83] have all consistently shown that in nonpolar hydrocarbon solvents (e.g. *n*-heptane, isooctane or cyclohexane), 2-bromo- and 2-chlorocyclohexanone exist predominantly in the axial conformer **71** (R = Br or Cl). For 2-fluorocyclohexanone approximately a 50:50 mixture of conformers exists in the same low dielectric constant solvents. As the polarity of the solvent increases, the proportion of the equatorial conformer **72** for the 2-halocyclohexanones increases. More specifically, in acetonitrile, Stothers determined that the equatorial mole fraction for 2-fluoro-, 2-chloro- and 2-bromocyclohexanone was 0.87,

0.65 and 0.50, respectively.[83] Hitherto, three main factors have been proposed to account for these results.[94] The first two factors, steric and dipole-dipole interactions, fall into a more classical explanation, while the third factor, orbital-orbital interactions, represents a nonclassical rationalization (*vide infra*).

Consultation of the recent literature for 2-methoxycyclohexanone (**74**) indicated that for this ketone the axial conformer **71** (R = OCH_3) is preferred, but quantitative estimates varied.[97-99] This conclusion was based on the research of Cantacuzene and Tordeux who, using 60 MHz ^1H NMR, found the mole fraction of **71** to be 0.63 and 0.16

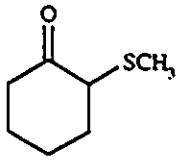

73

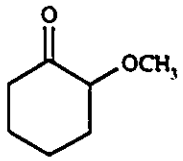

74

in carbon tetrachloride and acetonitrile, respectively.[100] Thus, as in the case of cyclohexanones bearing an α-halogen substituent, the proportion of the equatorial conformer increases as the solvent polarity increases. In contrast, an earlier paper in 1974 reported that compound **74** predominantly adopts the axial conformation; however, the mole fraction was independent of solvent.[101] Earlier equilibration studies by House[102], Casadevall[103] and Chodkiewicz[104] revealed, in contrast to later studies, that the equatorial conformer was preferred with the mole fraction being 0.86, 0.78 and 0.72 in methanol, carbon tetrachloride and ethanol, respectively. Lastly, Rittner *et al.* recently found using six distinct ^1H and ^{13}C NMR parameters at 400 and 100.6 MHz, respectively, an average value of 0.72±0.04 for the equatorial mole fraction in $CDCl_3$.[105]

For 2-methylthiocyclohexanone (**73**), an infrared study in 1980 indicated that the axial mole fraction was 0.70 in carbon tetrachloride.[106] An equilibration investigation of

2-methylthio-4-*t*-butylcyclohexanone yielded exactly the same result as obtained seven years earlier by Wladislaw, however, the solvent employed was methanol.[107] Finally, in addition to their study of **74**, Rittner and coworkers also determined the conformational preference for **73** and found the axial mole fraction to be 0.85±0.07.[105] Thus, the above results suggest an unexpected solvent effect. That is, as the solvent polarity decreases, the mole fraction of the axial conformer is expected to increase in a consistent fashion.

Hitherto, determinations of the magnitude of the equilibrium constant for 2-substituted cyclohexanones (i.e. equation 5) by ^{1}H NMR methods have used either the chemical shift[83] or the half-height bandwidth[83,100] for the methine proton at C2 as the NMR parameter since the investigation was limited by low field 60 MHz NMR. However, a more accurate approach would be to measure directly a single coupling constant (e.g. $J_{5',6}$). The magnitude of $J_{5',6}$ or any other vicinal coupling constant, represents a weighted average of the axial ($J_{5',6} = J_{aa}$) and equatorial ($J_{5',6} = J_{ee}$) conformers shown in equation 5 and thus application of equation 6 will provide a value for the axial mole fraction (n_a), the equatorial mole fraction (n_e) and K ($K = n_e/n_a$).[109]

$$J_{obs} = n_a J_{aa} + n_e J_{ee} \qquad [6]$$

In order to clarify the above inconsistent results for ketones **73** and **74**, we were prompted to measure the value of the equilibrium constant for **73** and **74** using high field 500 MHz ^{1}H NMR in a wide range of solvents from the nonpolar cyclohexane-d_{12} (ε = 2.0) to the polar solvent acetonitrile-d_3 (ε = 37.5). The use of high field NMR allowed for the direct measurement of $J_{5',6}$ and thus provided accurate data for the equilibrium shown in [5].

3.5 Results and Discussion

If equation 6 is to be employed, knowledge of the values of $J_{5',6}$ for the purely axial conformer **71** and the purely equatorial conformer **72** must be obtained. As a model we chose 4-*t*-butylcyclohexanone (**6**) since it is highly biased towards the equatorial conformation by the presence of the bulky *t*-butyl group (A value = 4.9 kcal/mol[71]). The 500 MHz ^{1}H NMR spectrum in acetone-d_6 provided the values of 13.7 Hz for J_{aa} (i.e. $J_{2ax,3ax}$ or $J_{5ax,6ax}$ in **6**) and 2.2 Hz for J_{ee} (i.e. $J_{2eq,3eq}$ or $J_{5eq,6eq}$ in **6**).[108] The magnitudes of these coupling constants were confirmed by spectral simulation using the commercially available program PCPMR (see Table 3.1 for spectral parameters).[80] However, the observed and calculated spectra are not in total agreement (see Figure 3.3). The proton coupling patterns for $H2_{ax}$ and $H2_{eq}$ were difficult to simulate. The patterns were very sensitive to the long range coupling between protons on C3 and C5 and C2 and C6. The program PCPMR is limited to an eight spin system (H4 was omitted) and thus we concluded that the differences observed between the observed and simulated spectra are acceptable. Overall, we believe the calculated values for n_a are accurate to within ±0.02 at values near 0.50 and to within ±0.04 at the extremes, which correspond to an accuracy in ΔG of ±0.1 to 0.4 kcal/mol.

The 500 MHz ^{1}H NMR spectrum of **74** in $CDCl_3$ is a first order spectrum (see Figure 3.4). More precisely, all nine protons exhibit the expected multiplet patterns and are free from overlap from any of the other proton absorptions. All nine protons were unequivocally assigned by standard COSY and HMQC two-dimensional spectra. The methine proton at C2 resonates at δ 3.23. The triplet coupling pattern indicates that the magnitude of the two vicinal coupling constants $J_{2,3}$ and $J_{2,3'}$ are both approximately 4.8 Hz. Thus, as observed, if the methine proton at C2 primarily adopts an equatorial conformation, one would expect to observe two vicinal coupling constants of approximately the same magnitude. If, however, the proton at C2 primarily adopts an

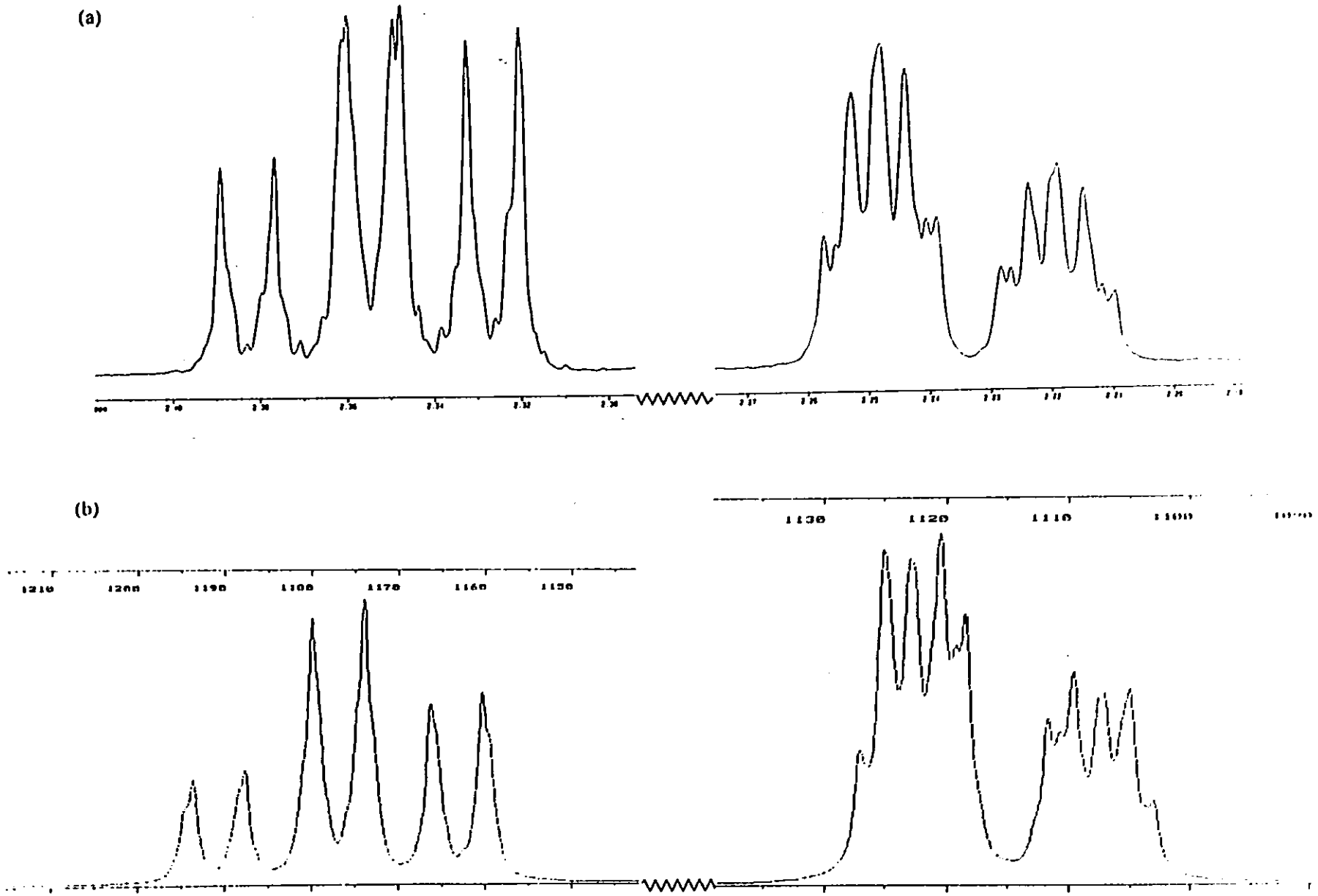

Figure 3.3 A portion of the 500 MHz ^{1}H NMR spectrum for 4-*t*-butylcyclohexanone in acetone-d_6: (a) the absorption for the axial (δ 2.31-2.39) and the equatorial (δ 2.21-2.26) protons at C2 and C6; (b) the spectrum calculated by PCPMR employing the parameters given in Table 3.1.

axial conformation, its coupling pattern would be expected to be a doublet of doublets with coupling constants of approximately 11 and 5 Hz (see Table 3.1).

Table 3.1 Spectral parameters for the simulation of (a) 4-*t*-butylcyclohexanone (6, in acetone-d_6) and (b) 2-methylthiocyclohexanone (73, in $CDCl_3$).

(a)

Chemical shifts (Hz from TMS): $H2_{ax} = H6_{ax}$ 1176, $H2_{eq} = H6_{eq}$ = 1116, $H3_{ax} = H5_{ax}$ = 705, $H3_{eq} = H5_{eq}$ = 1040

Coupling constants (Hz): $J_{2ax,2eq} = J_{6ax,6eq}$ = -14.5, $J_{3ax,3eq} = J_{5ax,5eq}$ = -12.3, $J_{2ax,3ax} = J_{5ax,6ax}$ = 13.7, $J_{2eq,3eq} = J_{5eq,6eq}$ = 2.2, $J_{2ax,3eq} = J_{5eq,6ax}$ = 6.1, $J_{2eq,3ax} = J_{5ax,6eq}$ = 4.6, $J_{2eq,6eq} = J_{3eq,5eq}$ = 2, $J_{3eq,5ax} = J_{3ax,5eq}$ = 1, $J_{2eq,6ax} = J_{2ax,6eq}$ = 0.8

(b)

Chemical shifts (Hz from TMS): H3 = 1030, H3′ = 1083, H4 = 934, H4′ = 837, H5 = 988, H5′ = 875, H6 = 1485, H6′ = 1119

Coupling constants (Hz): $J_{3,5}$ = 1.6, $J_{4',6'}$ = 1.6, $J_{3,4'}$ = 4.9, $J_{3,4}$ = 3.5, $J_{3',4'}$ = 3.8, $J_{3',4}$ = 10.1, $J_{3,3'}$ = -14.1, $J_{4',5'}$ = 3.8, $J_{4',5}$ = 4.9, $J_{4,5'}$ = 10.1, $J_{4,5}$ = 3.5, $J_{4,4'}$ = -13.6, $J_{5,5'}$ = -13.2, $J_{5,6'}$ = 4.8, $J_{5,6}$ = 5.8, $J_{5',6'}$ = 4.6, $J_{5',6}$ = 11.2, $J_{6,6'}$ = -14.5

The H6 axial proton of 73 appears at δ 2.94 as an octet (i.e. a doublet of doublet of doublets). The first order pattern allows for the determination of the geminal coupling constant $J_{6,6'}$ and the two vicinal coupling constants $J_{5,6}$ and $J_{5',6}$ (see inset in Figure 3.4).

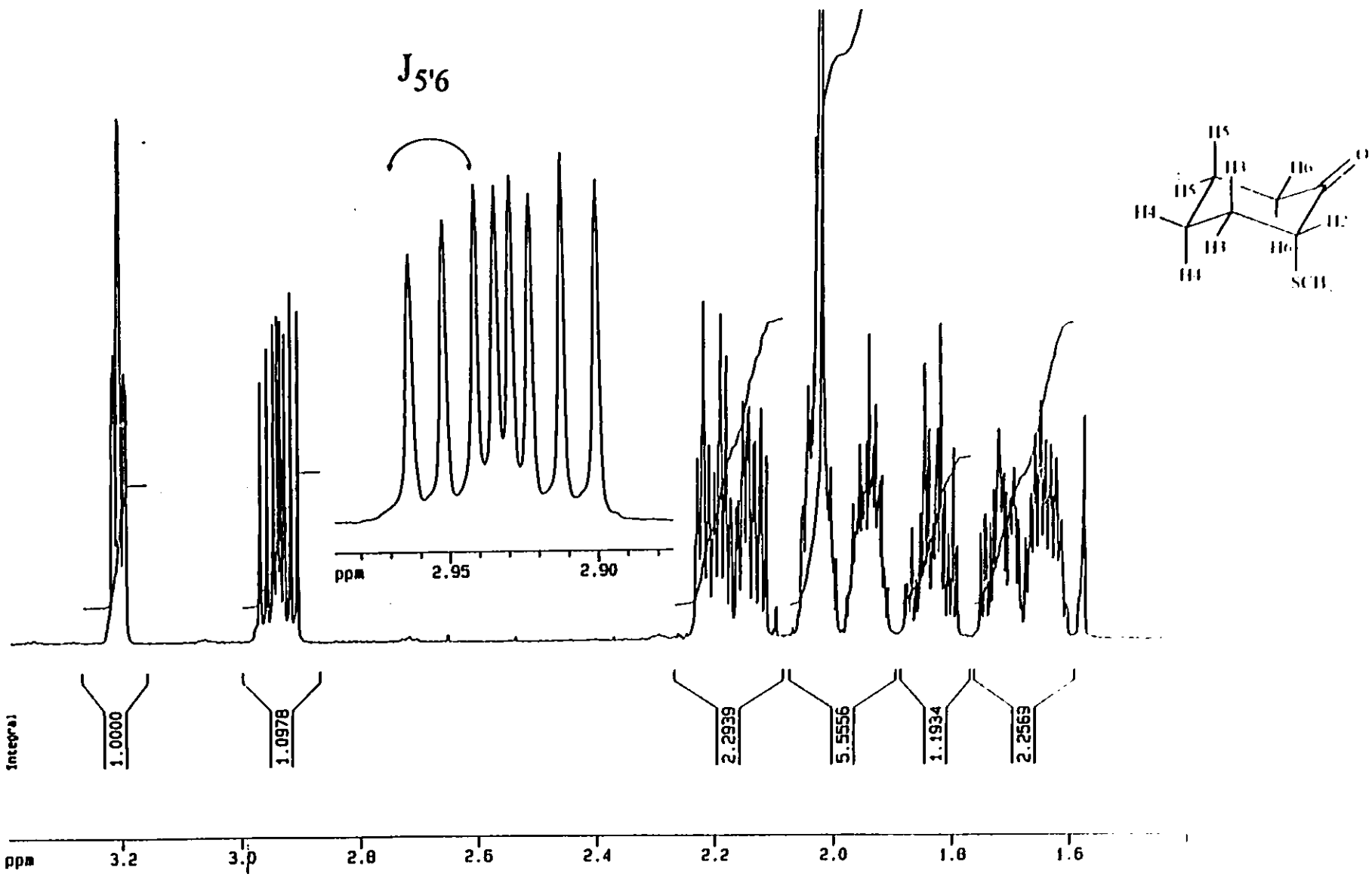

Figure 3.4 The 500 MHz ^{1}H NMR spectrum of 2-methylthiocyclohexanone (73) in $CDCl_3$. The inset shows the expansion of the octet for H6 at δ 2.94.

In principle, either $J_{5,6}$ or $J_{5',6}$ could be used as J_{obs} in equation 6, however, $J_{5',6}$ provides the more accurate values of K since it possesses the larger variation with conformation.

In order to determine the validity of our first order assumption, we simulated the 500 MHz ^{1}H NMR spectrum of **73** using PCPMR.[80] However, again, since this program is limited to eight nuclei, H2 was omitted. Satisfyingly, the octet pattern was reproduced to within 0.1 Hz by employing the parameters given in Table 3.1. The remaining seven protons exhibited similar agreement with the experimental spectrum, however, as expected, the H3 and H3′ coupling patterns were simplified.

The value obtained for $J_{5',6}$ in Figure 3.4 was 11.2 Hz and substitution into equation 6, where $n_a + n_e = 1$, yields a value of 0.78 for n_a and, in turn, gives K a value of 0.28 (see Table 3.2). The 500 MHz ^{1}H NMR spectra for **73** in the remaining solvents under study were obtained and with the observed value of $J_{5',6}$ afforded the final results listed in Table 3.2. The position of the equilibrium in equation 5 changes dramatically, as

Table 3.2 Conformational equilibrium data for 2-methylthiocyclohexanone (73).

Solvent	J_{obs} (Hz)	n_a	$K = \frac{[\text{equatorial } SCH_3]}{[\text{axial } SCH_3]}$	ΔG° (kcal/mol)
C_6D_{12}	13.0	0.94	0.064	1.6
CCl_4	12.7	0.91	0.099	1.4
$CDCl_3$	11.2	0.78	0.28	0.7
CD_3COCD_3	9.9	0.67	0.50	0.4
CD_3CN	9.0	0.59	0.71	0.2

demonstrated for 2-halocyclohexanones[82,83], with the proportion of axial SCH_3 conformer increasing as the solvent polarity decreases to a maximum of 94% in cyclohexane-d_{12}. Our result in $CDCl_3$ is in good agreement with that obtained by Basso and coworkers (n_a

= 0.85±0.07).[105] However, in carbon tetrachloride our result (n_a = 0.91) indicates that the value obtained by Wladislaw *et al.*[106] underestimates n_a.

In the case of 2-methoxycyclohexanone, **74**, it proved necessary to use an alternative vicinal coupling constant (i.e. $J_{2,3}$), since in acetone-d_6 and acetonitrile-d_3 severe overlap did not allow the magnitude of $J_{5',6}$ to be determined. As a result, we adjusted our model coupling constants J_{aa} and J_{ee} for the presence of the electronegative methoxy substituent on C2.[110] The magnitude of J_{aa} was decreased to 12.0 Hz and the magnitude for J_{ee} was increased to 2.7 Hz (see Figure 3.5). Utilization of these adjusted

ΔJ = -1.7 Hz ΔJ = +0.4 Hz

(relative to cyclohexane)

J_{aa} = 13.7 - 1.7 = 12.0 Hz

J_{ee} = 2.3 + 0.4 = 2.7 Hz

Figure 3.5 Estimation of J_{aa} and J_{ee} for 2-methoxycyclohexanone.

values and the observed $J_{2,3}$ values led, after application of equation 6, to the results given in Table 3.3. As observed for 2-methylthiocyclohexanone, the proportion of the axial conformer **71** increased as the polarity of the solvent decreased. However, contrary to previous evidence[100-104], **74** is biased towards the equatorial conformer, except in very nonpolar solvents such as cyclohexane-d_{12}.

Table 3.3 Conformational equilibrium data for 2-methoxycyclohexanone.

Solvent	J_{obs} (Hz)	n_a	K	ΔG° (kcal/mol)
C_6D_{12}	6.7	0.57(0.55)[a]	0.75	0.2
CCl_4	7.3	0.51(0.50)	0.96	0.0
$CDCl_3$	10.0	0.22(0.19)	3.5	-0.7
CD_3COCD_3	9.8	0.24	3.2	-0.7
CD_3CN	10.5	0.16	5.3	-1.0

[a] Values in parentheses were determined from $J_{5',6'}$.

3.5.1 Factors Influencing the Conformational Equilibrium

As mentioned in the introduction (Section 3.4), three main factors, steric, dipolar and orbital-orbital interactions, have been put forward to rationalize the observed equilibrium distribution of 2-substituted cyclohexanones.[94] The steric factor includes both torsional and van der Waals interactions. In cyclohexane derivatives, steric factors are responsible for the greater stability of the equatorial conformer **72**, which increases as the size of the substituent increases. For example, the free energy differences between the equatorial and axial conformers ($-\Delta G_{eq\text{-}ax}$ or A value) in methyl-, ethyl- and isopropylcyclohexane are 1.7, 1.8 and 2.2 kcal/mol, respectively.[111] In addition to torsional and van der Waals interactions, there is an additional effect, the 2-alkyl ketone effect, that is present in 2-substituted cyclohexanones. This effect, a type of $A^{1,3}$ strain[112], which favours the axial conformation as the steric bulk of the 2-substituent increases, is thought to be a result of a repulsive interaction between the lone pairs on oxygen and the 2-substituent (see Figure 3.6a). This additional effect is thought to be negligible for a methyl group, 1.0 and 1.7 kcal/mol for a ethyl and isopropyl group, respectively.[113] The second factor, the dipole-dipole interaction, favours the axial conformer since this

minimizes the repulsive interaction between the C-X and C=O dipoles (see Figure 3.6b).[114] The relative importance of this factor decreases as the dielectric constant (ε) of the medium increases. The third factor invoked is a two-electron stabilizing orbital-orbital interaction involving donation from either the $\sigma_{C2\text{-}X}$ orbital or the nonbonding lone pair on X into the carbonyl's π^* antibonding orbital.[115] This orbital-orbital interaction has been employed to explain the unexpected stability of the axial conformer for many 2-substituted cyclohexanones, since the axial conformer possesses the required antiperiplanar orbital-orbital alignment and thus provides the maximum stabilization. The equatorial conformer does not provide the correct orbital alignment and thus no such stabilization occurs.

In order to shed light upon the relative importance of the aforementioned factors,

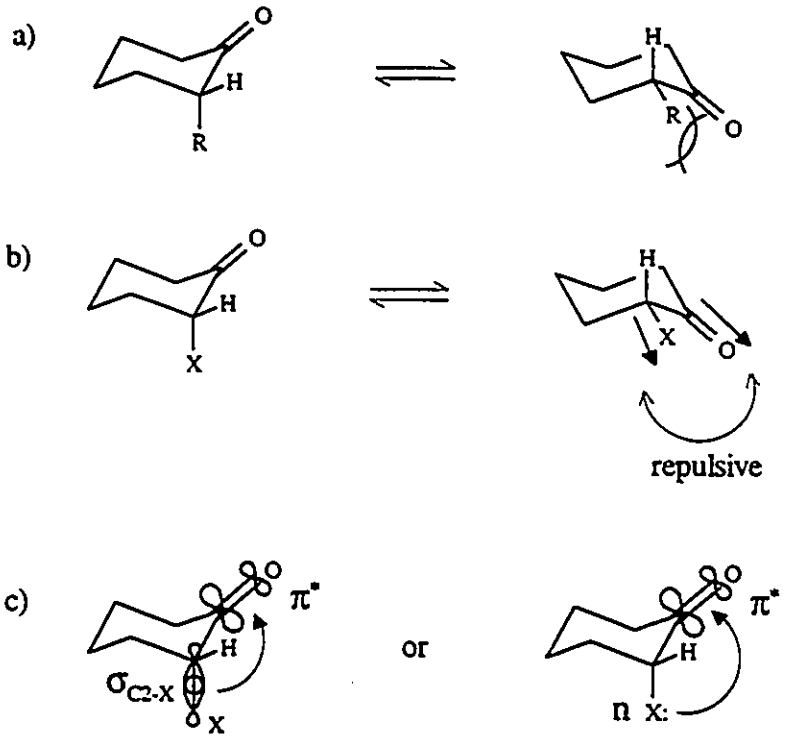

Figure 3.6 The (a) steric, (b) dipole-dipole repulsive interaction and (c) orbital-orbital interaction used to rationalize the conformational equilibrium in 2-substituted cyclohexanones.

we have collected the data for all of the previous ^{1}H NMR measurements of K and present the results in Table 3.4. The only solvents common to all measurements were CCl_4 and CD_3CN. As observed with **73** and **74**, the data in Table 3.4 show that the polar solvent acetonitrile exhibits the greater proportion of the equatorial conformer with the fluoro substituent showing the greatest preference and the methylthio and bromo substituents showing the least preference. Molecular mechanics calculations (*vide infra*) reveal that in the highly polar solvent acetonitrile, the dipole-dipole interaction shown in Figure 3.6b is negligible. Thus, assuming the dipole-dipole interaction is maximized in carbon tetrachloride, the difference in ΔG_{ea} (i.e. $\Delta\Delta G_{ea}$) reflects qualitatively the substituent's electronegativity and the data for acetonitrile, consequently, reflect solely the influence of steric and orbital-orbital interactions (see Table 3.4).

Table 3.4 Solvent effects on 2-substituted cyclohexanones.

	% Axial		ΔG_{ea}[a]			
Substituent	CCl_4	CD_3CN	CCl_4	CD_3CN	$\Delta\Delta G_{ea}$	$\Delta\Delta E_T$[b]
F	36	13 (ref. 83)	-0.3	-1.1	0.8	1.4
Cl	72	35 (ref. 83)	0.6	-0.4	1.0	0.9
Br	86	50 (ref. 83)	1.1	0.0	1.1	0.8
OCH_3	51	16 (this work)	0.0	-1.0	1.0	0.9
SCH_3	91	59 (this work)	1.4	0.2	1.2	1.1
OC_6H_5	46	21 (ref. 115)	-0.1	-0.8	0.7	
SC_6H_5	72	47 (ref. 115)	0.55	-0.1	0.65	
SeC_6H_5	73	49 (ref.115)	0.6	0.0	0.60	

[a] $\Delta G_{ea} = G_{eq} - G_{ax}$. [b] Calculated by PCMODEL.

3.5.2 Molecular Mechanics Calculations

In order to further investigate the importance of the various factors affecting the conformational equilibrium of 2-substituted cyclohexanones, we have carried out calculations on 2-fluoro-, 2-chloro-, 2-bromo-, 2-methoxy- and 2-methylthiocyclohexanone at the dielectric constants of 2.2 (CCl_4) and 37.5 (CH_3CN). As reported previously[82,83,117], the calculations indicate that in CCl_4 the dipole/charge term favours the axial conformer, but has a marginal influence in acetonitrile (see Table 3.5). Thus, the highly polar solvent CH_3CN effectively removes the dipole-dipole repulsion. The calculated energy difference ΔE_T ($\Delta E_T = E_{eq} - E_{ax}$) for $\varepsilon = 2.2$ and 37.5 agrees within 0.7 kcal/mol of the experimental ΔG_{ea} (last column in Table 3.5) for R = SCH_3, Br and Cl, but differs greatly for R = F and OCH_3 with the difference ranging from 1.5 to 2.2 kcal/mol. In 1993, Houk *et al.* concluded from *ab initio* methods that the torsional parameters used in MM2 and thus PCMODEL for both the C-C-C-O and C-C-C-F atom systems need to be corrected.[118] The MM2 torsional parameters were originally obtained from the A value of fluorocyclohexane and methoxycyclohexane. However, Houk points out that the torsional parameters for these systems are unique to these compounds and cannot by assumed to be valid for all molecules. Thus the poor agreement between theory and experiment for 2-fluorocyclohexanone and 2-methoxycyclohexanone is likely a result of the incorrectly parameterized torsional systems C-C-C-O and C-C-C-F. On the other hand, PCMODEL's estimation of the magnitude of the dipole-dipole interaction ($\Delta\Delta E_T$) agrees well with the experimental values $\Delta\Delta G_{ea}$ (see Table 3.4).

In acetonitrile, the proportion of the axial conformer increases in the order F<OCH_3<Cl<Br<SCH_3. Thus, since in this solvent the second factor, the dipole-dipole interaction, becomes effectively removed, this observed order suggests an inherent preference for the equatorial conformer and the increase in axial may simply reflect increasing steric repulsion (see Figure 3.6a). Our calculations reveal the same order of contribution for the van der Waals component (V) of the steric factor with a 0.9 kcal/mol

Table 3.5 Molecular mechanics calculations of steric energies of 2-substituted cyclohexanones.

	S[a]	B	S-B	T	V	D/C	E_T	ΔE_T	ΔG_{ea}[b]
				R = SCH_3					
ε = 2.2									
Axial	0.34	0.88	0.11	4.20	2.48	-1.67	6.34	1.83	1.4
Equatorial	0.39	1.13	0.11	4.33	3.12	-0.91	8.17		
ε = 37.5									
Axial	0.36	0.89	0.12	4.19	2.44	-0.10	7.90	0.70[c]	0.2
Equatorial	0.40	1.07	0.11	4.38	3.09	-0.05	9.00		
				R = OCH_3					
ε = 2.2									
Axial	0.57	1.60	0.14	4.24	5.48	-2.15	9.87	2.02	0.0
Equatorial	0.60	1.49	0.16	4.61	5.78	-1.25	11.89		
ε = 37.5									
Axial	0.59	1.61	0.15	4.23	5.44	-0.13	11.89	1.16	-1.0
Equatorial	0.62	1.91	0.16	4.67	5.76	-0.07	13.05		
				R = Br					
ε = 2.2									
Axial	0.34	0.71	0.11	4.56	3.17	-2.07	6.81	1.12	1.1
Equatorial	0.37	0.95	0.11	4.08	3.75	-1.32	7.93		
ε = 37.5									
Axial	0.32	0.74	0.10	4.56	3.14	-0.12	8.74	0.42	0.0
Equatorial	0.36	0.87	0.11	4.08	3.83	-0.08	9.16		
				R = Cl					
ε = 2.2									
Axial	0.34	0.60	0.09	6.11	3.26	-2.51	7.89	0.45	0.6
Equatorial	0.34	0.80	0.09	5.10	3.53	-1.52	8.34		
ε = 37.5									
Axial	0.33	0.61	0.09	6.16	3.20	-0.15	10.23	-0.48	-0.4
Equatorial	0.33	0.71	0.09	5.11	3.61	-0.09	9.75		
				R = F					
ε = 2.2									
Axial	0.35	0.60	0.05	7.15	3.23	-3.43	7.95	-1.84	-0.30
Equatorial	0.30	0.58	0.06	4.18	2.98	-1.99	6.11		
ε = 37.5									
Axial	0.33	0.53	0.05	7.27	3.18	-0.20	11.16	-3.21	-1.2
Equatorial	0.28	0.48	0.06	4.19	3.04	-0.11	7.95		

[a] S = stretch, B = bend, S-B = stretch-bend, T = torsional, V = van der Waals, D/C = dipole/charge, E_T = total steric energy, $\Delta E_T = E_{eq} - E_{ax}$, $\Delta G_{ea} = G_{eq} - G_{ax}$ (all in kcal/mol). [b] Experimental value. [c] Includes the entropy contribution due to two equivalent energy rotamers.

change in ΔV_{ea} over the series (see Table 3.5). This component, which supports the presence of a steric factor, can solely account for the experimentally observed variation of 1.3±0.4 kcal/mol. Therefore, as concluded by Rittner and coworkers[104], the need to consider a n-π^* or σ-π^* orbital-orbital interaction seems questionable.

3.6 Conclusions

In summary, we have evaluated the free energy difference (ΔG_{ea}) between the equatorial and axial conformers of 2-methoxycyclohexanone and 2-methylthiocyclohexanone in five solvents of varying polarity. Both compounds exhibit a strong solvent dependence with **74** existing predominantly in its axial conformer **71** (n_a = 0.94) in the nonpolar solvent cyclohexane-d_{12} while **73** exhibits a smaller preference (n_a = 0.56) in the same solvent. On the basis of molecular mechanics calculations, it is concluded that the order of conformational preference may simply reflect the varying strength in the van der Waals interaction between the carbonyl group and the 2-equatorial substituent. Thus, it appears that this same reasoning should apply to our α-substituted bridge biaryl ketones. However, for reasons not well understood, the α-fluoro substituent shows a significantly greater preference for the equatorial conformation than its analogue 2-fluorocyclohexanone.

Chapter 4 Competitive Reduction Rates of 5,7-dihydro-1,11-dimethyl-6*H*-dibenzo[a,c]cyclohepten-6-one and its α-methyl, -methylthio, -methoxy, -chloro and -fluoro derivatives

4.1 Introduction

As mentioned in Chapter 2, the main purpose of this thesis is to both probe the mechanistic properties and the validity of the various theoretical models that have gained widespread acceptance for predicting the preferred face of addition of nucleophiles to a carbonyl group possessing two heterotopic faces (see Sections 1.1 and 1.3). However, in contrast to most previous studies which have relied on π-facial selectivity (see Section 1.5), we have chosen to measure the π-facial reactivity for the addition of hydride ion to our conformationally fixed model ketone **44** and its α-methyl, -methylthio, -methoxy, -chloro and -fluoro quasi-axial and quasi-equatorial derivatives **45-53**. Because most, if not all, models were based on the diastereoselectivity observed in the nucleophilic addition of hydride ion, we decided to employ lithium aluminum hydride (in THF), sodium borohydride (in isopropanol) and triethylsilane (in acetonitrile) as our hydride source. The determination of π-facial reactivity provides a more definitive test of the aforementioned models than a study of π-facial selectivity, which only represents a ratio of the two diastereomeric products, since it offers no opportunity to test a variety of α-substituents.

The determination of π-facial reactivity may be carried out by one of two methods. The first method involves the evaluation of absolute rates for the nucleophilic addition to our bridged biaryl ketone model **44** and its α-derivatives **45-53**. The second method involves the determination of relative rates. More precisely, a mixture of the unsubstituted ketone **44** and an α-derivative is subjected to a competition for a given amount of hydride. However, the measurement of absolute rates has several problems associated with it. Namely, there are inherent inaccuracies associated with measuring these rapid reactions,

especially for lithium aluminum hydride reductions (*vide infra*). In addition, there exist several technical difficulties in determining the exact concentration of these water sensitive reagents. Lastly as observed with many metal alkoxide and aryloxide compounds[119], these reducing agents may aggregate and thus reproducing the exact reducing agents from run to run would be a formidable task. Indeed, ebullioscopic molecular weight measurements of lithium methoxyaluminohydrides indicate that these compounds readily aggregate.[120b]

Despite the above noted difficulties in determining absolute rates, several reports have utilized this method. Only a limited number of these have utilized 2-substituted cyclic ketones. These ketones provide the best opportunity for an assessment of the various factors responsible for π-facial selectivity. In 1970, Rickborn and Wuesthoff conducted a kinetic study of various alkyl substituted cyclohexanones using potentiometric and chromatographic methods.[29] They observed for example in the nucleophilic addition of SBH to 2-methylcyclohexanone, an approximate 5-fold decrease in reactivity and for 2,2-dimethylcyclohexanone an approximate 20-fold decrease in reactivity relative to cyclohexanone. Rickborn and Wuesthoff put forward no specific conclusions. They concluded that this decrease in reactivity was a result of inductive, steric and/or torsional effects. Subsequent to Rickborn's study, Wigfield and Phelps obtained kinetic data, again, for various alkyl substituted cyclohexanones.[121] In agreement with Rickborn and Wuesthoff's results, and in contrast to Brown's previous data which relied on the suspect iodate titration method[122], Wigfield observed an approximate 6-fold decrease in reactivity for 2-methylcyclohexanone relative to cyclohexanone. Wigfield *et al.* concluded that the reduction of 2-alkylcyclohexanones is mainly governed by changes in the activation enthalpy. Assuming additivity for the dialkyl substituted derivatives of cyclohexanone, the data revealed that a 2-equatorial methyl group causes a 1.2 kcal/mol increase in $\Delta H^{\ddagger}$ for axial attack and a 0.6 kcal/mol increase for equatorial attack. For an axial 2-methyl substituent, it was estimated that there is no effect upon axial attack (i.e. $\Delta H^{\ddagger} = 0$) and a 2.0 kcal/mol increase in equatorial attack. These results suggest, in contrast to Anh's[13] or

Cieplak's[40] predictions, that there is no effect on reactivity for an app methyl group. However, the results for these 2,2-dialkyl substituted conformationally mobile systems remain suspect.

Additional measurements of absolute rates were performed in 1974 by Sevin and Cense who, instead of studying the nucleophilic addition to ketones, investigated the electrophilic addition of p-$NO_2C_6H_4CO_3H$ to several 2-substituted methylenecyclohexane derivatives (see Table 4.1).[123] Their results were rationalized in terms of Felkin's torsional

Table 4.1 Face reactivity for the electrophilic addition of *p*-nitroperbenzoic acid in dichloromethane at 0°C.

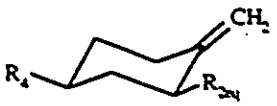

75a-f

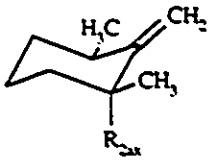

76a-b

Compound	R_2	R_4	% Axial Addition	Rate (L mol^{-1} sec^{-1}) ax + eq	ax	eq
75a	H	H	-	0.190		
b	H	*t*-Bu	70	0.222	0.156	0.067
c	CH_3	H	54	0.199	0.107	0.092
d	*i*-Pr	CH_3	43	0.118	0.051	0.067
e	*i*-Pr	H	49	0.121	0.059	0.062
f	CH_3	*t*-Bu	58	0.219	0.127	0.092
76a	H		45	0.209	0.094	0.115
b	CH_3		57	0.185	0.105	0.080

strain model. However, as mentioned previously for cyclohexanones, the possibility exists that these reactions are occurring through the twist boat conformation. In methylenecyclohexane, Anet using force-field methods determined that the various boat and twist-boat conformations are only 5-6 kcal/mol less stable than the chair conformation.[124]

The study of π-facial reactivity has also been carried out by determining relative rates. As mentioned previously in Section 2.1, Fraser measured the relative rates of acid catalyzed addition of $H_2{}^{18}O$ to the α-methyl, -methoxy and -chloro derivatives of **44** to investigate the app effect.[76] The study revealed a large rate retardation for antiperiplanar attack to the axial methyl ($\Delta\Delta G^{\ddagger}$ = 2.3 kcal/mol) in ketone **45** and the axial chloro ($\Delta\Delta G^{\ddagger}$ = 2.8 kcal/mol) in ketone **48** relative to the unsubstituted bridged biaryl ketone **44**. Interestingly, Fraser and coworkers found only a slightly greater rate retardation for the diaxial dimethyl derivative ($\Delta\Delta G^{\ddagger}$ = 2.7 kcal/mol). Lastly, the study revealed an extremely small rate retardation for an axial methoxy group ($\Delta\Delta G^{\ddagger}$ = 0.2 kcal/mol). Assuming additivity and steric effects were dominant, the data indicated that the value for the app effect (i.e. the Cieplak hyperconjugative effect) was only 0.4 and 0.7 kcal/mol for the axial methyl and chloro substituents, respectively, and a maximum of 0.2 kcal/mol for the axial methoxy substituent.

In addition to the above study, Senda *et al.* in 1993 measured the competitive rates of lithium aluminum hydride reduction of 2,2-disubstituted conformationally locked cyclohexanone derivatives.[125] The results are given below in Figure 4.1 and were explained in terms of Cieplak's proposal. Thus, since the electron donating ability is assumed to be C-H>C-C>C-O, replacement of the 2-axial hydrogen with a methyl or a methoxy group leads successively to a decrease in axial attack. Molecular mechanics calculations, determined that the steric environment for axial attack of the four cyclohexanone derivatives are essentially identical and therefore steric effects were not considered.

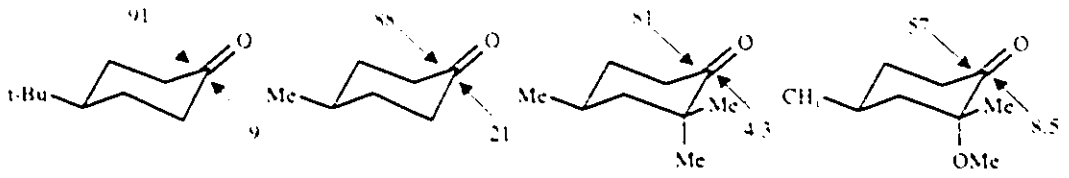

relative k_{ax}	100	97	89	63

Figure 4.1 Relative rates of addition for axial (ax) and equatorial attack.

The earliest study employing competitive rate kinetics was performed by Eliel and Senda in 1970.[25] They reported marginal changes in the rates of addition of lithium aluminum hydride and sodium borohydride to the axial and equatorial face of 2,2-dimethyl-4-*t*-butylcyclohexanone relative to 4-*t*-butylcyclohexanone. Eliel made no specific conclusions as to the origin of these results. In both the Eliel[25] and Senda[125] studies the reactions involved the total consumption of LAH (i.e. consumption of all four hydrides). Thus both these studies assumed that total disproportionation had occurred. An additional limitation is that both studies ignore steric effects in these 2,2-disubstituted cyclohexanone models.

To reiterate, the use of our bridged biaryl ketone offers several advantages over the previously mentioned systems. It allows for the determination of relative rates for α-derivatives possessing a wide range in induction and polarizability. Secondly, two diastereomeric α-derivatives can be prepared in which the substituents are oriented in a relatively fixed antiperiplanar (app) and anticlinal (ac) geometry relative to the incoming hydride. The app substituent allows for a direct assessment of the importance of the app effect, while the ac substituents provide a standard reactivity which because of the poor orbital-orbital alignment is only influenced by steric, torsional and/or electrostatic effects (i.e. classical effects). Thirdly, there will be a minimal amount of direct steric interaction between the incoming hydride and the app or ac substituent in the transition state and thus

steric effects will be assumed to be small. Lastly, as confirmed by molecular mechanics, our model ketone provides greater rigidity than cyclohexanone and it does not allow for the possibility of the reaction occurring through an additional conformation.[78,79]

The use of competitive kinetics provided reproducible results. It avoided the above noted complications associated with determining absolute rates which lessen both accuracy and precision.

The following sections will discuss the mechanisms for the three reactions under study.

4.1.1 Reductions using Lithium Aluminum Hydride in Tetrahydrofuran

Hitherto, the exact mechanism of the lithium aluminum hydride reduction of ketones remains essentially unknown. Nevertheless, much is known about this extremely common reaction.

In the concentration range of 10^{-5}-10^{-1} M, where all of our competitive reduction experiments were carried out, LAH is known to consist mainly of solvent separated ion pairs (77) in THF.[120]

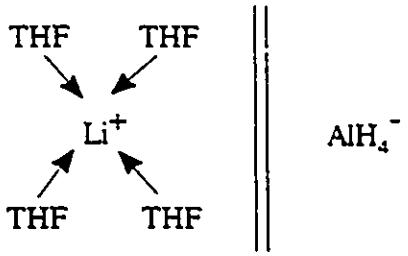

77

A complication in the mechanism of this reducing agent is that there are actually four separate reducing agents possible. That is, a molecule of ketone can react with LAH to generate a monoalkoxyaluminohydride species. This reducing agent can, in turn, react

with another molecule of ketone to afford the corresponding dialkoxyaluminohydride species and so on until all 4 hydrides have been consumed (see equations 7-10).

$$LiAlH_4 + \text{C=O} \xrightarrow{k_1} LiAl(OR)H_3 \qquad [7]$$

$$LiAl(OR)H_3 + \text{C=O} \xrightarrow{k_2} LiAl(OR)_2H_2 \qquad [8]$$

$$LiAl(OR)_2H_2 + \text{C=O} \xrightarrow{k_3} LiAl(OR)_3H \qquad [9]$$

$$LiAl(OR)_3H + \text{C=O} \xrightarrow{k_4} LiAl(OR)_4 \qquad [10]$$

Kinetic studies on mesityl phenyl ketone (**78**) and camphor (**79**) revealed the reaction to be first order in both ketone and LAH.[126,127] Interestingly, in diethyl ether, monomeric LAH was observed to be in equilibrium with dimeric LAH, with the dimer being the reactive species for mesityl phenyl ketone and both the monomer and dimer being the reactive species for the benzophenone derivatives **80** and **81**.[128]

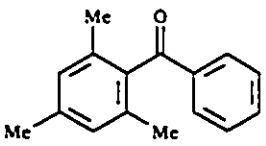

78

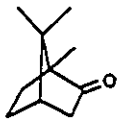

79

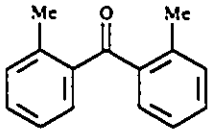

80

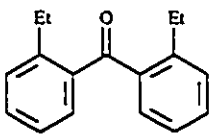

81

Studies by Eliel[129] and Brown[130] indicated that the intermediate reducing agents $LiAl(OR)_nH_{4-n}$ (n = 1 to 3) are stable to disproportionation when used for aldehydes, but unstable for ketones. For example, Eliel observed that in the reduction of 3,3,5-trimethylcyclohexanone, the diastereoselectivity was only minimally affected by varying

the ketone:LAH ratio. Thus, due to the increased bulk of the alkoxyaluminohydrides, Eliel and Haubenstock assumed that such species, if present, should result in significantly greater diastereoselectivities. It was concluded that secondary alkoxyaluminohydrides disproportionate rapidly to regenerate LAH (see equations 11 and 12), the only reducing agent that undergoes reaction with the substrate. However, later ^{27}Al and ^{13}C NMR studies in THF at room temperature provided evidence that for $LiAl(OR)_nH_{4-n}$ (n = 1 and 2, OR being primary, secondary or tertiary) disproportionation occurs readily with the extent being greatest for monalkoxy derivatives.[131] However, this study does not allow for an estimate of the relative rate of disproportionation versus the rate of reduction. In order for LAH to be the sole reducing agent, the rate of disproportionation must be much greater than the rate of reduction. In addition, the degree of disproportionation is reduced with increasing cation size, solvent polarity and reduction temperature.[132] Earlier studies by Brown[130a] on the addition of *t*-BuOH to LAH and subsequent studies by Barron[133] suggest that tetraalkoxy aluminohydride species cannot be formed. Apparently, too much steric strain is introduced about the aluminum atom. Therefore, disproportionations leading to aluminum tetraalkoxides are not considered.

$$2LiAl(OR)H_3 \longrightarrow LiAlH_4 + LiAl(OR)_2H_2 \qquad [11]$$

$$LiAl(OR)_2H_2 + LiAl(OR)H_3 \longrightarrow LiAl(OR)_3H + LiAlH_4 \qquad [12]$$

Both the rate and the stereoselectivity of the reduction of ketones are dependent on the cation M^+ in $MAlH_4$.[126,134] Several studies have also shown that ketones associate with Li^+ and that the rate of reaction with LAH is suppressed when a cation complexing agent is employed.[120,127,135] These facts suggest that the Li^+ cation is complexed to the carbonyl group in the transition state.

Kinetic isotope studies by Ashby[126] and Smith[127,128] on the LAH reduction of several benzophenone derivatives in THF and Et_2O show a k_H/k_D value of approximately

1.3. k_H/k_D represents both primary and secondary kinetic isotope effects and thus the small magnitude may be rationalized as consistent with a rate-determining step involving the transfer of hydride from the aluminum to the carbonyl carbon via an early reactant-like transition state, as predicted by the Hammond postulate for exothermic reactions.[37]

The consolidation of all the above facts led Ashby *et al.* in 1976 to propose the mechanism depicted in Figure 4.2.[126] For example for acetone, the first step involves the complexation of LAH to the carbonyl and displacement of one molecule of THF. The AlH_4^- ion then attacks the substrate at a Bürgi-Dunitz angle[14] to generate the corresponding bridged monoalkoxyaluminohydride **82**. Compound **82** can in turn react successively with three additional molecules of acetone in a similar fashion or disproportionate to regenerate LAH or some combination thereof. As noted above, the dialkoxy species may also undergo disproportionation.

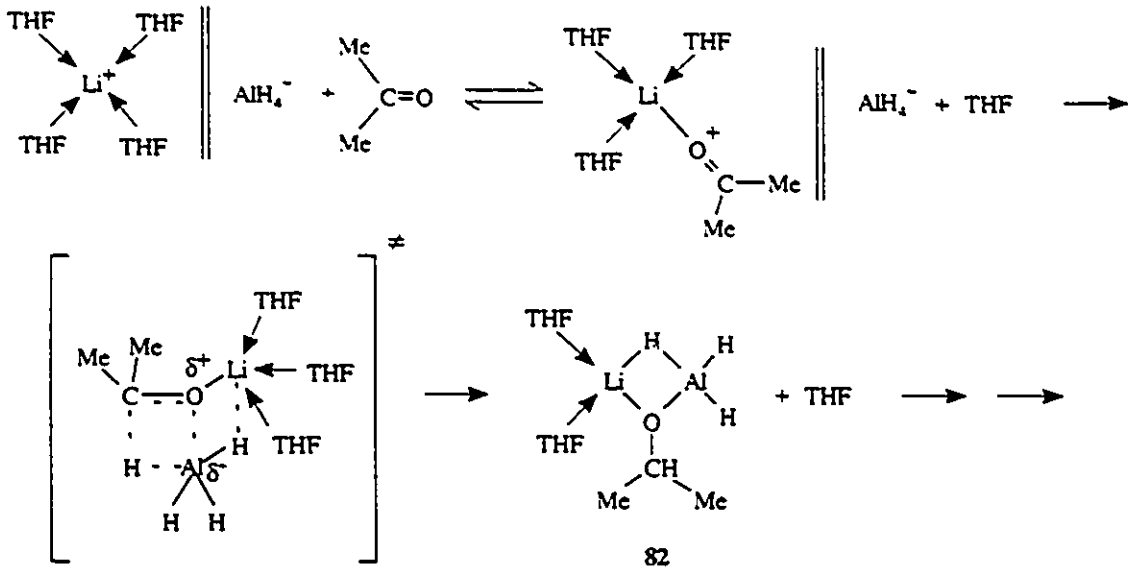

Figure 4.2 Proposed mechanism for the reduction of ketones with LAH in THF.

4.1.2 Reductions using Sodium Borohydride in Isopropanol

As for reductions involving LAH, the reduction of ketones with sodium borohydride involves, assuming a four to one ratio of ketone to SBH, four distinct

reducing agents. However, the mechanism is significantly simplified. Kinetic studies on the reduction of ketones with SBH in isopropanol show the reaction to be first order in both ketone and SBH with the transfer of the first hydride being the rate determining step (see equations 13-16).[29,121,136] Wigfield has shown that the alkoxy groups attached to

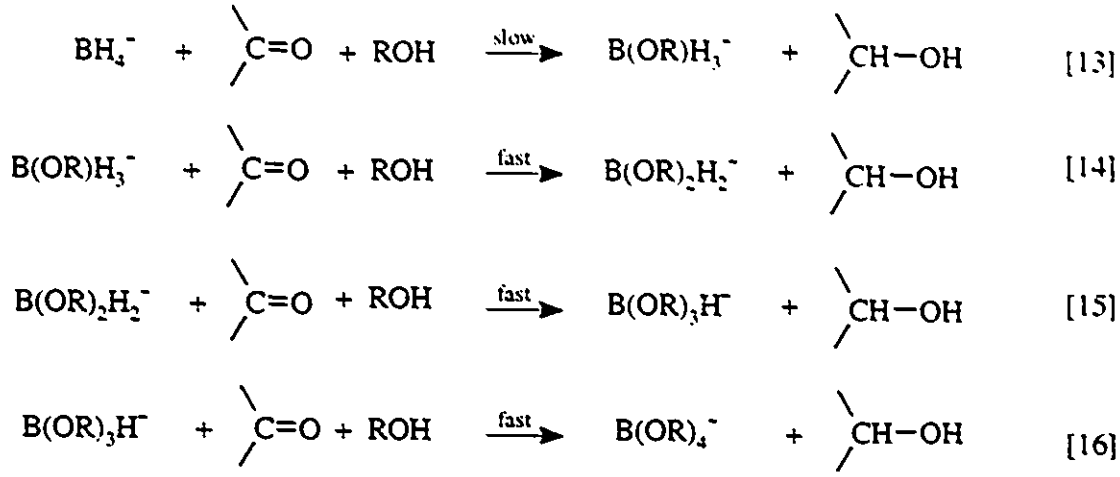

[13]

[14]

[15]

[16]

boron in the final product ($NaB(OR)_4$) are derived from the alcoholic solvent and not from the ketone.[136a] In the same paper, Wigfield observed that no exchange occurs between $NaB(OR)_4$ and the solvent R′OH when R and R′ are secondary, but does occur when they are primary. Thus, the fact that no exchange of alkoxy groups is observed for secondary alcohol solvents leads to the conclusion that any proposed mechanism must have the alkoxy groups in the product originating from the solvent in the initial reaction and not from subsequent exchange.

In 1978, Wigfield and Gowland reduced the ketones cyclohexanone and 3,3,5,5-tetramethylcyclohexanone with a mixture of SBH and $NaBD_4$ and found no mixed intermediates $NaBHD_{4-n}$ (n = 1-3).[137] They concluded that no disproportionation had occurred for the monoalkoxyborohydride species, but it subsequently reacts with another molecule of ketone to produce the corresponding dialkoxyborohydride intermediate (see equation 14). However, these experiments did not establish whether the dialkoxy or

trialkoxy intermediates are stable to disproportionation. Interestingly, Rickborn found modest changes in stereoselectivity as the reaction proceeded for some ketones, while other ketones exhibited no such changes.[29] Thus a modest amount of disproportionation may be occurring. Subsequent studies by Malmvik *et al.* found using ^{11}B NMR spectroscopy that acyloxyborohydrides in diglyme show a small degree of disproportionation, the system requires at least 12 hours to reach equilibrium (see equations 17 and 18).[138]

$$2NaB(OCOR)H_3 \overset{K_1}{\rightleftharpoons} NaB(OCOR)_2H_2 + NaBH_4 \qquad [17]$$

$$2NaB(OCOR)_2H_2 \overset{K_2}{\rightleftharpoons} NaB(OCOR)H_3 + NaB(OCOR)_3H \qquad [18]$$

$K_1 = 19$ ~12 h to reach equilibrium
$K_2 = 0.7$ ~48 h to reach equilibrium

For sodium borohydride/isopropanol reductions of ketones, the sodium cation does not participate in the transition state. This conclusion was based on the evidence that removal of Na^+ with crown ethers do not influence the reaction and, secondly, only a negligible increase in the rate of reduction was observed after the addition of NaI, while the addition of Li^+ caused a large increase.[135a,139]

Kinetic isotope studies on the SBH reduction show the value to be ~0.7.[121b,140] As in the LAH case, k_H/k_D represents a combination of primary and secondary kinetic isotope effects and thus the inverse value may be explained as consistent with an early, late or non-linear transition state.[141] However, based on Hammett ρ values, one of which had a known Bronsted coefficient, of SBH reductions and the value measured for an essentially symmetric Meerwein-Ponndorf reduction[142], Wigfield concluded that the transition state

was ~60-70% along the reaction coordinate.[143] A possible transition state that is consistent with the aforementioned evidence is shown in Figure 4.3.

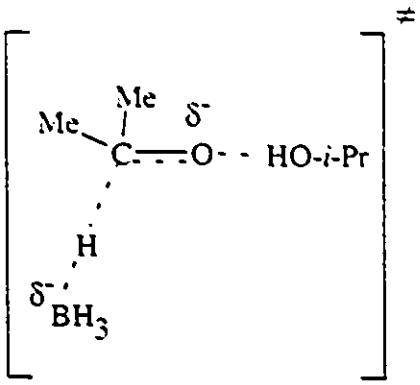

Figure 4.3 Proposed transition state for sodium borohydride reduction in isopropanol.

4.1.3 Boron Trifluoride Etherate Catalyzed Reductions using Triethylsilane

In order for a carbonyl group to be reduced by organosilanes, an acid catalyst such as trifluoroacetic acid or boron trifluoride etherate must be employed to activate the carbon atom of the carbonyl group. In contrast to TFA catalyzed triethylsilane reductions, BF_3•Et_2O catalyzed reductions provide no evidence for the presence of alkyl silyl ethers either during or following the reaction.[144] This fact led Doyle in 1976 to put forward two possible mechanisms (see Figure 4.4).[145] The reduction of carbonyl compounds (e.g. R_2C=O) at room temperature with Et_3SiH/BF_3•Et_2O occurs rapidly with BF_3 consumption yielding mainly borate esters and the oxidation product triethylsilylfluoride (Et_3SiF). The borate ester is subsequently hydrolyzed under acid or base catalysis to the corresponding alcohols. In order for all starting ketone to be consumed, the reaction requires a ketone:BF_3•Et_2O ratio of ≤3:1. As this ratio increases, a competing reaction leading to the symmetrical ether (e.g. R_2C-O-CR_2) becomes prominent.

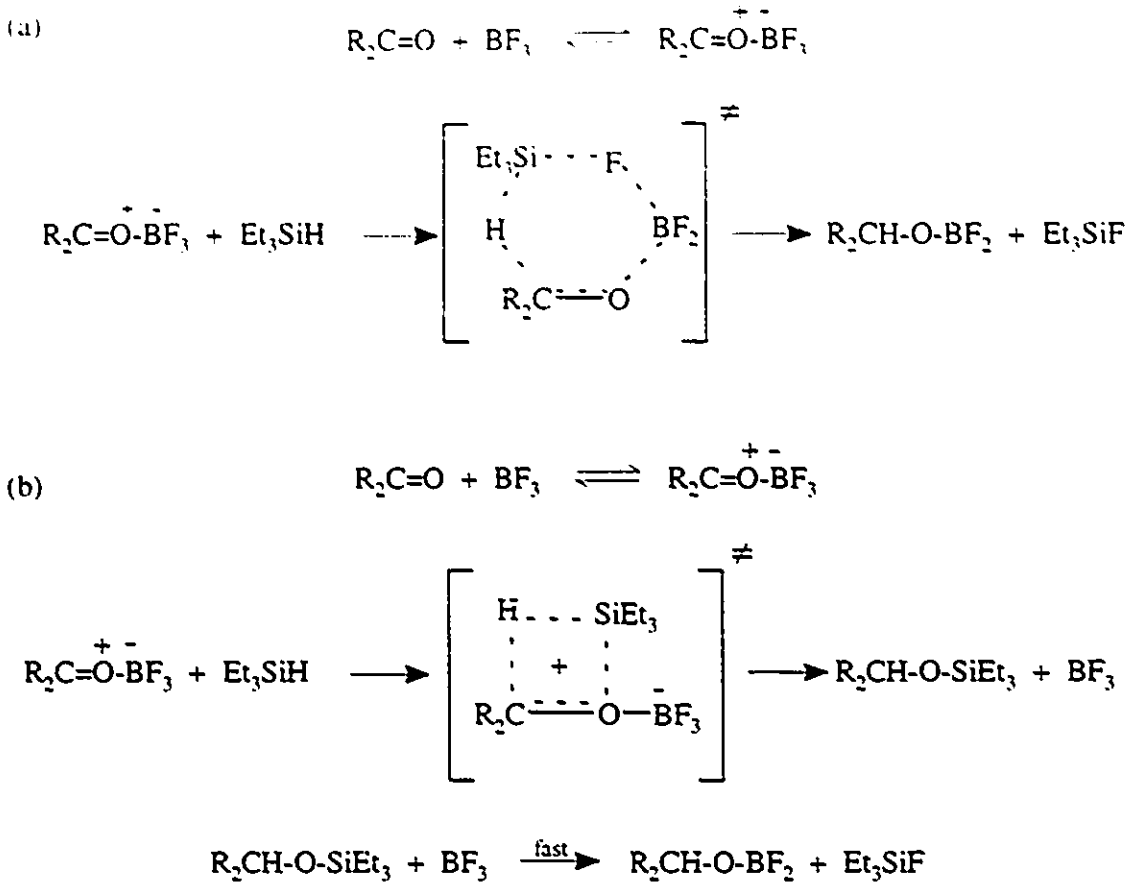

Figure 4.4 Proposed mechanisms for the reduction of ketones using Et_3SiH/BF_3-Et_2O .

If a chiral reducing agent is employed (e.g. R^*_3SiH), then in mechanism a, where hydride and fluoride transfer from silicon occur in a concerted fashion via a cyclic six-membered transition state, retention of configuration at silicon is expected to occur. For mechanism b, the overall reaction is assumed to lead to stereochemical inversion at silicon since the initial hydrosilylation is expected to occur via retention, while the second step is known to occur with inversion.[146] Reduction of acetone with (+)-α-naphthylphenylmethylsilane/BF_3-Et_2O yielded (-)-naphthylphenylmethylsilane in 11±2% ee and thus Doyle concluded that mechanism b was consistent with this result. However, at a molar ratio of acetone:BF_3-Et_2O of less than one, where all of our competitive reduction

study was performed (see Section 4.2.3). Doyle found only racemic α-naphthylphenylmethylsilane and thus this conclusion appears to be somewhat speculative

4.2 Results

4.2.1 Competitive Rates using Lithium Aluminum Hydride

In order to allow a direct comparison of our relative rate data, conditions were sought to limit the involvement of di- and trialkoxyaluminohydride reducing agents. More precisely, we sought to limit the consumption of available hydride to ≤50% since previous evidence indicated that the monoalkoxyaluminohydride species readily undergo disproportionation and thus LAH would be the effective reducing agent. Indeed, initial studies on the axial methyl derivative **45** showed that under sufficiently dilute conditions (a total of 0.050 mmol of ketones in 4 mL of THF), the involvement of $LiAl(OR)_2H_2$ and $LiAl(OR)_3H$ could be minimized.[147] In an attempt to limit the participation of the alkoxyaluminohydrides species further, Fraser *et al.* performed several competitive reduction experiments in the presence of water. It was reasoned that the presence of H_2O might quench the reaction *in situ* before the di- and trialkoxyaluminohydrides react with the substrate ketone. However, this investigation only led to irreproducible results. It was concluded that the water only partially reacted with the various reducing agents present to yield a complex mixture of polymeric oxygen bridged aluminohydrides. Accordingly, this route was not further pursued.

In an attempt to decipher the complexities associated with this reduction, low temperature 75 MHz ^{13}C NMR studies were conducted. However, even at -78°C, the monalkoxyaluminohydrides of cyclohexanone or 1,3-diphenylacetone could not be observed. More precisely, even after the preparation of samples containing 1 equiv of LAH and 0.25 equiv of ketone at -78°C and rapid the acquisition of 75 MHz ^{13}C NMR spectra (512 transients or 7.5 minutes), we were unable to observe the presence of the

monoalkoxyaluminohydride species. Thus it appears that the reduction of ketone is exceedingly rapid with its half-life being less than 2 minutes. However, as before this study did not provide information about the relative rate of disproportionation versus the rate of reduction. In addition, a significant number of unexpected absorbances were observed. It was concluded that a complex mixture of various possible aggregates had formed and thus, unfortunately, no additional information could be obtained without a more thorough investigation (e.g. labeling studies). However, this route was not followed.

The competitive rates measurements were normally employed using a 1:1 ratio of the α-derivative (i.e. **45-53**) and the unsubstituted bridged biaryl ketone **44** with a total amount of ketones of 0.050 mmol. After the addition of a standardized solution of LAH (0.00625 mmol), which if totally consumed would reduce 50% of the ketones present, the reaction mixture was quenched after 20 sec with HCl and analyzed using 500 MHz ^{1}H NMR spectroscopy. The relative rate constants were then calculated by employing equations 19-21, where $[A]_o$ and $[B]_o$ and [A] and [B] represent the initial and final

$$\frac{k_B}{k_A} = \frac{\log ([B]_o / [B])}{\log([A]_o / [A])} \qquad [19]$$

$$[A]_o = [A] + [C] \qquad [20]$$

$$[B]_o = [B] + [D] + [E] \qquad [21]$$

[C] = unsubstituted alcohol product (i.e. **65**)

[D] = axial or equatorial major alcohol product (i.e. **66** or **68**)

[E] = axial or equatorial minor alcohol product (i.e. **67** or **69**)

concentration of A (unsubstituted ketone **44**) and B (α-derivative **45-53**), respectively, under study. More precisely, the assumption was made that the reactions are first order in ketone and the same order in reducing agent. Details of the competitive rate experiments are presented in Appendix 2.

For example in entry 7 of Table 4.2, employing a 1:1 mixture of **44**:**45** and quenching with acid after 20 seconds yielded the mixture of three alcohols (**65**, **66a** and **67a**) and unreacted starting ketones **44** and **45** shown in Figure 4.5. Since each ketone and alcohol had been previously characterized, each component could be readily identified (see Figures 4.6-4.10). Measurement of the integral ratios for the absorption of **44** versus **65** and **45** versus **66a** and **67a** afforded the required relative concentrations, which after substitution into equation 19 provided the relative rate constant of 0.412.

Kinetic studies by Smith and Wiegers determined that the reduction of camphor was complete within one minute under the concentrations employed in our study.[127] Thus, given the fact the lithium aluminum hydride reductions are exceedingly rapid, the possibility that our competitive study may be diffusion controlled was considered. Under these circumstances, added LAH might react with the faster reacting ketone at the point of initial contact and then may react with the slower ketone before further access of the faster reacting ketone occurs. Thus the competitive rate ratio will not reflect the true ratio of rate constants, but will reflect a concentration ratio. In order to test for this possibility, we repeated the competitive reduction of the axial α-methyl ketone **45** versus **44** (see Table 4.2). However, unlike our initial competitive runs, the initial ratio of **45**:**44** was changed to ~3:1 and ~1:3 (see entries 1-4, 6 and 8 in Table 4.2). The results revealed an average increase of only 3.5% (average $k_{45}/k_{44} = 0.419$) for the 1:3 ratio and an average decrease of 19% (average $k_{45}/k_{44} = 0.328$) for the 3:1 ratio and therefore it was concluded that the lithium aluminum hydride reductions are not under diffusion control and hence the calculated relative rates represent the true ratio of rate constants.

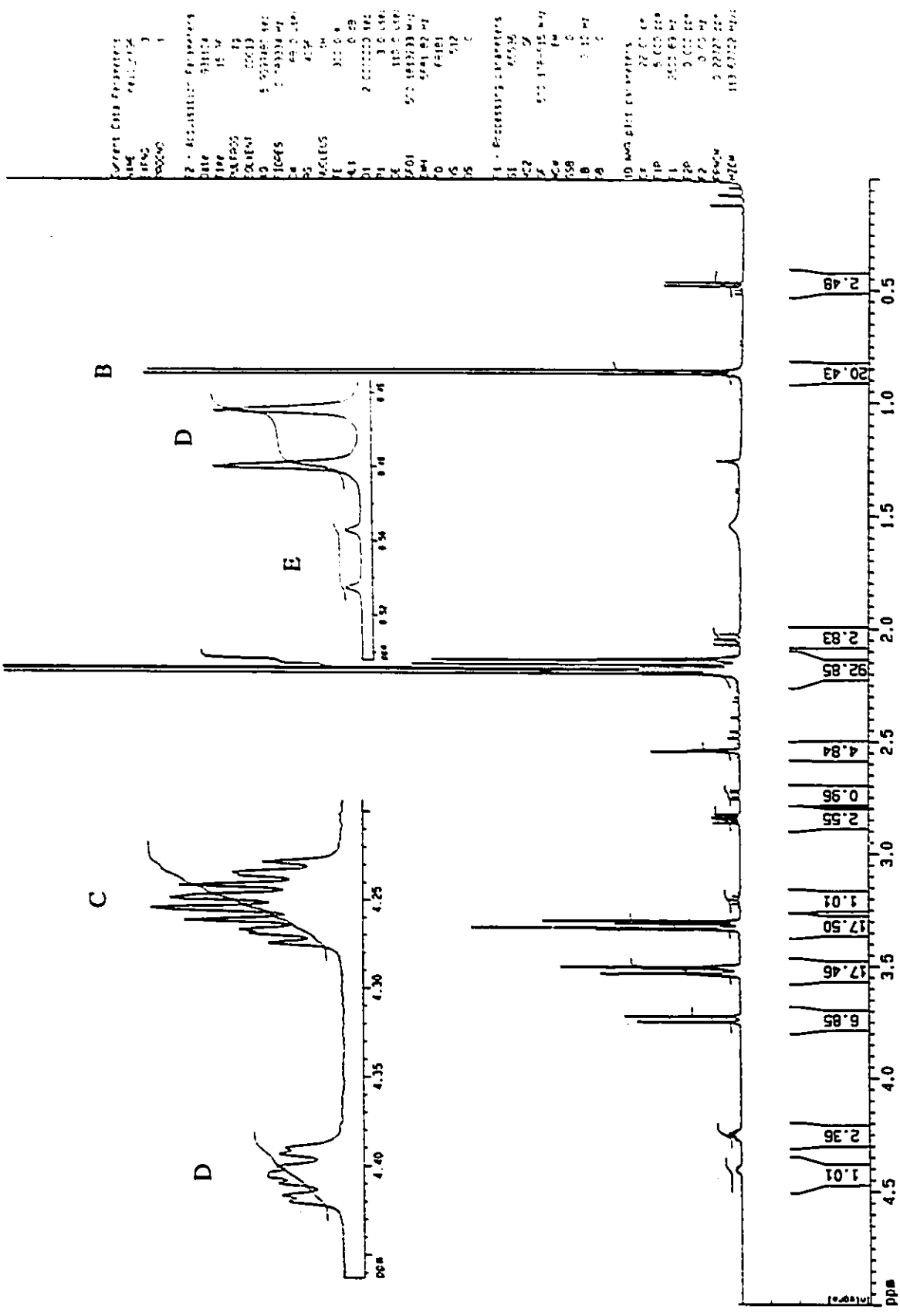

Figure 4.5 The 500 MHz ^{1}H NMR spectrum in $CDCl_3$ for the competitive reduction of entry 7 in Table 4.2.

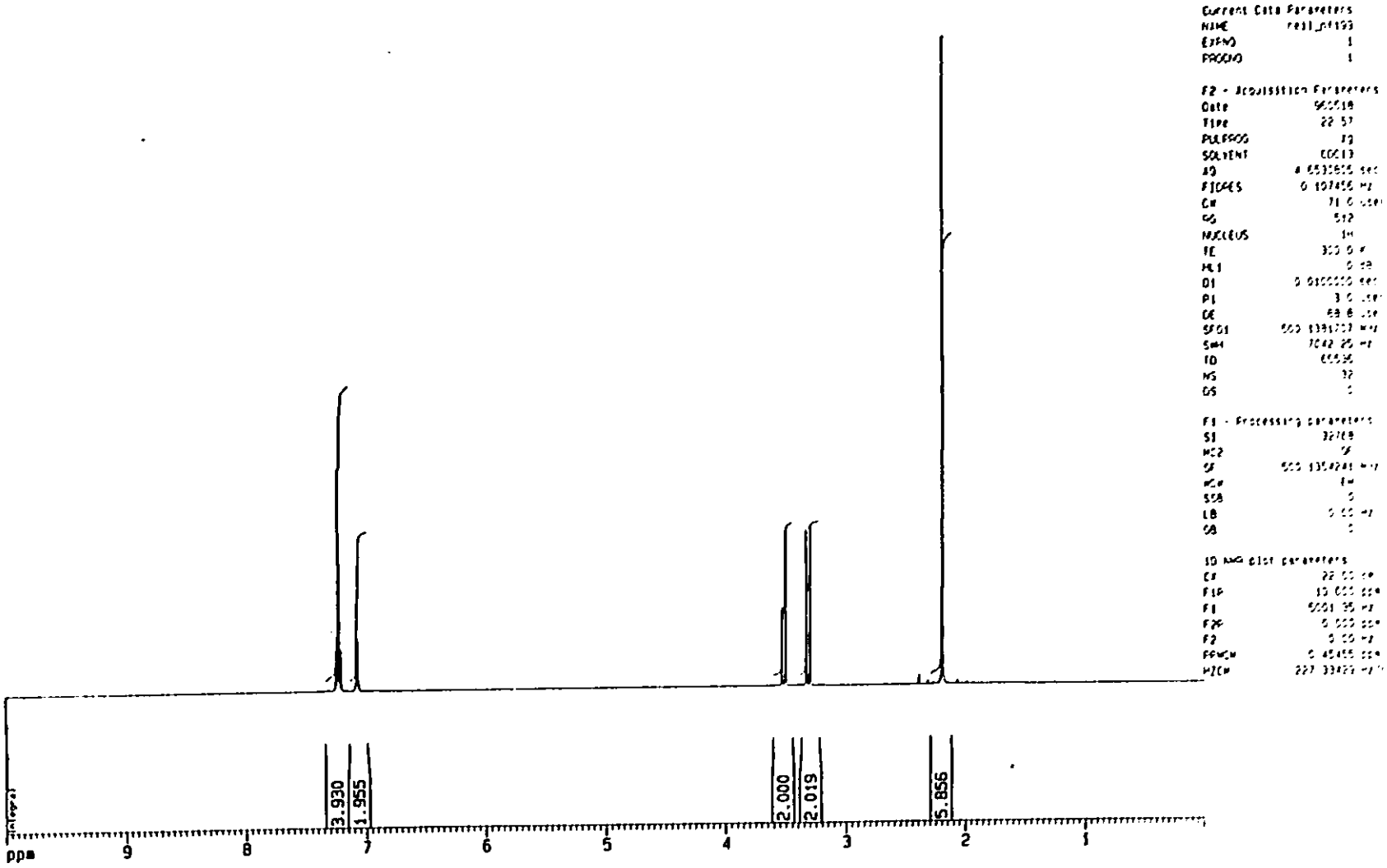

Figure 4.6 The 500 MHz ^{1}H NMR spectrum of the unsubstituted ketone 44 in $CDCl_3$.

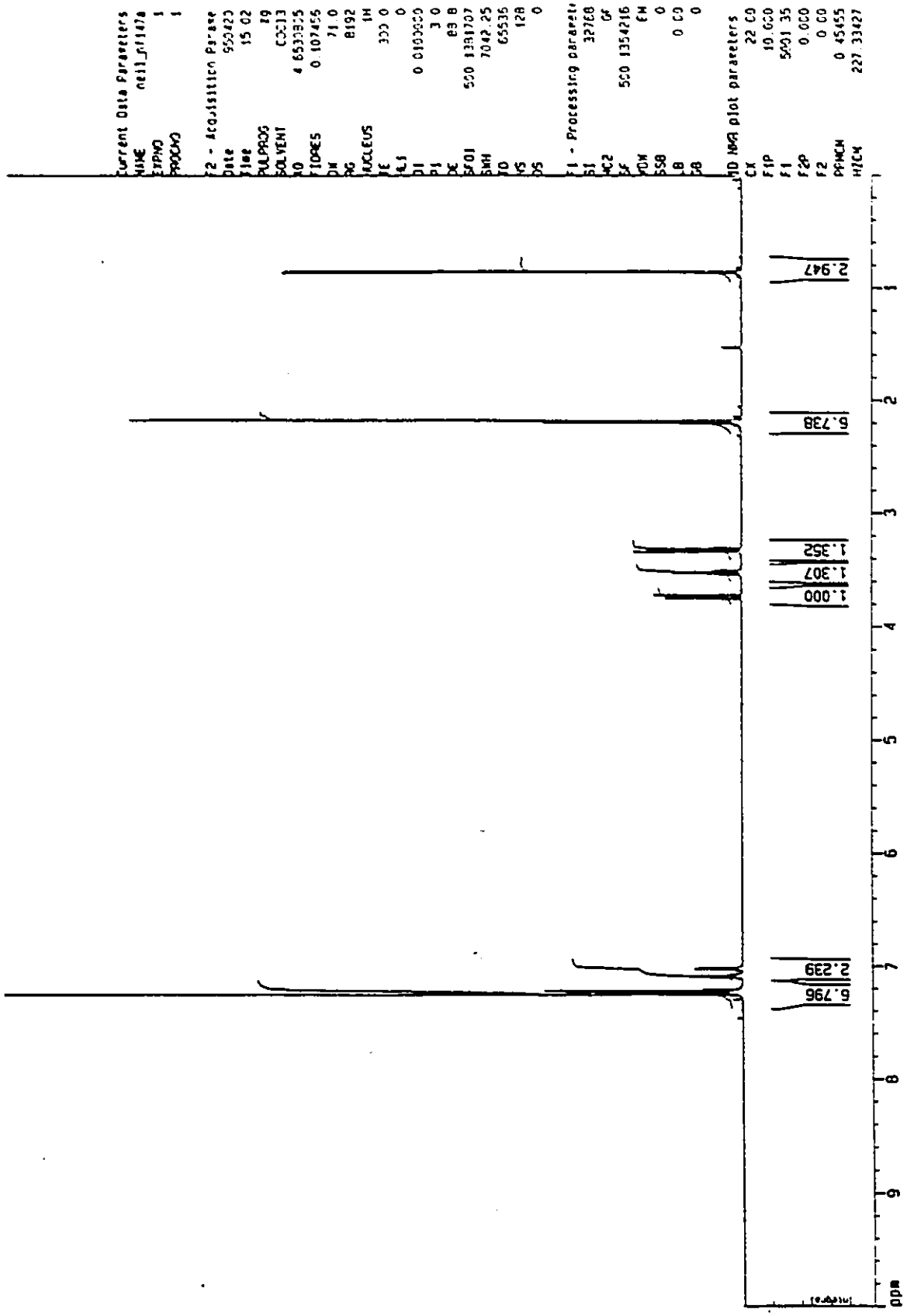

Figure 4.7 The 500 MHz ^{1}H NMR spectrum of the axial α-methyl ketone 45 in $CDCl_3$.[*]

[*] The crystalline sample contained 13.7% of the unsubstituted ketone 44 and thus the required amounts of 44 and 45 were adjusted as necessary.

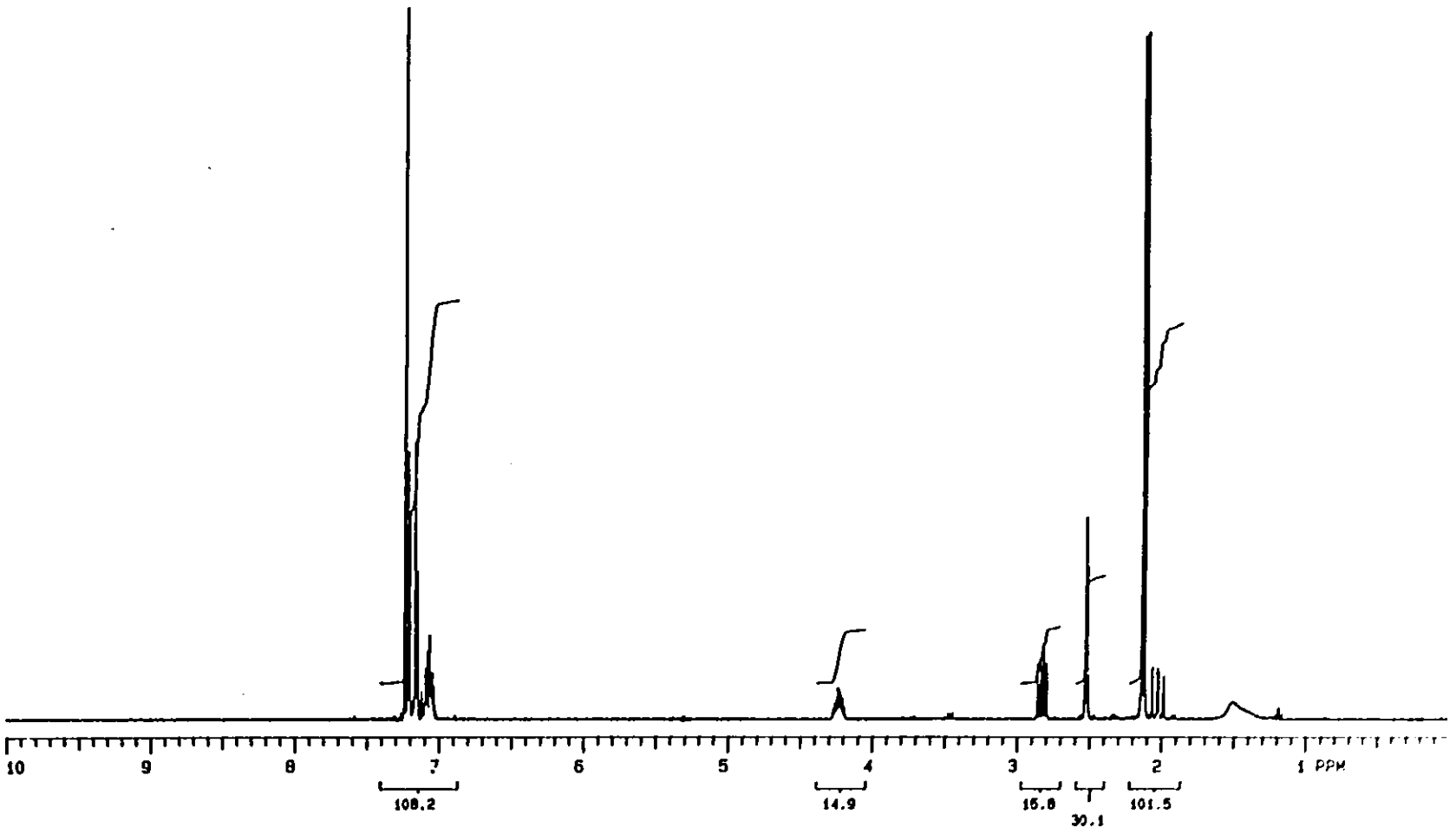

Figure 4.8 The 300 MHz ^{1}H NMR spectrum of the unsubstituted alcohol 65 in $CDCl_3$.

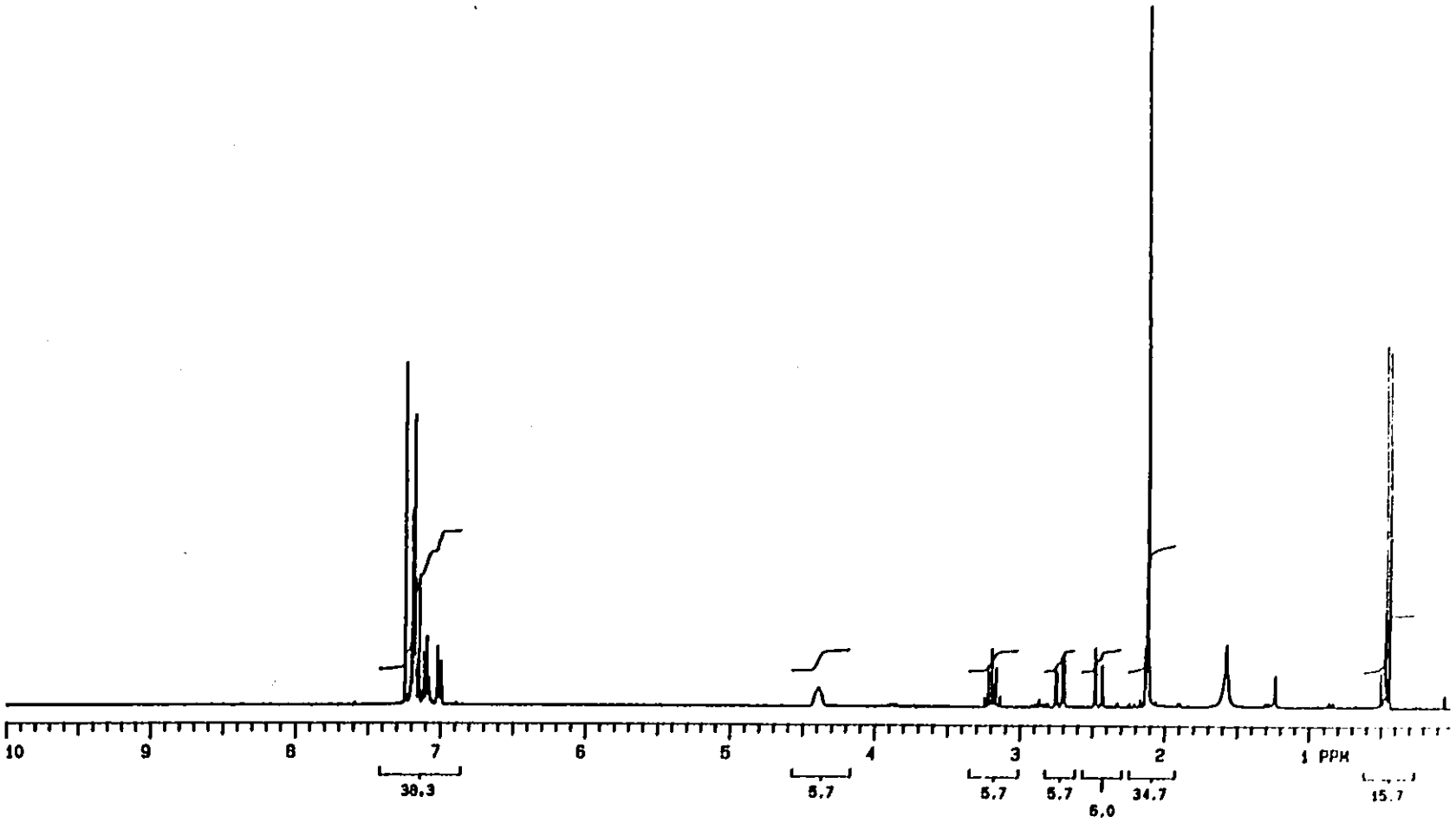

Figure 4.9 The 300 MHz ^{1}H NMR spectrum of the axial α-methyl major alcohol 66a in $CDCl_3$.

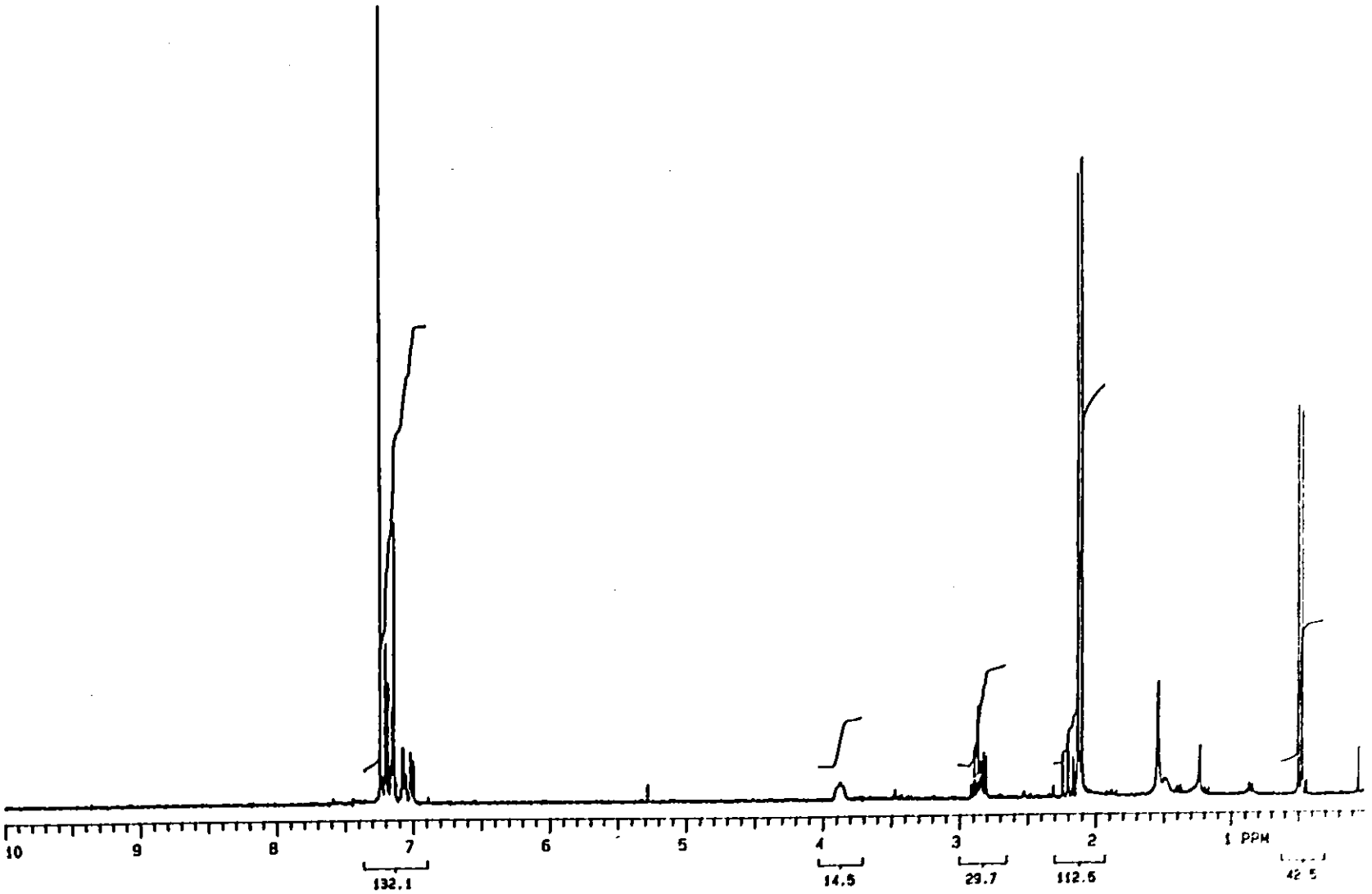

Figure 4.10 The 300 MHz ^{1}H NMR spectrum of the axial α-methyl minor alcohol 67a in $CDCl_3$.

Table 4.2 Competitive reduction of ketones 44 versus 45 with LAH in 4 mL THF at 0 °C (20 sec quench, 0.05 mmol of total ketones).

Entry	Ketone 44: Ketone 45	$LiAlH_4$ mmol	% 44 reduced	% 45 reduced	% Total Hydride Consumed	k_{45}/k_{44}
1	1:2.7	0.006	45	22	58	0.410
2	1:2.6	0.003	51	30	74	0.488
3	1:1.7	0.00275	63	32	87	0.388
4	1:2.7	0.006	54	26	69	0.391
5	1:1.1	0.006	34	15	50	0.398
6	2.8:1	0.006	23	9.0	29	0.333
7	1:1	0.006	30	14	38	0.412
8	3.1:1	0.006	22	7.6	40	0.322

[a] 0.025 mmol of total ketones in 10 mL. [b] 0.022 mmol of total ketones.

The decrease in relative rate constants for entries 6 and 8 may be due to incomplete disproportionation and thus involvement of alkoxyaluminohydride ions. It appears that the alkoxyaluminohydride species for the unsubstituted ketone are more stable towards disproportionation. Perhaps the presence of the α-methyl group in 45 introduces steric strain and thus facilitates disproportionation. Overall, it seems that the alkoxy reducing agents are even more reactive towards 44 than LAH itself and thus k_{45}/k_{44} decreases.

Employing the above reasoning, the results from entries 1-5 and 7 should be the most accurate. Accordingly, these results were used to obtain the required $k_{CH_3}^{app}/k_H$ which represents the relative rate for attack app to the α-methyl group relative to hydrogen and thus provides a direct test for the importance of the app effect as put forward by Anh[13] or Cieplak[40]. Entries 1-5 and 7 provided an average relative rate of

0.415. However, since the unsubstituted ketone **44** possesses two equivalent carbonyl faces, k_B/k_A (k_{45}/k_{44}) must be multiplied by two in order to compare the reactivity with respect to one face (see equation 22). As shown in Table 4.4, the average π-facial selectivity for ketone **45** was 11.9. Thus since the rate for attack of **45** represent the sum of antiperiplanar (app) and synperiplanar attack (sp) (i.e. equation 23), the rate for app attack rearranges to equation 24. Substitution of equation 24 into equation 22 provides the facial reactivity for attack app to a methyl group relative to hydrogen (i.e. equation 25).

$$\frac{k_{CH_{3ax}}}{k_H} = 0.415 \times 2 = 0.830 \qquad [22]$$

$$k_{CH_{3ax}} = k_{CH_3}^{app} + k_{CH_3}^{sp} = 1.084 \times k_{CH_3}^{app} \qquad [23]$$

$$k_{CH_3}^{app} = \frac{k_{CH_{3ax}}}{1.084} \qquad [24]$$

$$\frac{k_{CH_3}^{app}}{k_H} = \frac{0.830}{1.084} = 0.77 \qquad [25]$$

As shown in entries 1-3 and 5 in Table 4.3, the face reactivity for the equatorial α-methylthio bridged biaryl ketone **50** was determined by employing a mixture of the axial (**46**) and equatorial methylthio derivatives of **44**. In our preliminary studies of this ketone system, it was noticed that as the initial ratio of the **50**:**46** decreased, the relative rates increased from 3.35 to 8.23. As for the axial α-methyl ketone **45**, it was assumed that as the **50**:**46** ratio decreased, the participation of higher order and presumably both more sterically encumbered and polar alkoxyaluminohydrides species becomes more prominent

and could exaggerate the difference in reactivity between these ketones. The runs employing an approximate 1:1 ratio of ketones in Table 4.3 were thought to best represent the relative rate.

Table 4.3 Competitive reduction of ketones 50 versus 46 with LAH in 4 mL THF at 0°C (20 sec quench, 0.05 mmol of total ketones).

Entry	Ketone 50: Ketone 46	$LiAlH_4$ mmol	% 50 reduced	% 46 reduced	% Total Hydride Consumed	k_{50}/k_{46}
1	1.55:1	0.0062	48	18	70	3.35
2	1:1.46	0.006	60	16	70	4.92
3	1:4.88	0.0064	81	18	57	8.23
4	1:1[a]	0.00576	71	19	80	5.97
5	3.8:1[b]	0.015[c]				≥25.7

[a] Sample contained 0.0159 mmol of 44. [b] 0.0297 mmol of total ketones. [c] Reducing agent 83 was employed, 2 min quench.

In order to test our above proposed explanation for the SCH_{3eq} competitive reduction studies, the competitive reduction using a 3.8:1 mixture of **50:46** was repeated, however, the dialkoxy reducing agent **83** was employed. Compound **83** was generated by reacting **44** with 0.5 equiv of LAH (see equation 26). Interestingly, the relative rate increased dramatically to ≥25.7. The use of the dialkoxy aluminohydride forces the reaction to take place through high order alkoxyaluminohydrides. Therefore the observed increase presumably reflects a selectively increased reactivity of the SCH_{3eq} ketone **50** to the dialkoxy and trialkoxy reducing agent. This difference, although apparent in the α-methyl derivative **45**, is much more enhanced in ketone **50**.

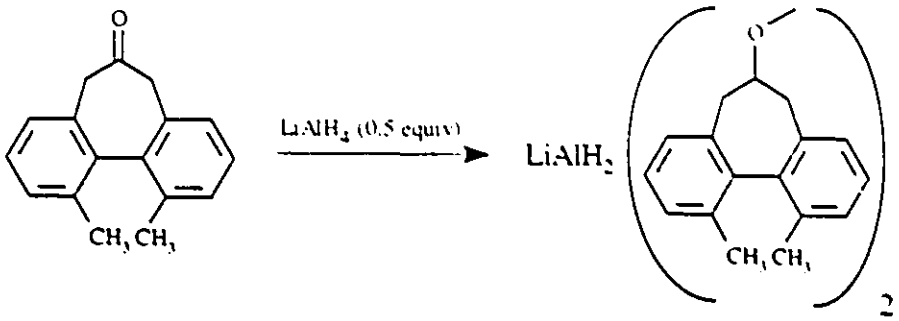

[26]

83

In order to corroborate our assumption, we repeated the competitive reduction of **46** and **50** in the presence of **44** and observed a relative rate of 5.97. The final result was obtained by taking the average of entries 2 and 4 (see Table 4.4). Because the competitive experiment in entry 4 of Table 4.3 was run in the presence of **44**, $k_{SCH_3}^{ax}/k_H$ could be calculated directly. The calculation of $k_{SCH_3}^{ax}/k_H$ from entry 4 yielded a value of 3.30, while via relay using k_{50}/k_{46} (see footnote in Table 4.4) yielded a value of 2.27. This difference likely reflects the inherent uncertainty associated with our method for the extremely concentration-sensitive equatorial α-SCH_3 ketone **50**.

The relative rates obtained for all of the remaining results showed no unusual behavior and were averaged and after application of their analogous equations 22-25 led to the final results listed in Table 4.4. Fortunately, the unexpected variability in the SCH_{3eq} ketone was not observed for these remaining substrates. Overall, in most instances we were able to limit the potential involvement of the trialkoxy species (i.e. <75% consumption of hydride) and in some instances the potential involvement of the dialkoxyaluminohydrides (i.e. <50% consumption of hydride). Nevertheless, we are quite confident in the validity of our results since previous results on the α-methyl derivative **45**, again, employing the reducing agent **83** showed only an approximate 15% change in the calculated relative rates.[147] As before, the use of **83**, presumably forces the reaction to occur through higher order alkoxyaluminohydrides.

Table 4.4 π-Facial reactivity[a] of the α-derivatives of 44 for reduction by LAH .

Substituent R	k_R/k_{44}	Number of Measurements	π-Facial Selectivity	k_R^{app}/k_H
H	-	-	1.0	1.0
CH_{3ax}	0.415	8	11.9	0.77
SCH_{3ax}	0.436	4	≥19	0.87
OCH_{3ax}	1.36	1	≥19	2.7
Cl_{ax}	2.81	1	≥19	5.6
				k_R^{ac}/k_H
CH_{3eq}	1.12	3	4.5	1.8
SCH_{3eq}	2.27	2	≥19	4.5[b]
OCH_{3eq}	4.07	2	≥19	8.1
Cl_{eq}	3.31	2	8.2	5.9
F_{eq}	3.68	4	7.6	6.5

[a] See experimental for precision. [b] Calculated via relay (i.e. $k_{SCH_3}^{ac}/k_H = k_{SCH_3}^{ac}/k_{SCH_3}^{app} \times k_{SCH_3}^{app}/k_H$).

4.2.2 Competitive Rates using Sodium Borohydride

As stated previously in the introduction (Section 4.1.2), the kinetics for the slower reacting SBH can be readily monitored. Wigfield, among others, found the reaction to be first order in ketone and SBH.[29,121,136] Isopropanol was chosen as solvent since it is less reactive towards SBH than either methanol or ethanol.[148] In order to determine whether our model ketone 44 was behaving as observed with other ketones in isopropanol, we

conducted preliminary rate studies on 1,3-diphenylacetone (84), an acyclic analogue of 44, and ketone 44.

For 1,3-diphenylacetone and 44, a 0.0318M and 0.00898M solution, respectively, in isopropanol was treated with SBH and quenched after 1.5, 15 and 180 minutes. The resulting solutions were worked-up and analyzed by 500 MHz ^{1}H NMR. The data for both ketones were treated by standard second-order kinetics and gave linear plots, although for 1,3-diphenylacetone the plot did not pass through the origin (see Figure 4.11). However, given the facts that the solutions for this preliminary investigation were not thermostated and the evaluation involved only three points, the results appear acceptable. The progress of the reaction is summarized in Table 4.5. From these data, it appears that fixing the two aromatic rings in ketone 44 causes an approximate 10 fold increase in reactivity.

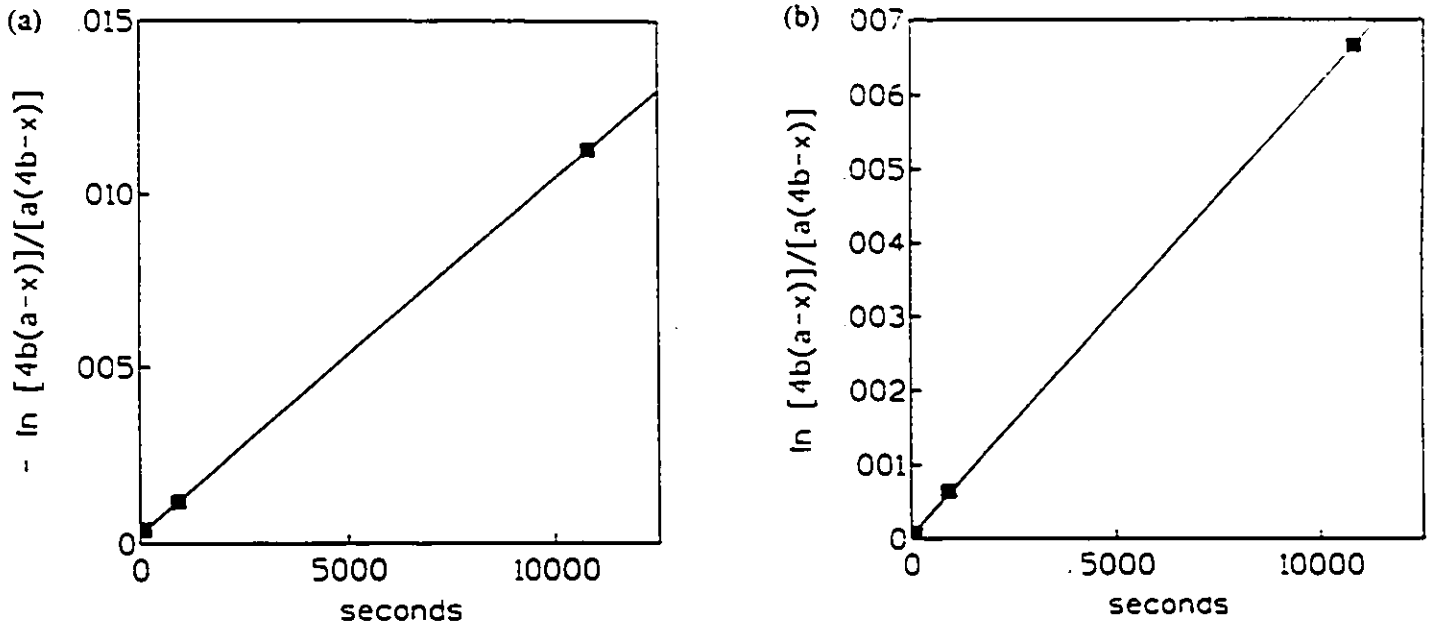

Figure 4.11 Kinetic plots for the reduction of (a) 1,3-diphenylacetone and (b) unsubstituted bridged biaryl ketone 44 by sodium borohydride (a = initial ketone concentration, b = initial borohydride concentration and x = concentration of ketone remaining at time *t*.

Table 4.5 Ketone reduction by SBH in isopropanol at rt.

Ketone	[M]	$NaBH_4$ [M]	Time (min)	% Ketone Reduced
			1.5	4.3
84	0.0318	0.00802	15	11.9
			180	56.7
			1.5	3.4
44	0.00898	0.00224	15	22.4
			180	74.8

Additionally, previous evidence indicated that the reduction normally occurs through a disproportionation mechanism and thus few alkoxyborohydride species participate in the reduction. If disproportionation occurs, one would expect the diastereoselectivity to increase as the reaction proceeds. Indeed, Rickborn[29] observed such an effect in the reduction of several substituted cyclohexanones. However, this behavior was not observed throughout the series of ketones studied. Accordingly, we were prompted to monitor the diastereoselectivity of compound **45** as a function of time, since it provided well separated and thus accurately integrated methyl doublets for the two alcohol products **66a** and **67a**. However, ketone **45** epimerized to the α-equatorial epimer **49** as the reaction proceeded. After three hours only 17% of the initial amount of **45** remained. As presented in Table 4.6, no change in selectivity within 5% was observed. Therefore since alkoxyborohydrides do not interconvert (i.e. disproportionate) these reducing agents appear to possess similar selectivities as SBH itself. Nevertheless, in order to minimize the possibility of interconversion, epimerization or rearrangement, conditions were adopted in our competitive study so as to keep the consumption of total hydride to no greater than 25%.

Table 4.6 Competitive Reduction of ketones 45 versus 44 for SBH in *i*-PrOH at rt.

Ketones (mmol)	$NaBH_4$ (mmol)	Quench Time (min)	% of Total Hydride Consumed	% of 45 Epimerized	π-Facial Selectivity
45 (0.0424) +	0.0123	1.5	0.37	< 0.5	6.0
44 (0.00713)		15	7.0	8.6	6.1
		60	20	67	5.8
		120	29	82	6.0
		180	38	83	6.4

The final results for the sodium borohydride reduction are given in Table 4.7 and represent the average for all runs shown in Appendix 2. For those cases where the π-facial selectivity was known, the data were treated as described for the LAH system. However, in contrast to the data for LAH, the relative rates for most entries were calculated by employing equation 27 where $[B]_o = [B] + [D]$. That is, because of the very low consumption of hydride, an accurate limit on the diastereoselectivity could not be determined due to poor signal to noise in the ^1H NMR spectra.

$$\frac{k_B}{k_A} = \frac{\log ([B]_o / [B]_o - [D])}{\log([A]_o / [A])} \qquad [27]$$

As long as the amount of reduction of ketone B remains low (i.e. <2%) and the diastereoselectivity is >1:1 (app:ac or ac:sc), knowledge of the diastereoselectivity is not required. If the stereoselectivity is included in the calculation, it would influence the relative rate constant by less than 1%. The initial experimental conditions such as ratio of ketones and quench time were based of the LAH results. The conditions were then adjusted as necessary to provide the optimum balance between the signal to noise ratio in

the ^1H NMR spectra and the amount of epimerization observed, while simultaneously attempting to keep the consumption of total hydride to <25%. Most competitive experiments were repeated twice and in those cases where a single result was obtained, our initial estimate of experimental conditions proved satisfactory and thus no additional adjustments were necessary (see Appendix 2). In the competitive experiments with the equatorial chloro ketone **52**, we were able to limit the consumption of hydride to ≤31% and in all other cases to ≤16%. Accordingly, we concluded that the data would be amenable for direct comparison.

For several of the entries noted in Table 4.7, epimerization of the α-substituted ketone was observed (see Appendix 2). In those instances a correction was made on the assumption that the rate of epimerization took place in a linear fashion. Thus an average value at the midpoint of the reaction was used for this epimerization correction. More specifically, the measured final concentration of B (α-substituted derivative of **44**), [B], was increased by the factor depicted in equation 28.

$$[B]_{corrected} = [B]_{measured} \times \frac{1}{1 - y/2} \qquad [28]$$

$$y = \frac{\text{per cent of initial } \alpha\text{-substituted ketone epimerized}}{100}$$

As before, in order to compare the reactivity with respect to one face of the unsubstituted bridged biaryl ketone **44**, the relative rates for k_R^{app}/k_{44} are obtained by multiplying by a factor of two. As noted above and in Table 4.7, the reactivities for **45**, **52** and **53** must be further subdivided in order to obtain the final facial reactivity.

Table 4.7 π-Facial reactivity[a] of the α-derivatives of 44 for reduction by SBH.

Substituent R	k_R/k_{44}	Number of Measurements	π-Facial Selectivity[b]	k_R^{syn}/k_H
H	-	-	1.0	1.0
CH_{3ax}	0.114	2	6.5	0.20
SCH_{3ax}	0.390	2		0.78
OCH_{3ax}	8.18	1	≥19	16.4
Cl_{ax}	40.0	2	≥19	80
				k_R^{ac}/k_H
CH_{3eq}	0.454	2	~2	0.91
SCH_{3eq}	4.34	1	≥9	8.7
OCH_{3eq}	42.1	2	≥19	84
Cl_{eq}	20.0	3	5.3	34
F_{eq}	60.0	2	5.9	103

[a] See appendix 2 for precision. [b] Blank regions were not determinable due to poor signal to noise.

4.2.3 Competitive rates using Triethylsilane/Boron Trifluoride Etherate

In 1976, Doyle reported that aldehydes and ketones could be reduced to alcohols with triethylsilane and BF_3•Et_2O (see Section 4.1.3).[145] In Fry's investigation similar results were observed, however, gaseous BF_3 was employed as catalyst in dichloromethane.[149] In a subsequent paper, Fry found that the reduction could also be performed using fluoride ion (F^-) as catalyst in acetonitrile.[150] These facts led us to study the competitive kinetics of triethylsilane for our bridged biaryl ketone **44** and its α-derivatives. Accordingly, preliminary investigations on the reduction of ketone **44**

employing 1 equiv of Et_3SiH and 3 equiv of $BF_3 \cdot Et_2O$ at 0°C in CH_3CN yielded, as revealed by 200 MHz ^1H NMR and TLC, an extremely clean reaction with the unsubstituted alcohol **65** being the sole product, while the same reaction in methylene chloride showed a mixture of products with **65** dominating. The isolation of the minor

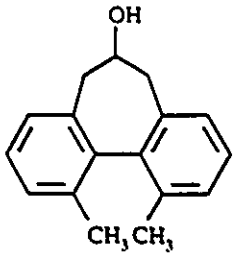

65

product from the reaction in dichloromethane was not attempted, but it appeared to be the symmetrical ether. Thus the competitive reductions were performed in acetonitrile employing a 3:1 ratio of $BF_3 \cdot Et_2O$:Et_3SiH.

As before in the SBH system, the optimum experimental conditions were obtained by performing a competitive reduction with the axial α-methyl ketone **45** and **44**. An initial concentration of 0.05 mmol of total ketones in 5 mL of CH_3CN was used. An aliquot from the reaction mixture was removed after 2, 15, 60 and 120 minutes. Interestingly, the results showed no significant change in diastereoselectivity as the reaction proceeded to 50% completion (see Table 4.8). However, despite exhibiting no change in selectivity, the three different possible catalysts (see Section 4.1.3) may influence the reactivity. Therefore, as before, to ensure that the reaction was occurring via a single catalyst (i.e. BF_3 and not $R_2CH\text{-}OBF_2$ or $(R_2CH\text{-}O)_2BF$), conditions were adopted so as to terminate the reaction as early as practically possible. Indeed, we were able to quench the reaction after ≤25% consumption of total hydride and in most cases ≤7% (see Appendix 2).

Table 4.8 Competitive reduction of ketones 45 versus 44 with $Et_3SiH/BF_3{\cdot}Et_2O$ in CH_3CN at 0°C.

Ketones (mmol)	Et_3SiH mmol	$BF_3{\cdot}Et_2O$ mmol	Quench Time min	% of Total Hydride Consumed	π-Facial Selectivity
45 (0.0441)	0.05	0.15	2	2.5	11.5
+ **44** (0.00586)			15	13.7	14.2
			60	35.0	12.4
			120	49.8	13.1

The results for the competitive reduction are shown in Table 4.9. However, again, in contrast to the LAH reductions, the relative rates for most entries in Table 4.9 were calculated by using equation 27. For the axial α-methoxy ketone **47**, no epimerization was observed, but an additional product was found. After isolation by column chromatography, both a 500 MHz ^1H and a ^1H-^1H COSY NMR spectra were obtained (see Figure 4.12). The spectra are consistent with compound **84**. Thus it

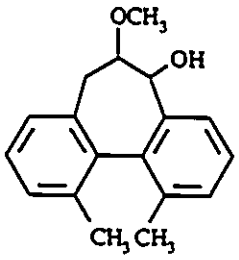

84

appears that the Lewis acid $BF_3{\cdot}Et_2O$ promotes a rearrangement reaction whose product ketone subsequently undergoes a rapid reduction with triethylsilane. Similarly, for the equatorial α-methoxy ketone **51**, a second component was found, but it was not identified. Lastly, for the equatorial α-methylthio ketone **50**, a combination of

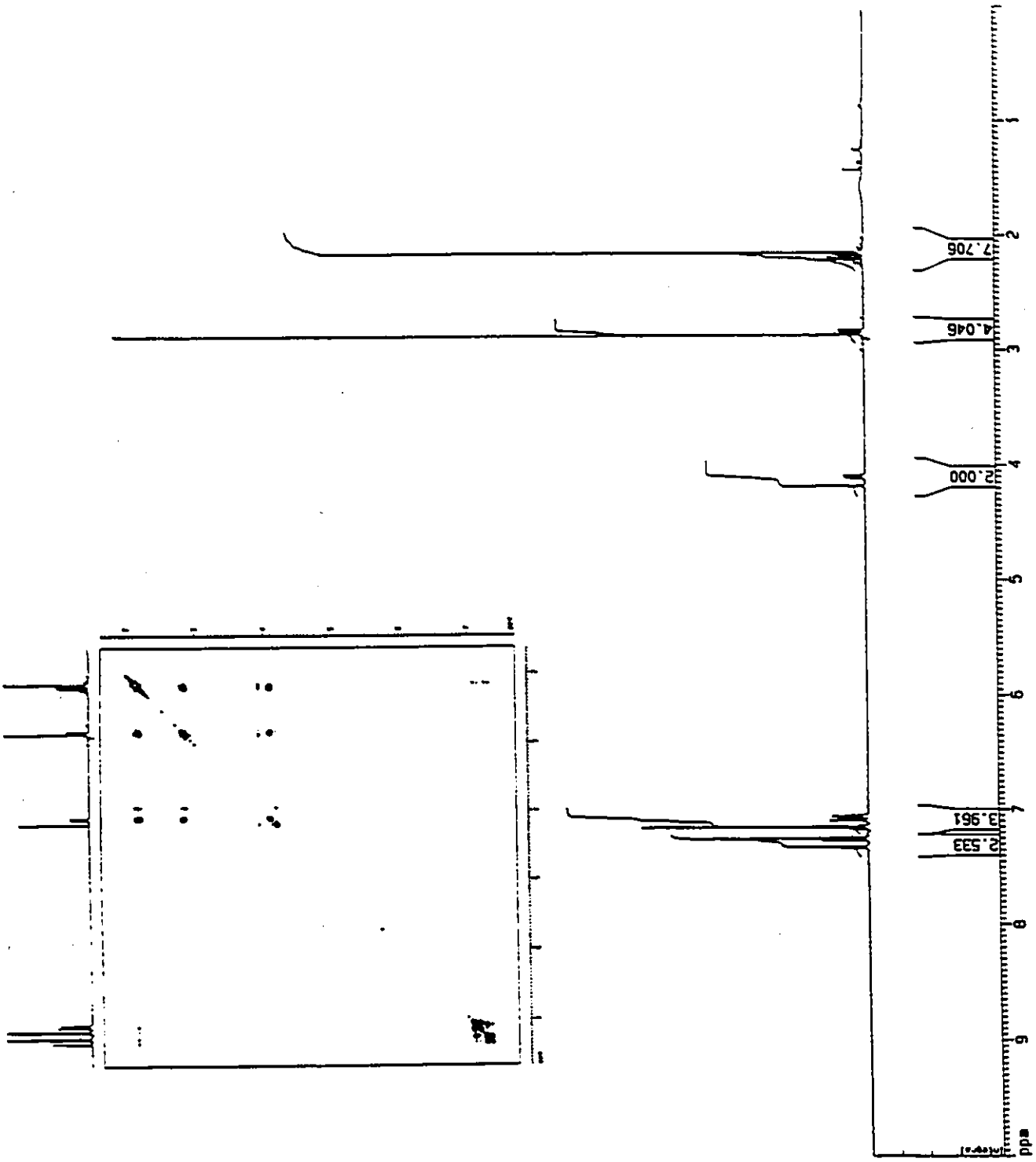

Figure 4.12 The 500 MHz ^1H and ^1H-^1H COSY NMR spectra of 84 in $CDCl_3$.

epimerization and rearrangement was observed, with the rearrangement route dominating. In all of these cases a similar correction, as noted in Section 4.2.2 was made, however, in equation 27 y no longer represents the per cent of epimerization, but represents the per cent of rearrangement that occurred. In the case of ketone **50** where both rearrangement and epimerization were observed, y represents the total amount of epimerization and rearrangement. The amount of rearrangement and/or epimerization observed for ketones

Table 4.9 π-Facial reactivity[a] of the α-derivatives of 44 for reduction by Et_3SiH/BF_3-Et_2O.

Substituent R	k_R^{app}/k_{44}	Number of Measurements	π-Facial Selectivity[b]	k_R^{app}/k_H
H	-	-	1.0	1.0
CH_{3ax}	0.155	1	11.5	0.28
SCH_{3ax}	0.00861	1		0.017
OCH_{3ax}	0.185	2	≥19	0.37
Cl_{ax}	0.0024	1		0.0048[c]
				k_R^{ac}/k_H
CH_{3eq}	0.156	1	~2	0.31
SCH_{3eq}	0.0915	2		0.18
OCH_{3eq}	0.921	2	≥19	1.8
Cl_{eq}	0.0659	1	7.0	0.12
F_{eq}	0.134	1	7.9	0.27

[a] See appendix 2 for precision. [b] Blank regions were not determinable due to poor signal to noise.
[c] Calculated via relay (i.e. $k_{Cl}^{app}/k_H = k_{Cl}^{app}/k_{Cl}^{ac} \times k_{Cl}^{ac}/k_H$).

47 and **50** was 28% and 22%, respectively. In all other cases, the maximum amount observed was 6%. In subsequent runs, we were successful in decreasing the rather high rearrangement observed for ketone **47** to 14%. Unfortunately, we were not successful in the case of **50**. Satisfyingly, we were able to reproduce the relative rates for both these ketones within experimental error and thus identification of the rearranged product and/or additional attempts to minimize its formation were not pursued (see Appendix 2).

4.3 Discussion

A summary of the competitive reduction data is given in Table 4.10. The results for lithium aluminum hydride show that as the electron withdrawing ability of R_{ax} (i.e. app to attacking hydride) increases a modest increase in reactivity is observed. An axial chloro substituent exhibits the largest influence with a 5.6 fold increase in the rate of reduction. The data for the equatorial substituents (i.e. ac to attacking hydride) show a similar trend. That is, again, as the electron withdrawing ability of the equatorial substituents increases a slight increase in π-facial reactivity is found with the electron withdrawing OMe substituent exhibiting the greatest reactivity ($k_{OMe}^{ac}/k_H = 8.1$).

For the sodium borohydride/isopropanol system, as in the LAH case, both axial and equatorial electron withdrawing substituents accelerate the π-facial reactivity. However, the influence is significantly enhanced. For example, an axial chloro substituent causes an 80 fold increase while an equatorial fluoro substituent causes a 103 fold increase in reactivity.

Interestingly, in the competitive reductions using triethylsilane/boron trifluoride etherate, the opposite trend was observed. The results show that electron withdrawing axial substituents strongly decelerate the rate of attack of triethylsilane relative to hydrogen. A similar result was obtained for the equatorial substituents, however, the rates are less affected by electronegative substituents.

Table 4.10 Face reactivity[a] of the α-derivatives of 44.

Substituent R	k_R/k_{unsub}			π-Facial Selectivity[c]			k_R^{app}/k_H		
	$LiAlH_4$	$NaBH_4$	Et_3SiH	$LiAlH_4$	$NaBH_4$	Et_3SiH	$LiAlH_4$	$NaBH_4$	Et_3SiH
H	-	-	-	1.0	1.0	1.0	1.0	1.0	1.0
CH_{3ax}	0.405 (8)[b]	0.114 (2)	0.155 (1)	11.9	6.5	11.5	0.77	0.20	0.28
SCH_{3ax}	0.436 (4)	0.390 (2)	0.00861 (1)	≥19			0.87	0.78	0.017
OCH_{3ax}	1.36 (1)	8.18 (1)	0.185 (2)	≥19	≥19	≥19	2.7	16.4	0.37
Cl_{ax}	2.81 (1)	40.0 (2)	0.0024 (1)	≥19	≥19		5.6	80	0.0048
							k_R^{ac}/k_H		
CH_{3eq}	1.12 (3)	0.454 (2)	0.156 (1)	4.5	~2	~2	1.8	0.91	0.31
SCH_{3eq}	2.27 (2)	4.34 (1)	0.0915 (2)	≥19	≥9		4.5	8.7	0.18
OCH_{3eq}	4.07 (2)	42.1 (2)	0.921 (2)	≥19	≥19	≥19	8.1	84	1.8
Cl_{eq}	3.31 (2)	20.0 (3)	0.0659 (1)	8.2	5.3	7.0	5.9	34	0.12
F_{eq}	3.68 (4)	60.0 (2)	0.134 (1)	7.6	5.9	7.9	6.5	103	0.27

[a] See experimental and appendix 2 for precision. [b] The number in parentheses gives the number of measurements. [c] Blank regions were not determinable due to poor signal to noise.

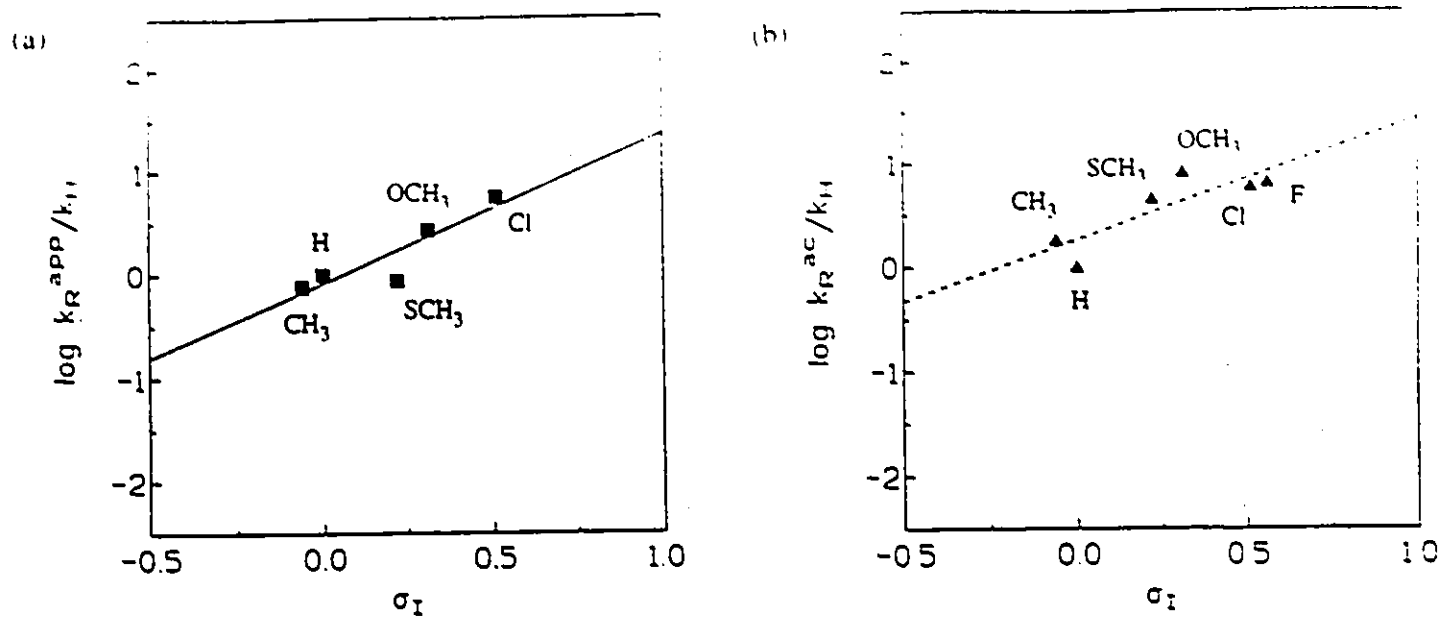

Figure 4.13 Plots of (a) log k_R^{app}/k_H and (b) log k_R^{ac}/k_H versus σ_I for LAH reduction of (a) 44-48 and (b) 44 and 49-53.

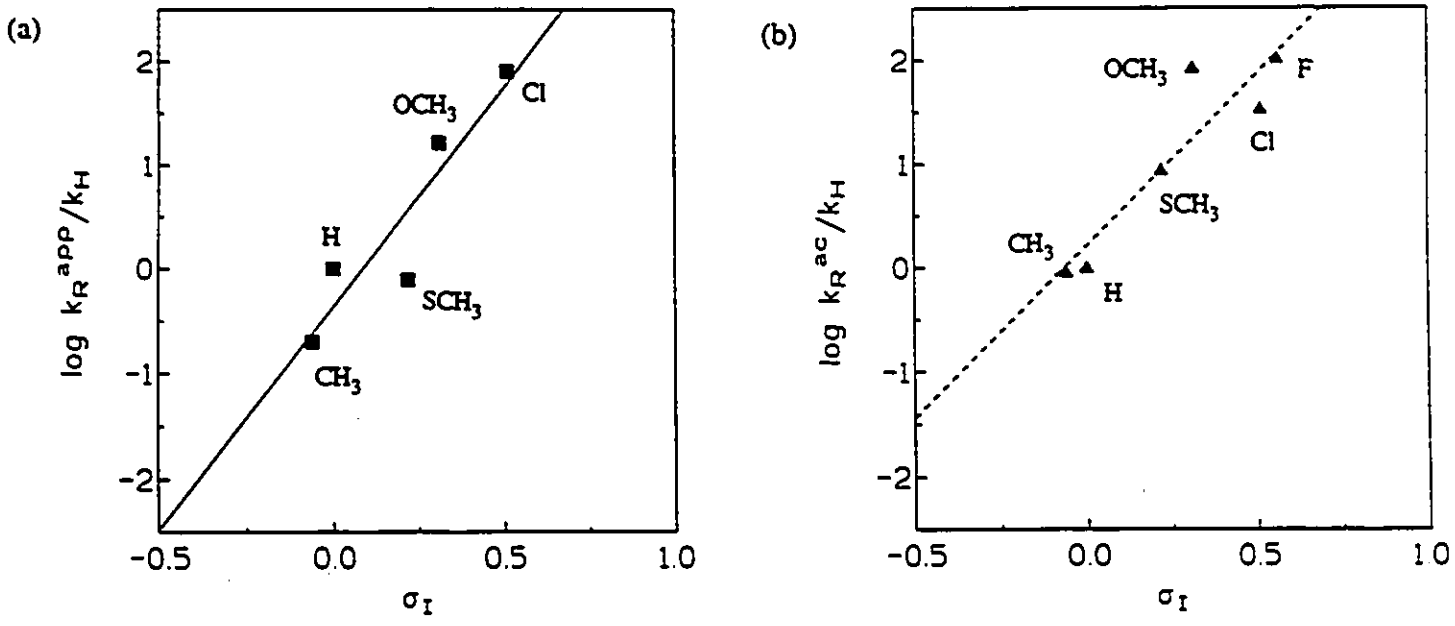

Figure 4.14 Plots of (a) log k_R^{app}/k_H and (b) log k_R^{ac}/k_H versus σ_I for SBH reduction of (a) 44-48 and (b) 44 and 49-53.

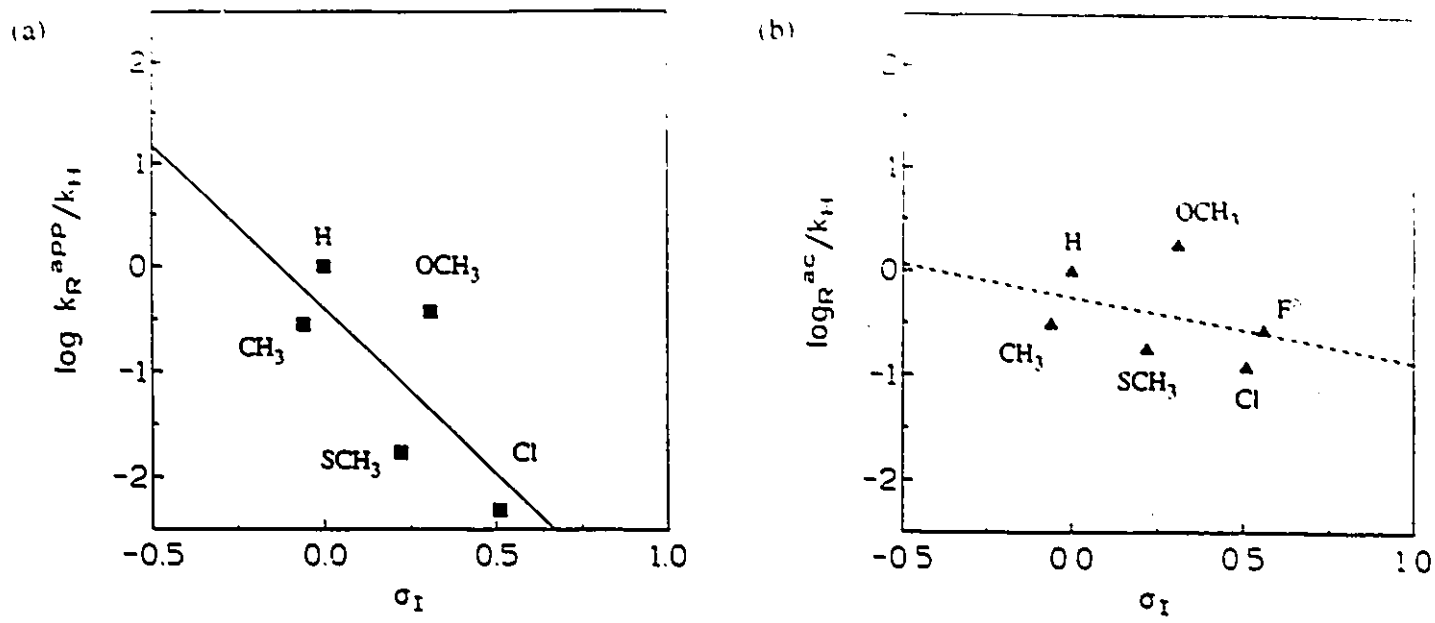

Figure 4.15 Plots of (a) log k_R^{app}/k_H and (b) log k_R^{ac}/k_H versus σ_I for triethylsilane reduction of (a) 44-48 and (b) 44 and 49-53.

In order to determine the importance of the polar effect, we were prompted to plot log (k_R^{app}/k_H) and (k_R^{ac}/k_H) versus the polar substituent constant σ_I for the three systems under study (see Figures 4.13-4.15). At present, there are numerous scales of σ_I available to the practicing physical organic chemist. However, recently Thornton and Das conducted a similar competitive reduction study for the aldol addition of pinacalone lithium enolate to various α-heterosubstituted ketones (see equation 29).[151] They observed excellent correlation when the Exner σ_I scale[152] was employed for both aliphatic ($r = 0.996$, $\rho = 6.62 \pm 0.24$) and aromatic ($r = 0.993$, $\rho = 7.61 \pm 0.60$) ketones, whereas other more recent scales gave poorer correlations. Thus in Figures 4.13, 4.15 and 4.15 the Exner σ_I scale was used.

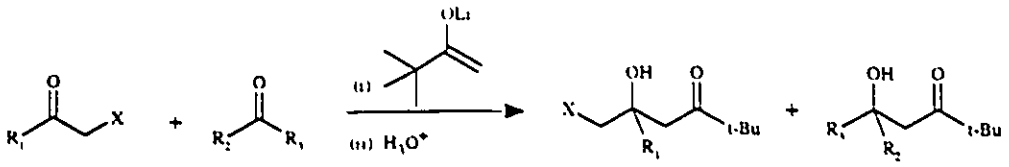

[29]

The Hammett plot for the lithium aluminum hydride system for the app substituents in Figure 4.13a exhibits a reasonable correlation (see Table 4.11). That is, the data show the general trend that the reactivity is mainly governed by polar effects.*

Table 4.11 Correlation coefficients and susceptibility constants of the Taft plots.

	$LiAlH_4$		$NaBH_4$		Et_3SiH	
	app	ac	app	ac	app	ac
r (correlation coefficient)	0.896	0.840	0.922	0.919	-0.743	-0.353
ρ (slope)	1.44	1.18	4.22	3.31	-3.14	-0.624

However, the rather shallow slope (ρ = 1.46) indicates that the effect is not pronounced. The plot for our standard system of equatorial substituents, where because of the poor orbital alignment no app effect should be present, indicates a similar conclusion. However, both the correlation and slope are reduced somewhat. The relatively shallow plots are indicative of the reaction coordinate shown in Figure 4.16 where, in agreement with the Hammond postulate[37], there is a minimal development of negative charge. More precisely, the shallow slopes are consistent with an early reactant-like transition state in which the overall change in charge from the ground state to the transition state, Δq in the carbonyl group, is ≤0.

* Polar effects are frequently referred to as inductive effects. This thesis will employ the latter term (see Section 4.3.2).

The plots of log (k_R^{app}/k_H) and log (k_R^{ax}/k_H) versus σ_I for the sodium borohydride study reveal even better correlations than that observed for the lithium aluminum hydride

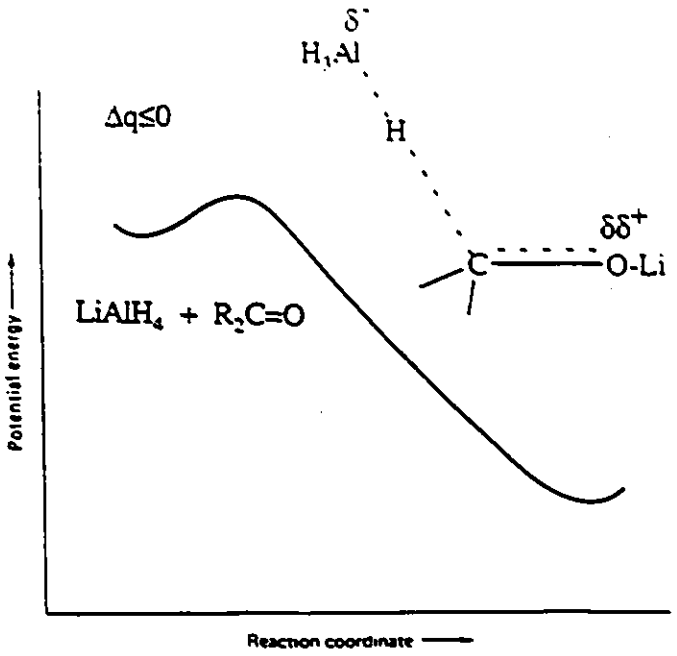

Figure 4.16 Free energy-reaction coordinate diagram representing reduction by lithium aluminum hydride.

reduction (see Figure 4.14 and Table 4.11). Thus, again, it appears that the nucleophilic addition of sodium borohydride to the α-derivatives of our model ketone is mainly due to inductive effects. However, reduction via sodium borohydride is almost three fold more sensitive to inductive effects. This increase in slope is consistent with the reaction coordinate depicted in Figure 4.17 where the reaction occurs via a much later transition state, perhaps mid-point along the reaction coordinate. This later transition state allows for the overall change in charge Δq for the sodium borohydride reaction to be significantly larger than that for the lithium aluminum hydride reduction and thus accounting for the approximately three fold increased in ρ. In his review article in 1979, Wigfield concluded

that for SBH reduction of ketones the transition state is approximately two-thirds along the reaction coordinate.[33b]

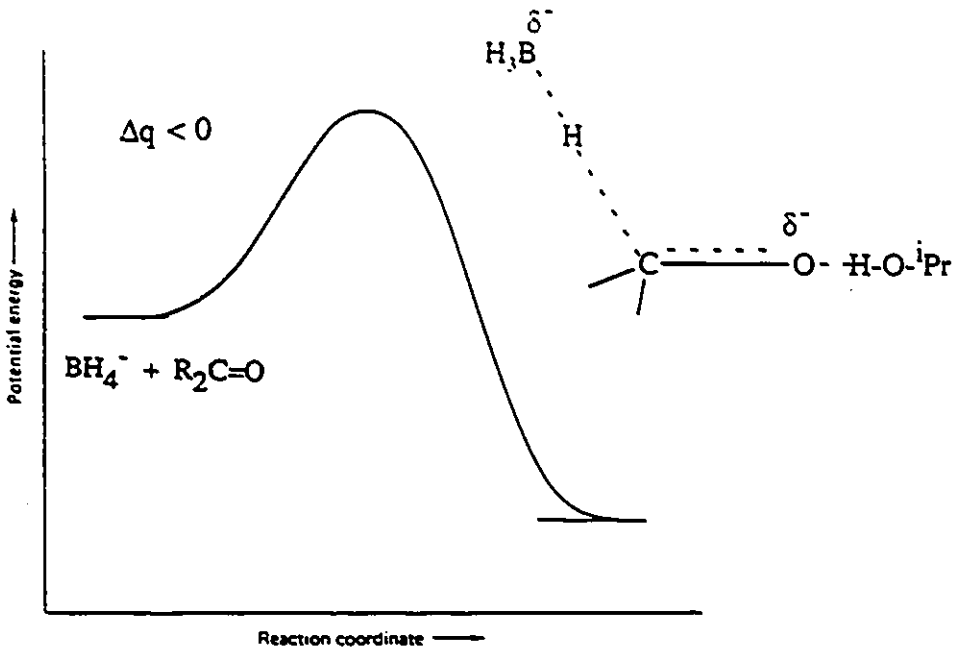

Figure 4.17 Free energy-reaction coordinate diagram representing reduction by sodium borohydride.

Lastly, the plots for the $Et_3SiH/BF_3{\cdot}Et_2O$ competitive reduction are given in Figure 4.9. As mentioned previously, the data reveal the opposite trend and thus the slopes are negative. The plot for the app substituents exhibits somewhat poor correlation (see Table 4.10). However, the plot shows the general trend that the addition of the nucleophile triethylsilane is mainly governed by inductive effects. The Hammett plot for the equatorial substituents shows a much poorer correlation and, as a result of its shallower slope, is less influenced by inductive effects. The negative slopes are consistent with the reaction coordinate diagram shown in Figure 4.18 in which the intermediate BF_3-ketone complex (85) is less stable than the starting materials since under these circumstances there is an

overall increase in the amount of carbocation character in the transition state. The activated ketone is then attacked by triethylsilane via a four centred transition state as proposed by Doyle.[145] Overall, the net change in charge (Δq) for the reaction is ≥ 0. The magnitude of positive charge developed is dependent on the character of the transition state (i.e. position along the reaction coordinate). The plot of log k_R^{app}/k_H vs σ_I seems to indicate an appreciably charged transition state.

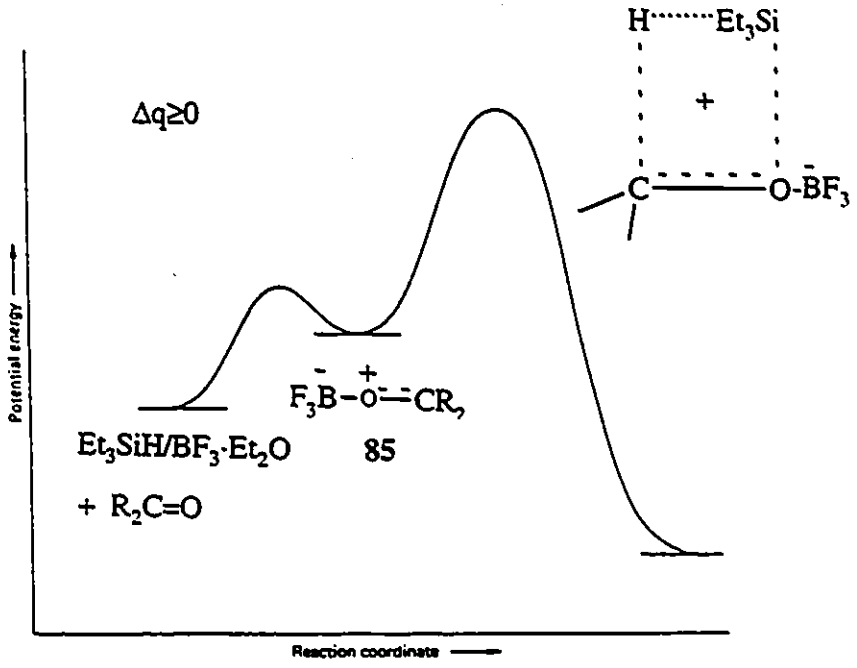

Figure 4.18 Free energy-reaction coordinate diagram representing reduction by triethylsilane.

Preliminary competitive rate studies with ketone **46** (axial SCH_3) indicated a severely retarded facial reactivity. It was initially proposed that for ketone **46** the enol tautomer may be energetically preferred. Thus the addition of the Lewis acid catalyzed the conversion from the keto to the enol form **86**. In order to test this proposal a 200 MHz ^1H NMR experiment was performed. Addition of 3 equivalents of BF_3•Et_2O to a 5mg sample of **46** in CD_3CN resulted in no observable change. Thus, it appears that the

keto tautomer is highly preferred. In addition, this lack of change indicates that 46-BF_3 complex is significantly less stable than the starting compound. This conclusion is in agreement with the proposed reaction coordinate shown in Figure 4.18.

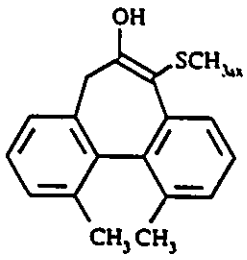

86

Overall, the plots of log k_R^{app}/k_H and log k_R^{ac}/k_H show the general trend that the differences in reactivity are predominantly due to inductive effects. In order to test the validity of the app effect, the log k_R^{app}/k_H plots were consulted. Because the plot of the LAH competitive reduction shows the least influence from inductive effects (ρ = 1.46), the LAH system should be the most likely to reveal an app effect as proposed by Cieplak.[40] An axial methyl group slightly retards the rate of app attack relative to hydrogen(i.e. $\Delta\Delta G^{\ddagger}$ = 0.14 kcal/mol). As commented on previously in Chapter 1, the Cieplak hyperconjugative model was originally based on the observed diastereoselectivity in the LAH or SBH reduction of 4-*t*-butylcyclohexanone. Thus because this ketone exhibits a 9:1 bias towards axial attack and since it possesses two antiperiplanar $\sigma_{C\text{-}H}/\sigma^*_{C\text{-}H}$ interactions at C2 and C6, the Cieplak theory represents a transition state destabilization (i.e. $\Delta\Delta G^{\ddagger}$) of 1.4/2 or 0.7 kcal/mol. However, our data reveals a value of only 0.14 kcal/mol. Perhaps the most informative value is for the axial methylthio substituent. For the series of substituents in our study, the methylthio substituent is the best sigma donor. Therefore an app SCH_3 group should provide the greatest transition state stabilization (i.e. $\Delta\Delta G^{\ddagger}$ should be large and negative) and consequently be the most reactive in the series.

However, this substituent causes a negligible change in reactivity ($\Delta\Delta G^{\ddagger}$ = 0.076 kcal/mol) and along with the methyl group is the least reactive in the series. Finally, the axial chloro substituent shows a 5.6 fold increase in reactivity which, again, is contrary to Cieplak's predictions. In Cieplak's theory, an app chlorine is predicted to decrease the reactivity of nucleophilic addition since the electron donating ability of a C-Cl sigma bond is significantly less than a C-H sigma bond. On the other hand, although the trend is in agreement with Anh's predictions, the reactivity for the axial chloro group falls well short of the extremely large increase calculated by Anh. In addition, for an app methyl group Anh predicts that the reactivity should be increased, but we observed a small decrease in reactivity. Hence, neither the Cieplak nor the Anh app effect are in agreement with the observed results.

4.3.1 Axial versus Equatorial Substituents

If the assumption is made that the results for the axial substituents represent a combination of inductive and app effects, whereas, because of poor orbital-orbital alignment, the reactivity for the equatorial substituents represent only inductive effects, a comparison between axial and equatorial data will provide an additional test for the validity of the Cieplak theory. The data for both axial and equatorial substituents for the three systems are readily compared by consulting Figure 4.19. For the LAH competitive reduction, the data show that an equatorial methyl group causes a greater increase in reactivity than an axial methyl group. This result is in agreement with Cieplak's theory since replacing an app H, as present in the axial α-methyl ketone **45**, with an app methyl should decrease the amount of transition state stabilization and thus should be the least reactive. In disagreement with Cieplak's theory, an axial methylthio group exhibits decreased reactivity relative to an equatorial SCH_3 group. Because Cieplak assumes an C-S sigma bond is a much better electron donor than a C-H bond, the model predicts that the axial ketone should show increased reactivity. The result for the methoxy substituent is

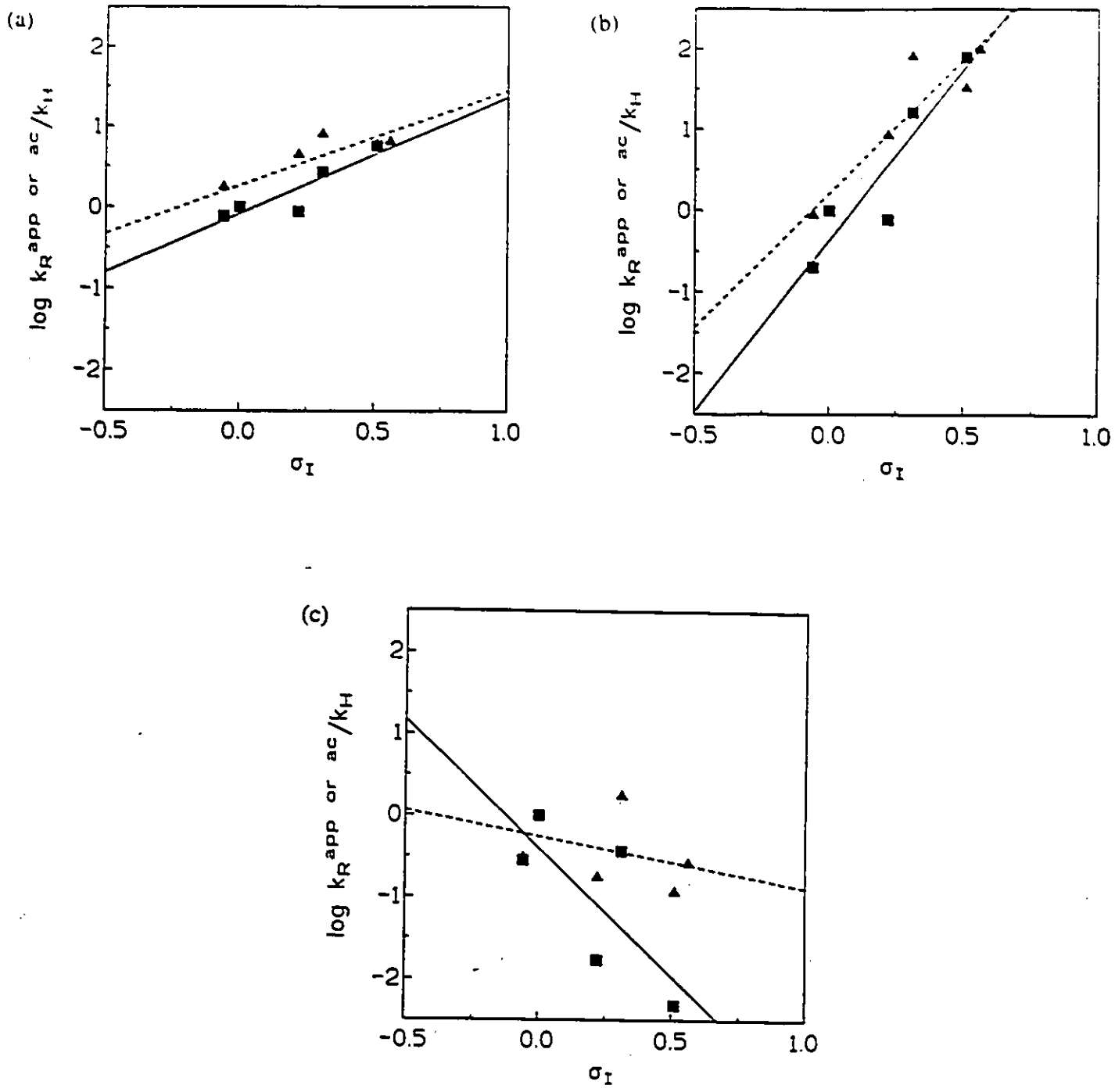

Figure 4.19 Plots of log k_R^{app}/k_H (■) and log k_R^{ac}/k_H (▲) versus σ_I for reduction by (a) LAH, (b) SBH and (c) triethylsilane.

consistent with Cieplak's theory, since, again, because Cieplak assumes a C-O σ bond is a poorer electron donor than a C-H bond, an axial OCH_3 group should diminish the reactivity. Lastly, for the chloro substituent, the Cieplak theory predicts that an app chloro group should cause a significant decrease in the π-facial reactivity since an app C-Cl sigma bond is properly oriented with the σ^*_{C-H} orbital. However, there is a negligible difference in reactivity between the axial and equatorial ketones **48** and **52**. Because the Anh hyperconjugative model makes the opposite predictions of the Cieplak model, all substituents above that were in agreement with Cieplak theory are now in disagreement with Anh's predictions (i.e. CH_3 and OCH_3*). However, because both the axial and equatorial chloro ketones exhibit a negligible difference in reactivity, both models yield the incorrect result.

For the SBH system and based on similar arguments as above, the data for the methyl and methoxy substituents are in agreement with Cieplak's theory, whereas the data for the methylthio and chloro substituents are not. Conversely, employing Anh's theory, the results reveal that the chloro substituent is in accord with his proposal, but the methyl and methoxy groups are not.

Finally, for the competitive reductions involving triethylsilane/boron trifluoride etherate, the data indicate that contrary to Cieplak's theory, which predicts that an app methyl group should be less reactive than an ac methyl, the axial and equatorial methyl groups exhibit only a negligible difference in π-facial reactivity. Our study shows that the methoxy and chloro substituents are in accord with Cieplak's app effect, while the methylthio substituent is not. In the case of Anh's hyperconjugative model, all substituents are in disagreement. Therefore for all three reducing agents under study, a very inconsistent trend is observed and thus it appears that both theories are rather dubious in nature.

---

* Although Anh never discussed an app methoxy substituent in his original proposal, it is assumed that this substituent should increase the reactivity (see reference 13).

4.3.2 A Closer Look at the Axial and Equatorial Plots

As the reaction conditions for a given chemical reaction are altered, the end result is normally a change in the rate of the chemical reaction or the position of the chemical equilibrium under study. These changes may include such factors as temperature, solvent or substituent electronegativity (i.e. substituent effects). If this series of changes influences the rate or equilibrium in exactly the same manner versus the adopted standard, except affecting it by an amount that is solely dependent on the specific change, the system is said to obey a linear free energy relationship. Hitherto, substituent effects have received by far the most attention.[153]

More than fifty years ago Hammett first recognized this fact and found that a linear free energy relationship exists for the acid dissociation equilibrium constants, K_a, for meta- and para-X-substituted benzoic acid and a number of derivatives thereof (e.g. X-$C_6H_4CH_2COOH$).[154] More specifically, Hammett observed that the data correlated well with the constant σ, the substituent effect (i.e. equation 30). In equation 30 K_x represents

$$\log \frac{K_x}{K_o} = \rho\sigma \qquad [30]$$

the acid dissociation constant for the X-substituted benzoic acid derivative under study and K_o represents the same dissociation constant, but for the unsubstituted substrate (i.e. X=H). The analogous expression [31] for the rates of reaction was subsequently found to be valid for a large number of aromatic compounds (e.g. hydrolysis of methyl benzoates).[155]

$$\log \frac{k_x}{k_o} = \rho\sigma \qquad [31]$$

In the early 1950s Taft put forward a proposal for broadening linear free energy relationships to aliphatic systems.[156] Based on the initial idea of Ingold[157], Taft recognized that equation 32 would allow for the estimation of the polar substituent constant σ^* for X assuming that the free energy of activation ($\Delta G^{\ddagger}$) can be divided into three independent contributions from inductive, resonance and steric effects. In addition, since the transition states for acid- and base-catalyzed ester hydrolysis (**88** and **89**, respectively) differ by only the presence of two small protons, the steric effects present in these two systems should be approximately equivalent. These transition states also allow for the assumption that the resonance effects are negligible. Therefore the substituent constant σ^* represents only the strength of the inductive effect of X relative to the standard methyl group. As mentioned previously in this discussion, a number of additional inductive substituent constant scales have be put forward with most using hydrogen as the standard.[152]

$$\sigma^* = \frac{\log (k_x/k_o)_B - \log (k_x/k_o)_A}{2.48} \qquad [32]$$

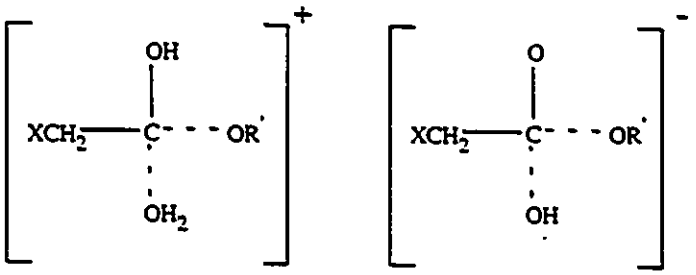

88 **89**

As in Taft's original system, where there exists a minimal amount of steric difference between the acid- and base-catalyzed hydrolysis of aliphatic esters, subsequent studies have shown to give normally good (i.e. $r>0.95$) correlations.[158] However, on occasion poor correlations have been found. For example, the correlation coefficient in the hydrogenation of aldehydes and ketones (i.e. equation 33) was found to be 0.65.[158a]

Therefore since the reduction of the α-derivatives of our bridged biaryl ketone **44** is not expected to be totally free from steric effects, the observed non-linearity is not surprising. As observed, the plots of face reactivity are expected to show increased steric strain due

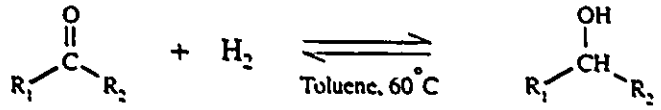

[33]

to van der Waals and torsional effects. That is, the α-substituents as part of Ar-CXH-CO-R′ oriented substituents should increase the amount of steric strain present in the transition state with M = AlH_3, BH_3 or $SiEt_3$ relative to that present in Taft's approximately symmetric transition state (see Figure 4.20). The much poorer correlation for the triethylsilane data is indicative of a much more tightly organized transition state such as the four centred transition state put forward by Doyle[145].

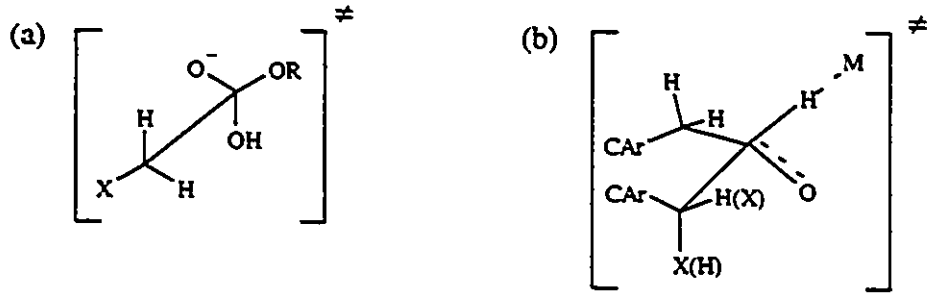

Figure 4.20 Three-dimensional representations of the transition states for (a) the Taft hydrolysis of aliphatic esters and (b) the reduction of our α-X substituted bridged biaryl ketones.

The inductive effect refers to the influence, other than steric, that nonconjugated substituents exert on reaction rates. The effect may transmit itself via two distinct mechanisms. Firstly, the transmission may occur through bonds via successive bond

polarization (**90**) and is referred as a through bond or sigma-inductive effect. The second mode of transmission is through space and this effect is dependent on the relative

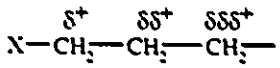

90

orientation of the dipoles present in the transition state. This effect is referred as either a field, through space or electrostatic effect. Numerous investigations have attempted to quantify this field effect.[159] However, because only an estimate of the polarity of the transition state, the effective dielectric constant or the shape of the molecule can be made, these models provide only a qualitative assessment. For example, if the dipoles are perpendicular to one another, the field effect will be negligible, whereas if the dipoles are parallel, a repulsive interaction is introduced and thus the rate of reaction is reduced as the electron withdrawing ability of the substituent increases. Several studies have been performed in order to determine which effect is dominant. Current evidence employing mostly carboxylic acids and their derivatives indicate that the field effect is the more important.[160] However, in more sophisticated models, both effects appear to be of equal value.[161]

In Taft's original proposal, the acyclic aliphatic esters $XCH_2COCOOR$ likely possess no conformational preference about the X-CH_2 bond. Thus the nature of X does not alter the relative orientation of the dipoles between X and the reaction centre. However, in cyclic or bicyclic substrates such as our model bridged biaryl ketones **45-53**, the relative orientation of the dipoles in the methoxy derivatives may be different from the monoatomic substituent (e.g. the chloro substituent). More specifically, the methoxy group will likely adopt the most favourable conformation and thus result in an additional stabilizing field effect.

In order to shed light onto the direction of the $^{\delta+}C\text{-}O^{\delta-}C^{\delta+}H_3$ dipole in the axial and equatorial ketones **47** and **51**, molecular mechanics calculations were carried out using the commercially available program PCMODEL.[80] As shown in Figures 4.21, the calculations on both the axial and equatorial derivatives indicated that there exists three stable rotamers about the O-C2 bond, two of which are favoured and available for occupancy.

(a)

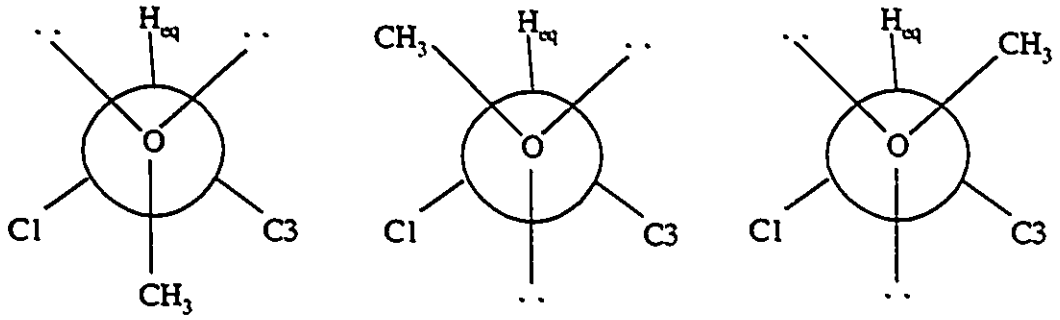

E = 31.79 27.97 27.77

(b)

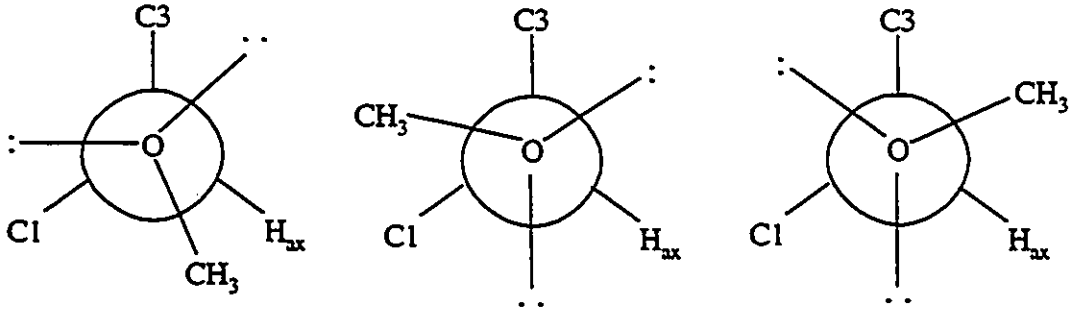

E = 30.94 33.80 31.20

Figure 4.21 Molecular mechanics calculations of the three rotamers about the O-C2 bond for the (a) axial α-methoxy ketone 47 and (b) equatorial α-methoxy ketone 51 and their respective steric energies (E) in kcal/mol.

An additional uncertainty is the orientation of the dipole in the carbonyl portion of the molecule. Unless, the exact nature of the transition state is known (i.e. position of all atoms and charges), any proposal remains quite speculative. Nevertheless, for the triethylsilane reduction of the axial and equatorial and methoxy derivatives of **44**, the dipoles appear to be oriented quite differently from the chloro derivatives (see Figure 4.22).[162] Therefore, the field effect of the methoxy group will contribute an additional stabilization through its ability to adopt the rotamer of most stabilizing dipole-dipole interaction in the transition state. This contribution through conformational adoption should provide greater stabilization for the equatorial derivative since this substituent is closer to the site of developing charge. This same line of reasoning is thought to apply to the SCH_3 derivatives. However, as observed, since the C-S bond dipole is expected to be greater than a C-O bond dipole, the effects should be larger. In addition, as noted in Table

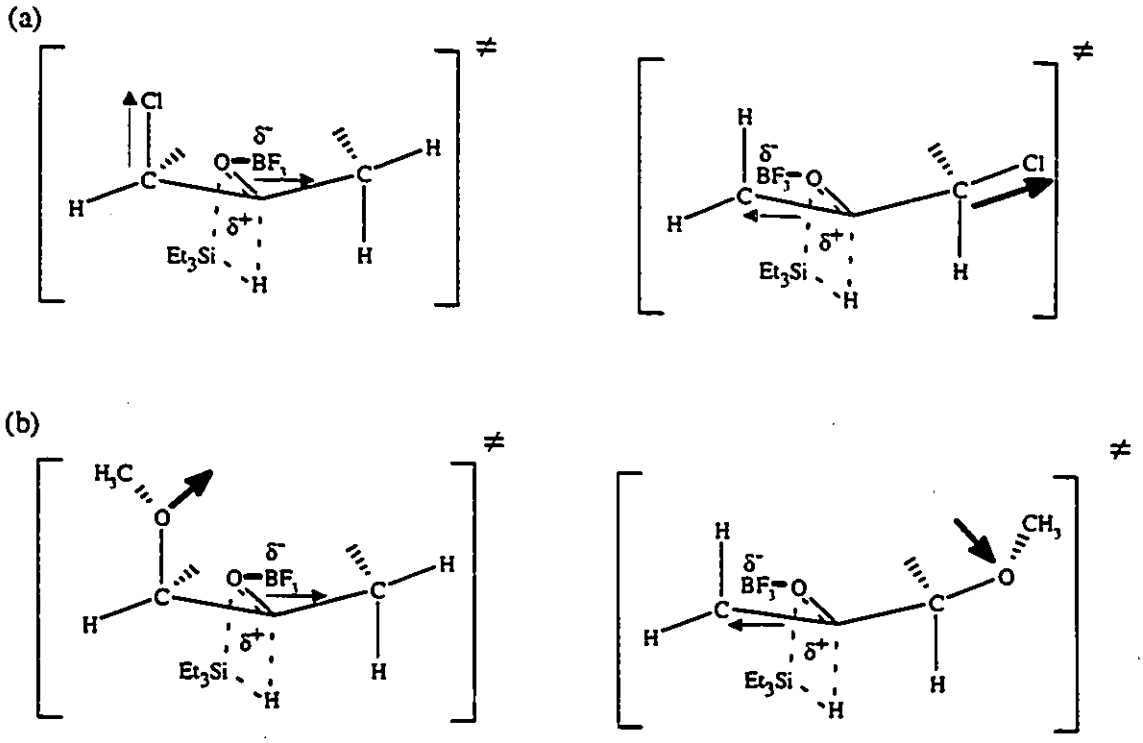

Figure 4.22 Proposed electrostatic interaction for the reduction of the axial and equatorial chloro derivatives (a) and methoxy derivatives (b) by triethylsilane.

4.11, the constant ρ (i.e. the slope) for the $Et_3Si/BF_3{\cdot}Et_2O$ plot is less negative for the equatorial substituents than the axial substituents. As can be seen in Figure 4.22, the app transition states appear to possess a greater dipole moment (i.e. more antiparallel or parallel) and thus is more influenced by inductive substituent effects.

In the transition states for the equatorial chloro derivative, the two dipoles are more closely opposed (i.e. antiparallel) than that present in the axial chloro derivative and thus an additional transition state stabilization interaction is introduced. Hence, as observed, the equatorial chloro substituent is expected to be more reactive than its axial stereoisomer.

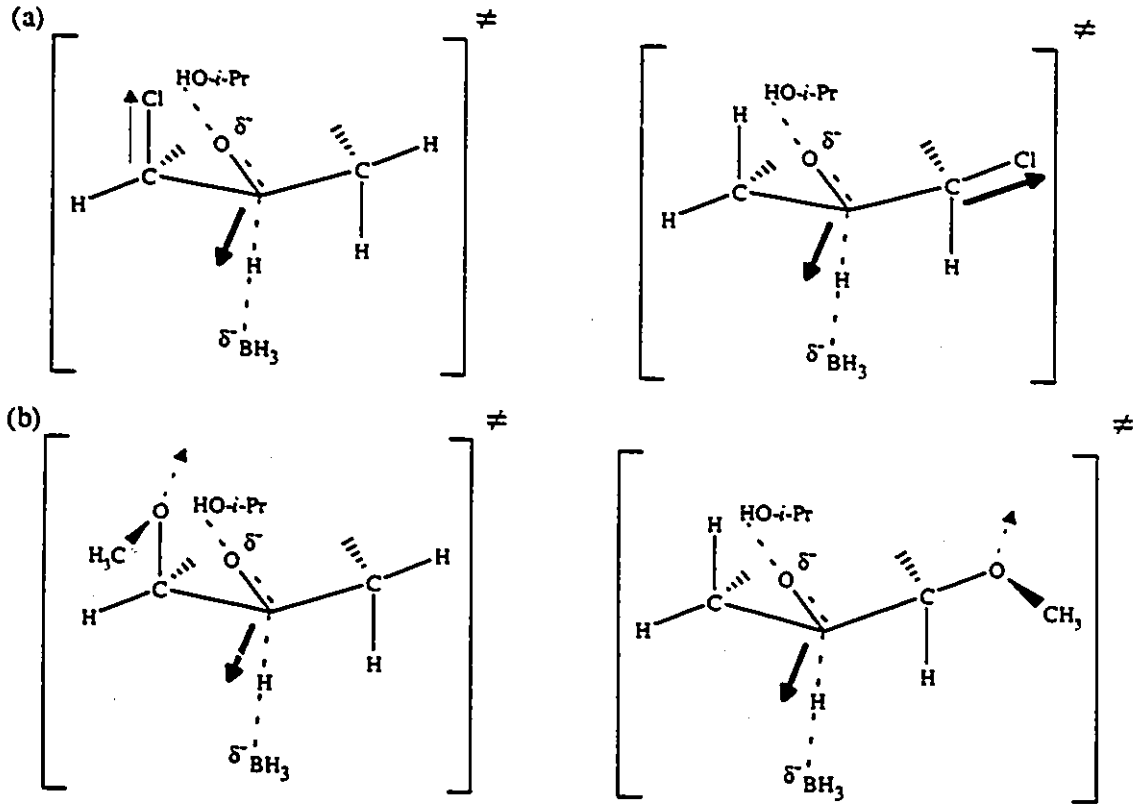

Figure 4.23 Proposed electrostatic interaction for the reduction of the axial and equatorial chloro derivatives (a) and methoxy derivatives (b) by sodium borohydride.

As shown in Figure 4.23 for the reductions using sodium borohydride, the orientation of the dipoles in the transition state for the axial and equatorial chloro and methoxy derivatives are different. Thus as in case of the triethylsilane results, one would expect that the field effect of the methoxy and methylthio groups will contribute an additional stabilization through their ability to adopt the most energetically favourable transition state interaction. As before, this contribution should provide greater stabilization of the equatorial derivatives. However, in the transition state for the equatorial chloro derivative and unlike that present in triethylsilane system, the two dipoles are more closely aligned (i.e. parallel) than that present in the axial chloro

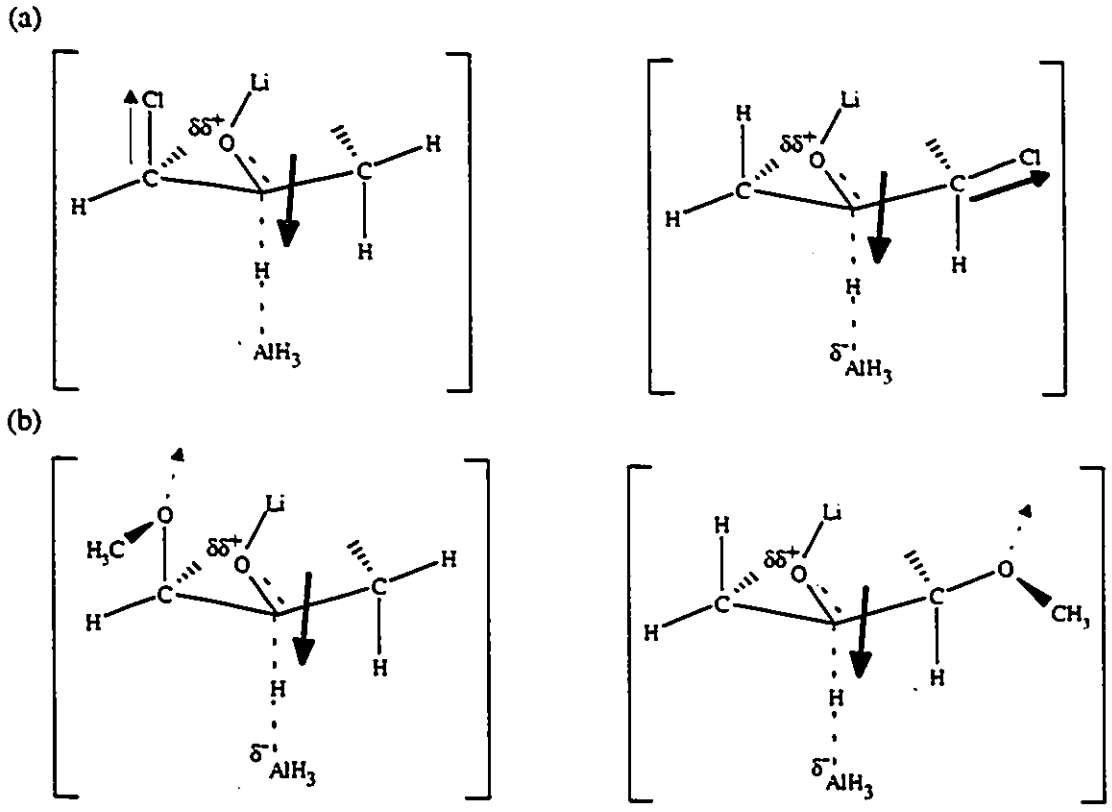

Figure 4.24 Proposed electrostatic interaction for the reduction of the axial and equatorial chloro derivatives (a) and methoxy derivatives (b) by lithium aluminum hydride.

derivative and thus an additional transition state destabilization interaction is introduced. This interaction causes the equatorial stereoisomer to be less reactive. As in the triethylsilane system, the slope of the app substituents is steeper than the ac substituents (ρ = 4.22 versus 3.31). As before, the field effect may be the cause of this difference.

Finally, in the LAH system a similar situation arises as present in the reductions employing SBH (see Figure 4.24). However, the importance of the inductive effect is diminished as indicated by the shallow plots in Figure 4.13 and the smaller difference in reactivity between the axial and equatorial chloro, methoxy and methylthio derivatives (see Figure 4.19). The slope for the ac substituents is less steep than the app substituents. However, the difference is significantly decreased relative to that observed for sodium borohydride (see Table 4.10). Overall, the shallow slopes, the smaller difference in slopes and the smaller differences in reactivities between the axial and equatorial α-chloro, -methoxy and -methylthio derivatives are all consistent with an early reactant-like transition state where there is little charge development in the transition state (i.e. possess small dipole moments).

4.4 Conclusions

We have established on the basis of a competitive reduction rate study on the axial and equatorial α-CH_3, -SCH_3, -OCH_3, -Cl and -F derivatives of **44** that the π-facial reactivity is mainly governed by sigma-inductive effects.

The results indicate an early reactant-like transition state for LAH reduction since this system shows the least influence from inductive effects, while the results for SBH reduction show much larger effects and thus indicates a more product-like transition state. In both instances, the reactivity increased as the electron withdrawing ability of the α substituent increased. For the triethylsilane reduction, the π-facial reactivity study revealed that as the electron withdrawing ability of the α-substituent increases, the reactivity decreases with the axial substituents showing the larger influence.

Because the face reactivity for the lithium aluminum hydride study exhibits the smallest inductive effect, it should be the most likely to reveal an additional app effect. However, contrary to Cieplak's proposal, the app CH_3 and SCH_3 substituents exhibit a negligible effect on reactivity. More specifically, Cieplak predicts that for an app CH_3 group, the change in free energy of activation ($\Delta\Delta G^{\ddagger}$) should be 0.7 kcal/mol, while our study reveals it to be 0.14 kcal/mol. For an app SCH_3 substituent, the Cieplak theory predicts $\Delta\Delta G^{\ddagger}$ should be large and negative, while we observed the small and positive value of 0.076 kcal/mol. Lastly, the chloro substituent should be the least reactive in the series, however, our study shows it to be the most reactive.

If the assumption was made that the reactivity for the axial substituents represents a combination of inductive and nonclassical Cieplak effects and for the equatorial substituents represents only inductive effects, the data for LAH, SBH and triethylsilane are, again, inconsistent with Cieplak's theory. Additionally, since Anh's theory makes the opposite predictions, application of this theory, again, leads to a series of inconsistent results.

The Hammett plots do not show a strong correlation. Of the three systems under study, the triethylsilane exhibits the poorest correlation. We have invoked the field effect to rationalize the results. This deviation is thought to arise from a variable dipole-dipole orientation. It is reasoned that for the three reactions the field effect is conformationally dependent and thus the plots of log k_R^{ax}/k_H and log k_R^{app}/k_H versus σ_I show more scatter. This field effect has also be used to explain the difference in ρ constants for the axial and equatorial substituents.

In summary, it appears that app orbital-orbital interactions as proposed by Cieplak[40] or Anh[13] do not contribute to π-facial reactivity. As stated by Felkin[3] and Houk[48d], our results indicate that steric, torsional and electrostatic effects are the dominating factors.

Chapter 5 Experimental

5.1 General Experimental

Melting points were measured with a Gallenkamp apparatus and are uncorrected. Thin-layer chromatography was performed using a commercial preparation (DC-Alufolien Kieselgel 60 F_{254} EM Separations Technology) and viewed using ultraviolet light. Chromatography was performed under a steady stream of nitrogen using 230-400 Mesh flash grade silica gel (equivalent to Merck 9385). Radial chromatography was performed using a Harrison Research Chromatatron model 7924 using silica gel 60-F254 rotors (1, 2, or 4 mm thickness). Mass spectra were obtained using a V6 7070-E spectrometer (EI). X-ray crystallography was performed using a Rigaku diffractometer operating at 295 K.

All ^1H NMR and ^{13}C NMR spectra were recorded on a Bruker AMX 500, Varian XL 300 or Gemini 200 spectrometer operating at 500, 300 and 200 MHz for protons and 125.7, 75.4 and 50.3 MHz for carbons, respectively. Spectra were recorded in $CDCl_3$ (purchased from Cambridge Isotope Laboratories) and chemical shifts are given in ppm relative to Me_4Si (0 ppm, ^1H) or $CDCl_3$ (77 ppm, ^{13}C) unless otherwise indicated.

All air and/or moisture sensitive reactions were performed under argon with oven-dried glassware (120°C) using standard syringe-septum cap techniques. A -78°C bath refers to a mixture of dry ice in acetone. All solvents (reagent grade) and reagents were obtained from commercial sources and used without further purification unless otherwise specified. Tetrahydrofuran (THF) and ether were distilled from sodium/benzophenone ketyl under an argon atmosphere. Acetonitrile and isopropanol were distilled from calcium hydride under an argon atmosphere prior to use. Hexanes used for chromatography was distilled prior to use. Solutions of MeLi in Et_2O (1.6 M) were purchased from Aldrich and titrated with diphenylacetic acid (Eastman Kodak) before its use. Solutions of LAH in THF (1.0 M) were obtained from Aldrich.

The plots and their least-squares analyses were obtained using the commercially available Graphpad Inplot Software v. 4.03.

5.2 Experimental for Chapter 2

NOE difference measurements of **46** were performed on a sealed degassed sample (5 mg) in 0.5 mL of $CDCl_3$. Ketone **46** and $CDCl_3$ were placed in a 5 mm NMR tube fitted with a one-way stopcock. The stopcock was closed, a vacuum line was attached and the contents degassed using four freeze-thaw-pump-thaw cycles. The stopcock was reclosed, the tube was reimmersed in liquid nitrogen and flame-sealed. The NMR tube was brought to room temperature and used accordingly.

Compound **44** was synthesized as described in the literature.[76] However, modification of the described procedure for **44** led to an improved overall yield.[88] **54** was synthesized as described in the literature.[89]

The preparation of **45**, **47-49** and **51-52** was carried out as described in the literature.[76] However, for the α-methoxy and -chloro ketones the final purification procedures were slightly modified.* The isolation of **48** was performed by flash column chromatography using Et_2O:AcOH:hexanes (2:1:100 v/v/v) as the eluent. The partial separation of **48** and **52** gave reproducibly a maximum **48**:**52** ratio of 2.5:1 (and <10% of dichloro disubstituted derivatives of **44**) and was used for the π-facial reactivity study in Chapter 4. Similarly, the separation of **47** and **51** was carried out by flash column chromatography employing Et_2O:AcOH:hexanes (4:1:100 v/v/v) as the eluent. In both instances, the elution of products was complete within 10-15 min. The purified or enriched (for ketone **48**) samples were subsequently used for our π-facial reactivity study (see Chapter 4).

---

* The syntheses described herein were based on the initial results of Fraser and Wu (see reference 90).

Solutions of lithium aluminum hydride in THF were prepared from a 1 M solution and calibrated as described in the Experimental of Chapter 4 of this thesis.

5-Methylthio-5,7-dihydro-1,11-dimethyl-6*H*-dibenzo[a,c]cyclohepten-6-one 46, Axial

To a stirred solution of LHMDS (2.1 mmol, prepared at 0°C from methyllithium and 1,1,1,3,3,3-hexamethyldisilazane (Aldrich) and allowed to stir for 1 h) in THF (1 mL) was added dropwise a solution of ketone **44** (473 mg, 2.0 mmol) in THF (2 mL) at -78°C and then the temperature was raised to 0°C. After 1 h at 0°C, the solution was cooled to -78°C and methylthiolmethylsulphonate[77] (purchased from Aldrich; 206 μL, 2.0 mmol) in THF (1 mL) was added and continued for 0.5 h at -15°C. The reaction mixture was quenched with ~1 mL of 0.75 N HCl, concentrated to remove the THF and extracted with Et_2O (3 x 10 mL). The combined organic extracts were dried (Na_2SO_4), filtered and concentrated *in vacuo*. The crude product (652 mg) was purified by flash column chromatography using Et_2O:hexanes (1:50 v/v) as eluent. Recrystallization from ether-hexanes afforded **46** (243 mg) in 43% yield (unoptimized): m.p. 110-113°C; R_f = 0.31 (Et_2O:hexanes, 1:5 v/v); ^1H NMR (500 MHz): 7.28-7.22 (m, 4H), 7.12-7.10 (m, 2H), 3.98 (s, 1H), 3.55 (AB q, 2H, J = 14.6 Hz), 2.18 (s, 3H), 2.17 (s, 3H), 2.08 (s, 3H); ^{13}C NMR (125.7 MHz): 205.8, 137.9, 137.6, 136.8, 136.6, 136.4, 132.4, 130.5, 129.0, 128.1, 127.5, 127.2, 125.9, 60.4, 48.3, 19.9, 19.6, 18.8; HRMS calcd for $C_{18}H_{18}OS$ (M^+) m/z 282.1078, found 282.1080.

A suitable sample for X-ray analysis was obtained by recrystallizing **46** from ether-hexanes.[91]

5-Methylthio-5,7-dihydro-1,11-dimethyl-6*H*-dibenzo[a,c]cyclohepten-6-one 50, Equatorial

Method A:

Compound **50** was obtained by isomerization of **46**. To a stirred solution of **46** (95 mg, 0.34 mmol) in acetonitrile (10 mL) was added sodium methoxide (24 mg, 0.57 mmol) at rt for 1 h. The solution was concentrated under vacuum and partitioned between ether (3 x 10 mL) and water (2 mL). The combined organic extracts were washed with water, dried (Na_2SO_4) and evaporated to a syrup (93 mg, **50:46**, 1:2.4). Purification by flash column chromatography over silica gel (150 fold, 13.95 g) using AcOH:Et_2O:hexanes (1:2:100 v/v/v) as eluent yielded after concentration a maximum **50:46** ratio of ~1:1 for the early fractions (R_f = 0.31, Et_2O:hexanes, 1:5 v/v). An appropriate pressure of N_2 was used to complete the chromatography within a maximum of 10-15 min.

Method B:

Ketone **50** was prepared by concentrating the mother liquor solution from the synthesis of **46**. Purification by flash column chromatography as described in Method A yielded after concentration a maximum **46:50** ratio of 1:6 for the early fractions: ^{1}H NMR (500 MHz) in the presence of **46**: 7.64-7.63 (m, 1H), 7.36-7.07 (m, 5H), 4.77 (s, 1H), 3.45 (AB q, 2H, J = 16.8 Hz), 2.26 (s, 6H), 1.93 (s, 3H); ^{13}C NMR (125.7 MHz): 204.8, 137.2, 137.0, 134.7, 133.1,130.0, 129.6, 128.1, 127.8, 126.4, 123.5, 61.1, 47.9, 19.9, 14.2; HRMS calcd for $C_{18}H_{18}OS$ (M^+) m/z 282.1078, found 282.1099.

5-Fluoro-5,7-dihydro-1,11-dimethyl-6*H*-dibenzo[a,c]cyclohepten-6-one 53, Equatorial

To a stirred solution of LDA (1.1 mmol, prepared at 0°C from methyllithium and diisopropylamine and allowed to stir for 1 h) in THF (2 mL) was added dropwise a solution of **44** (236 mg, 1 mmol) in THF (1 mL) at -78°C and then the temperature was

raised to 0°C. After 1 h at 0°C, the solution was cooled to -78°C and N-fluorodibenzensulphonamide[81] (347 mg, 1 mmol) in THF (1 mL) was added and continued for 0.5 h at 0°C. The ice bath was removed and the solution was allowed to stir for 1 h at rt. The reaction mixture was quenched with ~1 mL of 0.75 N HCl, concentrated to remove the THF and extracted with CH_2Cl_2 (3 x 10 mL). The combined organic extracts were dried with anhydrous sodium sulphate, filtered and concentrated under reduced pressure. The crude product (426 mg) was purified by flash chromatography using Et_2O:hexanes (1:50 v/v) as eluent to afford **53** (117 mg) in 46% yield (unoptimized): m.p. 108-110°C; R_f = 0.21 (Et_2O:hexanes, 1:10 v/v); ^1H NMR (500 MHz): 7.41-7.25 (m, 5H), 7.11-7.09 (m,1H), 5.76 (d, 1H, J = 47.3 Hz), 3.49 (AB part of ABX, 2H, J = 16.9 and 3.2 (upfield portion) Hz), 2.21 (s, 3H), 2.21 (s, 3H); ^{13}C NMR (125.7 MHz): 203.0, 137.1, 136.8, 135.9, 133.4, 133.3, 133.1, 133.0, 132.4, 130.3, 129.9, 128.2, 128.0, 126.7, 119.8, 119.7, 93.9, 92.4, 46.3, 19.8, 19.4; HRMS calcd for $C_{17}H_{15}FO$ (M^+) m/z 254.1107, found 254.1112.

A suitable sample for X-ray analysis was obtained by recrystallizing **53** from ether-hexanes.[91]

5,7-dihydro-6*H*-dibenzo[a,c]cyclohepten-6-ol 65

Ketone **44** (51 mg, 0.21 mmol) in THF (4 mL) was treated with a 0.088 M solution of $LiAlH_4$ in THF (0.73 mL, 0.64 mmol). The solution was stirred at 0°C and quenched with 0.75 N HCl (1 mL) after 2 h. The reaction mixture was concentrated to remove the THF and extracted with CH_2Cl_2 (3 x 10 mL). The combined organic extracts were dried (Na_2SO_4), filtered and concentrated under vacuum to afford a syrupy product. The crude product was crystallized from ether-hexanes to afford pure **65**: m.p. 124°C; ^1H NMR (500 MHz): 7.24-7.14 (m, 4H), 7.11-7.05 (m, 2H), 4.26-4.20 (m, 1H), 2.83 (dd, 1H, J = 12.4 and 6.5 Hz), 2.53 (m, 2H), 2.15 (s, 3H), 2.13 (s, 3H), 2.04 (dd, 1H, J = 12.4 and 10.1 Hz); ^{13}C NMR (125.7 MHz): 138.1, 137.9, 137.1, 136.3, 135.8, 135.2, 128.8,

128.7, 127.1, 126.9, 126.6, 125.5, 74.7, 41.2, 40.6, 19.7, 19.7; HRMS calcd for $C_{17}H_{18}O$ (M^+) m/z 238.1358, found 238.1358.

5-Methyl-5,7-dihydro-6*H*-dibenzo[a,c]cyclohepten-6-ol 66a and 67a, Axial Major and Minor

Ketone **45** (100 mg, 0.40 mmol) in Et_2O (2 mL) was treated with LAH (Aldrich, 20 mg, 0.53 mmol). The solution was stirred at rt and quenched with 0.75 N HCl (2 mL) after 1h. The reaction mixture was concentrated to remove the ether and extracted with CH_2Cl_2 (3 x 10 mL). The combined organic extracts were dried (Na_2SO_4), filtered and concentrated under vacuum to afford a syrupy product. The crude mixture of alcohols (**66a:67a**, 9:1) was purified by repeated radial silica gel chromatography using Et_2O:hexanes (3:5 v/v) as eluent to afford pure **66a** and **67a**. Data for **66a**: m.p. 131-132° C; R_f = 0.21 (Et_2O:hexanes, 1:2 v/v); ^1H NMR (300 MHz): 7.21-6.99 (m, 6H), 4.39-4.37 (m, 1H), 3.19 (q, 1H, J = 7.7 Hz), 2.59 (AB part of ABX, 2H, $J_{A,B}$ = 14.0, $J_{A,X}$ = 5.2 (downfield portion) and $J_{B,X}$ = 1.8 (upfield portion) Hz), 2.12 (s, 6H), 0.45 (d, 3H, J = 7.6 Hz); HRMS calcd for $C_{18}H_{20}O$ (M^+) m/z 252.1514, found 252.1528. Data for **67a**: R_f = 0.21 (Et_2O:hexanes, 1:2 v/v); ^1H NMR (300 MHz): 7.24-6.99 (m, 6H), 3.92-3.87 (m, 1H), 2.86 (q, 1H, J = 7.6 Hz), 2.83 (dd, 1H, J = 12.0 and 5.9 Hz), 2.20 (dd, 1H, J = 12.0 and 10.4 Hz), 2.13 (s, 3H), 2.10 (s, 3H), 0.48 (d, 3H, J = 7.8 Hz); HRMS calcd for $C_{18}H_{20}O$ (M^+) m/z 252.1514, found 252.1519.

5-Methyl-5,7-dihydro-6*H*-dibenzo[a,c]cyclohepten-6-ol 68a and 69a, Equatorial Major and Minor

Ketone **49** (138 mg, 0.55 mmol) in THF (5 mL) was treated with a 0.10 M solution of $LiAlH_4$ in THF (1.65 mL, 0.17 mmol). The solution was stirred at 0°C for 15 min. The ice bath was then removed and the solution was quenched with 0.75 N HCl (1 mL) after 15 min. The reaction mixture was concentrated to remove the THF and

extracted with CH_2Cl_2 (3 x 10 mL). The combined organic extracts were dried (Na_2SO_4), filtered and concentrated under vacuum to afford a syrupy product. The crude mixture of alcohols (**68a**:**69a**, 6:1) was purified by repeated column chromatography using Et_2O:hexanes (1:50 v/v) as eluent to yield pure **68a** and **69a**. Data for **68a**: m.p. 127-129° C; R_f = 0.24 (Et_2O:hexanes, 1:2 v/v); ^1H NMR (300 MHz): 7.29-7.04 (m, 6H), 3.99-3.90 (m, 1H), 2.89 (dd, 1H, J = 12.6 and 6.7 Hz), 2.60 (dq, 1H, J =7.3 and 4.0 Hz), 2.13 (s, 3H), 2.12 (s, 3H), 1.92 (dd, 1H, J =12.6 and 9.8 Hz), 1.29 (d, 3H, J = 7.3 Hz), 1.00 (d, 1H, J =8.8 Hz, OH); HRMS calcd for $C_{18}H_{20}O$ (M^+) m/z 252.1514, found 252.1533. Data for **69a**: m.p. 114-115°C; R_f = 0.24 (Et_2O:hexanes, 1:2 v/v); ^1H NMR (300 MHz): 7.26-7.05 (m, 6H), 3.65-3.60 (m, 1H), 2.50 (AB part of ABX, 2H, $J_{A,B}$ ~ 13.3, $J_{A,X}$ ~ 3.5 (downfield portion) and $J_{B,X}$ ~ 2.7 (upfield portion) Hz), 2.16 (dq, 1H, J = 9.2 and 6.9 Hz), 2.14 (s, 3H), 2.10 (s, 3H), 1.38 (d, 3H, J = 6.9 Hz); HRMS calcd for $C_{18}H_{20}O$ (M^+) m/z 252.1514, found 252.1512.

5-Methylthio-5,7-dihydro-6*H*-dibenzo[a,c]cyclohepten-6-ol 66b, Axial Major

Compound **46** (25 mg, 0.087 mmol) in THF (4 mL) was treated with a 0.11 M solution of $LiAlH_4$ in THF (0.25 mL, 0.028 mmol). The solution was stirred at 0°C and quenched with 0.75 N HCl (1 mL) after 2 h. The reaction mixture was concentrated to remove the THF and extracted with CH_2Cl_2 (3 x 10 mL). The combined organic extracts were dried (Na_2SO_4), filtered and concentrated under vacuum to afford a syrupy product. The crude product was crystallized from ether-hexanes to yield pure **66b**: m.p. 218-220° C; ^1H NMR (500 MHz): 7.32-7.08 (m, 6H), 4.47-4.42 (m, 1H), 3.73 (d, 1H, J = 6.9 Hz), 3.40 (d, 1H, J = 11.8 Hz, OH), 2.56 (AB part of ABX, 2H, $J_{A,B}$ = 13.9, $J_{A,X}$ = 5.1 (downfield portion) and $J_{B,X}$ = 1.6 (upfield portion) Hz), 2.13 (s, 3H), 2.12 (s, 3H), 1.98 (s, 3H); ^{13}C NMR (125.7 MHz): 140.5, 138.1, 138.1, 137.4, 137.1, 135.4, 129.7, 128.7, 127.6, 127.1, 126.9, 125.0, 74.8, 61.4, 40.4, 20.8, 19.6, 19.4; HRMS calcd for $C_{18}H_{20}OS$ (M^+) m/z 284.1235, found 284.1231.

5-Methylthio-5,7-dihydro-6*H*-dibenzo[a,c]cyclohepten-6-ol 68b, Equatorial Major

A 6:1 mixture of **50:46** (7.1 mg, 0.025 mmol) in THF (4 mL) was treated with $LiAlH_4$ (0.0075 mmol). The solution was stirred at 0°C and quenched with 0.75 N HCl (1 mL) after 2 h. The reaction mixture was purified by preparative TLC using EtOAc:hexanes (1:20 v/v) as eluent to afford pure **68b** as an oil: R_f = 0.26 (EtOAc:hexanes, 1:5 v/v); ^{1}H NMR (500 MHz): 7.32-7.00 (m, 6H), 4.12-4.07 (m, 1H), 3.51 (d, 1H, J = 3.8 Hz), 2.86 (dd, 1H, J = 12.6 and 6.6 Hz), 2.32 (d, 1H, J = 4.1 Hz, OH), 2.09 (s, 3H), 2.07 (s, 3H), 1.98 (dd, 1H, J = 12.6 and 9.9 Hz); ^{13}C NMR (125.7 MHz): 137.5, 137.4, 137.0, 135.8, 134.4, 129.5, 129.1, 127.4, 127.3, 125.8, 123.9, 74.0, 54.4, 40.2, 19.8, 14.4; HRMS calcd for $C_{18}H_{20}OS$ (M^+) m/z 284.1235, found 284.1247.

5-Methoxy-5,7-dihydro-6*H*-dibenzo[a,c]cyclohepten-6-ol 66c, Axial Major

Compound **47** (34 mg, 0.13 mmol) in THF (7 mL) was treated with $LiAlH_4$ (0.040 mmol). The solution was stirred at 0°C and quenched with 0.75 N HCl (1 mL) after 1 h. The reaction mixture was concentrated to remove the THF and extracted with CH_2Cl_2 (3 x 10 mL). The combined organic extracts were dried (Na_2SO_4), filtered and concentrated *in vacuo* to yield a syrupy product. The crude product was crystallized from ether-hexanes to afford pure **66c**: m.p. 130-132°C; ^{1}H NMR (500 MHz): 7.32-7.04 (m, 6H), 4.26 (d, 1H, J = 6.0 Hz), 4.23-4.17 (m, 1H), 3.19 (d, 1H, J =10.1 Hz, OH), 2.87 (s, 3H), 2.55 (AB part of ABX, 2H, $J_{A,B}$ = 14.0, $J_{A,X}$ = 4.8 (downfield portion) and $J_{B,X}$ = 1.6 (upfield portion) Hz), 2.13 (s, 3H), 2.13 (s, 3H); ^{13}C NMR (125.7 MHz): 138.3, 137.6, 137.4, 137.2, 136.4, 135.4, 130.8, 128.4, 127.0, 126.8, 126.5, 126.4, 84.1, 75.8, 56.1, 39.6, 19.5, 19.4; HRMS calcd for $C_{18}H_{20}O_2$ (M^+) m/z 268.1463, found 268.1470.

5-Methoxy-5,7-dihydro-6*H*-[a,c]cyclohepten-6-ol 68c, Equatorial Major

Compound **51** (68 mg, 0.26 mmol) in THF (8 mL) was treated with $LiAlH_4$ (0.080 mmol). The solution was stirred at 0°C and quenched with 0.75 N HCl after 1 h. The

reaction mixture was concentrated to remove the THF and extracted with CH_2Cl_2 (3 x 10 mL). The combined organic extracts were dried (Na_2SO_4), filtered and concentrated under vacuum to give a syrupy product. The crude product was purified by column chromatography using EtOAc:hexanes (1:10 v/v) as eluent to afford pure **68c**: m.p. 95-96 °C; R_f = 0.22 (EtOAc:hexanes, 1:5 v/v); ^{1}H NMR (500 MHz): 7.32-7.05 (m, 6H), 4.30-4.26 (m, 1H), 3.80 (d, 1H, J = 4.5 Hz), 3.38 (s, 3H), 2.83 (dd, 1H, J = 12.6 and 6.8 Hz), 2.44 (d, 1H, J = 2.1 Hz, OH), 2.14 (s, 3H), 2.12 (s, 3H), 2.00 (dd, 1H, J = 12.6 and 10.0 Hz); ^{13}C NMR (125.7 MHz): 137.1, 136.2, 136.0, 135.8, 135.1, 129.3, 129.0, 127.3, 127.1, 125.9, 121.7, 81.0, 74.3, 57.6, 38.5, 19.8, 19.5; HRMS calcd for $C_{18}H_{20}O_2$ (M^+) m/z 268.1463, found 268.1448.

5-Chloro-5,7-dihydro-6*H*-dibenzo[a,c]cyclohepten-6-ol 66d, Axial Major

A 2:1 mixture of **52**:**68** (33 mg, 0.12 mmol) in THF (2 mL) was treated with $LiAlH_4$ (0.04 mmol). The solution was stirred at 0°C and quenched with 0.75 N HCl (1 mL) after 1h. The combined organic extracts were dried (Na_2SO_4), filtered and concentrated under vacuum to give a syrupy product. The crude product was purified by column chromatography using EtOAc:hexanes (1:5 v/v) as eluent to give pure **66d**: m.p. 90-91°C; R_f = 0.28 (EtOAc:hexanes 1:5 v/v); ^{1}H NMR (500 MHz): 7.31-7.08 (m, 6H), 5.18 (d, 1H, J = 6.3 Hz), 4.33-4.30 (m, 1H), 2.65 (AB part of ABX, 2H, $J_{A,B}$ = 14.3, $J_{A,X}$ = 5.4 (downfield portion) and $J_{B,X}$ ~ 0 (upfield portion) Hz), 2.57 (d, 1H, J = 11.7 Hz, OH), 2.16 (s, 3H), 2.08 (s, 3H); ^{13}C NMR (125.7 MHz): 138.4, 138.2, 137.8, 137.1, 136.7, 134.5, 131.3, 129.0, 127.4, 126.9, 126.6, 125.8, 73.5, 67.1, 39.7, 19.7, 19.4; HRMS calcd for $C_{17}H_{17}ClO$ (M^+) m/z 272.0968, found 272.0948.

5-Chloro-5,7-dihydro-6*H*-dibenzo[a,c]cyclohepten-6-ol 68d, Equatorial Major

To a stirred solution of **52** (54 mg, 0.20 mmol) in THF (5 mL) was added $LiAlH_4$ (0.065 mmol) at 0°C. After 1 h the reaction mixture was quenched with 0.75 N HCl (1

mL). The combined organic extracts were dried (Na_2SO_4), filtered and concentrated under vacuum to give a 8.2:1 mixture of **68d**:**69d**. The crude product was purified by column chromatography using EtOAc:hexanes (1:5 v/v) as eluent to afford pure **68d**: m.p. 84-86° C; R_f = 0.32 (EtOAc:hexanes, 1:5 v/v); ^{1}H NMR (500 MHz): 7.51-7.07 (m, 6H), 4.79 (d, 1H, J = 3.7 Hz), 4.24-4.21 (m, 1H), 2.90 (dd, 1H, J = 12.8 and 6.8 Hz), 2.29 (d, 1H, J = 3.3 Hz, OH), 2.13 (s, 3H), 2.13, (s, 3H), 2.08 (dd, 1H, J = 12.8 and 9.9 Hz); ^{13}C NMR (125.7 MHz): 136.7, 136.6, 135.8, 135.6, 133.3, 130.1, 129.4, 127.7, 127.3, 126.0, 123.7, 76.4, 65.0, 39.5, 19.7, 19.6; HRMS calcd for $C_{17}H_{17}ClO$ (M^+) m/z 272.0968, found 272.0994.

5-Fluoro-5,7-dihydro-6*H*-dibenzo[a,c]cyclohepten-6-ol 68e and 69e, Equatorial Major and Minor

To a stirred solution of **53** (43 mg, 0.17 mmol) in THF (5 mL) was added $LiAlH_4$ (0.051 mmol) at 0°C. After 1 h the reaction was quenched with 0.75 N HCl (1 mL). The combined organic extracts were dried (Na_2SO_4), filtered and concentrated under vacuum to give a syrupy product. The crude mixture of alcohols (**68e**:**69e**, 7.6:1) was purified by preparative TLC using acetone:hexanes (1:10 v/v) as eluent to afford pure **68e** and **69e**. Data for **68e**: m.p. 112-114°C; R_f = 0.35 acetone:hexanes (1:2 v/v); ^{1}H NMR (500 MHz): 7.37-7.09 (m, 6H), 5.12 (dd, 1H, J = 45.6 and 4.5 Hz), 4.48-4.43 (m, 1H), 2.91 (ddd, 1H, J = 12.8, 7.2 and 3.7 Hz), 2.16-2.12 (m, 1H), 2.16 (s, 3H), 2.14 (s, 3H); ^{13}C NMR (125.7 MHz): 136.5, 136.5, 136.4, 135.7, 135.7, 135.2, 133.9, 133.9, 133.8, 133.7, 129.8, 129.3, 127.6, 127.2, 127.2, 126.0, 120.9, 120.8, 93.1, 91.7, 74.2, 74.0, 38.4, 38.3, 19.7, 19.7, 19.3, 19.3; HRMS calcd for $C_{17}H_{17}FO$ (M^+) m/z 256.1263, found 256.1265. Data for **69e**: R_f = 0.32 acetone:hexanes (1:2 v/v); ^{1}H NMR (500 MHz): 7.39-7.14 (m, 6H), 4.87 (dd, 1H, J = 49.6 and 7.5 Hz), 4.15-4.09 (m, 1H), 2.59 (d, 2H), 2.15 (s, 3H), 2.15 (s, 3H); ^{13}C NMR (125.7 MHz): 136.2, 136.1, 136.0, 135.7, 135.6, 135.3, 134.0, 133.9,

130.0, 129.2, 127.7, 127.2, 127.1, 126.8, 119.6, 119.5, 97.5, 96.1, 78.6, 78.4 38.2, 38.1, 19.7, 19.3, 19.3; HRMS calcd for $C_{17}H_{17}FO$ (M^+) m/z 256.1263, found 256.1260.

5.3 Experimental for Chapter 3 Part B

All NMR spectra were recorded on a Bruker AMX 500 spectrometer using an inverse detection probe with homogeneity optimized to afford resolution of ≤0.4 Hz. $CDCl_3$ (99.8%), acetone-d_6 (99.9%) and acetonitrile-d_3 (99.8%) were obtained from Cambridge Isotopes Laboratories, carbon tetrachloride (99.7%) was obtained from BDH and cyclohexane-d_{12} (99.5%) was obtained from Aldrich. Acetonitrile-d_3 was dried over calcium hydride before its use.

Due to the unresolved long range couplings in **73** and **74**, which are expected to be between 0.8 and 1.0 Hz, the measured coupling constants J_{obs} are estimated to be accurate within 0.2 Hz.

2-Methoxycyclohexanone (**74**) was purchased from Aldrich and used without further purification. 2-Methylthiocyclohexanone (**73**) was synthesized by the addition of methylmethanethiolsulphonate to the cyclohexanone lithium enolate as described in the literature.[77]

5.4 Experimental for Chapter 4

Standardization of $LiAlH_4$ Solutions

A mixture of approximately 0.4 mL of 1.0 M $LiAlH_4$ solution in THF (Aldrich) and 19.6 mL of THF was added to a 25 mL round bottom flask fitted with a septum capped adapter bearing a one-way stopcock. The resulting solution was stirred and sealed with parafilm. In a separate 10 mL round bottom flask was placed ~40 mg (0.190 mmol) of accurately weighed 1,3-diphenylacetone (Aldrich) and 4 mL of THF. To the 1,3-diphenylacetone solution was added 2 mL of the freshly prepared $LiAlH_4$ solution. The

reaction mixture was stirred at rt and quenched with ~1 mL of 0.75N HCl after 2 h. The resulting solution was concentrated *in vacuo* to remove the THF, extracted with $CHCl_3$ (3 x 10 mL), washed with H_2O and dried over sodium sulphate. The filtered $CHCl_3$ solution was concentrated under reduced pressure and analyzed by either 300 or 500 MHz ^1H NMR. The molarity of the $LiAlH_4$ solution was determined by employing the following equation: M of $LiAlH_4$ = ab/8, where a = mmol of 1,3 diphenylacetone and b = % of 1,3-diphenylacetone reduced.

Standardization of $NaBH_4$ Solutions

The standardization of sodium borohydride was accomplished as described in the literature with some minor changes.[163] An approximately 16 mg (0.423 mmol) sample of $NaBH_4$ was dissolved in 20 mL of *i*-PrOH and stirred for ~15 min. The solution was then filtered and a 5 mL aliquot was added to an Erlenmeyer flask containing 25 mL of 0.5 N NaOH. A 0.1500 N solution of KIO_3 was added immediately and the flask was stirred vigorously. After 30 seconds, KI (~400 mg) and 20 mL of 4 N H_2SO_4 were then added. The subsequent procedure is identical to that described in reference 163.

General Procedure for the Competitive Reductions by LAH

To a 10 or 25 mL round bottom flask was added the mixture of ketones under study (total ~0.05 mmol) and an appropriate amount of THF to give a final total volume of 4-10 mL of THF (see Appendix 2). The solution was stirred vigorously at 0°C for 15 min and ~0.00625 mmol of a standardized solution of $LiAlH_4$ (~0.015 M) was added and the reaction mixture was quenched after 20 seconds with ~1 mL of 0.75 N HCl. The resulting solution was diluted with ~20 mL of H_2O, extracted with $CHCl_3$ (5 x 10 mL) and washed with H_2O. The combined organic extracts were dried over Na_2SO_4 and concentrated by careful rotary evaporation (i.e. water bath < 35°C). The remaining traces of solvent were removed under high vacuum (~25 mT). The oily residue was then

analyzed by 500 MHz ^{1}H NMR and the relative rates were determined as described in Section 4.2. The 500 MHz ^{1}H NMR spectra for the competitive reduction of the α-methoxy ketone **51/44** were obtained in benzene-d_6 to remove peak overlap.

As mentioned in Section 4.2.1, the decrease in relative rate constants for entries 6 and 8 in Table 4.2 may be due to incomplete disproportionation and thus involving alkoxyaluminohydride ions. Accordingly, the average from entries 1-5 and 7 was used to calculate $k_{CH_3}^{app}/k_H$. Due to the uncertainty associated with this assumption, we estimate the accuracy of the relative rate constant for the axial α-methyl ketone **45** to be ±20%.

In addition, as mentioned in Section 4.2.1, the relative rate constant for the equatorial α-methylthio ketone **50** was determined by employing a mixture of **50** and **46**. As for the axial methyl ketone **45**, it was assumed that as the **50**:**46** ratio decreased, the participation of higher order alkoxyaluminohydrides becomes more prominent and could exaggerate the difference in reactivity between these ketones. The runs using a ~1:1 ratio were thought to best represent the relative rate. Due to the uncertainty associated with this assumption, we estimate the accuracy of $k_{SCH_3}^{ax}/k_H$ to be ± 30%.

For all remaining substituents this variability was not observed. We estimate the integrals in the ^{1}H NMR spectra to be accurate within 1%. This corresponds to a precision in the relative rate constants of ±5%.

General Procedure for the Competitive Reductions by SBH

To a 10 or 25 mL round bottom flask was added the mixture of ketones under study (total ~0.05 mmol) and an appropriate amount of *i*-PrOH to give a final total volume of 4-10 mL (see Appendix 2). The solution was stirred vigorously at 23°C for 15 min and ~0.0125 mmol of a standardized solution of $NaBH_4$ (~0.02 M) was added and the reaction mixture was quenched after 0.75-15 min with ~2 mL of 0.75 N HCl. The resulting solution was diluted with ~20 mL of H_2O, extracted with $CHCl_3$ (5 x 10 mL) and washed with H_2O. The combined organic extracts were dried over Na_2SO_4 and

concentrated by careful rotary evaporation (i.e. water bath < 35°C). The remaining traces of solvent were removed under high vacuum (~25 mT). The oily residue was then analyzed by 500 MHz ^{1}H NMR and the relative rates were determined as described in Section 4.2. The 500 MHz ^{1}H NMR spectra for the competitive reduction of the α-methoxy ketone **51/44** were obtained in benzene-d_6 to remove peak overlap.

General Procedure for the Competitive Reductions by Triethylsilane[164]

To a 10 mL round bottom flask was added the mixture of ketones under study (total ~0.05 mmol) and 5 mL of CH_3CN (see Appendix 2). The solution was stirred vigorously at 0°C and Et_3SiH (~0.05 mmol, 8.0 μL) was added. After 15 min, BF_3•Et_2O (~0.15 mmol, 19 μL) was added and the solution was quenched after 0.75-16 min with ~2 mL of 0.75 N HCl. The resulting solution was diluted with ~20 mL of H_2O, extracted with $CHCl_3$ (5 x 10 mL) and washed with H_2O. The combined organic extracts were dried over Na_2SO_4 and concentrated by careful rotary evaporation (i.e. water bath < 35° C). The remaining traces of solvent were removed under high vacuum (~25 mT). The oily residue was then analyzed by 500 MHz ^{1}H NMR and the relative rates were determined as described in Section 4.2. The 500 MHz ^{1}H NMR spectra for the competitive reduction of the α-methoxy ketone **51/44** were obtained in benzene-d_6 to remove peak overlap.

References

1. (a) McKenzie, A. *J. Chem. Soc.* **1904**, *85*, 1249. (b) Turner, E.E.; Harris, M.M.; *Q. Rev., Chem. Soc.* **1947**, *1*, 299. (c) Bovey, D.M.; Turner, E.E. *J. Chem. Soc.* **1951**, 3223.
2. For a more comprehensive review see: (a) Morrison, J.D.; Mosher, H.S. *Asymmetric Organic Reactions*; Prentice-Hall: Englewood Cliffs, NJ, 1971; Chapter 3. (b) Eliel, E.L. In *Asymmetric Synthesis*; Morrison, J.D., Ed.; Academic Press: New York, 1983; Vol. 2 p 125.
3. (a) Chérest, M.; Felkin, H.; Prudent, N. *Tetrahedron Lett.* **1968**, 2199. (b) Chérest, M.; Felkin, H. *Tetrahedron Lett.* **1968**, 2205.
4. Cram, D.J.; Elhafez, F.A.A. *J. Am. Chem. Soc.* **1952**, *74*, 5828.
5. Cram, D.J.; Kopecky, K.R. *J. Am. Chem. Soc.* **1959**, *81*, 2748.
6. Cornforth, J.W.; Cornforth, R.H.; Mathew, K.K. *J. Chem. Soc.* **1959**, 112.
7. This topic has been the subject of a review see: reference 2a.
8. For recent contributions on the chelate controlled model see: (a) Paquette, L.A.; Lobben, P.C. *J. Am. Chem. Soc.* **1996**, *118*, 1917. (b) Chen, X.; Hortelano, E.R.; Eliel, E.L.; Frye, S.V. *J. Am. Chem. Soc.* **1992**, *114*, 1778.
9. Sauleau, J. *Bull. Soc. Chim. Fr. II* **1978**, 474.
10. Karabatsos, G.J.; Hsi, N. *J. Am. Chem. Soc.* **1965**, *87*, 2864 and references therein.
11. Karabatsos, G.J. *J. Am. Chem. Soc.* **1967**, *89*, 1367.
12. (a) Schleyer, P.v.R. *J. Am. Chem. Soc.* **1967**, *89*, 699. (b) Schleyer, P.v.R. *J. Am. Chem Soc.* **1967**, *89*, 701. (c) Garbisch, E.W., Jr.; Schildcrout, S.; Patterson, D.B.; Spreecher, C.M. *J. Am. Chem. Soc.* **1965**, *87*, 2932.
13. (a) Anh, N.T. *Nouv. J. Chim.* **1977**, *1*, 61. (b) Anh, N.T. *Top. Curr. Chem.* **1980**, *88*, 145.

14. (a) Bürgi, H.B; Dunitz, J.B.; Shefter, E. *J. Am. Chem. Soc.* **1973**, *95*, 5065. (b) Bürgi, H.B.; Lehn, J.M.; Wipff, G. *J. Am. Chem. Soc.* **1974**, *96*, 1956. (c) Bürgi, H.B.; Dunitz, J.D.; Lehn, J.M.; Wipff, G. *Tetrahedron* **1974**, *30*, 1563.

15. Liotta, C.L.; Burgess, E.M.; Eberhardt, W.H. *J. Am. Chem. Soc.* **1984**, *106*, 4849.

16. Fukui, K. *Acc. Chem. Res.* **1971**, *4*, 57.

17. Lodge, E.P.; Heathcock, C.H. *J. Am. Chem. Soc.* **1987**, *109*, 3353.

18. Wu, Y.-D.; Houk, K.N. *J. Am. Chem. Soc.* **1987**, *109*, 908.

19. Wipke, W.T.; Gund, P. *J. Am. Chem. Soc.* **1976**, *98*, 8107.

20. Perlberger, J.-C.; Müller, P. *J. Am. Chem. Soc.* **1977**, *99*, 6316.

21. Paddon-Row, M.N.; Rondan, N.G.; Houk, K.N. *J. Am. Chem. Soc.* **1982**, *104*, 7162.

22. (a) Wong, S.S.; Paddon-Row, M.N. *J. Chem. Soc., Chem. Commun.* **1990**, 456. (b) Wong, S.S.; Paddon-Row, M.N. *J. Chem. Soc., Chem. Commun.* **1991**, 327.

23. Frenking, G.; Köhler, K.F.; Reetz, M.T. *Tetrahedron* **1991**, *47*, 9005.

24. For a thorough review of the diastereoselectivity in cyclohexanone and other cyclic ketone substrates see: (a) Kamernitzky, A.V.; Akhrem, A.A. *Tetrahedron* **1962**, *18*, 705. (b) Boone, J.R.; Ashby, E.C. *Top. Stereochem.* **1979**, *11*, 53. (c) Houk, K.N.; Wu, Y.-D. In *Stereochemistry of Organic and Bioorganic Transformations*; Bartmann, W., Sharpless, K.B., Eds.; VCH, Weinheim, Germany, 1987, p 247. (d) Gung, B.W. *Tetrahedron* **1996**, *52*, 5263.

25. Eliel, E.L.; Senda, Y. *Tetrahedron* **1970**, *26*, 2411.

26. Wigfield, D.C.; Phelps, D.J. *J. Org. Chem.* **1976**, *41*, 2396.

27. Lansbury, P.T.; MacLeay, R.E. *J. Org. Chem.* **1963**, *28*, 1940.

28. Cense, J.-M. *Tetrahedron Lett.* **1972**, 2153.

29. Rickborn, B.; Wuesthoff, M.T. *J. Am. Chem. Soc.* **1970**, *92*, 6894.

30. Ashby, E.C.; Boone, J.R. *J. Org. Chem.* **1976**, *41*, 2890.

31. Haubenstock, H.; Eliel, E.L. *J. Am. Chem. Soc.* **1962**, *84*, 2363.

32. Kobayashi, Y.M.; Lambrecht, J.; Jochims, J.C.; Burkert, U. *Chem. Ber.* **1978**, *111*, 3442.

33. This topic has been the focus of several reviews see: (a) reference 24b. (b) Wigfield, D.C. *Tetrahedron* **1979**, *35*, 449. (c) reference 24c. (d) Li, H.; le Noble, W.J. *Recl. Trav. Chim. Pays-Bas* **1992**, *111*, 199. (e) reference 24d.

34. Barton, D.H.R. *J. Chem. Soc.* **1953**, 1027.

35. Dauben, W.G.; Fonken, G.J.; Noyce, D.S. *J. Am. Chem. Soc.* **1956**, *78*, 2579.

36. Brown, H.C.; Deck, H.R. *J. Am. Chem. Soc.* **1965**, *87*, 5620.

37. Hammond, G.S. *J. Am. Chem. Soc.* **1955**, *77*, 334.

38. (a) Eliel, E.L.; Ro, R.S. *J. Am. Chem. Soc.* **1957**, *79*, 5992. (b) Eliel, E.L.; Schroeter, S.H. *J. Am. Chem. Soc.* **1965**, *87*, 5031.

39. For another example where the observed ratio of alcohol products is greater than that observed at equilibrium for 7-norbornanone derivatives see: Ashby, E.C.; Noding, S.A. *J. Org. Chem.* **1977**, *42*, 264.

40. (a) Cieplak, A.S. *J. Am. Chem. Soc.* **1981**, *103*, 4540. (b) Cieplak, A.S.; Tait, B.D.; Johnson, C.R. *J. Am. Chem. Soc.* **1989**, *111*, 8447.

41. (a) Lau, J.; Gonikberg, E.M.; Hung, J.; le Noble, W.J. *J. Am. Chem. Soc.* **1995**, *117*, 11421. (b) Bellucci, G.; Chiappe, C.; Moro, G.L.; Ingrosso, G. *J. Org. Chem.* **1995**, *60*, 6214. (c) Mehta, G.; Khan, F.A.; Gadre, S.R.; Shirsat, R.N.; Ganguly, B.; Chandrasekhar, J. *Angew. Chem., Int. Ed. Engl.* **1994**, *33*, 1390. (d) Jones, G.R.; Vogel, P.; *J. Chem. Soc., Chem. Commun.* **1993**, 769. (e) Halterman, R.L.; McEvoy, M.A. *J. Am. Chem. Soc.* **1992**, *114*, 980. (f) Srivastava, S.; le Noble, W.J. *J. Am. Chem. Soc.* **1987**, *109*, 5874.

42. (a) Halterman, R.L.; McCarthy, B.A.; McEvoy, M.A. *J. Org. Chem.* **1992**, *57*, 5585. (b) Coxon, J.M.; McDonald, D.Q. *Tetrahedron Lett.* **1992**, *33*, 651. (c) Chung, W.-S.; Turro, N.J.; Srivastava, S.; le Noble, W.J. *J. Org. Chem.* **1991**, *56*, 5020. (d) Li, H.; Silver, J.E.; Watson, W.H.; Kashyap, R.M.; le Noble, W.J. *J.*

Org. Chem. **1991**, *56*, 5932. (e) Macaulay, J.B.; Fallis, A.G. *J. Am. Chem. Soc.* **1990**, *112*, 1136.

43. Bodepudi, V.R.; le Noble, W.J. *J. Org. Chem.* **1991**, *56*, 2001.

44. (a) Song, I.H.; le Noble, W.J. *J. Org. Chem.* **1994**, *59*, 58. (b) Lin, M.-H.; Cheung, C.K.; le Noble, W.J. *J. Am. Chem. Soc.* **1988**, *110*, 6562. (c) Cheung, C.K.; Tseng, L.T.; Lin, M.-H.; Srivastava, S.; le Noble, W.J. *J. Am. Chem. Soc.* **1986**, *108*, 1598; **1987**, *109*, 7239.

45. Mukherjee, A.K.; le Noble, W.J. *J. Org. Chem.* **1993**, *58*, 7955.

46. Muhkerjee, A.; Venter, E.M.M.; le Noble, W.J.; Watson, W.H.; Kashyap, R.P. *Tetrahedron Lett.* **1992**, *33*, 3837.

47. (a) Mukherjee, A.; Wu, Q.; le Noble, W.J. *J. Org. Chem.* **1994**, *59*, 3270. (b) Mukherjee, A.; Schulman, E.M.; le Noble, W.J. *J. Org. Chem.* **1992**, *57*, 3120. (c) Lin, M.-H.; Watson, W.H.; Kashyap, R.P.; le Noble, W.J. *J. Org. Chem.* **1990**, *55*, 3597. (d) Lin, M.-H.; le Noble, W.J. *J. Org. Chem.* **1989**, *54*, 997.

48. (a) Raghavachari, K.; Whiteside, R.A.; Pople, J.A.; Schleyer, P.v.R. *J. Am. Chem. Soc.* **1981**, *103*, 5649. (b) Rozeboom, M.D.; Houk, K.N. *J. Am. Chem. Soc.* **1982**, *104*, 1189. (c) Koch, W.; Liu, B.; Schleyer, P.v.R. *J. Am. Chem. Soc.* **1989**, *111*, 3479. (d) Wu, Y.-D.; Tucker, J.A.; Houk, K.N. *J. Am. Chem. Soc.* **1991**, *113*, 5018.

49. (a) Adcock, W.; Abeywickrema, A.N. *J. Org. Chem.* **1982**, *47*, 2957. (b) Kirchen, R.P.; Ranganayakulu, K.; Sorensen, T.S. *J. Am. Chem. Soc.* **1987**, *109*, 7811. (c) Finne, E.S.; Gunn, J.R.; Sorensen, T.S. *J. Am. Chem. Soc.* **1987**, *109*, 7816. (d) Laube, T.; Stilz, H.U. *J. Am. Chem. Soc.* **1987**, *109*, 5876. (e) Laube, T.; Ha, T.-K. *J. Am. Chem. Soc.* **1988**, *110*, 5511. (f) Dutter, R.; Rauk, A.; Sorensen, T.S.; Whitworth, S.M. *J. Am. Chem. Soc.* **1989**, *111*, 9024.

50. Wu, Y.-D.; Houk, K.N.; Paddon-Row, M.N. *Angew. Chem., Int. Ed. Engl.* **1992**, *31*, 1019.

51. Coxon, J.M.; Luibrand, R.T. *Tetrahedron Lett.* **1993**, *34*, 7097.

52. Shi, Z.; Boyd, R.J. *J. Am. Chem. Soc.* **1993**, *115*, 9614.

53. For a review of earlier experimental investigations see: references 24a,b and c.

54. le Noble based the symmetric assumption for **17a-b** on X-ray crystallographic evidence of similar compounds see: (a) Fernandez, M.J.; Galvez, E.; Lorente, A.; Soler, J.A.; Florencio, F.; Sonz, J. *J. Heterocycl. Chem.* **1989**, *26*, 349. (b) McCabe, P.H.; Milne, N.J.; Sim, G.A. *Acta Crystallogr.* **1989**, *C45*, 114. (c) Goncharov, A.V.; Panov, V.N.; Maleev, A.V.; Potekin, K.A.; Kurkutova, E.N. Stuchkov, Y.T.; Palyvulin, V.A.; Zefirov, N.S. *Dokl. Akad. Nauk. SSSR* **1991**, *318*, 907.

55. (a) Lantvoev, V.I. *J. Org. Chem. USSR (Engl. Transl.)* **1980**, *16*, 1409. (b) Adcock, W.; Trout, N.A. *J. Org. Chem.* **1991**, *56*, 3229. (c) Xie, M.; le Noble, W.J. *J. Org. Chem.* **1989**, *54*, 3836. (d) Hahn, J.M.; le Noble, W.J. *J. Am. Chem. Soc.* **1992**, *114*, 1916. (e) Gonikberg, E.M.; le Noble, W.J. *J. Org. Chem.* **1995**, *60*, 7751. (f) Kaselj, M.; Adcock, J.L.; Luo, H.; Zhang, H.; Li, H.; le Noble, W.J. *J. Am. Chem. Soc.* **1995**, *117*, 7088.

56. Ganguly, B.; Chandrasekhar, J.; Khan, F.A.; Mehta, G. *J. Org. Chem.* **1993**, *58*, 1734.

57. Coxon, J.M; Houk, K.N.; Luibrand, R.T. *J. Org. Chem.* **1995**, *60*, 418.

58. Gung, B.W.; Wolf, M.A. *J. Org. Chem.* **1996**, *61*, 232.

59. Halterman, R.L.; McEvoy, M.A. *J. Am. Chem. Soc.* **1990**, *112*, 6690.

60. (a) Mehta, G.; Khan, F.A.; *J. Am. Chem. Soc.* **1990**, *112*, 6140. (b) Mehta, G.; Khan, F.A. *Tetrahedron Lett.* **1992**, *33*, 3065. (c) Kumar, V.A.; Venkatesan, K.; Ganguly, B.; Chandrasekhar, J.; Khan, F.A.; Mehta, G. *Tetrahedron Lett.* **1992**, *33*, 3069.

61. Paddon-Row, M.N.; Wu, Y.-D.; Houk, K.N. *J. Am. Chem. Soc.* **1992**, *114*, 10638.

62. (a) Okada, K.; Tomita, S.; Oda, M. *Tetrahedron Lett.* **1986**, *27*, 2645. (b) Okada, K.; Tomita, S.; Oda, M. *Bull. Chem. Soc. Jpn.* **1989**, *62*, 459.

63. (a) Wipf, P.; Kim, Y.; Fritch, P.C. *J. Org. Chem.* **1993**, *58*, 7195. (b) Wipf, P.; Kim, Y. *J. Org. Chem.* **1993**, *58*, 1649.

64. Wipf, P.; Kim, Y. *J. Am. Chem. Soc.* **1994**, *116*, 11678.

65. Adcock, W.; Cotton, J.; Trout, N.A. *J. Org. Chem.* **1994**, *59*, 1867.

66. Kwart, H.; Takeshita, T. *J. Am. Chem. Soc.* **1962**, *84*, 2833.

67. Mislow, K.; Glass, M.A.W.; O'Brien, R.E.; Rutkin, P.; Steinberg, D.H.; Weiss, J.; Djerassi, C. *J. Am. Chem. Soc.* **1962**, *84*, 1455.

68. Mislow, K.; Gordon, A.J. *J. Am. Chem. Soc.* **1963**, *85*, 3521.

69. The 200 MHz ^{1}H NMR spectrum of **54** in $CDCl_3$ exhibits two diastereotopic α-hydrogens at rt (i.e. AB pattern, $\Delta\nu$ = 20.5 Hz).

70. Anet, F.A.L.; Chmurny, G.N.; Krane, J. *J. Am. Chem. Soc.* **1973**, *95*, 4423.

71. Manoharan, M.; Eliel, E.L. *Tetrahedron Lett.* **1984**, *25*, 3267.

72. Allinger, N.L.; Chen, K.; Rahman, M.; Pathiaseril, A. *J. Am. Chem. Soc.* **1991**, *113*, 4505.

73. Fraser, R.R.; Champagne, P.J. *Can. J. Chem.* **1976**, *54*, 3809.

74. Trimitsis, G.B.; Van Dam, E.M. *J. Chem. Soc., Chem. Commun.* **1974**, 610.

75. Corey, E.J.; Sneen, R.A. *J. Am. Chem. Soc.* **1956**, *78*, 6269.

76. (a) Fraser, R.R.; Stanciulesçu, M. *J. Am. Chem. Soc.* **1987**, *109*, 1580. (b) Fraser, R.R.; Kong, F.; Stanciulesçu, M.; Wu, Y.-D.; Houk, K.N. *J. Org. Chem.* **1993**, *58*, 4431.

77. Scholz, D. *Synthesis* **1983**, 944.

78. Fraser, R.R.; Bensimon, C.; Kong, F.; Wu, X. *Can. J. Chem.* **1993**, *71*, 685.

79. Fraser, R.R.; Bensimon, C.; Faibish, N.C.; Kong, F. *Can. J. Chem.* **1994**, *72*, 1481.

80. Purchased from Serena Software, P.O. Box 3076, Bloomington, IN 47402, U.S.A. For a detailed description of PCMODEL see: Gajewski, J.J.; Gilbert, K.E.; McKelvey, J. *Adv. Mol. Model.* **1990**, 2, 65.

81. Differding, E.; Ofner, H. *Synlett* **1991**, 187.

82. (a) Eliel, E.L.; Allinger, N.L.; Angyal, S.J.; Morrison, G.A. *Conformational Analysis*, Interscience; New York, 1965, pp 460-466.

83. Pan, Y.-H.; Stothers, J.B. *Can. J. Chem.* **1967**, *45*, 2943.

84. The epimerization of 4-*t*-butyl-2-fluorocyclohexanone in a wide range of solvents has been successfully perfomed by using HCl, see: Moreau, P.; Casadevall, A.; Casadevall, E. *Bull Soc. Chim. Fr.* **1969**, 2013.

85. Mooney, E.F.; Winson, P.H. *Annual Review of NMR Spectroscopy*; Mooney, E.F., Ed.; Academic Press: New York, 1968; Vol. 1 p 255.

86. The reduction products of the axial and equatorial methyl ketones (**45** and **49**) have been previously characterized and the details of the ^{1}H NMR and HRMS are given in the Experimental (see Section 2.6); Fraser, R.R.; Kong, F.; Bednarski, K. unpublished results.

87. (a) Karplus, M. *J. Chem. Phys.* **1959**, *30*, 11. (b) Karplus, M. *J. Am. Chem. Soc.* **1963**, *85*, 2870.

88. Stanciulesçu, M., M.Sc. Thesis, University of Ottawa, 1985.

89. Cope, A.C.; Smith, R.D. *J. Am. Chem. Soc.* **1956**, *78*, 1012.

90. Fraser, R.R.; Wu, Q.Q. unpublished results.

91. We thank Mr. Q.Q. Wu for preparing the X-ray samples of compounds **46** and **53**.

92. (a) Favini, G.; Maggi, A.; Todeschini, R. *J. Mol. Struct.* **1983**, *105*, 17. (b) Saebo, S.; Boggs, J.E. *J. Mol. Struct.* **1982**, *87*, 365.

93. (a) Kirkwood, J.G.; Westheimer, F.H. *J. Chem. Phys.* **1938**, *6*, 506. (b) Eliel, E.L.; Wilen, S.H. *Stereochemistry of Organic Compounds*, Wiley-Interscience, New York, 1994, pp 37-39.

94. For a review of the conformational properties of 2-substituted cyclohexanones see: Lambert, J.B. In *The Conformational Analysis of Cyclohexenes, Cyclohexadienes and Related Hydroaromatic Compounds*, Ed. P. Rabideau, VCH, Weinheim, Germany, 1989, Chap. 2.

95. Allinger, N.L.; Allinger, J.; Freiberg, L.A.; Czajar, R.F.; LeBel, N.A. *J. Am. Chem. Soc.* **1960**, *82*, 5876.

96. (a) Allinger, N.L.; Blatter, H.M. *J. Org. Chem.* **1962**, *27*, 1523. (b) Allinger, N.L.; Allinger, J. LeBel, N.A. *J. Am. Chem. Soc.* **1960**, *82*, 2926.

97. Kirby, A.J. *The Anomeric Effect and Related Stereoelectronic Effects at Oxygen*, Springer-Verlag, Berlin, 1983.

98. Paquette, L.A.; Branan, B.M.; Freidrich, D.; Edmonson, S.D.; Rogers, R.D. *J. Am. Chem. Soc.* **1994**, *116*, 506.

99. Denmark, S.E.; Dappen, M.S.; Sear, N.L.; Jacobs, R.T. *J. Am. Chem. Soc.* **1990**, *112*, 3466.

100. Cantacuzene, S.E.; Tordeux, M. *Can. J. Chem.* **1976**, *54*, 2759.

101. Robinson, M.J.T. *Tetrahedron* **1974**, *30*, 1971.

102. House, H.O.; Thompson, H.W. *J. Org. Chem.* **1963**, *28*, 164.

103. Battioni, J.-P.; Chodkiewicz, W. *Bull. Soc. Chim. Fr.* **1977**, 320.

104. Mion, L.; Casadevall, A.; Casadevall, E. *Bull. Soc. Chim. Fr.* **1970**, 984.

105. Basso, E.A.; Kaiser, C.; Rittner, R.; Lambert, J.B. *J. Org. Chem.* **1993**, *58*, 7865.

106. Wladislaw, B.; Viertler, H.; Olivato, P.R.; Calegãgo, I.C.C.; Pardini, V.L.; Rittner, R. *J. Chem. Soc. Perkin Trans. 2* **1980**, 435.

107. Carreño, M.C.; Domínguez, E.; García-Ruano, J.L.; Rubio, A. *J. Org. Chem.* **1987**, *52*, 3619.

108. Anet, F.A.L. *J. Am. Chem. Soc.* **1962**, *84*, 1053.

109. The values of these coupling constants are in agreement within 0.5 Hz of those observed in 4,4-diphenylcyclohexanone see: Lambert, J.B.; Carhart, R.E.; Corfield, P.W.R.; Enemark, J.H. *J. Chem. Soc., Chem. Commun.* **1968**, 999.

110. Höfner, D.; Lesko, S.A.; Binsch, G. *Org. Magn. Reson.* **1978**, *11*, 179.

111. Booth, H.; Everett, J.R. *J. Chem. Soc. Perkin* 2 **1980**, 255.

112. Johnson, F. *Chem. Rev.* **1968**, *68*, 375.

113. Rickborn, B. *J. Am. Chem. Soc.* **1962**, *84*, 2414.

114. Corey, E.J.; Burke, H.J. *J. Am. Chem. Soc.* **1955**, *77*, 5418.

115. Eisenstein, O.; Anh, N.T.; Jean, Y.; Devaquet, A.; Cantacuzene, J.; Salem, L. *Tetrahedron* **1974**, *30*, 1717.

116. Ozbal, H.; Zajak, W.W., Jr. *Tetrahedron Lett.* **1979**, 4821.

117. Dosen-Micovic, L.; Jeremic, D.; Allinger, N.L. *J. Am. Chem. Soc.* **1983**, *105*, 1723.

118. Houk, K.N.; Eksterowicz, J.E.; Wu, Y.-D.; Fuglesang, C.D.; Mitchell, D.B. *J. Am. Chem. Soc.* **1993**, *115*, 4170.

119. Bradley, D.C. *Adv. Chem. Ser.* **1959**, *23*, 10.

120. (a) Ashby, E.C.; Dobbs, F.R.; Hopkins, H.P., Jr. *J. Am. Chem. Soc.* **1973**, *95*, 2823. (b) Ashby, E.C.; Dobbs, F.R.; Hopkins, H.P., Jr. *J. Am. Chem. Soc.* **1975**, *97*, 3158.

121. (a) Wigfield, D.C.; Phelps, D.J. *J. Chem. Soc. Perkin Trans. 2* **1972**, 680. (b) Wigfield, D.C.; Phelps, D.J. *Can. J. Chem.* **1972**, *50*, 388. (c) Wigfield, D.C.; Phelps, D.J. *J. Am. Chem. Soc.* **1974**, *96*, 543.

122. (a) Brown, H.C.; Wheeler, O.H.; Ichikawa, K. *Tetrahedron* **1957**, *1*, 214. (b) Brown, H.C.; Ichikawa, K. *Tetrahedron* **1957**, *1*, 221. (c) Brown, H.C.; Muzzio, J. *J. Am. Chem. Soc.* **1966**, *88*, 2811.

123. Sevin, A.; Cense, J.-M. *Bull Chim. Soc. Fr.* **1974**, 964.

124. Anet, F.A.L.; Yavari, I. *Tetrahedron* **1978**, *34*, 2879.

125. Senda, Y.; Nakano, S.; Kunii, H.; Itoh, H. *J. Chem. Soc. Perkin Trans. 2* **1993**, 1009.

126. Ashby, E.C.; Boone, J.R. *J. Am. Chem. Soc.* **1976**, *98*, 5524.

127. Wiegers, K.E.; Smith, S.G. *J. Org. Chem.* **1978**, *43*, 1126.

128. Wiegers, K.E.; Smith, S.G. *J. Am. Chem. Soc.* **1977**, 99, 1480.

129. Haubenstock, H.; Eliel, E.L. *J. Am. Chem. Soc.* **1962**, *84*, 2363.

130. (a) Brown, H.C.; McFarlin, R.F. *J. Am. Chem. Soc.* **1958**, *80*, 5372. (b) Brown, H.C.; Shoaf, C.J. *J. Am. Chem. Soc.* **1964**, *86*, 1079.

131. Malmvik, A.-C.; Obenius, U.; Henridsson, U. *J. Chem. Soc. Perkin Trans. 2* **1986**, 1905.

132. Hermanek, S.; Kriz, O.; Fusek, J.; Cerny, Z.; Casensky, B. *J. Chem. Soc. Perkin Trans. II* **1989**, 987.

133. Healy, M.D.; Barron, A.R. *Angew. Chem. Int. Ed. Engl.* **1992**, *31*, 921.

134. (a) Ashby, E.C.; Boone, J.R.; Oliver, J.P. *J. Am. Chem. Soc.* **1973**, *95*, 5427. (b) Ashby, E.C.; Boone, J.R. *J. Org. Chem.* **1976**, *41*, 2890.

135. (a) Pierre, J.L.; Handel, H. *Tetrahedron Lett.* **1974**, 2317. (b) Handel, H.; Pierre, J.L. *Tetrahedron Lett.* **1976**, 2029. (c) Loupy, A.; Seyden-Penne, J.; Tchoubar, B. *Tetrahedron Lett.* **1976**, 1677. (d) Pierre, J.L.; Handel, H. Perraud, R. *Tetrahedron* **1975**, *31*, 2795. (e) Handel, H.; Pierre, J.L. *Tetrahedron* **1975**, *31*, 997.

136. (a) Wigfield, D.C.; Gowland, F.W. *Tetrahedron Lett.* **1976**, 3373. (b) Wigfield, D.C.; Phelps, D.J. *J. Org. Chem.* **1976**, *41*, 2396. (c) Wigfield, D.C.; Gowland, F.W. *J. Org. Chem.* **1977**, *42*, 1108.

137. Wigfield, D.C.; Gowland, F.W. *Can. J. Chem.* **1978**, *56*, 786.

138. Malmvik, A.-C.; Obenius, U.; Henriksson, U. *J. Org. Chem.* **1988**, *53*, 221.

139. Brown, H.C.; Ichikawa, K. *J. Am. Chem. Soc.* **1961**, *83*, 4372.

140. Wigfield, D.C.; Phelps, D.J. *J. Chem. Soc., Chem. Commun.* **1970**, 1152.

141. Thornton, E.R. In *Isotope Effects in Chemical Reactions*, Eds. Collins, C.J.; Bownan, N.S. Van Nostrand Reinhold, New York, 1971, p 238.

142. (a) Burnett, R.D.; Kirk, D.N. *J. Chem. Soc. Perkin Trans. 2* **1976**, 1523. (b) Geneste, P.; Lamaty, G.; Roque, J.-P. *Tetrahedron Lett.* **1970**, 5007.

143. Wigfield, D.C.; Gowland, F.W. *Tetrahedron Lett.* **1979**, 2209.

144. (a) Doyle, M.P.; DeBruyn, D.J.; Donnelly, S.J.; Kooistra, D.A.; Odubela, A.A.; West, C.T.; Zonnebelt, S.M. *J. Org. Chem.* **1974**, *39*, 2740. (b) Doyle, M.P.; West, C.T. *J. Org. Chem.* **1975**, *40*, 3835.

145. Doyle, M.P.; West, C.T.; Donnelly, S.J.; McOsker, C.C. *J. Orgmet. Chem.* **1976**, *117*, 129.

146. (a) Sommer, L.H.; Frye, C.L.; Parker, G.A.; Michael, K.W. *J. Am. Chem. Soc.* **1964**, *86*, 3271. (b) Sommer, L.H.; Citron, J.D.; Parker, G.A. *J. Am. Chem. Soc.* **1969**, *91*, 4729.

147. Fraser, R.R.; Kong, F.; Bednarski, K. unpublished results.

148. Brown, H.C.; Mead, E.J.; Subba Rao, B.C. *J. Am. Chem. Soc.* **1955**, *77*, 6209.

149. Fry, J.L.; Orfanopoulos, M.; Adlington, M.G.; Dittman, W.R., Jr.; Silverman, S.B. *J. Org. Chem.* **1978**, *43*, 374.

150. Fry, J.L.; McAdam, M.A. *Tetrahedron Lett.* **1984**, *25*, 5859.

151. Das, G.; Thornton, E.R. *J. Am. Chem. Soc.* **1993**, *115*, 1302.

152. Charton, M. *Prog. Phys. Org. Chem.* **1981**, *13*, 119-251, p 171.

153. For a comprehensive list of review articles see: Lowry, T.H.; Richardson, K.S. *Mechanism and Theory in Organic Chemistry*, 3rd Edition, Harper and Row, New York 1987, p 143 reference 28.

154. Hammett, L.P. *J. Am. Chem. Soc.* **1937**, *59*, 96.

155. Jaffe, H.H. *Chem. Rev.* **1953**, *53*, 191.

156. (a) Taft, R.W., Jr. *J. Am. Chem. Soc.* **1952**, *74*, 3120. (b) Taft, R.W., Jr. *J. Am. Chem. Soc.* **1953**, *75*, 4231.

157. Ingold, C.K. *J. Chem. Soc.* **1930**, 1032.

158. (a) Taft, R.W., Jr. In *Steric Effects in Organic Chemistry*, Ed. Newman, M.S.; John Wiley & Sons, New York 1956, pp. 607-610. (b) Charton, M. *J. Am. Chem. Soc.* **1977**, *99*, 5687. (c) Charton, M. *J. Org. Chem.* **1979**, *44*, 903. (d) Bordwell, F.G.; Bartmess, J.E.; Hautala, J.A. *J. Org. Chem.* **1978**, *43*, 3095.

159. Hine, J. *Structural Effects on Equilibria in Organic Chemistry*, Wiley-Interscience: New York, 1975, pp 32-37.

160. (a) Reynolds, W.F. *J. Chem. Soc. Perkin Trans.* 2 **1980**, 985. (b) Bowden, K.; Grubbs, E.J. *Prog. Phys. Org. Chem.* **1993**, *19*, 183.

161. Exner, O.; Friedl, Z.; Laboratory, T. *Prog. Phys. Org. Chem.* **1993**, *19*, 259.

162. The BF_3-ketone complexes in Figure 4.22 are expected to have boron in the π-nodal plane of the ketone as found by X-ray for an aluminum complex of benzophenone. Power, M.B.; Bott, S.G.; Atwood, J.L.; Barron, A.R. *J. Am. Chem. Soc.* **1990**, *112*, 3446.

163. Lyttle, D.A.; Jensen, E.H.; Struck, W.A. *Analyt. Chem.* **1952**, *24*, 1843.

164. We thank Professor D.A. Evans for suggesting Et_3SiH/BF_3-Et_2O as a reducing agent for our π-facial reactivity study.

Claims to Original Research

1. The axial and equatorial α-methylthio and the equatorial α-fluoro derivatives of **44** were prepared. The stereochemistry of ketones **46** and **53** was confirmed by X-ray crystallography.

2. The reduction products of the bridged biaryl ketone **44** and its α-methylthio, -methoxy, -chloro and -fluoro derivatives have been prepared and fully characterized.

3. It was demonstrated using molecular mechanics that ketone **44** is a suitable model to test importance of the app effect.[1] Molecular mechanics also provided evidence that the axial α-methylthio and the axial and equatorial α-methoxy derivative of **44** possess three stable rotamers about the S-C2 and O-C2 bond, respectively, two of which are energetically favoured.

4. The measurement of ΔG_{ea} for 2-methoxy- and 2-methylthiocyclohexanone in five solvents of varying polarity was carried out using 500 MHz ^{1}H NMR spectroscopy. With the aid of molecular mechanics, it was concluded that the conformational preference for 2-substituted cyclohexanones may simply reflect the varying strength in the van der Waals interaction between the carbonyl group and the 2-equatorial substituent.[2]

5. The relative rate constants for the addition of LAH, SBH and triethylsilane to **44** and its α-methyl, -methylthio, -methoxy, -chloro and -fluoro derivatives were

---

[1] Fraser, R.R.; Bensimon, C.; Faibish, N.C.; Kong, F. *Can. J. Chem.* **1994**, *72*, 1481.
[2] Fraser, R.R.; Faibish, N.C. *Can. J. Chem.* **1995**, *73*, 88.

determined. It was concluded that the π-facial reactivity is mainly influenced by sigma-inductive effects. The competitive rate study yielded compelling evidence that neither the Cieplak nor the Anh app effect contribute to π-facial reactivity.[3]

[3] Fraser, R.R.; Faibish, N.C.; Kong, F.; Wu, Q.Q.; Bednarski, K. *Manuscript in Preparation.*

Appendix 1: X-Ray Data for Ketones 46 and 53.

EXPERIMENTAL

1. Data Collection

A plate crystal of SOC18H18 having approximate dimensions of .2,.1,.3 mm was mounted on a glass capillary. All the measurements were made on a Rigaku diffractometer with Mo Kalpha radiation.

Cell constants and an orientation matrix for data collection, were obtained from least-squares refinement using the setting angles of 25 reflections in the range 40<2theta<45 corresponded to an orthorombic cell with dimensions:

a = 11.082(7)
b = 15.518(5)
c = 8.7868(24)

For Z= 4 and FW= 282.40, the calculated density is 1.241g/cm3. Based on the systematic absences, the space group was determined to be P 21 21 21.

The data was collected at a temperature of -110 degrees using the omega-2theta scan technique to a maximum 2theta value of 44.9 degrees.

2. Data reduction

A total of 1141 reflections was collected. The unique set contains only 1141 reflections. The standards were measured after every 150 reflections. No crystal decay was noticed. The data were collected for Lorentz and polarisation effects (1).

3. Solution and refinement:

The structure was solved by direct methods. All the atoms were refined anisotropically except the hydrogen. The hydrogen atoms were found by differences fourier map. The benzene rings were all refined as rigid group to increase the ratio reflection/parameters, because the crystal was not diffractin g
a lot. The final cycle of full matrix least-squares refinement was based on 958 observed reflections (I>2.5 sigma(I)) and 182 variable parameters. Weights based

on counting statistics were used. The maximum and minimum peaks on the final differences Fourier map corresponded to .310 and -.270 e/a3, respectively.

All the calculations were performed using the NRCVAX crystallographic software package (2).

EXPERIMENTAL DETAILS

Empirical formula	SOC18H18
Formula weight	282.40
Crystal shape	PLATE
Crystal dimensions (mm)	.2,.1,.3
Crystal system	orthorombic
No. Reflection used for unit cell dimension (2theta range)	25 40-45
Lattice parameters	a=11.082(7) b=15.518(5) c=8.7868(24)
Space group	P 212121
Z value	4
Dcalc (g.cm-3)	1.241
F(000)	600.62
mu (mm-1)	.21
No of reflection measured	1141
No of reflection unique	1141
No of reflection observed	958
No of atoms	38
No of variables	182
Rf (sign refl)	.055
Rw (sign refl)	.032
Rf (all refl)	.075
Rw (all.refl)	.032
Goodness of fit	3.54
Last difference fourier map	
max peak	.310
min peak	-.270

References

1. D.F. Grant and E.J. Gabe
J. Appl. Crystallogr., 11, 114 (1978)
2. E.J. Gabe, F.L. Lee and Y. Lepage
J. Appl. Crystallogr., 22, 384 (1989)

Space Group and Cell Dimensions Orthorhombic P 212121
a 11.082(7) b 15.518(5) c 8.7868(24)
Volume 1511.0(12)A**3

Empirical formula : S O C18 H18

Cell dimensions were obtained from 24 reflections with 2Theta angle
in the range 40.00 - 50.00 degrees.

Crystal dimensions : 0.20 X 0.20 X 0.20 mm

FW = 282.40 Z = 4 F(000) = 600.62

Dcalc 1.241Mg.m-3, mu 0.21mm-1, lambda 0.70930A, 2Theta(max) 44.9

The intensity data were collected on a Rigaku diffractometer,
using the theta/2theta scan mode.
The h,k,l ranges used during structure solution and refinement are :--
Hmin,max 0 10; Kmin,max 0 16; Lmin,max 0 9
No. of reflections measured 1141
No. of unique reflections 1141
No. of reflections with Inet > 2.5sigma(Inet) 958
Merging R-value on intensities 0.000
No correction was made for absorption

The last least squares cycle was calculated with
38 atoms, 182 parameters and 958 out of 1141 reflections.
Weights based on counting-statistics were used.

The residuals are as follows :--
For significant reflections, RF 0.055, Rw 0.032 GoF 3.54
For all reflections, RF 0.075, Rw 0.032.
where RF = Sum(Fo-Fc)/Sum(Fo),
Rw = Sqrt[Sum(w(Fo-Fc)**2)/Sum(wFo**2)] and
GoF = Sqrt[Sum(w(Fo-Fc)**2)/(No. of reflns - No. of params.)]
The maximum shift/sigma ratio was 0.149.

In the last D-map, the deepest hole was -0.270e/A**3,
and the highest peak 0.310e/A**3.

Secondary ext. coeff. 0.292260 sigma 0.013984

The following references are relevant to the NRCVAX System.

1. Full System Reference :
Gabe, E.J., Le Page, Y., Charland,.J.-P., Lee, F.L. and White, P.S.
(1989) J. Appl. Cryst., 22, 384-387.

2. Scattering Factors from Int. Tab. Vol. 4 :
International Tables for X-ray Crystallography, Vol. IV, (1974)
Kynoch Press, Birmingham, England.

The following references may also be relevant.

3. ORTEP Plotting :
Johnson, C.K., (1976) ORTEP - A Fortran Thermal Ellipsoid Plot Program, Technical Report ORNL-5138, Oak Ridge

4. Pluto Plotting :
S. Motherwell, University Chemical Laboratory, Cambridge, 1978

5. Missing Symmetry Treatment by MISSYM :
Le Page, Y., (1988) J. Appl. Cryst., 21, 983-984.

7. Extinction Treatment :
Larson, A.C., (1970) p.293, Crystallographic Computing, Munksgaard, Copenhagen.

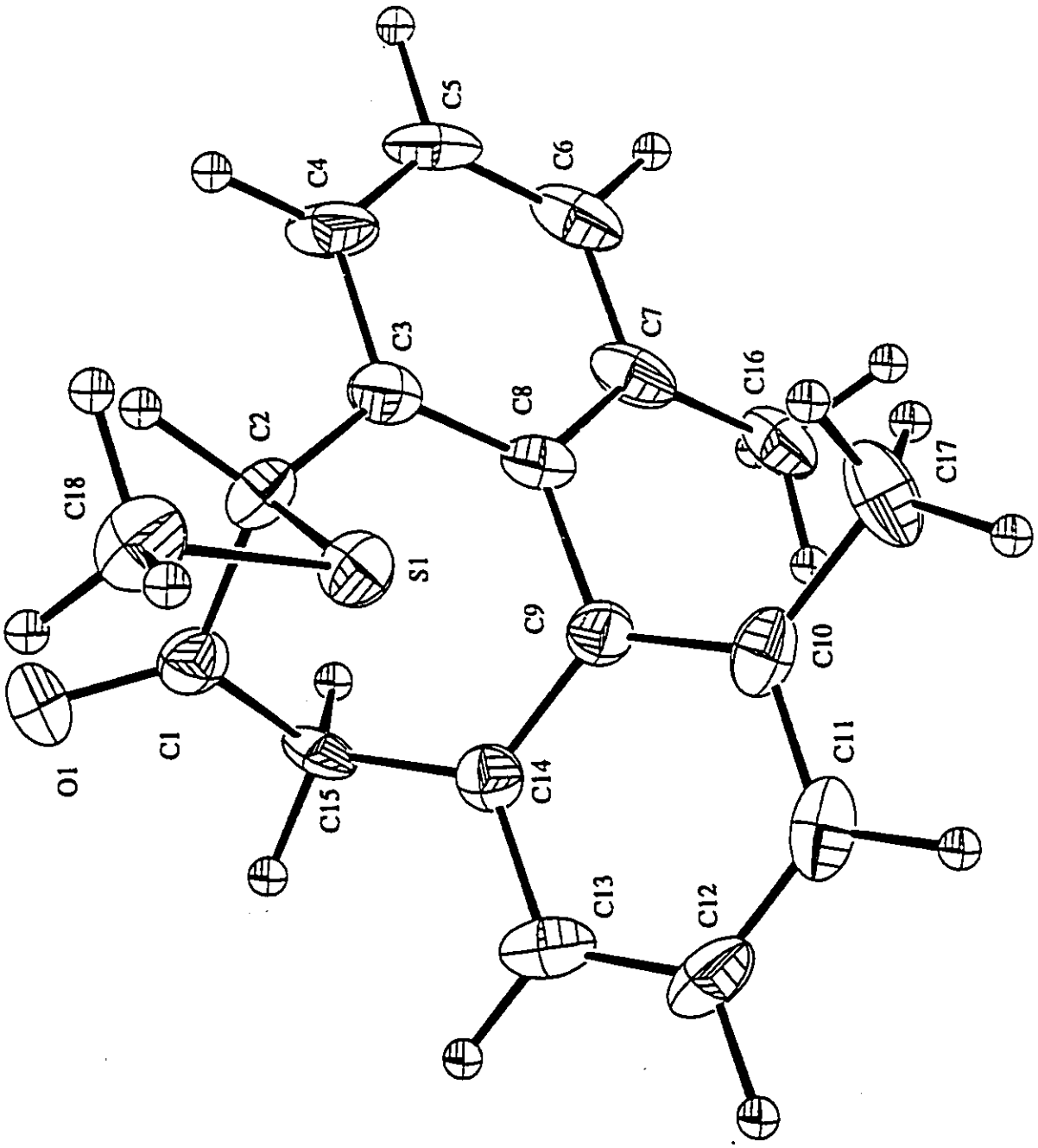
C5
C4
C6
C3
C7
C16
C8
C2
C18
C17
S1
C9
C10
C1
C11
O1
C15
C14
C13
C12

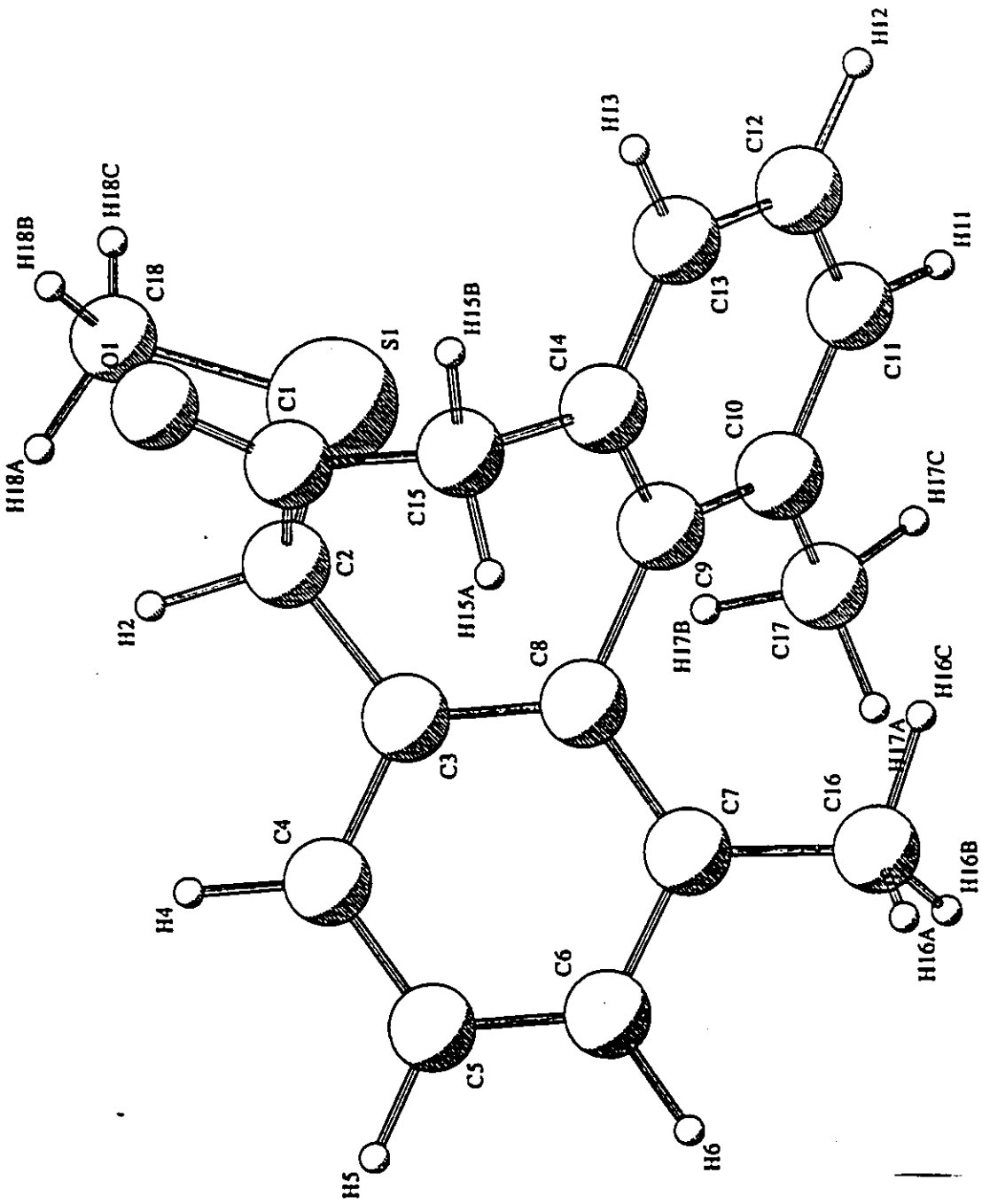
H18B
H18C
C18
O1
H18A
C1
S1
H15B
C14
H13
C12
H12
C13
C11
H11
C10
C15
H15A
H17C
C9
H17B
C17
H2
C2
C8
H16C
H17A
C3
C16
C7
C4
H16B
H4
C6
H16A
C5
H5
H6

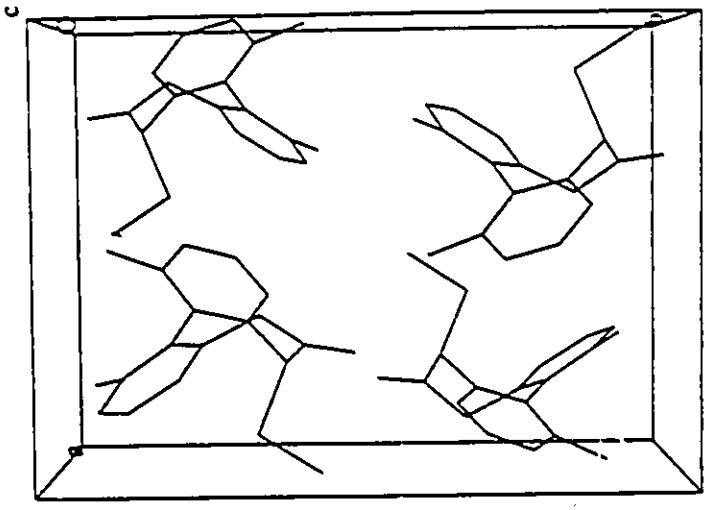
c
a

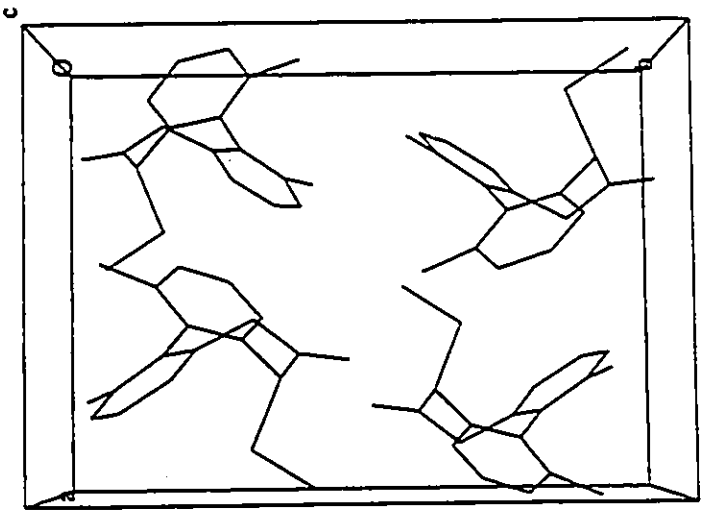
c
a

Table of Atomic Parameters x,y,z and Biso.
E.S.Ds. refer to the last digit printed.

	x	y	z	Biso
S1	0.38797(17)	0.16810(12)	0.16609(21)	2.31(9)
O1	0.2015 (4)	0.0186 (3)	0.0056 (5)	3.5 (3)
C1	0.1873 (6)	0.0934 (4)	0.0451 (7)	2.3 (4)
C2	0.2362 (6)	0.1242 (4)	0.2023 (7)	2.2 (3)
C3	0.1526 (5)	0.1853 (4)	0.2815 (7)	2.4 (4)
C4	0.1025 (6)	0.1569 (4)	0.4199 (6)	3.2 (4)
C5	0.0204 (6)	0.2099 (5)	0.4933 (7)	3.5 (4)
C6	-0.0133 (6)	0.2893 (5)	0.4308 (7)	3.4 (4)
C7	0.0357 (6)	0.3190 (4)	0.2920 (7)	2.8 (4)
C8	0.1223 (6)	0.2665 (4)	0.2213 (7)	2.3 (4)
C9	0.1868 (6)	0.2970 (4)	0.0809 (7)	2.2 (4)
C10	0.2576 (6)	0.3719 (4)	0.0826 (8)	2.7 (4)
C11	0.3163 (6)	0.3983 (4)	-0.0537 (8)	3.3 (4)
C12	0.3049 (6)	0.3488 (4)	-0.1880 (8)	3.4 (4)
C13	0.2391 (6)	0.2733 (4)	-0.1857 (7)	3.0 (4)
C14	0.1781 (6)	0.2446 (4)	-0.0524 (7)	2.2 (4)
C15	0.1176 (6)	0.1584 (4)	-0.0490 (6)	2.6 (4)
C16	-0.0116 (7)	0.4020 (4)	0.2283 (8)	3.1 (4)
C17	0.2838 (6)	0.4221 (4)	0.2259 (9)	3.8 (4)
C18	0.4746 (6)	0.0708 (4)	0.1961 (8)	3.0 (4)
H2	0.250	0.065	0.274	3.1
H4	0.129	0.095	0.469	3.7
H5	-0.021	0.189	0.602	4.2
H6	-0.076	0.332	0.492	3.9
H11	0.373	0.455	-0.053	3.9
H12	0.346	0.371	-0.294	3.9
H13	0.230	0.233	-0.290	3.6
H15A	0.028	0.166	-0.003	3.5
H15B	0.110	0.134	-0.165	3.5
H16C	0.034	0.416	0.121	4.3
H16A	-0.107	0.398	0.209	4.3
H16B	0.007	0.455	0.307	4.3
H17C	0.342	0.476	0.202	4.6
H17A	0.202	0.443	0.277	4.6
H17B	0.331	0.379	0.307	4.6
H18C	0.571	0.084	0.182	4.1
H18A	0.462	0.047	0.313	4.1
H18B	0.449	0.021	0.118	4.1

Biso is the Mean of the Principal Axes of the Thermal Ellipsoid

Table of u(i,j) or U values *100.
E.S.Ds. refer to the last digit printed

	u11(U)	u22	u33	u12	u13	u23
S1	2.66(11)	3.10(11)	3.00(10)	0.14(12)	-0.35(11)	0.25(12)
O1	6.5 (4)	2.6 (3)	4.1 (3)	0.3 (3)	0.3 (3)	-1.0 (3)
C1	2.9 (5)	3.1 (5)	2.9 (5)	-0.6 (4)	0.4 (4)	0.3 (4)
C2	2.8 (5)	2.8 (4)	3.0 (5)	0.1 (4)	-0.1 (4)	0.9 (4)
C3	3.2 (5)	3.6 (5)	2.4 (4)	-0.2 (4)	0.2 (4)	-0.2 (4)
C4	4.4 (5)	5.7 (6)	2.0 (4)	2.2 (6)	0.9 (5)	0.3 (5)
C5	4.7 (6)	7.1 (7)	1.4 (4)	-0.3 (5)	0.5 (4)	-0.1 (5)
C6	3.9 (5)	5.9 (6)	2.9 (5)	1.2 (5)	-0.1 (4)	-1.8 (5)
C7	2.9 (5)	4.9 (6)	2.7 (5)	1.1 (5)	0.2 (4)	-1.3 (5)
C8	3.1 (5)	3.7 (5)	1.8 (4)	-0.1 (5)	-0.1 (4)	-0.3 (4)
C9	2.7 (5)	2.6 (5)	2.9 (5)	0.1 (4)	0.7 (4)	0.1 (4)
C10	2.8 (5)	2.4 (4)	4.9 (5)	0.2 (4)	0.1 (5)	0.8 (5)
C11	3.9 (5)	2.5 (5)	6.1 (6)	-0.6 (5)	-0.5 (5)	0.5 (5)
C12	3.9 (5)	4.3 (6)	4.6 (5)	-0.4 (5)	1.3 (5)	1.9 (5)
C13	3.2 (5)	5.6 (5)	2.4 (4)	0.7 (5)	0.4 (4)	0.8 (5)
C14	2.6 (5)	2.9 (5)	2.8 (5)	0.2 (4)	0.1 (4)	0.0 (4)
C15	4.6 (5)	3.7 (5)	1.5 (4)	-0.3 (5)	-0.2 (4)	-1.1 (4)
C16	4.5 (5)	3.9 (6)	3.5 (5)	0.9 (5)	-0.1 (5)	-1.6 (5)
C17	4.5 (6)	3.9 (5)	6.1 (6)	-0.9 (5)	-1.2 (5)	-2.2 (5)
C18	2.7 (5)	4.2 (5)	4.6 (5)	1.1 (4)	0.4 (5)	0.9 (5)

Anisotropic Temperature Factors are of the form
Temp=-2*Pi*Pi*(h*h*u11*astar*astar+----+2*h*k*u12*astar*bstar+---)

Table of Atomic Bond Distances in Angstroms

S1-C2	1.842(7)	C14-C13	1.424(9)
S1-C18	1.808(7)	C14-C15	1.496(9)
O1-C1	1.223(8)	C13-C12	1.379(9)
C1-C2	1.559(9)	C13-H13	1.110(7)
C1-C15	1.516(9)	C12-C11	1.414(10)
C2-C3	1.497(9)	C12-H12	1.093(7)
C2-H2	1.121(6)	C11-C10	1.423(10)
C3-C4	1.408(8)	C11-H11	1.082(7)
C3-C8	1.408(9)	C10-C17	1.509(10)
C4-C5	1.385(10)	C15-H15A	1.078(7)
C4-H4	1.089(7)	C15-H15B	1.091(6)
C5-C6	1.400(10)	C16-H16C	1.089(7)
C5-H5	1.108(7)	C16-H16A	1.076(7)
C6-C7	1.413(9)	C16-H16B	1.091(7)
C6-H6	1.101(7)	C17-H17C	1.074(7)
C7-C8	1.403(9)	C17-H17A	1.068(7)
C7-C16	1.499(10)	C17-H17B	1.106(7)
C8-C9	1.502(9)	C18-H18C	1.096(7)
C9-C14	1.429(9)	C18-H18A	1.097(7)
C9-C10	1.402(9)	C18-H18B	1.071(7)

Table of Atomic Angles in Degrees

C2-S1-C18	98.7(3)	C14-C13-H13	117.6(6)
O1-C1-C2	119.9(6)	C12-C13-H13	120.5(6)
O1-C1-C15	122.9(6)	C13-C12-C11	119.7(6)
C2-C1-C15	117.2(5)	C13-C12-H12	119.8(6)
S1-C2-C1	106.1(4)	C11-C12-H12	120.4(6)
S1-C2-C3	114.2(4)	C12-C11-C10	120.4(6)
S1-C2-H2	105.8(4)	C12-C11-H11	120.2(6)
C1-C2-C3	113.0(5)	C10-C11-H11	119.4(6)
C1-C2-H2	107.3(5)	C9-C10-C11	119.0(6)
C3-C2-H2	109.9(5)	C9-C10-C17	123.0(6)
C2-C3-C4	116.6(6)	C11-C10-C17	117.8(6)
C2-C3-C8	122.7(5)	C1-C15-C14	112.1(5)
C4-C3-C8	120.7(6)	C1-C15-H15A	109.8(5)
C3-C4-C5	118.4(6)	C1-C15-H15B	108.4(5)
C3-C4-H4	120.8(6)	C14-C15-H15A	108.5(5)
C5-C4-H4	120.8(6)	C14-C15-H15B	109.1(5)
C4-C5-C6	121.0(6)	H15A-C15-H15B	108.8(5)
C4-C5-H5	119.8(7)	C7-C16-H16C	109.8(6)
C6-C5-H5	119.3(6)	C7-C16-H16A	110.9(6)
C5-C6-C7	121.6(6)	C7-C16-H16B	109.9(6)
C5-C6-H6	120.3(6)	H16C-C16-H16A	109.1(6)
C7-C6-H6	118.1(6)	H16C-C16-H16B	108.0(6)
C6-C7-C8	117.1(6)	H16A-C16-H16B	109.0(6)
C6-C7-C16	117.9(6)	C10-C17-H17C	110.7(6)
C8-C7-C16	124.9(6)	C10-C17-H17A	110.3(6)
C3-C8-C7	121.1(6)	C10-C17-H17B	108.4(6)
C3-C8-C9	118.5(6)	H17C-C17-H17A	110.8(6)
C7-C8-C9	120.4(6)	H17C-C17-H17B	108.0(6)
C8-C9-C14	117.5(5)	H17A-C17-H17B	108.4(7)
C8-C9-C10	121.2(6)	S1-C18-H18C	110.1(5)
C14-C9-C10	121.2(6)	S1-C18-H18A	110.2(5)
C9-C14-C13	117.6(6)	S1-C18-H18B	111.4(5)
C9-C14-C15	121.5(5)	H18C-C18-H18A	107.1(6)
C13-C14-C15	120.6(6)	H18C-C18-H18B	109.0(6)
C14-C13-C12	121.9(6)	H18A-C18-H18B	108.9(6)

1 Table . Distances(A) to the least-squares planes.

Plane no. 1

Equation of the plane : 8.217(21)X + 6.82(4)Y + 4.457(22)Z = 3.785(9)

Distances(A) to the plane from the atoms in the plane.

C3	-0.013(8)	C4	-0.002(9)
C5	0.013(9)	C6	-0.002(9)
C7	-0.015(9)	C8	0.023(8)

Chi squared for this plane 15.865

Plane no. 2

Equation of the plane : 8.973(18)X - 8.09(4)Y + 2.372(23)Z = 0.514(16)

Distances(A) to the plane from the atoms in the plane.

C9	-0.020(8)	C10	0.014(8)
C11	0.004(9)	C12	-0.017(9)
C13	0.009(8)	C14	0.010(8)

Chi squared for this plane 15.796

1 Dihedral angle between planes A and B

A	B	Angle(deg)
1	2	59.45(23)

Torsion angles

C18	S1	C2	C1	-91.0(	5)	C18	S1	C2	C3	143.8(	5)
C18	S1	C2	H2	22.9(	3)	C2	S1	C18	H18C	-178.8(	6)
C2	S1	C18	H18A	-60.9(	4)	C2	S1	C18	H18B	60.1(	4)
O1	C1	C2	S1	93.2(	6)	O1	C1	C2	C3	-140.9(	8)
O1	C1	C2	H2	-19.6(	3)	C15	C1	C2	S1	-89.9(	5)
C15	C1	C2	C3	36.1(	4)	C15	C1	C2	H2	157.3(	8)
O1	C1	C15	C14	-138.4(	8)	O1	C1	C15	H15A	100.9(	7)
O1	C1	C15	H15B	-17.9(	3)	C2	C1	C15	C14	44.8(	4)
C2	C1	C15	H15A	-76.0(	6)	C2	C1	C15	H15B	165.3(	8)
S1	C2	C3	C4	-122.8(	6)	S1	C2	C3	C8	58.6(	4)
C1	C2	C3	C4	115.7(	7)	C1	C2	C3	C8	-62.9(	5)
H2	C2	C3	C4	-4.1(	3)	H2	C2	C3	C8	177.3(	8)
C2	C3	C4	C5	-177.1(	8)	C2	C3	C4	H4	4.3(	3)
C8	C3	C4	C5	1.5(	4)	C8	C3	C4	H4	-177.0(	9)
C2	C3	C8	C7	174.4(	8)	C2	C3	C8	C9	-6.9(	3)
C4	C3	C8	C7	-4.1(	4)	C4	C3	C8	C9	174.5(	8)
C3	C4	C5	C6	0.9(	4)	C3	C4	C5	H5	179.8(	9)
H4	C4	C5	C6	179.4(	9)	H4	C4	C5	H5	-1.7(	0)
C4	C5	C6	C7	-0.8(	4)	C4	C5	C6	H6	-177.9(	10)
H5	C5	C6	C7	-179.7(	9)	H5	C5	C6	H6	3.2(	0)
C5	C6	C7	C8	-1.6(	4)	C5	C6	C7	C16	176.1(	8)
H6	C6	C7	C8	175.5(	9)	H6	C6	C7	C16	-6.8(	3)
C6	C7	C8	C3	4.1(	4)	C6	C7	C8	C9	-174.5(	8)
C16	C7	C8	C3	-173.5(	8)	C16	C7	C8	C9	7.9(	4)
C6	C7	C16	H16C	-179.5(	9)	C6	C7	C16	H16A	-58.8(	5)
C6	C7	C16	H16B	61.8(	5)	C8	C7	C16	H16C	-2.0(	3)
C8	C7	C16	H16A	118.7(	8)	C8	C7	C16	H16B	-120.7(	8)
C3	C8	C9	C14	58.7(	5)	C3	C8	C9	C10	-118.3(	7)
C7	C8	C9	C14	-122.7(	7)	C7	C8	C9	C10	60.3(	5)
C8	C9	C14	C13	180.0(	8)	C8	C9	C14	C15	-5.9(	3)
C10	C9	C14	C13	-3.0(	4)	C10	C9	C14	C15	171.1(	8)
C8	C9	C10	C11	-179.6(	8)	C8	C9	C10	C17	5.9(	4)
C14	C9	C10	C11	3.5(	4)	C14	C9	C10	C17	-171.0(	8)
C9	C14	C13	C12	0.1(	4)	C9	C14	C13	H13	-178.6(	9)
C15	C14	C13	C12	-174.0(	8)	C15	C14	C13	H13	7.3(	3)
C9	C14	C15	C1	-67.7(	5)	C9	C14	C15	H15A	53.9(	5)
C9	C14	C15	H15B	172.3(	9)	C13	C14	C15	C1	106.3(	7)
C13	C14	C15	H15A	-132.2(	8)	C13	C14	C15	H15B	-13.8(	3)
C14	C13	C12	C11	2.2(	4)	C14	C13	C12	H12	-176.7(	9)
H13	C13	C12	C11	-179.2(	9)	H13	C13	C12	H12	2.0(	0)
C13	C12	C11	C10	-1.7(	4)	C13	C12	C11	H11	175.9(	10)
H12	C12	C11	C10	177.2(	9)	H12	C12	C11	H11	-5.2(	0)
C12	C11	C10	C9	-1.1(	4)	C12	C11	C10	C17	173.7(	8)
H11	C11	C10	C9	-178.7(	9)	H11	C11	C10	C17	-4.0(	3)
C9	C10	C17	H17C	178.2(	9)	C9	C10	C17	H17A	-58.8(	5)
C9	C10	C17	H17B	59.8(	5)	C11	C10	C17	H17C	3.6(	3)
C11	C10	C17	H17A	126.7(	9)	C11	C10	C17	H17B	-114.7(	8)

Intramolecular distances in Angstroms

H15A	C1	2.1375
	C2	2.9994
	C3	2.8750
	C8	2.7185
	C9	2.7840
	C14	2.1040
H15B	C1	2.1293
	C13	2.5994
	C14	2.1208
H2	C1	2.1742
	C3	2.1536
	C4	2.5171
	C18	2.5818
C16	C17	3.2885

Space Group and Cell Dimensions Triclinic, P -1
a 10.924(7) b 14.012(5) c 9.0360(23)
alpha 103.08(3) beta 93.89(3) gamma 74.14(4)
Volume 1295.9(10)A**3

Empirical formula : F O C17 H15 + 1/8 Ow

Cell dimensions were obtained from 24 reflections with 2Theta angle
in the range 40.00 - 50.00 degrees.

Crystal dimensions : 0.20 X 0.20 X 0.20 mm

FW = 256.30 Z = 4 F(000) = 540.23

Dcalc 1.314Mg.m-3, mu 0.06mm-1, lambda 0.70930A, 2Theta(max) 49.9

The intensity data were collected on a Rigaku diffractometer,
using the theta/2theta scan mode.
The h,k,l ranges used during structure solution and refinement are :--
Hmin,max -12 12; Kmin,max 0 16; Lmin,max -10 10
No. of reflections measured 4816
No. of unique reflections 4554
No. of reflections with Inet > 2.5sigma(Inet) 3965
Merging R-value on intensities 0.009
No correction was made for absorption

The last least squares cycle was calculated with
69 atoms, 460 parameters and 3965 out of 4554 reflections.
Weights based on counting-statistics were used.
The weight modifier K in KFo**2 is 0.000250

The residuals are as follows :--
For significant reflections, RF 0.068, Rw 0.091 GoF 4.09
For all reflections, RF 0.075, Rw 0.091.
where RF = Sum(Fo-Fc)/Sum(Fo),
Rw = Sqrt[Sum(w(Fo-Fc)**2)/Sum(wFo**2)] and
GoF = Sqrt[Sum(w(Fo-Fc)**2)/(No. of reflns - No. of params.)]
The maximum shift/sigma ratio was 0.284.

In the last D-map, the deepest hole was -0.400e/A**3,
and the highest peak 0.450e/A**3.

Secondary ext. coeff. 1.888412 sigma 0.136564

The following references are relevant to the NRCVAX System.

1. Full System Reference :
Gabe, E.J., Le Page, Y., Charland,.J.-P., Lee, F.L. and White, P.S.
(1989) J. Appl. Cryst., 22, 384-387.

2. Scattering Factors from Int. Tab. Vol. 4 :

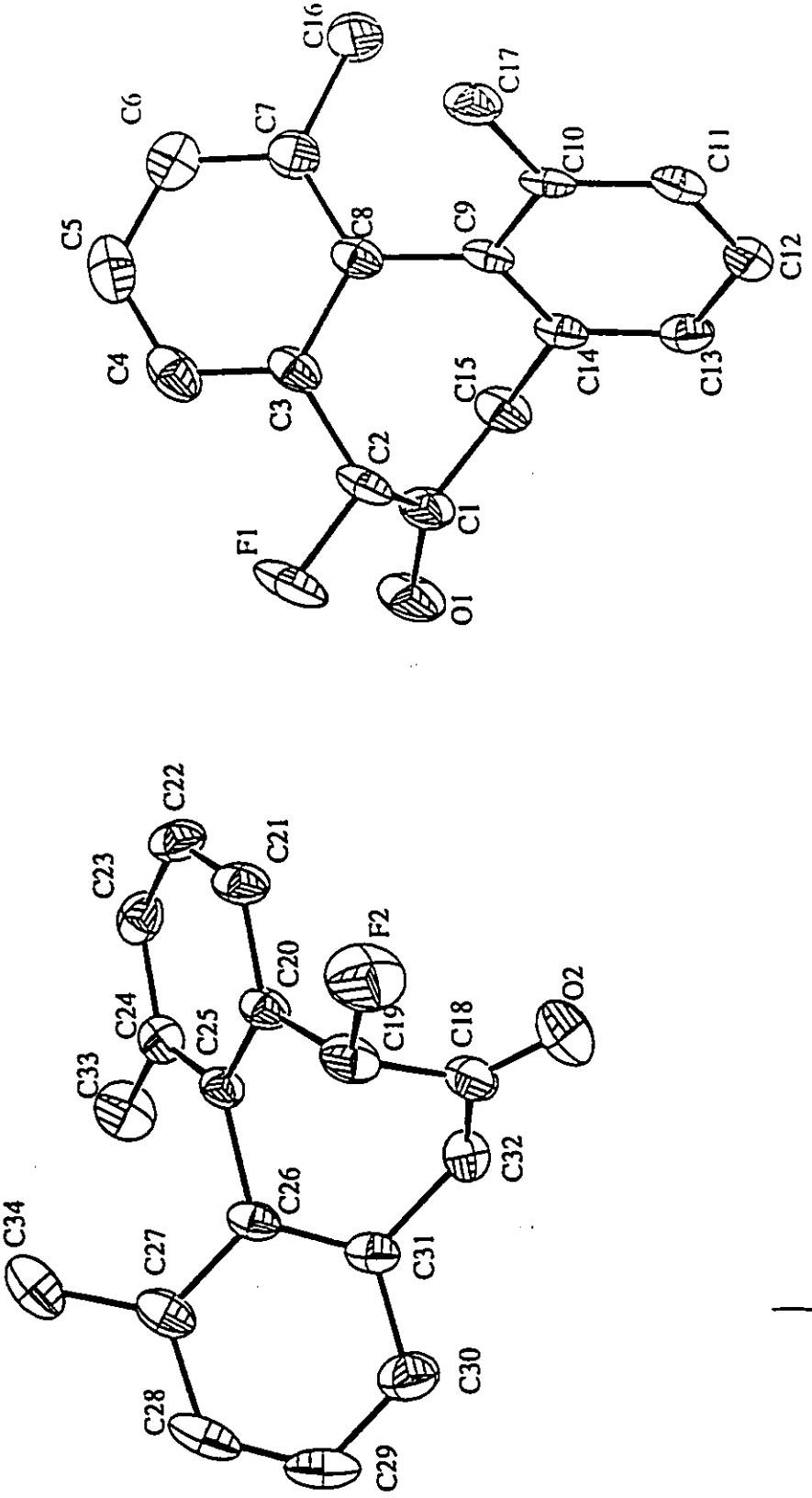
C16
C17
C6
C7
C10
C11
C5
C8
C9
C12
C4
C3
C15
C14
C13
C2
C1
F1
O1
C22
C21
C23
F2
C20
C24
C25
C19
C18
O2
C33
C32
C26
C34
C27
C31
C30
C28
C29

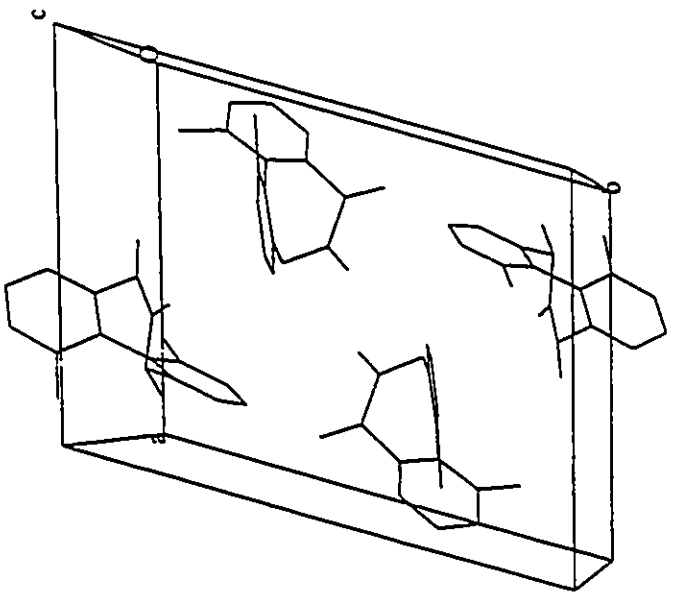
c
o
o

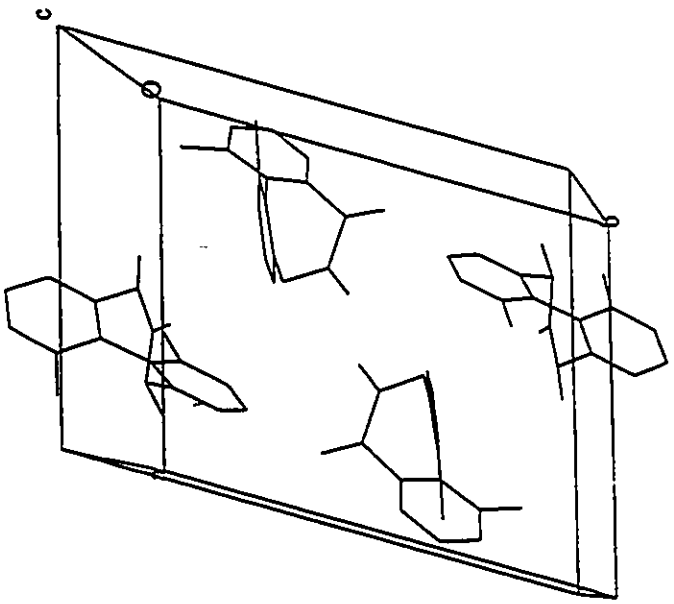
c
o
o

Table of Atomic Parameters x,y,z and Biso.
E.S.Ds. refer to the last digit printed.

	x	y	z	Biso
F1	0.83662(17)	0.44593(13)	0.61038(20)	4.21(8)
F2	0.85535(18)	0.10603(14)	0.54154(18)	4.58(9)
O1	0.59347(19)	0.53242(16)	0.65730(22)	4.01(10)
O2	0.61962(24)	0.10774(18)	0.47000(23)	4.94(12)
C1	0.6418 (3)	0.56061(20)	0.5640 (3)	2.71(11)
C2	0.78253(25)	0.51671(19)	0.5234 (3)	2.54(11)
C3	0.84658(23)	0.60168(19)	0.5535 (3)	2.23(10)
C4	0.92105(25)	0.61733(22)	0.6811 (3)	2.92(12)
C5	0.9716 (3)	0.70052(23)	0.7151 (3)	3.39(13)
C6	0.9412 (3)	0.77125(22)	0.6214 (3)	3.18(12)
C7	0.86561(25)	0.75690(19)	0.4937 (3)	2.49(11)
C8	0.81893(22)	0.67071(18)	0.4546 (3)	2.00(9)
C9	0.74077(21)	0.64956(16)	0.31606(25)	1.76(9)
C10	0.78707(22)	0.63658(16)	0.1674 (3)	1.83(9)
C11	0.70912(24)	0.61819(17)	0.0443 (3)	2.10(10)
C12	0.58759(24)	0.60883(18)	0.0593 (3)	2.30(10)
C13	0.54335(23)	0.61719(18)	0.2038 (3)	2.28(10)
C14	0.61856(22)	0.63727(17)	0.3299 (3)	1.95(9)
C15	0.56809(24)	0.64450(20)	0.4865 (3)	2.52(11)
C16	0.8310 (3)	0.83885(21)	0.4022 (4)	3.97(15)
C17	0.92150(24)	0.63745(19)	0.1405 (3)	2.53(11)
C18	0.6528 (3)	0.09815(19)	0.5961 (3)	2.91(12)
C19	0.7862 (3)	0.09484(20)	0.6553 (3)	2.70(12)
C20	0.78100(22)	0.17634(18)	0.7960 (3)	2.04(10)
C21	0.80370(24)	0.26776(19)	0.7888 (3)	2.53(11)
C22	0.78541(24)	0.34631(19)	0.9143 (3)	2.70(12)
C23	0.74153(24)	0.33471(19)	1.0479 (3)	2.58(11)
C24	0.71748(23)	0.24324(19)	1.0588 (3)	2.23(10)
C25	0.73850(22)	0.16262(18)	0.9330 (3)	1.99(10)
C26	0.71226(23)	0.06218(17)	0.9310 (3)	2.14(10)
C27	0.7786 (3)	-0.00144(20)	1.0278 (3)	2.69(11)
C28	0.7478 (3)	-0.09370(22)	1.0165 (3)	3.74(14)
C29	0.6608 (3)	-0.12424(21)	0.9164 (4)	4.05(15)
C30	0.5973 (3)	-0.06262(21)	0.8181 (3)	3.41(14)
C31	0.62515(24)	0.02961(18)	0.8253 (3)	2.38(10)
C32	0.5604 (3)	0.09289(20)	0.7132 (3)	2.82(11)
C33	0.6620 (3)	0.23908(23)	1.2057 (3)	3.47(13)
C34	0.8783 (3)	0.02432(23)	1.1387 (3)	3.54(13)
H2	0.7844 (22)	0.4810 (17)	0.417 (3)	2.2 (5)
H4	0.942 (3)	0.5644 (22)	0.735 (3)	4.3 (7)
H5	1.0312 (25)	0.7110 (19)	0.799 (3)	3.2 (6)
H6	0.9730 (24)	0.8333 (19)	0.659 (3)	2.9 (6)
H11	0.7367 (24)	0.6020 (19)	-0.050 (3)	2.5 (5)
H12	0.5388 (22)	0.5908 (17)	-0.027 (3)	2.1 (5)
H13	0.4562 (22)	0.6074 (17)	0.201 (3)	2.1 (5)
H15a	0.5799 (24)	0.7082 (19)	0.559 (3)	2.8 (6)
H15b	0.469	0.641	0.474	3.2
H16a	0.777 (3)	0.8209 (21)	0.320 (3)	3.6 (6)
H16b	0.889 (4)	0.875 (3)	0.437 (4)	9.5 (12)
H16c	0.776 (5)	0.905 (4)	0.476 (5)	12.1 (15)

H17a	0.979	(3)	0.6272	(21)	0.224	(3)	4.0 (7)
H17b	0.956	(3)	0.5820	(25)	0.048	(4)	5.7 (8)
H17c	0.927	(4)	0.709	(3)	0.127	(4)	7.2 (10)
H19	0.8324	(21)	0.0257	(16)	0.6783	(24)	1.6 (5)
H21	0.838	(3)	0.2650	(23)	0.701	(3)	5.1 (8)
H22	0.8006	(23)	0.4116	(18)	0.914	(3)	2.4 (5)
H23	0.7254	(22)	0.3907	(18)	1.135	(3)	2.1 (5)
H28	0.793	(3)	-0.1305	(23)	1.081	(3)	5.2 (8)
H29	0.643	(3)	-0.1871	(23)	0.898	(3)	4.6 (7)
H30	0.537	(3)	-0.0868	(20)	0.737	(3)	3.6 (6)
H32A	0.530	(3)	0.1687	(21)	0.772	(3)	4.1 (7)
H32B	0.489		0.056		0.648		3.6
H33A	0.727	(3)	0.2386	(24)	1.290	(4)	5.5 (8)
H33B	0.595	(3)	0.307	(3)	1.260	(4)	7.0 (9)
H33C	0.620	(4)	0.185	(3)	1.194	(4)	8.3 (11)
H34A	0.921	(3)	0.0783	(22)	1.121	(3)	3.9 (7)
H34B	0.855	(3)	0.0528	(22)	1.242	(3)	4.4 (7)
H34C	0.952	(3)	-0.0319	(22)	1.142	(3)	4.6 (7)
OW	0.4711	(12)	0.0782	(9)	0.6236	(13)	7.4 (3)

Biso is the Mean of the Principal Axes of the Thermal Ellipsoid

Table of u(i,j) or U values *100.
E.S.Ds. refer to the last digit printed

	u11(U)	u22	u33	u12	u13	u23
F1	5.46(11)	5.33(10)	6.30(11)	-0.39(9)	0.55(9)	4.63(9)
F2	7.51(13)	6.44(12)	4.15(10)	-2.30(10)	2.17(9)	1.39(8)
O1	5.02(13)	6.66(14)	5.04(12)	-1.81(11)	1.39(10)	3.61(11)
O2	8.58(18)	7.63(16)	4.03(12)	-3.55(14)	-2.27(12)	3.22(11)
C1	4.13(16)	4.04(15)	2.90(13)	-1.54(13)	0.82(11)	1.54(11)
C2	3.63(14)	3.27(14)	3.29(13)	-0.36(12)	0.42(11)	2.34(11)
C3	2.35(12)	3.47(14)	2.79(12)	-0.08(10)	0.89(10)	1.54(10)
C4	3.01(14)	5.02(17)	3.10(13)	-0.10(13)	0.55(11)	2.00(12)
C5	3.26(15)	6.11(19)	3.10(14)	-0.69(14)	-0.36(12)	0.95(13)
C6	3.76(16)	4.20(16)	4.09(15)	-1.28(13)	-0.08(13)	0.58(13)
C7	3.28(14)	2.84(13)	3.27(13)	-0.56(11)	0.30(11)	0.74(11)
C8	2.22(12)	2.74(12)	2.73(12)	-0.20(10)	0.81(10)	1.13(10)
C9	2.53(12)	1.72(11)	2.62(12)	-0.13(9)	0.62(10)	1.18(9)
C10	2.59(12)	1.77(11)	2.98(12)	-0.40(10)	0.74(10)	1.34(9)
C11	3.47(14)	2.44(12)	2.42(12)	-0.66(11)	0.58(10)	1.19(10)
C12	3.21(14)	2.67(13)	3.08(13)	-0.72(11)	-0.30(11)	1.28(10)
C13	2.42(13)	2.70(13)	4.00(14)	-0.70(10)	0.39(11)	1.51(11)
C14	2.54(12)	2.27(12)	2.89(12)	-0.36(10)	0.71(10)	1.30(10)
C15	2.63(13)	4.10(15)	3.10(13)	-0.38(11)	1.30(11)	1.52(11)
C16	7.38(22)	2.90(14)	5.65(18)	-2.48(15)	-2.23(17)	1.91(13)
C17	2.87(13)	3.85(15)	3.61(14)	-1.10(12)	0.56(11)	1.88(11)
C18	5.50(18)	2.68(13)	3.18(14)	-1.26(13)	-0.83(13)	1.24(11)
C19	4.51(16)	3.68(14)	2.45(12)	-1.05(13)	1.00(11)	1.19(11)
C20	2.45(12)	2.87(13)	2.77(12)	-0.63(10)	0.48(10)	1.27(10)
C21	2.90(14)	3.32(14)	4.04(14)	-0.98(11)	0.76(11)	1.71(11)
C22	2.66(14)	2.99(14)	5.18(16)	-1.16(11)	0.56(12)	1.38(12)
C23	2.54(13)	3.10(14)	3.86(14)	-0.68(11)	-0.04(11)	0.24(11)
C24	2.24(12)	3.47(14)	2.87(12)	-0.57(11)	0.41(10)	1.00(10)
C25	2.44(12)	3.04(13)	2.59(12)	-0.89(10)	0.13(10)	1.38(10)
C26	2.93(13)	2.52(12)	3.00(12)	-0.53(10)	0.72(10)	1.31(10)
C27	3.86(15)	3.40(14)	3.09(13)	-0.21(12)	0.95(12)	1.60(11)
C28	5.97(20)	3.73(16)	5.02(17)	-0.21(14)	0.93(15)	3.07(14)
C29	6.81(22)	3.16(15)	6.52(20)	-1.85(15)	0.87(17)	2.35(14)
C30	4.74(17)	3.69(16)	5.35(17)	-1.97(14)	0.24(14)	1.50(13)
C31	3.18(14)	2.52(13)	3.69(14)	-0.80(11)	0.52(11)	1.20(11)
C32	3.29(14)	3.59(14)	4.07(15)	-1.11(12)	-0.94(12)	1.32(12)
C33	5.09(18)	5.14(18)	2.81(14)	-0.88(15)	1.48(13)	0.73(12)
C34	4.61(18)	5.20(18)	3.50(15)	-0.08(14)	0.12(13)	2.10(13)

Anisotropic Temperature Factors are of the form
Temp=-2*Pi*Pi*(h*h*u11*astar*astar+---+2*h*k*u12*astar*bstar+---)

Table of Atomic Bond Distances in Angstroms

F1-C2	1.386(3)	C19-C20	1.497(3)
F2-C19	1.377(3)	C19-H19	1.023(21)
O1-C1	1.213(3)	C20-C21	1.386(3)
O2-C18	1.198(3)	C20-C25	1.421(3)
C1-C2	1.528(4)	C21-C22	1.372(4)
C1-C15	1.516(4)	C21-H21	0.89(3)
C2-C3	1.504(4)	C22-C23	1.387(4)
C2-H2	0.975(22)	C22-H22	0.973(24)
C3-C4	1.376(4)	C23-C24	1.402(4)
C3-C8	1.422(3)	C23-H23	0.965(23)
C4-C5	1.387(4)	C24-C25	1.390(3)
C4-H4	0.95(3)	C24-C33	1.515(4)
C5-C6	1.404(4)	C25-C26	1.507(3)
C5-H5	0.98(3)	C26-C27	1.414(3)
C6-C7	1.382(4)	C26-C31	1.394(4)
C6-H6	1.00(3)	C27-C28	1.403(4)
C7-C8	1.401(3)	C27-C34	1.491(4)
C7-C16	1.515(4)	C28-C29	1.355(5)
C8-C9	1.486(3)	C28-H28	0.90(3)
C9-C10	1.423(3)	C29-C30	1.397(4)
C9-C14	1.409(3)	C29-H29	0.93(3)
C10-C11	1.374(3)	C30-C31	1.394(4)
C10-C17	1.508(3)	C30-H30	1.02(3)
C11-C12	1.388(4)	C31-C32	1.510(3)
C11-H11	0.882(24)	C32-H32A	1.05(3)
C12-C13	1.392(3)	C32-H32B	1.114(3)
C12-H12	0.942(23)	C32-OW	1.255(12)
C13-C14	1.381(3)	C33-H33A	1.00(3)
C13-H13	0.997(23)	C33-H33B	1.07(4)
C14-C15	1.526(3)	C33-H33C	0.97(4)
C15-H15a	1.015(25)	C34-H34A	1.04(3)
C15-H15b	1.092(3)	C34-H34B	0.95(3)
C16-H16a	0.95(3)	C34-H34C	0.96(3)
C16-H16b	0.91(4)		
C16-H16c	1.06(5)		
C17-H17a	0.96(3)		
C17-H17b	1.01(3)		
C17-H17c	1.06(4)		
C18-C19	1.509(4)		
C18-C32	1.538(4)		

Table of Atomic Bond Angles in Degrees

O1-C1-C2	121.64(23)	C19-C20-C25	118.61(21)
O1-C1-C15	122.14(24)	C21-C20-C25	120.59(22)
C2-C1-C15	116.16(19)	C20-C21-C22	120.28(22)
F1-C2-C1	108.55(19)	C20-C21-H21	112.4(20)
F1-C2-C3	111.06(21)	C22-C21-H21	127.0(20)
F1-C2-H2	108.2(14)	C21-C22-C23	119.76(22)
C1-C2-C3	109.09(20)	C21-C22-H22	123.0(14)
C1-C2-H2	105.7(14)	C23-C22-H22	117.3(14)
C3-C2-H2	114.0(14)	C22-C23-C24	121.35(23)
C2-C3-C4	120.70(21)	C22-C23-H23	119.9(14)
C2-C3-C8	118.25(21)	C24-C23-H23	118.7(14)
C4-C3-C8	120.81(24)	C23-C24-C25	119.14(22)
C3-C4-C5	120.58(24)	C23-C24-C33	117.94(22)
C3-C4-H4	115.5(17)	C25-C24-C33	122.83(23)
C5-C4-H4	123.6(17)	C20-C25-C24	118.85(21)
C4-C5-C6	119.16(24)	C20-C25-C26	117.60(20)
C4-C5-H5	123.0(15)	C24-C25-C26	123.48(20)
C6-C5-H5	117.8(15)	C25-C26-C27	121.54(22)
C5-C6-C7	120.8(3)	C25-C26-C31	118.67(20)
C5-C6-H6	115.1(14)	C27-C26-C31	119.71(22)
C7-C6-H6	124.0(14)	C26-C27-C28	117.13(25)
C6-C7-C8	120.45(23)	C26-C27-C34	123.63(24)
C6-C7-C16	118.01(23)	C28-C27-C34	119.23(24)
C8-C7-C16	121.50(22)	C27-C28-C29	123.14(25)
C3-C8-C7	118.11(22)	C27-C28-H28	112.7(20)
C3-C8-C9	119.05(21)	C29-C28-H28	124.1(20)
C7-C8-C9	122.84(20)	C28-C29-C30	119.8(3)
C8-C9-C10	122.26(20)	C28-C29-H29	126.3(18)
C8-C9-C14	119.66(19)	C30-C29-H29	113.5(18)
C10-C9-C14	118.03(21)	C29-C30-C31	119.0(3)
C9-C10-C11	119.15(21)	C29-C30-H30	120.8(15)
C9-C10-C17	121.82(21)	C31-C30-H30	120.1(15)
C11-C10-C17	118.97(20)	C26-C31-C30	121.16(23)
C10-C11-C12	122.36(21)	C26-C31-C32	120.57(21)
C10-C11-H11	122.3(16)	C30-C31-C32	118.26(23)
C12-C11-H11	114.7(16)	C18-C32-C31	112.80(22)
C11-C12-C13	118.94(22)	C18-C32-H32A	102.5(16)
C11-C12-H12	120.6(14)	C18-C32-H32B	106.67(22)
C13-C12-H12	120.2(14)	C18-C32-OW	98.0(6)
C12-C13-C14	120.10(22)	C31-C32-H32A	108.0(15)
C12-C13-H13	112.2(13)	C31-C32-H32B	107.74(22)
C14-C13-H13	127.7(13)	C31-C32-OW	127.0(6)
C9-C14-C13	121.33(21)	H32A-C32-H32B	119.2(16)
C9-C14-C15	119.82(21)	H32A-C32-OW	105.7(17)
C13-C14-C15	118.84(21)	H32B-C32-OW	19.5(6)
C1-C15-C14	113.89(20)	C24-C33-H33A	110.9(18)
C1-C15-H15a	102.8(14)	C24-C33-H33B	115.8(18)
C1-C15-H15b	108.20(21)	C24-C33-H33C	113.1(23)
C14-C15-H15a	109.9(14)	H33A-C33-H33B	96(3)
C14-C15-H15b	108.34(21)	H33A-C33-H33C	113(3)
H15a-C15-H15b	113.8(15)	H33B-C33-H33C	105(3)

C7-C16-H16a	109.7(16)	C27-C34-H34A	117.5(15)
C7-C16-H16b	101.6(25)	C27-C34-H34B	118.3(18)
C7-C16-H16c	105(3)	C27-C34-H34C	113.9(18)
H16a-C16-H16b	145(3)	H34A-C34-H34B	98.9(23)
H16a-C16-H16c	106(3)	H34A-C34-H34C	100.4(24)
H16b-C16-H16c	76(4)	H34B-C34-H34C	105.3(24)
C10-C17-H17a	114.9(17)		
C10-C17-H17b	108.2(19)		
C10-C17-H17c	112.5(21)		
H17a-C17-H17b	108.4(25)		
H17a-C17-H17c	101(3)		
H17b-C17-H17c	111(3)		
O2-C18-C19	123.1(3)		
O2-C18-C32	122.2(3)		
C19-C18-C32	114.61(20)		
F2-C19-C18	107.98(21)		
F2-C19-C20	112.40(21)		
F2-C19-H19	105.2(12)		
C18-C19-C20	109.43(21)		
C18-C19-H19	112.1(13)		
C20-C19-H19	109.7(12)		
C19-C20-C21	120.42(21)		

Torsion angles

O1	C1	C2	F1	-0.82(22)	O1	C1	C2	C3	-122.0(5)
O1	C1	C2	H2	115. (3)	C15	C1	C2	F1	176.5(6)
C15	C1	C2	C3	55.3(3)	C15	C1	C2	H2	-67.7(25)
O1	C1	C15	C14	-153.3(6)	O1	C1	C15	H15a	88. (3)
O1	C1	C15	H15b	-32.8(3)	C2	C1	C15	C14	29.4(3)
C2	C1	C15	H15a	-89. (3)	C2	C1	C15	H15b	149.9(6)
F1	C2	C3	C4	-16.91(25)	F1	C2	C3	C8	168.7(5)
C1	C2	C3	C4	102.7(5)	C1	C2	C3	C8	-71.7(4)
H2	C2	C3	C4	-139. (3)	H2	C2	C3	C8	46.2(24)
C2	C3	C4	C5	-174.8(6)	C2	C3	C4	H4	12. (3)
C8	C3	C4	C5	-0.5(3)	C8	C3	C4	H4	-174. (3)
C2	C3	C8	C7	172.0(5)	C2	C3	C8	C9	-7.15(23)
C4	C3	C8	C7	-2.3(3)	C4	C3	C8	C9	178.5(5)
C3	C4	C5	C6	2.8(3)	C3	C4	C5	H5	-174. (3)
H4	C4	C5	C6	176. (3)	H4	C4	C5	H5	-1. (4)
C4	C5	C6	C7	-2.3(3)	C4	C5	C6	H6	174. (3)
H5	C5	C6	C7	175. (3)	H5	C5	C6	H6	-9. (4)
C5	C6	C7	C8	-0.7(3)	C5	C6	C7	C16	176.9(6)
H6	C6	C7	C8	-176. (3)	H6	C6	C7	C16	1. (3)
C6	C7	C8	C3	2.9(3)	C6	C7	C8	C9	-178.0(6)
C16	C7	C8	C3	-174.6(6)	C16	C7	C8	C9	4.5(3)
C6	C7	C16	H16a	-178. (3)	C6	C7	C16	H16b	16. (5)
C6	C7	C16	H16c	-63. (5)	C8	C7	C16	H16a	-1. (3)
C8	C7	C16	H16b	-166. (5)	C8	C7	C16	H16c	114. (5)
C3	C8	C9	C10	-120.4(5)	C3	C8	C9	C14	56.7(3)
C7	C8	C9	C10	60.5(3)	C7	C8	C9	C14	-122.4(5)
C8	C9	C10	C11	-179.4(5)	C8	C9	C10	C17	3.62(24)
C14	C9	C10	C11	3.46(24)	C14	C9	C10	C17	-173.6(5)
C8	C9	C14	C13	-179.8(5)	C8	C9	C14	C15	-0.73(23)
C10	C9	C14	C13	-2.51(24)	C10	C9	C14	C15	176.5(5)
C9	C10	C11	C12	-1.90(24)	C9	C10	C11	H11	-172. (3)
C17	C10	C11	C12	175.2(5)	C17	C10	C11	H11	5. (3)
C9	C10	C17	H17a	18. (3)	C9	C10	C17	H17b	139. (3)
C9	C10	C17	H17c	-98. (4)	C11	C10	C17	H17a	-160. (3)
C11	C10	C17	H17b	-38. (3)	C11	C10	C17	H17c	85. (4)
C10	C11	C12	C13	-0.75(24)	C10	C11	C12	H12	-175. (3)
H11	C11	C12	C13	170. (3)	H11	C11	C12	H12	-4. (4)
C11	C12	C13	C14	1.76(24)	C11	C12	C13	H13	-178.4(24)
H12	C12	C13	C14	176. (3)	H12	C12	C13	H13	-4. (3)
C12	C13	C14	C9	-0.10(24)	C12	C13	C14	C15	-179.1(5)
H13	C13	C14	C9	-179.9(24)	H13	C13	C14	C15	1.1(24)
C9	C14	C15	C1	-65.3(4)	C9	C14	C15	H15a	49. (3)
C9	C14	C15	H15b	174.2(6)	C13	C14	C15	C1	113.7(5)
C13	C14	C15	H15a	-132. (3)	C13	C14	C15	H15b	-6.71(20)
C7	C16	H16b	H16c	-104. (6)	H16a	C16	H16b	H16c	101. (8)
H16c	C16	H16b	H16c	0. (6)	C7	C16	H16c	H16b	99. (7)
H16a	C16	H16c	H16b	-145. (10)	H16b	C16	H16c	H16b	0. (6)
O2	C18	C19	F2	0.85(25)	O2	C18	C19	C20	123.5(6)
O2	C18	C19	H19	-114.6(23)	C32	C18	C19	F2	-176.6(6)

C32	C18	C19	C20	-54.0(3)	C32	C18	C19	H19	67.9(22)
O2	C18	C32	C31	150.1(6)	O2	C18	C32	H32A	-94. (3)
O2	C18	C32	H32B	32.0(3)	O2	C18	C32	OW	14.1(10)
C19	C18	C32	C31	-32.5(3)	C19	C18	C32	H32A	83. (3)
C19	C18	C32	H32B	-150.5(6)	C19	C18	C32	OW	-168.4(12)
F2	C19	C20	C21	21.1(3)	F2	C19	C20	C25	-166.0(6)
C18	C19	C20	C21	-98.9(5)	C18	C19	C20	C25	74.1(4)
H19	C19	C20	C21	137.8(23)	H19	C19	C20	C25	-49.3(22)
C19	C20	C21	C22	172.9(6)	C19	C20	C21	H21	-14. (4)
C25	C20	C21	C22	0.0(3)	C25	C20	C21	H21	174. (4)
C19	C20	C25	C24	-171.6(5)	C19	C20	C25	C26	5.34(24)
C21	C20	C25	C24	1.3(3)	C21	C20	C25	C26	178.3(5)
C20	C21	C22	C23	-1.3(3)	C20	C21	C22	H22	180. (3)
H21	C21	C22	C23	-174. (4)	H21	C21	C22	H22	7. (4)
C21	C22	C23	C24	1.2(3)	C21	C22	C23	H23	-178. (3)
H22	C22	C23	C24	-180. (3)	H22	C22	C23	H23	1. (4)
C22	C23	C24	C25	0.2(3)	C22	C23	C24	C33	-176.3(6)
H23	C23	C24	C25	179. (3)	H23	C23	C24	C33	2.5(25)
C23	C24	C25	C20	-1.42(25)	C23	C24	C25	C26	-178.2(5)
C33	C24	C25	C20	174.9(5)	C33	C24	C25	C26	-1.9(3)
C23	C24	C33	H33A	-72. (3)	C23	C24	C33	H33B	36. (3)
C23	C24	C33	H33C	159. (4)	C25	C24	C33	H33A	112. (3)
C25	C24	C33	H33B	-140. (3)	C25	C24	C33	H33C	-18. (4)
C20	C25	C26	C27	120.1(5)	C20	C25	C26	C31	-56.5(3)
C24	C25	C26	C27	-63.1(4)	C24	C25	C26	C31	120.3(5)
C25	C26	C27	C28	-179.6(6)	C25	C26	C27	C34	0.1(3)
C31	C26	C27	C28	-3.0(3)	C31	C26	C27	C34	176.7(6)
C25	C26	C31	C30	179.9(6)	C25	C26	C31	C32	1.12(24)
C27	C26	C31	C30	3.3(3)	C27	C26	C31	C32	-175.5(5)
C26	C27	C28	C29	1.4(3)	C26	C27	C28	H28	-180. (4)
C34	C27	C28	C29	-178.3(7)	C34	C27	C28	H28	0. (3)
C26	C27	C34	H34A	-20. (3)	C26	C27	C34	H34B	98. (3)
C26	C27	C34	H34C	-137. (3)	C28	C27	C34	H34A	160. (3)
C28	C27	C34	H34B	-82. (3)	C28	C27	C34	H34C	42. (3)
C27	C28	C29	C30	0.1(3)	C27	C28	C29	H29	173. (3)
H28	C28	C29	C30	-179. (4)	H28	C28	C29	H29	-5. (5)
C28	C29	C30	C31	0.1(3)	C28	C29	C30	H30	175. (3)
H29	C29	C30	C31	-174. (3)	H29	C29	C30	H30	1. (4)
C29	C30	C31	C26	-1.7(3)	C29	C30	C31	C32	177.1(6)
H30	C30	C31	C26	-177. (3)	H30	C30	C31	C32	2. (3)
C26	C31	C32	C18	67.6(4)	C26	C31	C32	H32A	-45. (3)
C26	C31	C32	H32B	-174.9(6)	C26	C31	C32	OW	-171.9(12)
C30	C31	C32	C18	-111.2(5)	C30	C31	C32	H32A	136. (3)
C30	C31	C32	H32B	6.23(23)	C30	C31	C32	OW	9.2(10)
C18	C32	H32B	OW	-66. (3)	C31	C32	H32B	OW	173. (3)
H32A	C32	H32B	OW	49. (4)	OW	C32	H32B	OW	0. (3)
C18	C32	OW	H32B	118. (3)	C31	C32	OW	H32B	-8.6(22)
H32A	C32	OW	H32B	-137. (5)	H32B	C32	OW	H32B	0.0(19)
C24	C33	H33A	H33B	121. (4)	H33B	C33	H33A	H33B	0. (4)
H33C	C33	H33A	H33B	-110. (7)	C24	C33	H33B	H33A	-117. (5)
H33A	C33	H33B	H33A	0. (4)	H33C	C33	H33B	H33A	117. (7)
C27	C34	H34A	H34B	128. (4)	C27	C34	H34A	H34C	-124. (4)
H34B	C34	H34A	H34B	0. (4)	H34B	C34	H34A	H34C	107. (5)
H34C	C34	H34A	H34B	-107. (5)	H34C	C34	H34A	H34C	0. (4)

C27	C34	H34B	H34A	-128. (4)	C27	C34	H34B	H34C	129. (4)
H34A	C34	H34B	H34A	0. (3)	H34A	C34	H34B	H34C	-103. (5)
H34C	C34	H34B	H34A	103. (5)	H34C	C34	H34B	H34C	0. (4)
C27	C34	H34C	H34A	127. (4)	C27	C34	H34C	H34B	-131. (4)
H34A	C34	H34C	H34A	0. (3)	H34A	C34	H34C	H34B	102. (5)
H34B	C34	H34C	H34A	-102. (5)	H34B	C34	H34C	H34B	0. (4)
C16	H16b	H16c	C16	0.0(11)	C32	H32B	OW	C32	0.0(4)
C33	H33A	H33B	C33	0.0(5)	C34	H34A	H34B	C34	0.0(6)
C34	H34A	H34B	H34C	43. (3)	H34C	H34A	H34B	C34	-43. (4)
H34C	H34A	H34B	H34C	0. (3)	C34	H34A	H34C	C34	0.0(5)
C34	H34A	H34C	H34B	-43. (3)	H34B	H34A	H34C	C34	43. (4)
H34B	H34A	H34C	H34B	0. (3)	C34	H34B	H34C	C34	0.0(4)
C34	H34B	H34C	H34A	49. (4)	H34A	H34B	H34C	C34	-49. (4)
H34A	H34B	H34C	H34A	0. (3)					

Appendix 2: Competitive Reduction of Ketones 44-53 using LAH, SBH and triethylsilane

Table A2.1a Competitive reduction of ketones A (unsubstituted) versus B (axial α-substituted) for $LiAlH_4$ in 4 mL THF at 0°C (20 sec quench).

Substituent	Unsubstituted Ketone (A) mmol	Substituted Ketone (B) mmol	$LiAlH_4$ mmol	% A reduced	% B reduced	% Total Hydride Consumed	k_B/k_A
CH_{3ax}	0.0135	0.0365	0.006	45	22	58	0.410
CH_{3ax}[a]	0.00694	0.0181	0.003	51	30	74	0.488
CH_{3ax}	0.00815	0.0139	0.00275	63	32	87	0.388
CH_{3ax}	0.0135	0.0365	0.006	54	26	69	0.391
CH_{3ax}	0.0238	0.0262	0.006	34	15	50	0.398
CH_{3ax}	0.0368	0.0132	0.006	23	9.0	29	0.333
CH_{3ax}	0.025	0.025	0.006	30	14	38	0.412
CH_{3ax}	0.0379	0.0121	0.006	22	7.6	40	0.322
SCH_{3ax}[b,c]	0.0259	0.0241	0.006	30	14	46	0.400
SCH_{3ax}[a,b]	0.0275	0.0225	0.006	26	14	43	0.481
SCH_{3ax}[a,d]	0.0258	0.0242	0.006	47	28	79	0.505
SCH_{3ax}	0.0269	0.0231	0.00625	33	14	49	0.382
OCH_{3ax}	0.0307	0.0193	0.006	36	28	54	1.36
Cl_{ax}	0.0220	0.0220 + 0.006 (Cl_{eq})	0.006	39 (Cl_{ax})	16	65	2.81[e]

[a] In 10 mL. [b] 30 sec quench. [c] In 5 mL. [d] 15 sec quench. [e] $k_B/k_A = k_{Clax}/k_{unsub}$.

Table A2.1b Competitive reduction of ketones A (unsubstituted) versus B (equatorial α-substituted) for $LiAlH_4$ in 4 mL THF at 0°C (20 sec quench).

Substituent	Unsubstituted Ketone (A) mmol	Substituted Ketone (B) mmol	$LiAlH_4$ mmol	% A reduced	% B reduced	% Total Hydride Consumed	k_B/k_A
CH_{3eq}[a,b]	0.0271	0.0229	0.006	24	28	52	1.21
CH_{3eq}[a,c]	0.0496	0.0504	0.012	32	35	67	1.08
CH_{3eq}	0.0254	0.0246	0.00625	33	35	68	1.08
SCH_{3eq}	0.0200[d]	0.0309	0.0062	18	48	70	3.35[e]
SCH_{3eq}	0.0291[d]	0.0199	0.006	16	60	70	4.92[e]
SCH_{3eq}	0.0432[d]	0.00885	0.0064	18	81	57	8.23[e]
SCH_{3eq}	0.0159 + 0.0163[d]	0.0163	0.00576	19 (SCH_{3ax})	71	80	5.97[e]
SCH_{3eq}[f]	0.00614[d]	0.0236	0.015[g]				≥25.7[e]
OCH_{3eq}	0.0289	0.0231	0.006	20	56	72	3.58
OCH_{3eq}	0.0385	0.0135	0.0065	20	65	61	4.72
Cleq	0.0276	0.0224	0.006	16	45	61	3.39
Cleq	0.0273	0.0227	0.00313	8	25	64	3.23
Feq	0.025	0.025	0.00625	19	48	67	3.16
Feq	0.0361	0.0139	0.00625	20	61	62	4.32
Feq	0.00904	0.00347	0.00156	13	42	42	3.99
Feq	0.025	0.025	0.00313	8.8	26	68	3.23

[a] Reference 147. [b] 1 min quench. [c] In 8 mL, 45 sec quench. [d] Axial α-methylthio ketone 46. [e] $k_B/k_A = k_{SCH3eq}/k_{SCH3ax}$. [f] 2 min quench. [g] Reduced with compound 83.

Table A2.2a Competitive reduction of ketones A (unsubstituted) versus B (axial α-substituted) for $NaBH_4$ (1 equiv) in 20 mL *i*-PrOH at 23°C (45 sec quench).

Substituent	Unsubstituted Ketone (A) mmol	Substituted Ketone (B) mmol	% A reduced	% B reduced	% Total Hydride Consumed	% of B Epimerized	k_B/k_A[a]
CH_{3ax}[b]	0.00713	0.0424	28	2.9	7.0	8.6	0.113
CH_{3ax}[c]	0.00686	0.0431	23	2.7	5.8	3.7	0.115
SCH_{3ax}	0.00618	0.0439	2.2	0.88	1.6	3.0	0.401
SCH_{3ax}[d]	0.0238	0.0262	1.6	0.62	1.5	5.6	0.378
OCH_{3ax}	0.0413	0.00868	2.4	18	5.4	2.6	8.18
Cl_{ax}	0.0350	0.007 + 0.008 (Cl_{eq})	1.2	40 (Cl_{ax})	12	7.7	41.4[e]
Cl_{ax}	0.0458	0.00180 + 0.00239 (Cl_{eq})	1.3	41 (Cl_{ax})	3.5	9.2	41.3[e]

[a] The accuracy of the integrals in the ^1H NMR spectra is estimated to be ±1%. This corresponds to a precision in k_B/k_A of ± 5%. [b] In 5 mL at rt, 15 min quench. [c] In 5 mL at rt, 7.5 min quench. [d] 2.25 min quench. [e] $k_B/k_A = k_{Clax}/k_{unsub}$.

Table A2.2b Competitive reduction of ketones A (unsubstituted) versus B (equatorial α-substituted) for $NaBH_4$ (1 equiv) in 20 mL *i*-PrOH at 23°C (45 sec quench).

Substituent	Unsubstituted Ketone (A) mmol	Substituted Ketone (B) mmol	% A reduced	% B reduced	% Total Hydride Consumed	% of B Epimerized	k_B/k_A[a]
CH_{3eq}	0.0255	0.0245	0.35	0.17	0.26	<2	0.484
CH_{3eq}[b]	0.0182	0.0318	1.1	0.46	0.68	<2	0.424
SCH_{3eq}	0.0385	0.00633 + 0.00518 (SCH_{3ax})	1.4	6.3	1.6	9.6 (SCH_{3eq})	4.44[c]
SCH_{3eq}	0.0308	0.00839 + 0.0108 (SCH_{3ax})	2.5	11	3.2	4.2 (SCH_{3eq})	4.24[c]
OCH_{3eq}	0.0333	0.0167	1.4	44	16	3.6[d]	40.5
OCH_{3eq}	0.0450	0.00495	1.2	42	5.3	4.1[d]	43.7
Cl_{eq}[e]	0.0299	0.0201	6.9	77	31	9.6	19.7
Cl_{eq}[b]	0.0292	0.0208	5.1	68	28	8.3	21.1
Cl_{eq}	0.0119	0.0131	3.2	47	28	7.1	19.2
F_{eq}	0.0442	0.00575	2.3	76	11	0	62.1
F_{eq}	0.0424	0.00763	2.2	73	13	0	57.8

[a] The accuracy of the integrals in the ^1H NMR spectra is estimated to be ±1%. This corresponds to a precision in k_B/k_A of ± 5%. [b] 90 sec quench. [c] $k_B/k_A = k_{SCH3eq}/k_{unsub}$. [d] % rearrangement. [e] 90 sec quench at rt.

Table A2.3 Competitive reduction of ketones A (unsubstituted) versus B (α-substituted) for Et_3SiH (1 equiv)/BF_3-Et_2O (3 equiv) in 5 mL CH_3CN at 0°C (2 min quench).

Substituent	Unsubstituted Ketone (A) mmol	Substituted Ketone (B) mmol	% A reduced	% B reduced	% Total Hydride Consumed	% of B Epimerized	k_B/k_A[a]
CH_{3ax}	0.00586	0.0441	9.4	1.5	2.5	0.7	0.155
SCH_{3ax}	0.00382	0.0462	11	0.099	0.95	3.6	0.00861
OCH_{3ax}	0.00683	0.0432	1.9	0.6	25	28[b]	0.189
OCH_{3ax}[c]	0.0112	0.0393 + 0.00217 (Cleq)	4.1	0.80 (OCH_{3ax})	10	13.7[b] (OCH_{3ax})	0.181[d]
Cl_{ax}[e]	0.00523	0.0276 + 0.0180 (Cleq)	50	0.2 (Cl_{ax})	7.1	6.7 (OCH_{3ax})	0.0024[f]
CH_{3eq}[g]	0.0181	0.0319	1.9	0.3	0.9	0	0.156
SCH_{3eq}[h]	0.0109	0.0271 + 0.00912 (SCH_{3ax})	5.1	0.52 (SCH_{3eq})	1.6	21.9[i] (SCH_{3eq})	0.0905[j]
SCH_{3eq}[c]	0.00302	0.0195 + 0.0233 (SCH_{3ax})	6.8	0.73 (SCH_{3eq})	1.5	22.2[i] (SCH_{3eq})	0.0924[j]
OCH_{3eq}	0.0102	0.0439	10	9.7	14	6.1[b]	0.938
OCH_{3eq}[h]	0.0317	0.0254	6.5	6.0	8.0	4.0[b]	0.904
Cleq	0.00772	0.0423	6.4	0.4	1.3	1.5	0.0576
Feq[k]	0.00568	0.0443	11	1.8	2.9	0	0.134

[a] The accuracy of the integrals in the ^1H NMR spectra is estimated to be ±1%. This corresponds to a precision in k_B/k_A of ± 5%. [a] % rearrangement. [b] 40 sec quench. [c] $k_B/k_A = k_{OCH3ax}/k_{unsub}$. [d] 16 min quench. [e] $k_B/k_A = k_{Clax}/k_{unsub}$, calculated via relay (i.e. $k_{Clax}/k_{unsub} = k_{Clax}/k_{Cleq} \times k_{Cleq}/k_{unsub}$). [f] 45 sec quench. [g] 1 min quench. [h] % epimerization and rearrangement. [i] $k_B/k_A = k_{SCH3eq}/k_{unsub}$. [j] 4 min quench.

Appendix 3: Supplementary ^{1}H NMR Spectra

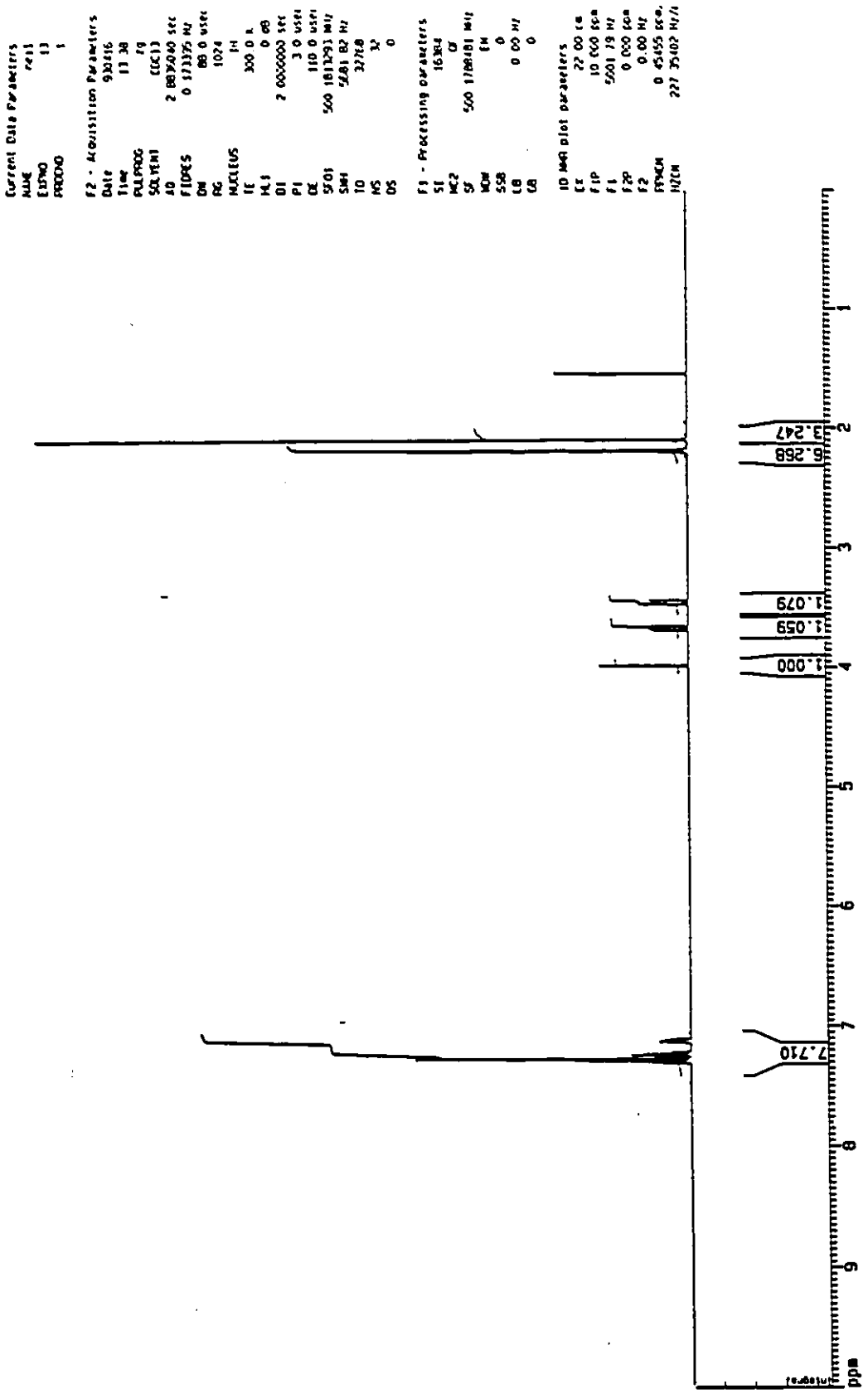

Figure A3.1 The 500 MHz ^{1}H NMR spectrum of the axial α-methylthio ketone 46 in $CDCl_3$.

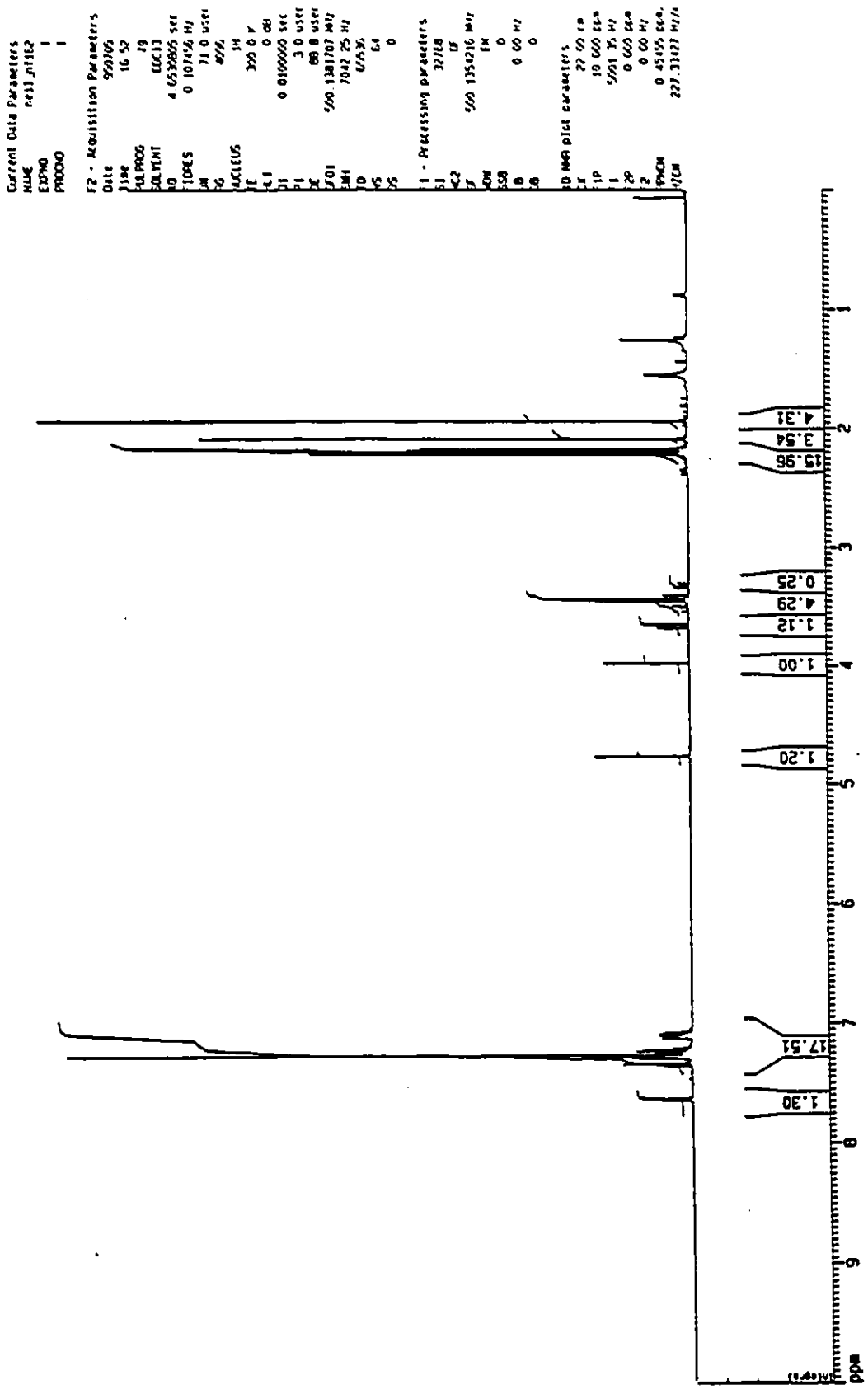

Figure A3.2 The 500 MHz ^{1}H NMR spectrum of a mixture of the axial and equatorial α-methylthio ketones 46 and 50 in $CDCl_3$ (50:46, 1.22:1; sample contained 5.6% of the unsubstituted ketone 44).

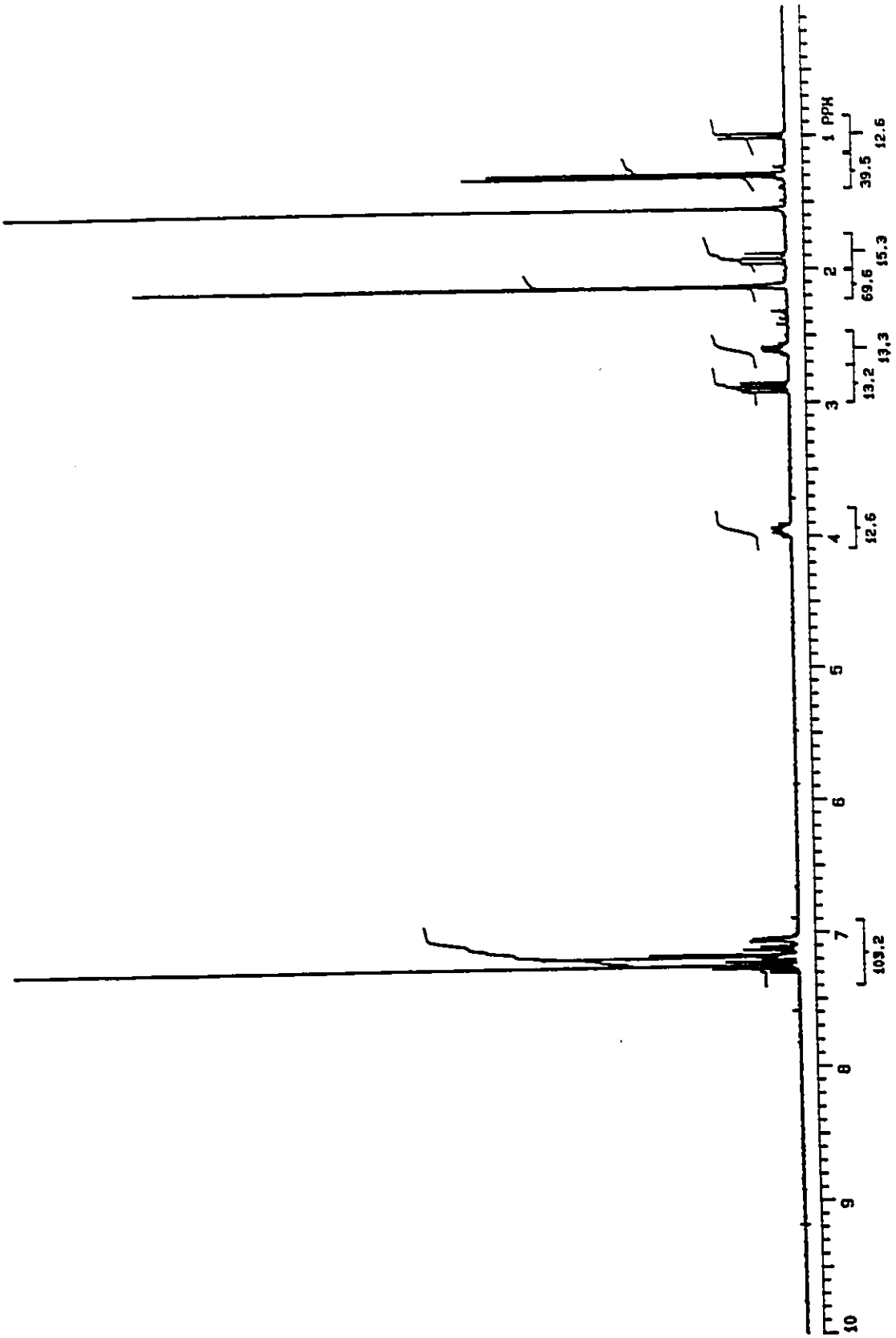

Figure A3.3 The 300 MHz ^{1}H NMR spectrum of the equatorial α-methyl major alcohol 68a in $CDCl_3$.

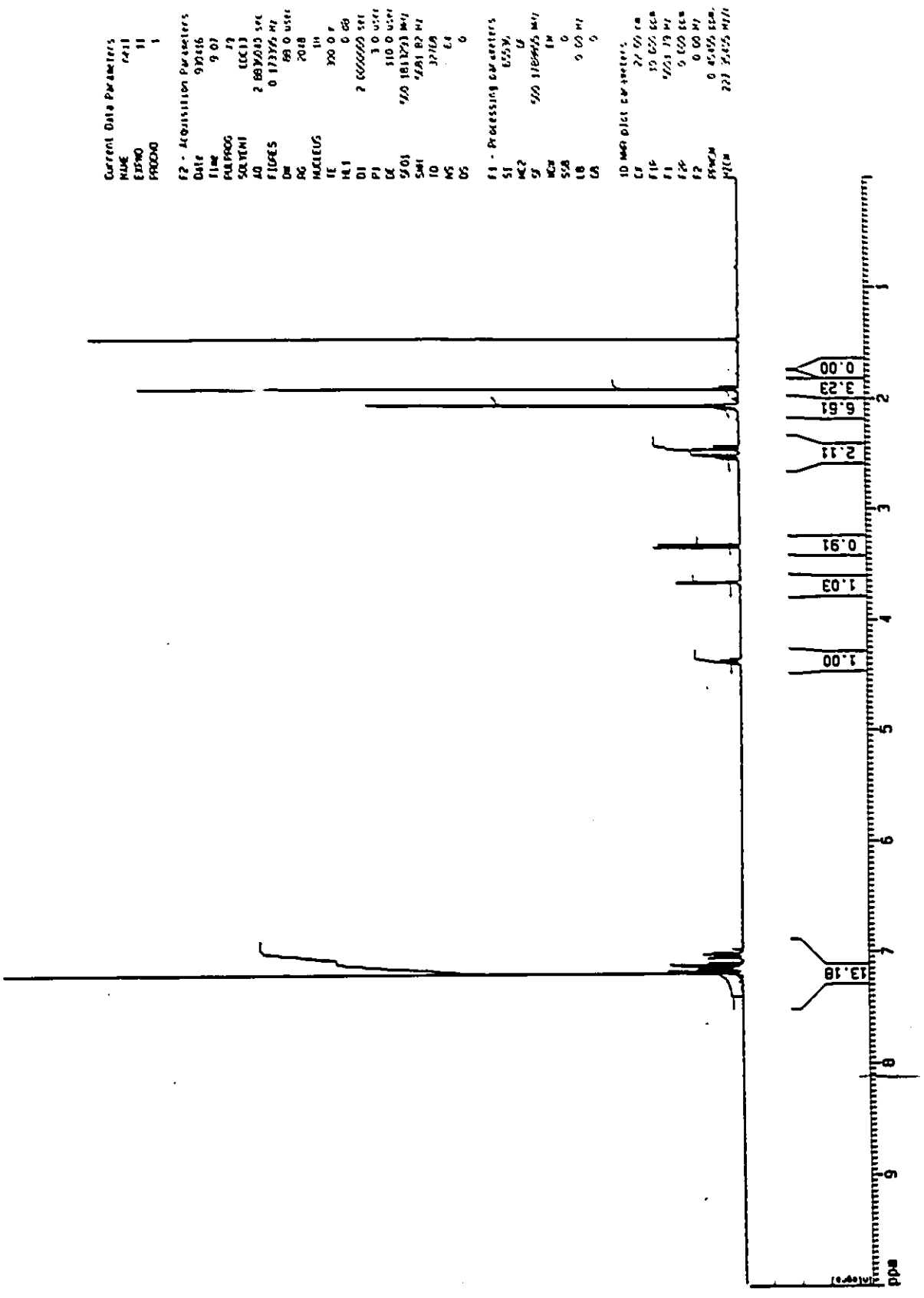

Figure A3.4 The 500 MHz ^{1}H NMR spectrum of the axial α-methylthio major alcohol 66b in $CDCl_3$.

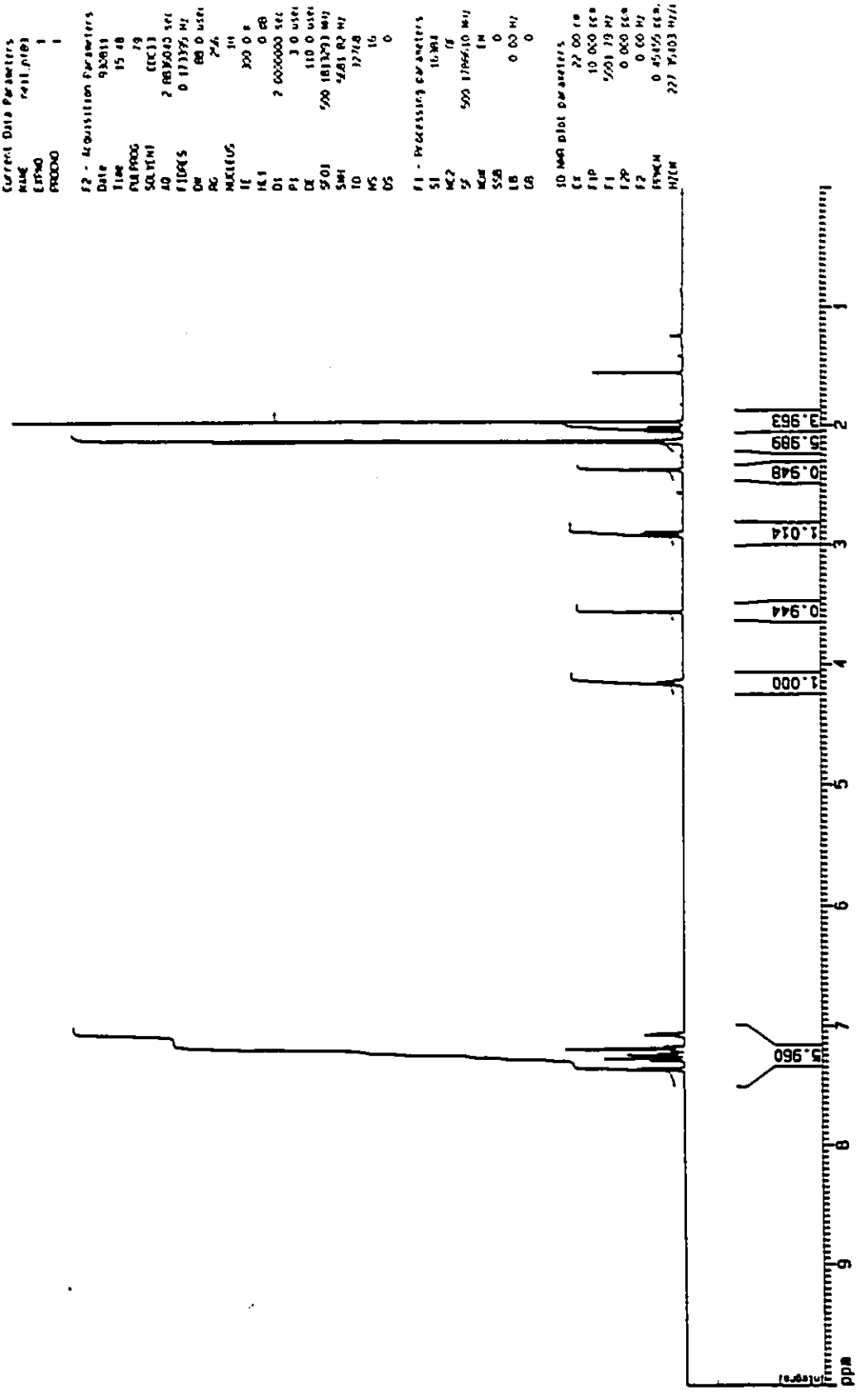

Figure A3.5 The 500 MHz ^{1}H NMR spectrum of the equatorial α-methylthio major alcohol 68b in $CDCl_3$.

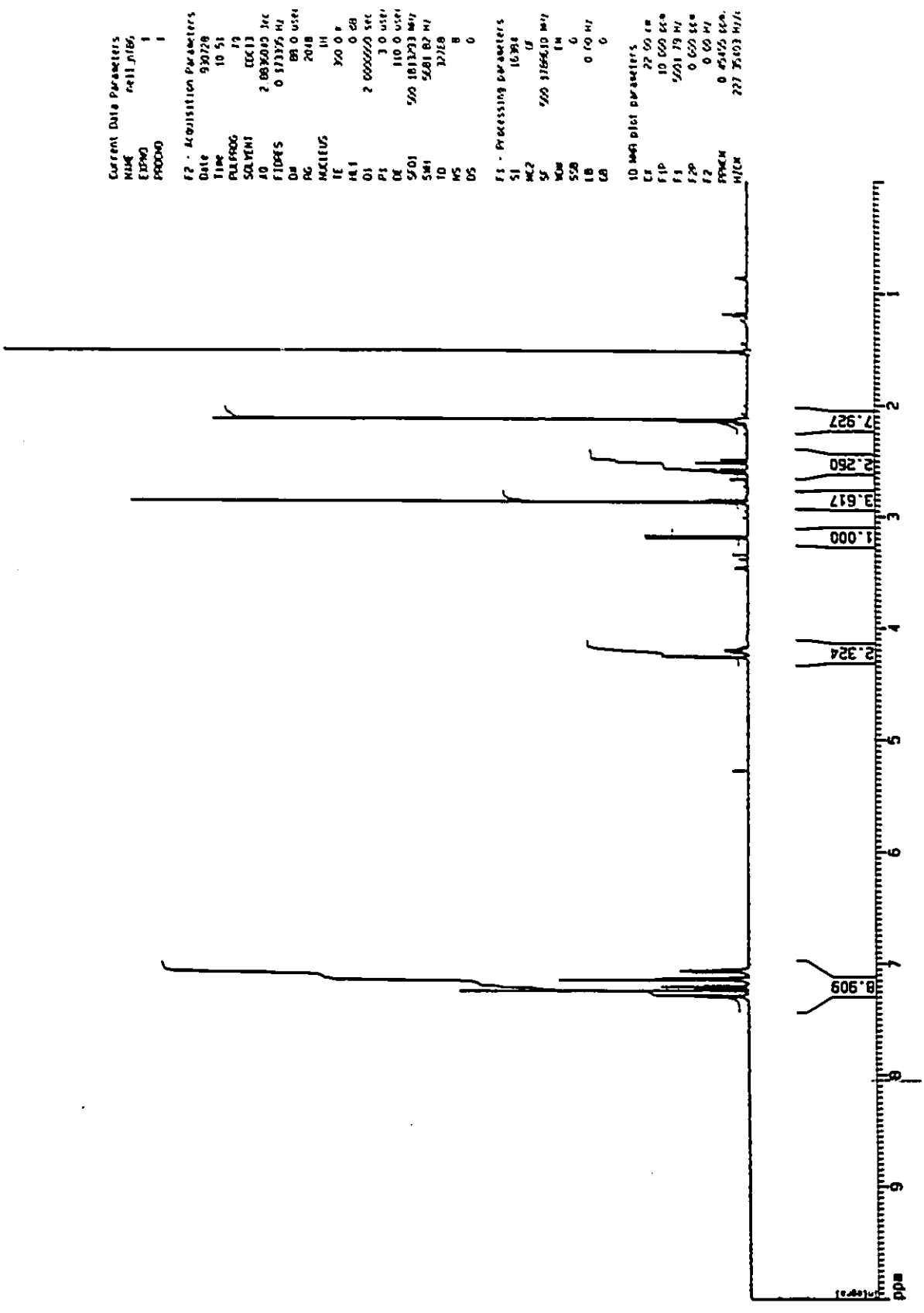

Figure A3.6 The 500 MHz ^{1}H NMR spectrum of the axial α-methoxy major alcohol 66c in $CDCl_3$.

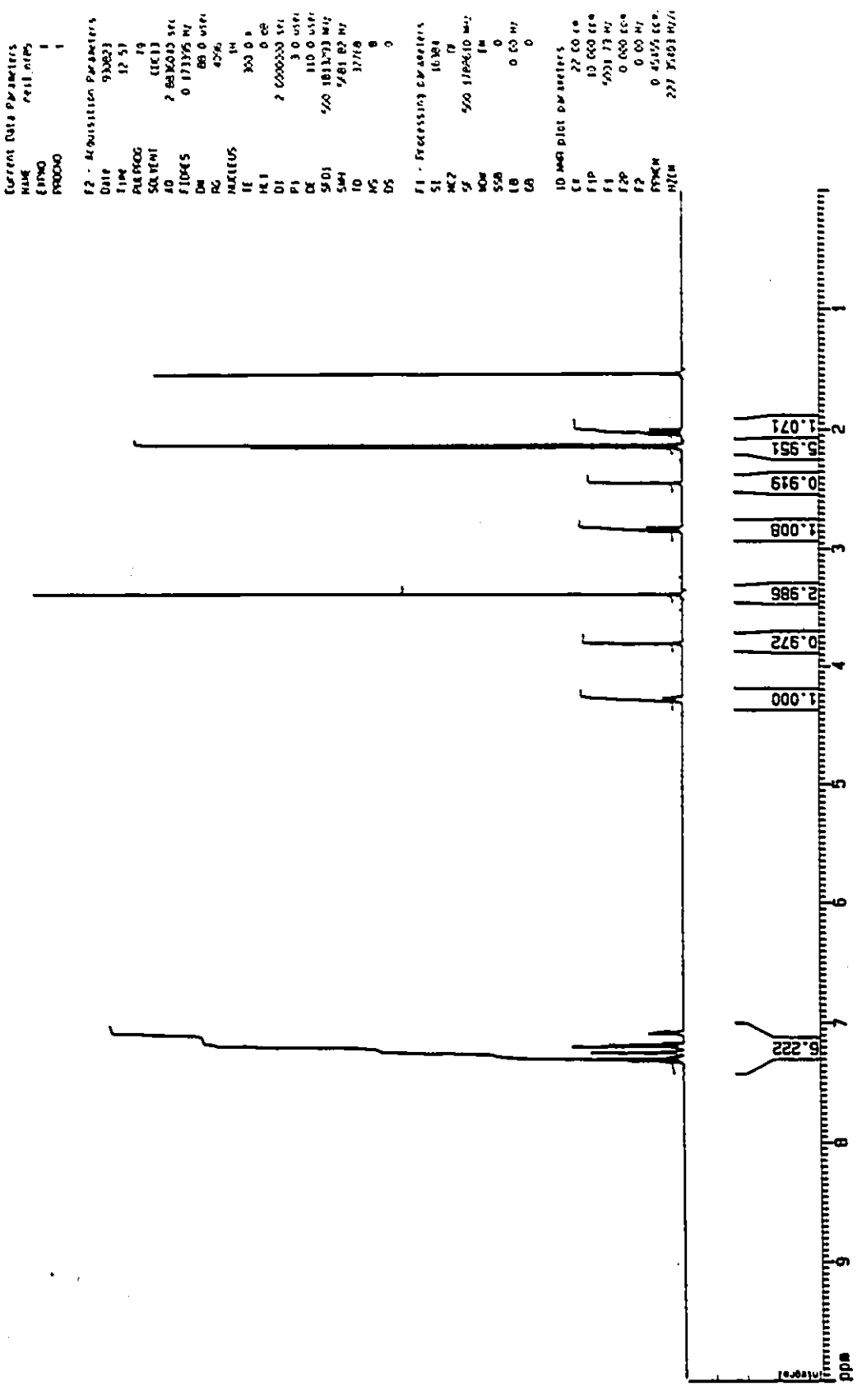

Figure A3.7 The 500 MHz ^{1}H NMR spectrum of the equatorial α-methoxy major alcohol 68c in $CDCl_3$.

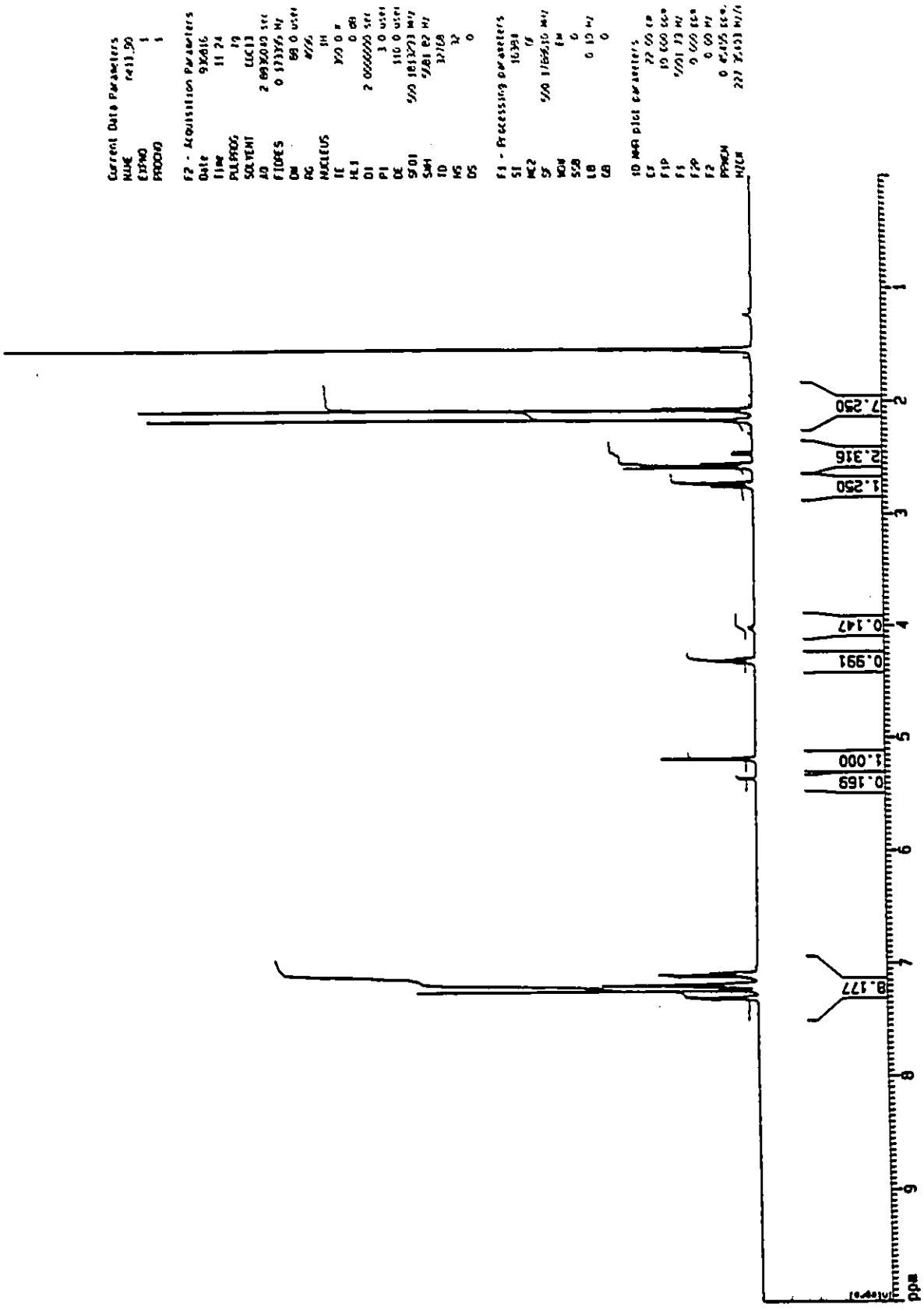

Figure A3.8 The 500 MHz ^{1}H NMR spectrum of the axial α-chloro major alcohol 66d in $CDCl_3$.

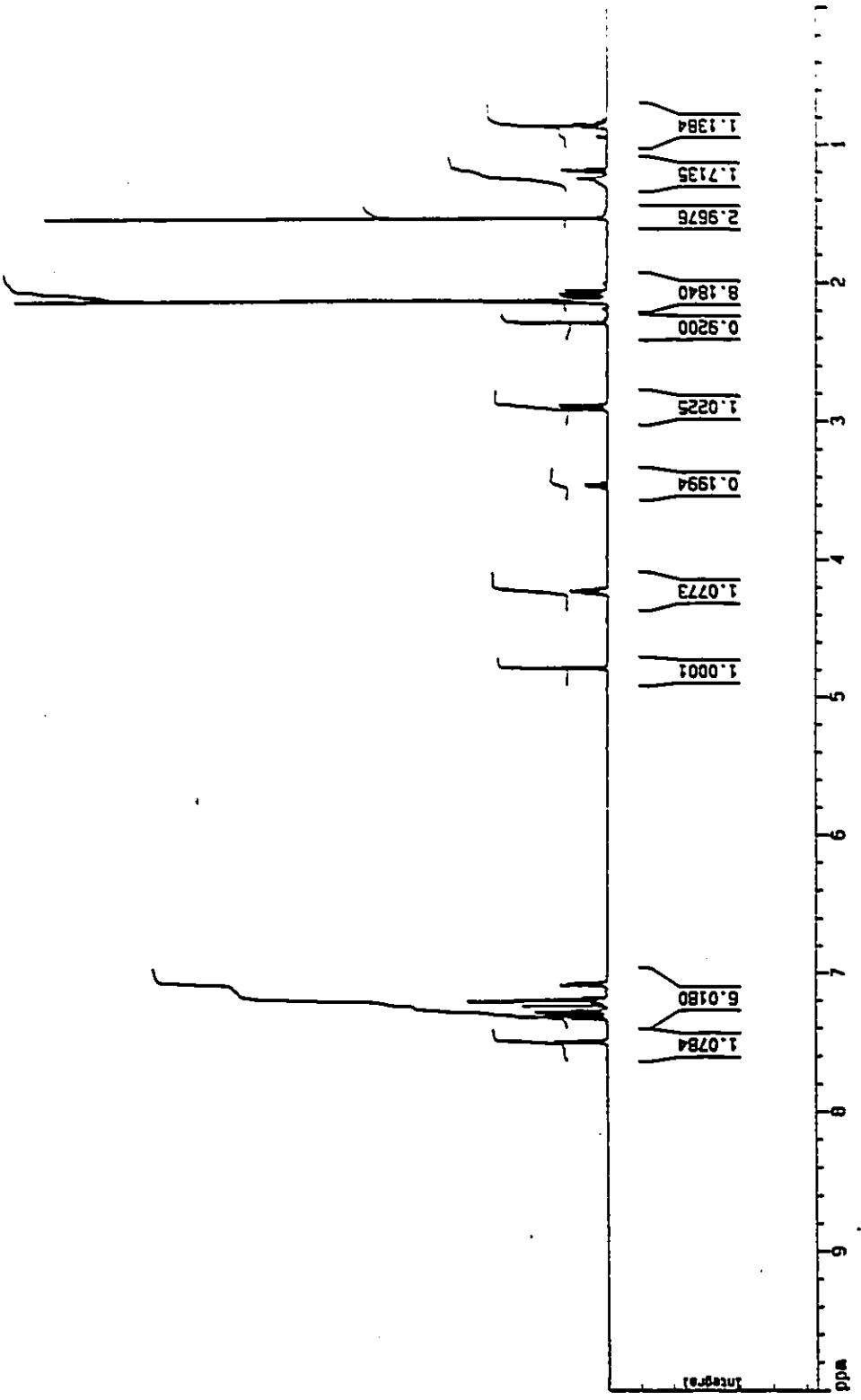

Figure A3.9 The 500 MHz ^{1}H NMR spectrum of the equatorial α-chloro major alcohol 68d in $CDCl_3$.

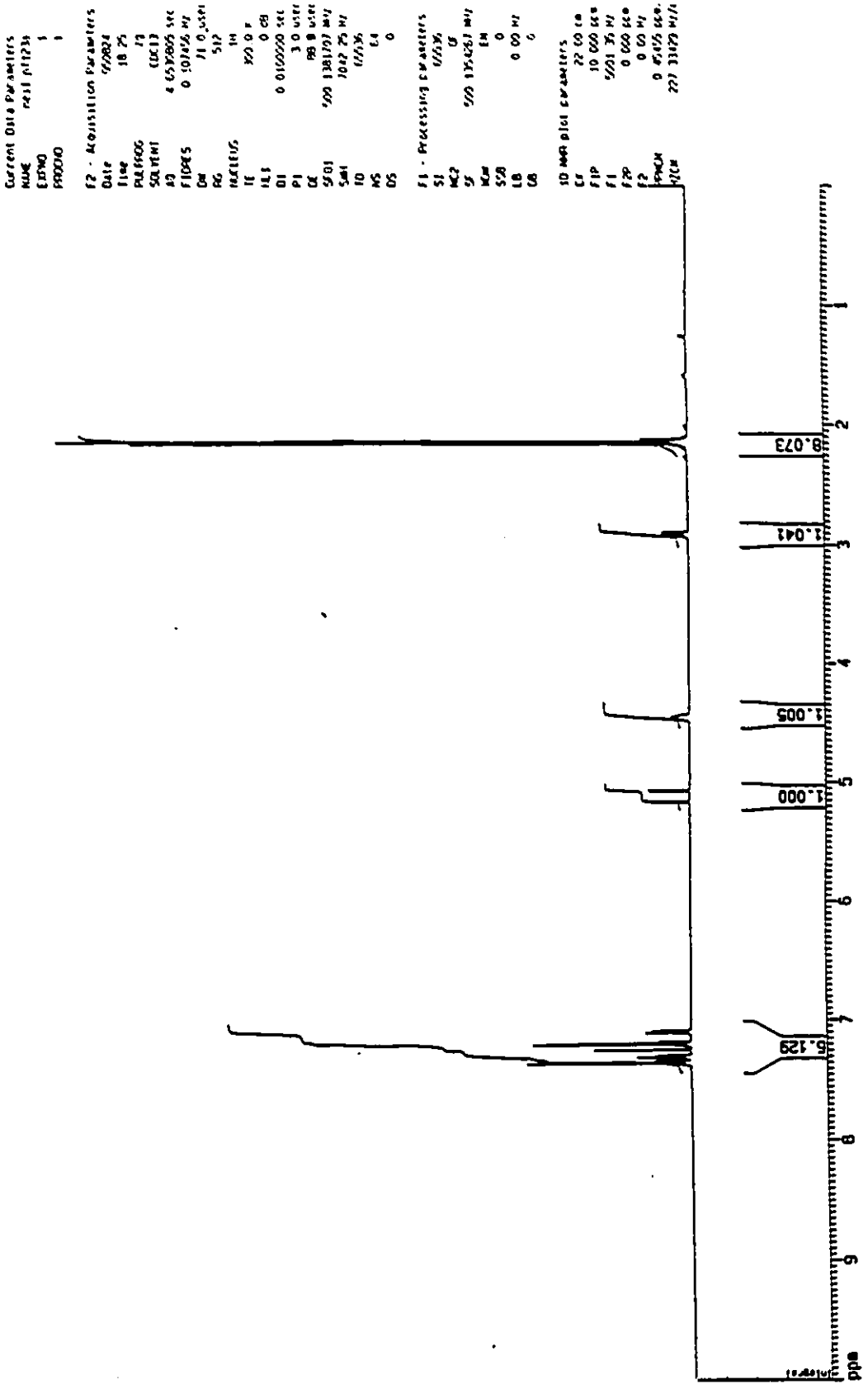

Figure A3.10 The 500 MHz ^{1}H NMR spectrum of the equatorial α-fluoro major alcohol 68e in $CDCl_3$.